Anna Karczewska and Piotr Rozmej

Shallow water waves - extended Korteweg - de Vries equations

– Second order perturbation approach –

September 5, 2018

Preface

This book provides an up-to-date (2018) presentation of the shallow water problem according to a theory which goes beyond the Korteweg-de Vries equation. When we began studying nonlinear partial differential equations in 2012, we were struck by the high number of seemingly miraculous results obtained within the KdV theory. Yet, realizing that this marvelous theory had been derived from more general laws of hydrodynamics serving solely as a first order perturbative approximation with respect to some small parameters, we were curious about the consequences of an extension of the perturbative approach to the next (second) order.

The direct extension of KdV to the second order has been known since 1990 as the *extended KdV equation*. For short we call it **KdV2**. This equation is derived under the same assumptions as KdV and applies to the flat-bottom case.

As beginners in the field, we asked whether it was possible to derive an extended KdV type equation for an uneven bottom according to the same perturbative approach. It was evident that this could not be done in the first order regime. The boundary condition at the non-flat bottom required at least a second order perturbation approach. So, in 2014, we derived the KdV2 equation for an uneven bottom, called by us **KdV2B**, in this regime and showed that such a derivation in higher orders could not be done for a general form of the bottom function. In this derivation, some unorthodox (unconventional) steps were necessary to obtain the final result. Unfortunately, the KdV2 for the case of an uneven bottom could not be, in general, solved analytically. Then we found many exciting features in numerical simulations of wave motion according to this equation, while studying it for different initial

conditions and different bottom functions. These results were obtained using the finite difference method (FDM). Only as recently as in 2017 did we find approximate analytic solitonic solutions to this equation.

In 2014, we found an analytic single soliton solution for the KdV2 equation. This solution, quite unexpectedly, has the same functional form as the single soliton solution to KdV, but with slightly different coefficients. Then we conjectured that the same property could occur for other types of KdV and KdV2 solutions, that is, periodic solutions (known as cnoidal waves) and so-called superposition (composed) solutions. This was proved in subsequent years. The analytic solutions to KdV2 (periodic type or superposition type) have the same functional form as corresponding KdV solutions, but with modified coefficients. Moreover, the KdV2 equation imposes one more condition on these coefficients than the KdV, putting more restrictions on ranges of these coefficients than KdV.

In the meantime, we have discussed conservation laws and invariants for the KdV equation and KdV2 equations with a flat bottom and with an uneven one. For KdV2 we found only one exact invariant related to mass (volume) conservation. For the KdV2 equation with the flat bottom, we found adiabatic (approximate) invariants related to momentum and energy conservation. Through the numerical approach, we extended the finite element method (FEM) used for solving the KdV problem numerically to KdV2 both in deterministic and some stochastic cases.

We would like to express our gratitude to Eryk Infeld and George Rowlands for their contributions in six published papers, as well as through numerous essential discussions and exchange of ideas. The influence of their in-depth knowledge and experience in the field of nonlinear physics cannot be overestimated, particularly in the early stage of our engagement in the subject of nonlinear waves.

Anna Karczewska and Piotr Rozmej

Zielona Góra, July 2018

Contents

1

Introduction and general outline

The physics of nonlinear waves belongs to the fields of science which experienced explosive growth during the last half-century. In this time hundreds of monographs and many thousands of papers have been published. Applications have appeared in many fields, such as hydrodynamics, plasma physics, quantum optics, electric systems, biology, medicine, and neuroscience. In many cases, linear equations and theories provide a good description of the considered phenomena. However, in many other cases, nonlinear wave equations emerge even in first order approximations to more general sets of fundamental equations describing the dynamics of a given system.

In this book, we focus on the *shallow water problem*, in particular on solutions to equations which go beyond the Korteweg-de Vries equation.

1.1 Historical remarks

The history of scientific research which has brought the scientific community to its present stage of understanding of nonlinear waves is by itself a fascinating subject. Much information of this kind can be found, for instance, in the review paper by Craik [30] and in Chapter 1 of the Osborne book [123].

The first person who attempted to create a theory of water waves was Isaac Newton. In *Book II*, *Prop. XLV* of *Principia* (1687) he correctly deduced that the frequency of deep-water waves must be inversely proportional to the square root of "breadth of the wave". Newton derived his conclusion from the analogy with oscillations in a U-tube and was aware that this result was approximate.

In the middle of the eighteen century (1757, 1761) Leonhard Euler derived equations for hydrodynamics. Soon after that Pierre-Simon Laplace (1776) reexamined wave motion. His work was disregarded despite the considerable progress obtained. At almost the same time, perhaps independently, Louis Lagrange (1781, 1786) derived linearised governing equations for small amplitude waves. Lagrange obtained the solution for the limiting case of long plane waves in shallow water. In *Mechanique Analitique (1788)* he wrote "the speed of propagation of waves will be that which a heavy body would acquire falling from the height of the water in the canal", that is, $\sqrt{gh}$, where h is the fluid depth, and g is gravitational acceleration.

Substantial progress in wave theory was achieved in the 1820s by Augustin-Louis Cauchy and Siméon D. Poisson. Their works, however, did not receive their worthy full attention because of mathematical sophistication and results seeming contrary to intuition.

The first observations of a solitary wave by John Scott Russel in 1834 [131] and his next experiments made a significant impact on the progress in research on wave theory. Russel observed a solitary wave on a channel of constant depth and followed its motion on his horse for several miles. He described several specific properties of the propagation of new waves, called by him "waves of translation". He wrote "The observed waves are stable, and they may travel long distances without change of shape. The wave velocity depends on its height, and the width depends on the water depth. If the crest of the created wave is too high concerning the depth of the fluid, then the wave divides into two smaller waves of different amplitudes".

Observations of unusual wave properties by Russel became a great challenge for wave theory. Although only a few years later (1847) Stokes pointed out that waves described by nonlinear models can be periodic [135], it took more than one hundred years for such solutions to be derived. Almost forty years passed from Russel's observations before Joseph Valentin Boussinesq (1871) [20] and John William Strutt (Lord Rayleigh) (1876) [136] found proper mathematical approach. The next important step was performed by Diederik Korteweg and Gustav de Vries (1985) [96]. For shallow water gravity waves, they derived a nonlinear wave equation, nowadays commonly known as the **Korteweg-de Vries equation** (**KdV** for short), and its analytic solution which describes properties of solitary waves.

New impulses in the development of theories of nonlinear waves did not appear until the 1960s. Significant progress in computational methods allowed

scientists a deeper understanding of nonlinear phenomena. The paper by N.J. Zabusky and M.D. Kruskal (1965) [150] initiated an "explosion" of research in this field. Zabusky and Kruskal, while doing a numerical study of the propagation of nonlinear waves in plasma, noticed that impulses (solitary waves) of different amplitudes and therefore different velocities conserve their properties after collisions with each other. Since this kind of behavior resembles particle properties, they introduced the term **soliton** for such waves. Two years later, in 1967, Zabusky [149] observed in a numerical experiment the emergence of a train of solitons of decreasing amplitudes from an initial cosine wave, evolving according to the KdV equation. This observation gave rise to intensive research in which multi-soliton solutions for several kinds of nonlinear wave equations were discovered and a general method for the construction of such solutions, called *Inverse Scattering Transform* method (IST for short), was established [48, 98, 110–113, 125]. Soon after that subsequent studies showed that the nonlinear KdV-type wave equations appear in many fields as first order approximations (in the sense of the perturbation approach with respect to some small parameter(s)) of some more fundamental equations governing the system. It turned out that soliton solutions appear much more often than had been expected earlier. Scientists and engineers understood that stable localized nonlinear waves could have significant applications in many fields, such as nonlinear optics [104, 121], hydrodynamics [1, 13, 16, 123, 144], plasma physics [71, 75], electric circuits [127, 145] and many others. In particular, such waves can be used in the transmission of signals.

At present soliton solutions appear in electrodynamics, magnetohydrodynamics and field theory, where, among others, nonlinear Schödinger equations have been introduced. Work in these fields has led to descriptions of "bions", that is, bounded states of solitons in Born-Infeld theory, and their oscillations called "breathers". A great area of applications appeared in fiber optics, where "dark solitons" and "vector solitons" have been discovered. Solitons appear in contemporary biology, in the collective motion of proteins and DNA molecules and the propagation of impulses in neuron networks. In some equations for water waves, which are of a different type than KdV, e.g., Camassa-Holm and Fornberg-Whitham equations, there appear "peacon" solitons, which have a discontinuous first derivative at the crest.

The KdV equation and soliton theory have been described in many monographs, see, e.g., [1–3, 5, 10, 33, 36, 40, 60, 66, 72, 117, 121, 123, 127, 144] and countless scientific papers. An extension of KdV for two dimensions is the

Kadomtsev-Petviashvili equation [73, 76] (KP equation for short). Models with equations of higher order (in the sense of higher order space derivatives) have been studied as well, [27], [105], [88], [107], [139], [23], [97], [24], [62], [61], [152] (citation in chronological order). In parallel with analytic studies broad research using numerical methods has been undertaken, e.g., [31, 32, 49, 74, 133, 138, 141, 147, 148] and many others. Besides soliton solutions the periodic (cnoidal) ones have been studied [18, 100, 110], as well as the stability of solutions [67–69, 71] and conservation laws [31, 102, 106]. For almost twenty years there have been appearing research papers studying stochastic nonlinear equations of KdV-type, e.g., [19, 32, 84–86, 119, 120].

Derivations of nonlinear wave equations, such as KdV, KP and their modifications, are based on the assumption that the bottom of the fluid is flat. However, one of the most important aims of the water wave theory is to understand changes in wave amplitudes and velocities when waves approach shallower regions (among other problems, understanding the creation of tsunamis). Many different theoretical models have been created for these purposes, see, e.g., [11, 15, 33, 41, 50–52, 55, 56, 58, 59, 77, 89, 106, 111, 115, 116, 118, 124, 126, 134, 140, 151]. None of them, however, have led to a wave equation which directly incorporates bottom fluctuations. Only recently has such a wave equation been derived by our co-workers and us in [78, 79]. The derivation, however, requires a second order perturbation approach and a special trick (see, sect. 4.2.2).

1.2 Outline of Book

The book is organized as follows. In Chapter 2 we discuss the hydrodynamic model of an incompressible, inviscid fluid and its irrotational motion governed by gravitational forces. The model allows us to derive the set of four partial differential equations describing the movement of the liquid. This set consists of the Laplace equation for velocity potential, kinematic boundary conditions at the bottom and the (unknown) surface, and the dynamic boundary condition at the surface.

In Chapter 3 dimensionless variables are introduced which allow us to apply perturbation expansion with respect to some parameters assumed to be small. These parameters are: $\alpha = \frac{a}{H}$ - the ratio of the wave amplitude to the fluid depth, and $\beta = (\frac{H}{L})^2$ - square of the ratio of the fluid depth to the wavelength. Limiting perturbative approach to first order with respect to small parameters results in the derivation of the Korteweg-de Vries equation

for the long surface waves of small amplitudes. Also, several types of analytic solutions are discussed, that is, single soliton solutions, periodic solutions and multi-soliton solutions to KdV.

The main body of the book is based on the original research performed by our co-workers and us. The results of these studies have been published in the following papers [70, 78–84, 128–130].

Chapter 4 is devoted to the derivation of the extended KdV equations. First, the second order perturbation approach is recalled for the case of a flat bottom. This derivation results in the *extended KdV* equation which we call *KdV2*. This equation is sometimes named the *fifth-order KdV* equation since it contains the fifth space derivative of the wave function as the highest one. Next, the case with an uneven bottom is considered. For this case another small parameter is defined, $\delta = \frac{a_h}{H}$ - the ratio of the amplitude of bottom changes to the average fluid depth. Then the derivation of the equation for surface waves in the presence of an uneven bottom, called by us the *KdV2B* equation, is shown. For this point we use derivations presented in [78, 79].

In Chapter 5 we present an algebraic approach to the KdV2 equation. Assuming the same functional forms for solutions to KdV2 as forms of solutions to KdV we derive the coefficients of single soliton solutions and periodic cnoidal solutions. It is stressed that physically relevant solutions have to fulfill the volume conservation condition, often neglected in papers studying mathematical properties of KdV-type equations. This chapter is based on our papers [70, 79].

Chapter 6 deals with analytic solutions to KdV and KdV2 in forms of superpositions "$\mathsf{dn}^2 \pm \sqrt{m}\,\mathsf{cn}\,\mathsf{dn}$". These periodic solutions were found for KdV not until 2013 [90]. They are slightly different from the usual cnoidal solutions known earlier. In this chapter, we first focus on mathematical aspects of these solutions in order to compare them to the KdV solutions obtained in [90]. Next, we discuss physical constraints on these solutions imposed by the volume conservation condition. In this chapter we follow the approach presented in [129] and [130].

In Chapter 7 we derive the approximate analytic solution to KdV2B (the case with the uneven bottom) and observe its qualitative agreement with the "exact" numerical evolution. This analytic solution approximates well the changes of the soliton's amplitude and velocity but is not able to reproduce subtle second order details of the evolution. Here we use the results of the paper [128].

Chapter 8 contains a comprehensive discussion of conservation laws for KdV and KdV2 equations. A variational approach to KdV type equations is reviewed. Invariants of KdV equations are recalled. It is shown that despite the presence of the infinite number of invariants, the energy of the wave, fulfilling the KdV in the fixed reference frame, is not exactly conserved. Quantitative deviations from exact energy conservation are illustrated by numerical calculations. Moreover, it is shown that for the KdV2 and KdV2B equations there exist only one exact invariant corresponding to volume (mass) conservation of the fluid. This chapter is based on [80].

The problems related to invariants of the extended KdV equations (KdV2) are discussed in detail in Chapter 9. Since the higher exact invariants do not exist, adiabatic ones, that is, expressed in the same order as the order of the equation, are helpful. Several forms of adiabatic invariants of KdV2 are constructed, and their small deviations from constant values are presented in numerical tests. Particular attention is drawn to the momentum and energy of the fluid. The content of this chapter extends substantialy results obtained in [82].

In Chapter 10 we first describe the FDM (finite difference method) algorithm which has been used by us for most of the calculations of the time evolution of surface waves according to KdV, KdV2 and KdV2B (extended KdV for the uneven bottom) equations presented in previous chapters. Next, we analyze the time evolution of several initially different waves encountering different bottom profiles in accordance with the KdV2B equation. Some of these examples were taken from [79].

Chapter 11 contains description and tests of another useful numerical method, FEM (finite element method). We have extended the FEM introduced for the KdV in [32] to KdV2 and KdV2B, both in deterministic and stochastic cases. Then we present several examples of the time evolution of some soliton and cnoidal waves according to this numerical scheme. It has been shown that the FEM approach could reproduce details of the evolution known from FDM calculations. It requires, however, larger computing times. Next, we show a study of the wave motion according to KdV2 and KdV2B equations when the surface is exposed to white noise simulating the influence of atmospheric pressure fluctuations, which we were first to perform. This study shows that both solitonic and periodic solutions to KdV and KdV2 are very robust for such weak random impulses. The content of this chapter is based on articles [83, 84].

2
_____

Hydrodynamic model

The general problem of fluid motion in arbitrary boundary conditions leads
to a set of _Navier-Stokes equations_. In most cases attempts to solve these
equations lead to extremely difficult problems. Therefore in many cases some
simplified models are introduced. For shallow water problem physicists use
the ideal fluid model. This means that fluid is assumed to be incompressible
and inviscid with additional assumption that the fluid motion is irrotational.
Since in normal conditions water viscosity and compressibility are very small
the model should reproduce the fluid motion with reasonable accuracy, until
waves on the surface do not break.

In this chapter a standard derivation of the _Euler equations_ for this model
is presented. In this derivation we follow arguments and reasoning presented
in several textbooks, see, e.g., [1, 99, 127, 144]. An important role is played
by conservation laws. The continuity equation results from mass or (due to
fluid's incompressibility) volume conservation. The assumption of irrotational
motion supplies the Laplace equation for velocity potential. The kinematic and
dynamic boundary conditions supplement the final set of the Euler equations.

2.1 Mass invariance

Let us cosider an arbitrary volume V of the fluid bounded by a closed sur-
face S, see figure 2.1 . When the fluid density is denoted by ϱ, the mass M of
fluid contained in V is given by

$$M = \int_V \varrho \, dV. \tag{2.1}$$
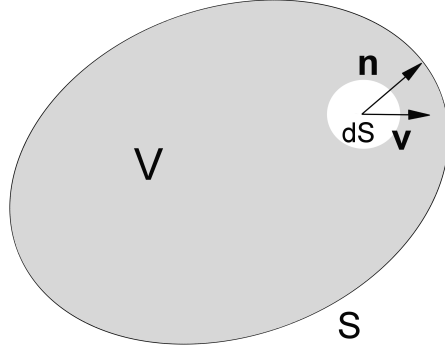
Fig. 2.1. Volume element of fluid V contained in a closed surface S. $\mathbf{v}(x, y, z, t)$ is a velocity of a fluid particle and $\mathbf{n}$ is the normal to the surface.

The change of mass in the volume V per unit of time results from flow of the fluid with flux density $\varrho\mathbf{v}$ through surface S. Then

$$\frac{\partial M}{\partial t} = -\int_S \varrho\mathbf{v} \cdot d\mathbf{S} = -\int_S \varrho(\mathbf{v} \cdot \mathbf{n})dS, \tag{2.2}$$

where $\mathbf{v} = \mathbf{v}(x, y, z, t)$ is the velocity of a particle of fluid and $\mathbf{n}$ denotes the normal to the surface element dS. On the other hand from (2.1)

$$\frac{\partial M}{\partial t} = \int_V \frac{\partial \varrho}{\partial t} \, dV. \tag{2.3}$$

Then

$$\int_V \frac{\partial \varrho}{\partial t} \, dV = -\int_S \varrho(\mathbf{v} \cdot \mathbf{n})dS. \tag{2.4}$$

Transforming surface integral to volume integral by Green's theorem yields

$$\int_V \left(\frac{\partial \varrho}{\partial t} + \nabla \cdot (\varrho\mathbf{v})\right) dV = 0. \tag{2.5}$$

The equation (2.5) holds for arbitrary volume V. It implies a fundamental *continuity equation*

$$\frac{\partial \varrho}{\partial t} + \nabla \cdot (\varrho\mathbf{v}) = 0. \tag{2.6}$$

2.2 Momentum conservation

Assume for a while that the only force acting on the fluid is due to pressure $p = p(x, y, z, t)$. Then the total force acting on element V is equal to the integral of the pressure over the surface S. Once more we transform the surface integral into the volume one, yielding

$$\mathbf{F} = -\int_S p\mathbf{n}\,dS = -\int_V (\nabla p)\,dV. \qquad (2.7)$$

Equation (2.7) shows that any element of fluid exerts a force $d\mathbf{F} = -(\nabla p)dV$.

Now we can write down the equation of motion of a volume element in the fluid by equating the force $-\nabla p$ to the product of the mass per unit volume (ϱ) and the acceleration $\frac{d\mathbf{v}}{dt}$. Then Newton's *second law of Mechanics* for the motion of fluid element is

$$\varrho\frac{d\mathbf{v}}{dt} = -\nabla p. \qquad (2.8)$$

The velocity of a fluid particle is a function of space coordinates and time. The derivative $\frac{d\mathbf{v}}{dt}$ which appears in (2.8) does not denote the rate of change of the fluid velocity at a fixed point in space, but the rate of change of the velocity of a given fluid particle as it moves about in space. This derivative has to be expressed in terms of quantities referring to points fixed in space. Then the change of velocity $d\mathbf{v}$ can be written as

$$d\mathbf{v} = \frac{\partial\mathbf{v}}{\partial t}dt + \frac{\partial\mathbf{v}}{\partial x}dx + \frac{\partial\mathbf{v}}{\partial y}dy + \frac{\partial\mathbf{v}}{\partial z}dz = \frac{\partial\mathbf{v}}{\partial t}dt + (d\mathbf{r}\cdot\nabla)\mathbf{v}. \qquad (2.9)$$

In (2.9), the derivative $\frac{\partial\mathbf{v}}{\partial t}$ is taken at a constant point in space, i.e. for x, y, z constant. Dividing by dt results in

$$\frac{d\mathbf{v}}{dt} = \frac{\partial\mathbf{v}}{\partial t} + (\mathbf{v}\cdot\nabla)\mathbf{v}. \qquad (2.10)$$

Substitution (2.10) into (2.8) gives

$$\frac{\partial\mathbf{v}}{\partial t} + (\mathbf{v}\cdot\nabla)\mathbf{v} = -\frac{1}{\varrho}\nabla p. \qquad (2.11)$$

Equation (2.11) is known in fluid mechanics as the *Euler equation of motion*, first derived by L. Euler in 1755. It can be generalized by taking into account an external force $\varrho\mathbf{f}$ other than that due to the pressure p. That force has to be added to the right-hand side of the (2.8). The generalized Euler equation takes the following form

$$\frac{\partial \mathbf{v}}{\partial t} + (\mathbf{v} \cdot \nabla)\mathbf{v} = -\frac{1}{\varrho}\nabla p + \mathbf{f}. \qquad (2.12)$$

From standard vector analysis we have

$$\frac{1}{2}\nabla \mathbf{v}^2 = \mathbf{v} \times (\nabla \times \mathbf{v}) + (\mathbf{v} \cdot \nabla)\mathbf{v}.$$

Using the above identity one can write (2.12) as

$$\frac{\partial \mathbf{v}}{\partial t} + \frac{1}{2}\nabla \mathbf{v}^2 + \omega \times \mathbf{v} = -\frac{1}{\varrho}\nabla p + \mathbf{f}, \qquad (2.13)$$

where $\omega = \nabla \times \mathbf{v}$ is defied as *vorticity*.

2.3 Irrotational flow of incompressible fluid

In many cases fluid can be consider as incompressible. In particular, compressibility of water under gravity can be safely neglected for shallow water problems. In such cases $\varrho = const$ and continuity equation (2.6) simplifies to

$$\nabla \cdot \mathbf{v} \equiv u_x + v_y + w_z = 0, \qquad (2.14)$$

where $u = \frac{dx}{dt}, v = \frac{dy}{dt}, w = \frac{dz}{dt}$. In the following we will use low indexes for denoting partial derivatives, for instance $u_x \equiv \frac{\partial u}{\partial x}, \phi_{2xt} \equiv \frac{\partial^3 \phi}{\partial x^2 \partial t}$ and so on.

In many problems (particularly when velocities of fluid particles are relatively small) flow of fluid is irrotational, $\omega = 0$. In such cases the Euler equation (2.13) takes a simpler form

$$\frac{\partial \mathbf{v}}{\partial t} + \frac{1}{2}\nabla \mathbf{v}^2 = -\frac{1}{\varrho}\nabla p + \mathbf{f}. \qquad (2.15)$$

When any vector field has its curl equals zero then it can be expressed as a gradient of a scalar function called its potential. For irrotational flow velocity can be written as a gradient of the *velocity potential* $\phi(x, y, z, t)$

$$\mathbf{v} = \nabla \phi = \mathbf{e}_x \phi_x + \mathbf{e}_y \phi_y + \mathbf{e}_z \phi_z, \qquad (2.16)$$

where $\mathbf{e}_x, \mathbf{e}_y, \mathbf{e}_z$ are unit vectors in x, y, z directions, respectively. Insertion of (2.16) into the continuity equation (2.6) yields the *Laplace equation* for the velocity potential

$$\Delta \phi = \phi_{2x} + \phi_{2y} + \phi_{2z} = 0, \qquad (2.17)$$

which holds for the whole volume of the fluid.

Inserting (2.16) into (2.15) one obtains

$$\nabla \left(\phi_t + \frac{1}{2}(\nabla\phi)^2 + \frac{p}{\varrho} \right) = \mathbf{f}. \tag{2.18}$$

If there are no other volume forces different than gravity ($\mathbf{f} = \mathbf{g}$), then (2.18) becomes

$$\nabla \left(\phi_t + \frac{1}{2}(\nabla\phi)^2 + \frac{p}{\varrho} + gz \right) = 0. \tag{2.19}$$

Integration of (2.19) over space variables gives

$$\phi_t + \frac{1}{2}(\nabla\phi)^2 + \frac{p - p_0}{\varrho} + gz = C(t). \tag{2.20}$$

Since the velocity is the space derivative of the potential ϕ, it is invariant with respect to a gauge transformation of the velocity potential consisting of an addition to ϕ an arbitrary function of time. The replacement of ϕ by $\phi + \int (C(t) + \frac{p_0}{\varrho})dt$ allows us to remove term $-p_0/\varrho$ from (2.20) yielding

$$\phi_t + \frac{1}{2}(\nabla\phi)^2 + \frac{p}{\varrho} + gz = 0. \tag{2.21}$$

Equation (2.21) carries the name the *Bernoulli equation.*

2.4 Boundary conditions

The Laplace equation (2.17) and the Bernoulli equation (2.21) have to be supplemented by boundary conditions both at a free surface and at the bottom of the fluid container. The surface is defined by the equation

$$z = \eta(x, y, t).$$

Taking time derivative and expressing velocity through velocity potential one obtains

$$\phi_z = \eta_x \phi_x + \eta_y \phi_y + \eta_t \qquad \text{for} \qquad z = \eta(x, y, t). \tag{2.22}$$

This is so called *kinematic boundary condition* at the surface.

In a slimilar way the *kinematic boundary condition* at the bottom can be defined for $z = h(x, y)$. Taking time derivative one gets

$$\phi_z = h_x \phi_x + h_y \phi_y \qquad \text{for} \qquad z = h(x, y). \tag{2.23}$$

In particular case, when the bottom is even $h(x) = $ const., the boundary condition (2.23) reduces to

$$\phi_z = 0 \qquad \text{for} \qquad z = h. \tag{2.24}$$

For shallow water problem the pressure at the surface is the constant atmospheric pressure p_a, then Bernoulli's equation at the surface $z = \eta(x, y, t)$ is

$$\phi_t + \frac{1}{2}(\nabla\phi)^2 + \frac{p_a}{\varrho} + gz = 0. \tag{2.25}$$

The constant atmospheric pressure can be eliminated by another gauge transformation of the velocity potential $\phi \to \phi - (p_a/\varrho)t$. Using (2.16) one obtains the *dynamic boundary condition* at the surface

$$\phi_t + \frac{1}{2}\left(\phi_x^2 + \phi_y^2 + \phi_z^2\right) + g\eta = 0 \qquad \text{for} \qquad z = \eta(x, y, t). \tag{2.26}$$

Finally the motion of the fluid under gravity for shallow water problem is described by the set of four partial differential equations for two unknown functions $\eta(x, y, t)$ and $\phi(x, y, z, t)$

$$\phi_{2x} + \phi_{2y} + \phi_{2z} = 0 \quad \text{for} \quad h(x, y) < z < \eta(x, y, t), \tag{2.27}$$

$$\phi_z - (\eta_x\phi_x + \eta_y\phi_y + \eta_t) = 0 \quad \text{for} \quad z = \eta(x, y, t), \tag{2.28}$$

$$\phi_t + \frac{1}{2}(\phi_x^2 + \phi_y^2 + \phi_z^2) + g\eta = 0 \quad \text{for} \quad z = \eta(x, y, t), \tag{2.29}$$

$$\phi_z - (h_x\phi_x + h_y\phi_y) = 0 \quad \text{for} \quad z = h(x, y). \tag{2.30}$$

3

Approximations: KdV - first order wave equation

In this chapter, we present the derivation of the famous Korteweg - de Vries (KdV for short) equation and its solutions. KdV is obtained within perturbation approach as first order approximation with respect to some small parameters related to the physical system. Despite the low order of approximation KdV proved to be a powerful tool for describing nonlinear weakly dispersive waves on the surface of the shallow water and in many other physical systems.

3.1 Korteweg - de Vries equation

In many cases, like in the first observation of the solitary wave by John Scott Russel in 1834, the wave exhibits translational invariance with respect to direction perpendicular to wave propagation. In other words the wave function does not depend on one of space coordinates (e.g., y). Then the unknown functions are $\eta = \eta(x,t)$ and $\phi = \phi(x,z,t)$. The system of Euler equations (2.27)-(2.30) reduces to (2+1) dimensions

$$\phi_{2x} + \phi_{2z} = 0 \quad \text{for} \quad h(x) < z < \eta(x,t), \tag{3.1}$$

$$\phi_z - (\eta_x \phi_x + \eta_t) = 0 \quad \text{for} \quad z = \eta(x,t), \tag{3.2}$$

$$\phi_t + \frac{1}{2}(\phi_x^2 + \phi_z^2) + g\eta = 0 \quad \text{for} \quad z = \eta(x,t), \tag{3.3}$$

$$\phi_z - h_x \phi_x = 0 \quad \text{for} \quad z = h(x). \tag{3.4}$$

The simplest possible case occures when the bottom is flat, that is, for $h = \text{const}$. In this case one usually chooses $z = 0$ at the bottom and the set (3.1)-(3.2) reads as

$$\phi_{2x} + \phi_{2z} = 0 \quad \text{for} \quad 0 < z < h + \eta(x,t), \tag{3.5}$$

$$\phi_z - (\eta_x \phi_x + \eta_t) = 0 \quad \text{for} \quad z = \eta(x,t), \tag{3.6}$$

$$\phi_t + \frac{1}{2}(\phi_x^2 + \phi_z^2) + g\eta = 0 \quad \text{for} \quad z = \eta(x,t), \tag{3.7}$$

$$\phi_z = 0 \quad \text{for} \quad z = 0. \tag{3.8}$$

Even for this simplest case, analytic solutions of the above sets of nonlinear differential equations are not known. [Only numerical approach can give us some insight, but with many constraints.] Therefore some simplifications or approximations are needed.

Till now, all equations were written in primary, dimensional variables. In this form, it is difficult to estimate which terms are more important than the others and how to obtain a simplified approximate set of equations. Therefore the next step consists in the transformation to dimensionless variables, see, e.g., [24, 36, 41, 78, 79, 105]. Denote by a the amplitude of a surface wave, by L its mean wavelength and by H the depth of the container. Introduction of the dimensionless variables in the form

$$\tilde{\phi} = \frac{H}{La\sqrt{gH}}\phi, \quad \tilde{x} = x/L, \quad \tilde{\eta} = \eta/a, \quad \tilde{z} = z/H, \quad \tilde{t} = t/(L/\sqrt{gH}) \tag{3.9}$$

with notations $\alpha = \frac{a}{H}$ and $\beta = (\frac{H}{L})^2$ transforms the set of equations (3.5)-(3.6) into

$$\beta\tilde{\phi}_{2x} + \tilde{\phi}_{2z} = 0, \quad \text{for} \quad 0 < z < 1 + \alpha\tilde{\eta}(x,t), \tag{3.10}$$

$$\frac{1}{\beta}\tilde{\phi}_z - (\alpha\tilde{\eta}_x\tilde{\phi}_x + \tilde{\eta}_t) = 0, \quad \text{for} \quad z = 1 + \alpha\tilde{\eta}(x,t), \tag{3.11}$$

$$\tilde{\phi}_t + \frac{1}{2}(\alpha\tilde{\phi}_x^2 + \frac{\alpha}{\beta}\tilde{\phi}_z^2) + \tilde{\eta} = 0, \quad \text{for} \quad z = 1 + \alpha\tilde{\eta}(x,t), \tag{3.12}$$

$$\tilde{\phi}_z = 0, \quad \text{for} \quad z = 0. \tag{3.13}$$

Next, one assumes that parameters α, β are small and of the same order of magnitude, $\alpha, \beta \ll 1$, which allows us to apply a perturbation approach. Then we can expect that the results obtained with perturbation theory will be a good approximation for long waves with an amplitude much less than the depth of the water. In the following we will use the dimensionless variables omitting the sign $\tilde{\ }$.

In standard perturbation approach [36, 144] one looks for dimensionless velocity potential in the form

$$\phi(x,z,t) = \sum_{m=0}^{\infty} z^m \phi^{(m)}(x,t), \tag{3.14}$$

where $\phi^{(m)}(x,t)$ are yet unknown functions.

Insertion $\phi(x,y,t)$ given by (3.14) into the Laplace equation (3.10) allows us to express the set of functions $\{\phi^{(m)}\}$ by partial derivatives of the first two of them, that is, by derivatives of $\phi^{(0)}$ and $\phi^{(1)}$

$$
\begin{aligned}
\phi^{(2m)} &= \frac{(-\beta)^m}{(2m)!}\,\phi^{(0)}_{2mx} && \text{for even terms} \\
\phi^{(2m+1)} &= \frac{(-\beta)^m}{(2m)!}\,\phi^{(1)}_{2mx} && \text{for odd terms.}
\end{aligned}
\tag{3.15}
$$

For even bottom the condition (3.13) ensures

$$
\phi^{(1)}(x,t) = 0.
\tag{3.16}
$$

This condition together with (3.15) causes vanishing of all odd terms in the series (3.14) which takes the form

$$
\phi(x,z,t) = \phi^{(0)} - \frac{1}{2}\beta z^2 \phi^{(0)}_{2x} + \frac{1}{24}\beta^2 z^4 \phi^{(0)}_{4x} - \frac{1}{720}\beta^3 z^6 \phi^{(0)}_{6x} + \dots
\tag{3.17}
$$

Now, insertion of the velocity potential in the form (3.17) into kinematic (3.11) and dynamic (3.12) boundary conditions at the surface yields the set of the Boussinesq equations for two unknown functions $\eta(x,t)$ and $w(x,t) \equiv \phi^{(0)}_x$. Since $\alpha, \beta \ll 1$ perturbation solutions can be considered on different order of approximation.

When the Boussinesq equations are limited to first order in α, β they take the following form

$$
\eta_t + w_x + \alpha(\eta w)_x - \beta \frac{1}{6} w_{3x} = 0,
\tag{3.18}
$$

$$
\eta_x + w_t + \alpha w w_x - \beta \frac{1}{2} w_{2xt} = 0.
\tag{3.19}
$$

It is possible to eliminate the function w from this set and obtain a single wave equation for surface elevation function η. In order to do this one begins with zeroth (with respect to α, β) approximation of (3.18)-(3.19), that is, with linear equations

$$
\eta_t + w_x = 0, \quad \eta_x + w_t = 0.
\tag{3.20}
$$

Equations (3.20) imply

$$
w = \eta, \quad \eta_t = -\eta_x \quad \text{and} \quad w_t = -w_x.
\tag{3.21}
$$

Now, one assumes that in the first order equations (3.18)-(3.19)

$$
w = \eta + \alpha Q^{(\alpha)} + \beta Q^{(\beta)},
\tag{3.22}
$$

where $Q^{(\alpha)}$ and $Q^{(\beta)}$ are functions of η and its derivatives with respect to x.

Insertion of (3.22) into (3.18) and (3.19) and neglection of terms with powers of α, β greater than 1 yields

$$\alpha \left(Q_x^{(\alpha)} + 2\eta\eta_x \right) + \beta \left(Q_x^{(\beta)} - \frac{1}{6}\eta_{3x} \right) = 0, \tag{3.23}$$

$$\alpha \left(Q_t^{(\alpha)} + \eta\eta_x \right) + \beta \left(Q_t^{(\beta)} + \frac{1}{2}\eta_{3x} \right) = 0. \tag{3.24}$$

Since the corrections $Q^{(\alpha)}$ i $Q^{(\beta)}$ enter already in first order, that is with small factors, then the relations between their x and t partial derivatives can be chosen the same as corresponding relations in zeroth order (3.21), that is,

$$Q_t^{(\alpha)} = -Q_x^{(\alpha)}, \quad Q_t^{(\beta)} = -Q_x^{(\beta)}. \tag{3.25}$$

(The opposite assumption, e.g., $Q_t^{(\alpha)} = -Q_x^{(\alpha)} + \alpha F_1 + \beta F_2$ and $Q_t^{(\beta)} = -Q_x^{(\beta)} + \alpha G_1 + \beta G_2$ do not change the further results since after insertion into (3.23) i (3.24) terms of the order higher than the first in α and β have to be rejected.)

Substraction (3.24) and (3.23) with the use of (3.25) and setting to zero terms at the coefficients α and β separately (α and β may be arbitary within some intervals) results in

$$Q_x^{(\alpha)} = -\frac{1}{2}\eta\eta_x, \qquad Q_x^{(\beta)} = \frac{1}{3}\eta_{3x}. \tag{3.26}$$

Integration yields

$$Q^{(\alpha)} = -\frac{1}{4}\eta^2, \qquad Q^{(\beta)} = \frac{1}{3}\eta_{2x}. \tag{3.27}$$

So, equations (3.22) and (3.24) take the following forms

$$w = \eta - \frac{1}{4}\alpha\eta^2 + \frac{1}{3}\beta\eta_{2x}, \tag{3.28}$$

$$\eta_t + \eta_x + \frac{3}{2}\alpha\eta\eta_x + \frac{1}{6}\beta\eta_{3x} = 0. \tag{3.29}$$

The equation (3.29) is the famous *KdV equation* in **fixed reference frame**. Remember that it is expressed in dimensionless quantities.

We stress this point since we use this reference frame across the whole book.

3.1.1 Other forms of KdV equation

Consider transformation of variables to a moving reference frame

$$\hat{x} = (x - t) \quad \text{and} \quad \hat{t} = t. \tag{3.30}$$

Application of (3.30) to (3.29) gets rid of η_x and yields the KdV equation in **moving reference frame**

$$\eta_{\hat{t}} + \frac{3}{2}\alpha\eta\eta_{\hat{x}} + \frac{1}{6}\beta\eta_{3\hat{x}} = 0. \tag{3.31}$$

It is worth to note that this reference frame moves with respect to the fixed frame with velocity equal to one (in dimensionless variables). In dimension variables this velocity corresponds to $\sqrt{gH}$.

In the case $\alpha = \beta$ one can use another transformation of variables

$$\hat{x} = \sqrt{\frac{3}{2}}(x - t) \quad \text{and} \quad \hat{t} = \frac{1}{4}\sqrt{\frac{3}{2}}\alpha t \,, \tag{3.32}$$

which converts the equation (3.29) to so called *standard KdV* form

$$\eta_{\hat{t}} + 6\eta\eta_{\hat{x}} + \eta_{3\hat{x}} = 0. \tag{3.33}$$

With slightly different variables KdV can be written as

$$\eta_{\hat{t}} + \eta\eta_{\hat{x}} + \eta_{3\hat{x}} = 0. \tag{3.34}$$

The forms (3.33) or (3.34) of KdV are preferred in mathematical papers, see, e.g., [87, 101].

It is worth to note that the variable transformation of the type (3.32) but with different coefficients allows us to obtain coefficients of equation (3.34) arbitrary. Therefore, in some papers one can encounter equations (3.33) or (3.34) with some signs changed.

Transformation to non-dimensional variables makes studying of mathematical aspects of KdV equation simpler. Sometimes, however, it is worth to present the KdV in original dimensional variables. Then the KdV equations are

$$\eta_t + c\eta_x + \frac{3}{2}\frac{c}{H}\eta\eta_x + \frac{cH^2}{6}\eta_{xxx} = 0, \tag{3.35}$$

in a fixed frame of reference and

$$\eta_t + \frac{3}{2}\frac{c}{H}\eta\eta_x + \frac{cH^2}{6}\eta_{xxx} = 0, \tag{3.36}$$

in a moving frame. In both, $c = \sqrt{gH}$, and (3.36) is obtained from (3.35) by setting $x' = x - ct$ and dropping the prime sign. One has to remember that using equations (3.35) or (3.36) makes sense only when the appropriate ratios of the wave amplitude, length and water depth are small.

3.2 Analytic solutions - standard methods

KdV equation for the fixed reference frame, written in dimensionless variables is given by (3.29). There exist three types of analytic solutions of this equation: single solitonic, periodic and multi-solitonic ones. The standard approach to solve the equation (3.29) is described in several monographs, see, e.g., [33, 36, 144].

3.2.1 Single soliton solutions

Looking for solution of unidirectional wave with permanent shape one introduces new variable $\xi = x - ct$, where $c = 1 + \alpha c_1$. Then dividing KdV equation by α one obtains an ODE equation

$$-c_1 \eta_\xi + \frac{3}{2} \eta \eta_\xi + \frac{1}{6} \frac{\beta}{\alpha} \eta_{3\xi} = 0. \tag{3.37}$$

Integration gives (r is an integration constant)

$$-c_1 \eta + \frac{3}{4} \eta^2 + \frac{1}{6} \frac{\beta}{\alpha} \eta_{2\xi} = \frac{1}{4} r. \tag{3.38}$$

Then multiplication by η_ξ and next integration yields

$$\frac{1}{3} \frac{\beta}{\alpha} (\eta_\xi)^2 = -\eta^3 + 2c_1 \eta^2 + r\eta + s =: f(\eta), \tag{3.39}$$

where s is another integration constant.

    Now, consider the solitonic case, that is, solutions are such that $\eta(\xi) \to 0$ when $\xi \to \pm\infty$. Then from (3.38) and (3.39) $r = s = 0$. So, in this case $f(\eta) = \eta^2(2c_1 - \eta)$ and

$$\frac{1}{3} \frac{\beta}{\alpha} (\eta_\xi)^2 = \eta^2(2c_1 - \eta). \tag{3.40}$$

The right hand side is real when $\eta \leq 2c_1$. Denote $q = \sqrt{\frac{2c_1}{\eta}}$. Then (3.40) becomes

$$\frac{2}{3c_1} \frac{\beta}{\alpha} q_\xi^2 = q^2 - 1. \tag{3.41}$$

Integration of (3.41) gives

$$\pm \sqrt{\frac{3c_1 \alpha}{2\beta}} \xi = \int_{q(0)}^{q(\xi)} \frac{d\hat{q}}{\sqrt{\hat{q}^2 - 1}} = \operatorname{arc cosh}(q). \tag{3.42}$$

Then
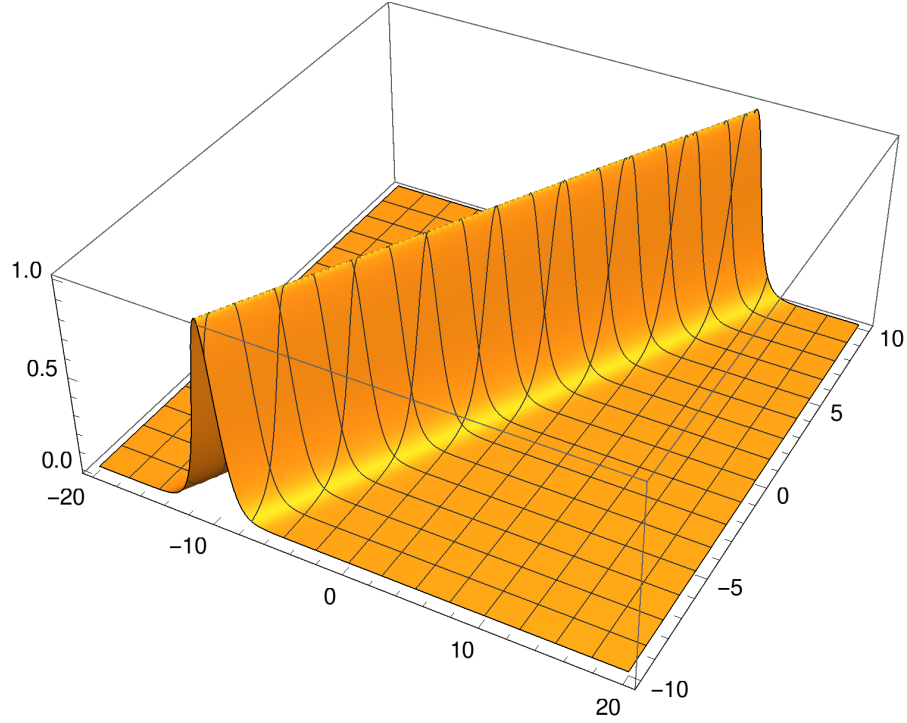
Fig. 3.1. Example of single soliton solution (3.45) for $\alpha = \beta = 0.1$.

$$q = \sqrt{\frac{2c_1}{\eta}} = \cosh\left(\sqrt{\frac{3c_1\,\alpha}{2\,\beta}}\xi\right) \tag{3.43}$$

and

$$\eta(\xi) = 2c_1\text{sech}^2\left(\sqrt{\frac{3c_1\,\alpha}{2\,\beta}}\xi\right). \tag{3.44}$$

Denote the amplitude $2c_1 = A$. Then finally the single soliton solution of KdV takes, in dimensionless variables x, t, the following form

$$\eta(x,t) = A\,\text{sech}^2\left[\sqrt{\frac{3\,\alpha}{4\,\beta}A}\left(x - t\left(1 + \frac{\alpha}{2}\right)\right)\right]. \tag{3.45}$$

Waves represented by such solutions move with the fixed shape and constant velocity $v = 1 + \frac{\alpha}{2}$ as illustrated in figure 3.1.

3.2.2 Periodic solutions

The path to obtaining exact periodic solutions is much more involved. The most detailed discussion of this problem is contained in [33]. Below, we remind

only a few essential steps and formulas. In general, integration constants can be nonzero. Then, assuming that $\eta_1 < \eta_2 < \eta_3$ are roots of polynomial $f(\eta)$, the polynomial can be written as

$$f(\eta) = -(\eta - y_1)(\eta - y_2)(\eta - y_3). \tag{3.46}$$

By comparison of equations (3.39) and (3.46) one sees that the roots y_k have to fulfil the following relations

$$y_1 + y_2 + y_3 = 2c_1,$$
$$y_1 y_2 + y_2 y_3 + y_3 y_1 = -r, \tag{3.47}$$
$$y_1 y_2 y_3 = s > 0.$$

The datail discussion (see, e.g., [33]) reveals that the bounded solutions exist only when two roots are negative and one is positive. Denote

$$y_1 = \eta_1 > 0, \qquad y_2 = -\eta_2, \qquad y_3 = -\eta_3 \qquad \text{with} \qquad \eta_3 > \eta_2 > 0.$$

The quantities η_2, η_2, η_3 now replace the three unknowns $2c_1, r$ and s.

For $d\eta/d\xi$ to be real and bounded it is necessary that $-\eta_2 \leq \eta \leq \eta_1$. This condition means that η_1 is the amplitude of the wave crest (with respect to undisturbed water level) and η_2 is the amplitude of the wave trough.

Then solution of (3.39) can be found in the form

$$\eta(\xi) = \eta_1 \cos^2 \chi(\xi) - \eta_2 \sin^2 \chi(\xi). \tag{3.48}$$

With (3.48) equation (3.39) takes form

$$\frac{4\beta}{3\alpha} {\chi_\xi}^2 = (\eta_1 + \eta_3) - (\eta_1 + \eta_2)\sin^2\chi. \tag{3.49}$$

Denoting $m = \frac{\eta_1 + \eta_2}{\eta_1 + \eta_3} \in [0,1]$ and $\Delta^2 = \frac{4\beta}{3\alpha(\eta_1 + \eta_3)}$ one obtains from (3.39)

$$\Delta^2 \chi_\xi^2 = 1 - m\sin^2\chi. \tag{3.50}$$

Integration yields

$$\frac{1}{\Delta} \int_0^\xi d\hat{\xi} = \mp \int_0^\chi \frac{d\hat{\chi}}{\sqrt{1 - m\sin^2\hat{\chi}}} \quad \Longrightarrow \quad \pm \frac{\xi}{\Delta} = F(\chi|m), \tag{3.51}$$

where $F(\chi|m)$ is the incomplete elliptic integral of the first kind. Since the inverse functions are

$$\cos\chi = \operatorname{cn}\left(\frac{\xi}{\Delta}\middle|m\right), \qquad \sin\chi = \operatorname{sn}\left(\frac{\xi}{\Delta}\middle|m\right) \tag{3.52}$$

then from (3.49) solution is obtained in the form

$$\eta(\xi) = -\eta_2 + (\eta_1 + \eta_2)\,\mathsf{cn}^2\left(\frac{\xi}{\Delta}\Big|m\right). \tag{3.53}$$

In next steps Dingemans [33] stresses three conditions which allows him to express η_1, η_2, η_3 through physical quantities. Two of these conditions come from definitions of dimensionless variables. Since distance x has been made dimensionless with the wavelength, then dimensionless wavelength should be equal to 1. Non-dimensionalization of vertical variable has been made with H so dimensionless amplitude should be equal to 1, as well (this argument was used already in derivation of soliton solution (3.45)). The third condition requires that the mean free surface elevation should coincide with still water surface.

Knowing that KdV possesses analytic solutions expressed by the Jacobi elliptic functions it is easier to obtain them by algebraic method described in chapter 5. Then such solutions can be written as

$$\eta(x,t) = A\,\mathsf{cn}^2[B(x - vt), m] + D, \tag{3.54}$$

where

$$B = \sqrt{\frac{3\alpha}{4\beta}\frac{A}{m}}, \quad v = 1 - \frac{\alpha}{2}\frac{A}{m}\left[3\frac{E(m)}{K(m)} + m - 2\right], \quad D = -\frac{A}{m}\left[\frac{E(m)}{K(m)} + m - 1\right]. \tag{3.55}$$

In (3.55), $E(m)$, $K(m)$ denote the complete elliptic integral and the complete elliptic integral of the first kind, respectively. The elliptic parameter $m \in [0, 1]$.

An example of periodic solution of KdV (3.29) is displayed in figure 3.2.

It is worth to note that in the limit $m \to 1$ the distance between the crests of solution (3.54) tends to infinity and $D \to 0$, giving finally single soliton solution (3.45). When $m \to 0$ the solution (3.54) tends to usual cosine wave.

Sometimes cnoidal solutions (3.54) are presented in the form of dn^2 function, that is, as

$$\eta(x,t) = A'\,\mathsf{dn}^2[B(x - vt), m] + D'. \tag{3.56}$$

This formula is equivalent to (3.54) when

$$A' = \frac{A}{m}, \quad \text{and} \quad D' = D + \frac{A(m-1)}{m} = -\frac{A}{m}\frac{E(m)}{K(m)}.$$
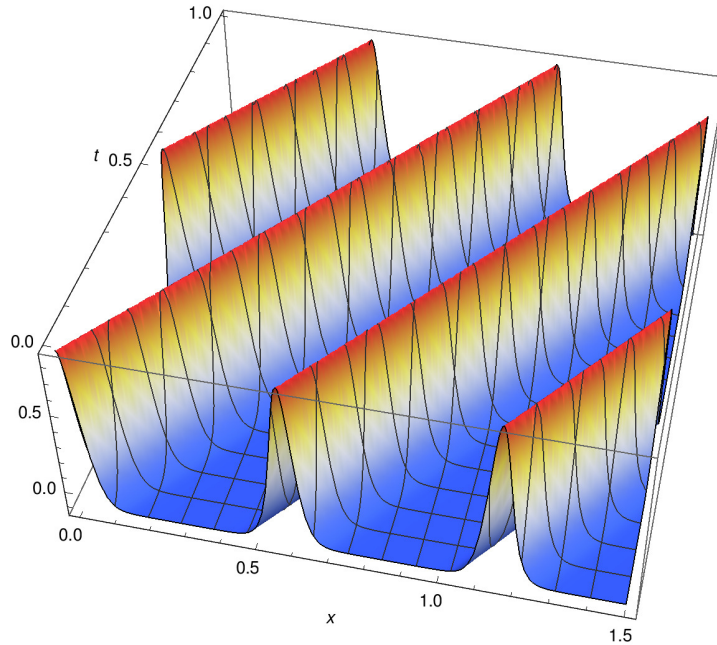
Fig. 3.2. Example of periodic solution (3.54). Here $m = 0.99999$ and $\alpha = 0.1$.

3.2.3 Multi-soliton solutions

One of the most exciting properties of the KdV equation is the existence of multi-soliton solutions. The first indication of that property was noticed by Zabusky and Kruskal [150] in their famous numerical experiment. They assumed initial wave in the form of the usual cosine function and numerically evolved it according to KdV equation using periodic boundary conditions. To authors' surprise the cosine wave was evolving into a train of solitons of decreasing amplitudes. The paper [150] inspired intensive studies which resulted in the development of a general method, by Gardner, Green, Kruskal and Miura [48], called *IST (Inverse Scattering Transform)*, see, e.g., [2,4,5,40, 123], as well. The IST allows us to construct the whole family of multi-soliton solutions.

There exist also simpler methods for construction of multi-soliton solutions to KdV. Some of them use Bäcklund transformations [46] or Lax's pairs [98]. There is also Hirota's direct method [64, 66]. Below, following [21], we show explicit forms of the exact 2- and 3-soliton solutions.
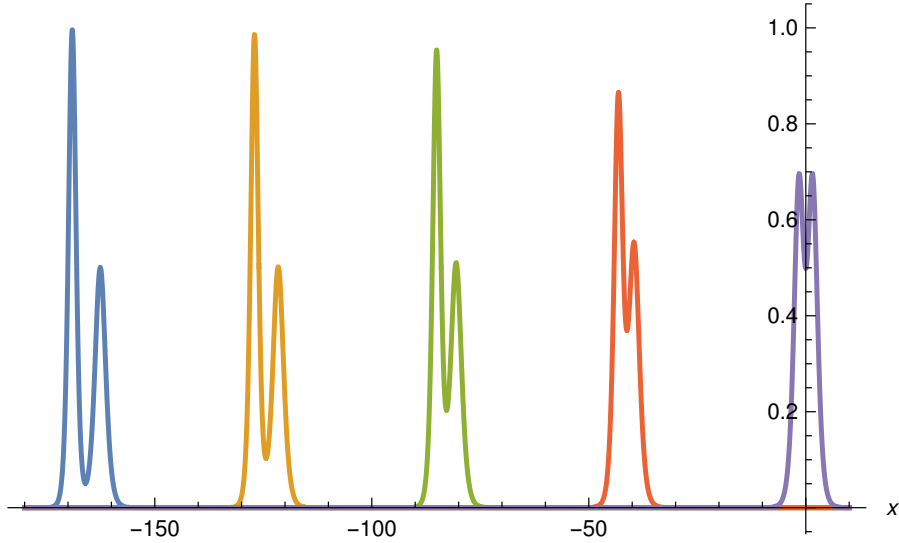
Fig. 3.3. Example of profiles of 2-soliton solution (3.58) for $\alpha = \beta = 0.1$ at time instants $t = -160, -120, -80, -40, 0$, respectively. The amplitudes of solitons are $A_1 = 0.5$ and $A_2 = 1$. For time instants $t = 40, 80, 120, 160$ the corresponding profiles are symmetric to the displayed ones with respect to $x = 0$.

Denote by $A_2 > A_1$ the amplitudes of higher and lower solitons, respectively. Set

$$\Theta_i(x,t) = \sqrt{\frac{3\,\alpha}{4\,\beta}A_i}\left[x - t\left(1 + \frac{\alpha}{2}A_i\right)\right]. \tag{3.57}$$

Then 2-soliton solution of (3.29) is given by

$$\eta(x,t) = \frac{(A_2 - A_1)\left(A_1 \operatorname{sech}^2\left[\Theta_1(x,t)\right] + A_2 \operatorname{csch}^2\left[\Theta_2(x,t)\right]\right)}{\left(\sqrt{A_1}\tanh\left[\Theta_1(x,t)\right] - \sqrt{A_2}\coth\left[\Theta_2(x,t)\right]\right)^2}, \tag{3.58}$$

but 3-soliton solution $(A_3 > A_2 > A_1)$ has more complicated form. Denote

$$X_1(x,t) = -\frac{2(A_1 - A_2)\left(A_1 \operatorname{sech}^2\left[\Theta_1(x,t)\right] + A_2 \operatorname{csch}^2\left[\Theta_2(x,t)\right]\right)}{\left(\sqrt{2A_1}\tanh\left[\Theta_1(x,t)\right] - \sqrt{2A_2}\coth\left[\Theta_2(x,t)\right]\right)^2}, \tag{3.59}$$

$$X_2(x,t) = \frac{(-A_1 + A_3)\left(-A_1 \operatorname{sech}^2\left[\Theta_1(x,t)\right] + A_3 \operatorname{sech}^2\left[\Theta_3(x,t)\right]\right)}{\left(-\sqrt{2A_1}\tanh\left[\Theta_1(x,t)\right] + \sqrt{2A_3}\tanh\left[\Theta_3(x,t)\right]\right)^2}, \tag{3.60}$$

$$X_3(x,t) = \frac{2(A_1 - A_2)}{-\sqrt{2A_1}\tanh\left[\Theta_1(x,t)\right] + \sqrt{2A_2}\coth\left[\Theta_2(x,t)\right]}, \tag{3.61}$$

$$X_4(x,t) = \frac{2(-A_1 + A_3)}{-\sqrt{2A_1}\tanh\left[\Theta_1(x,t)\right] + \sqrt{2A_3}\tanh\left[\Theta_3(x,t)\right]}. \tag{3.62}$$
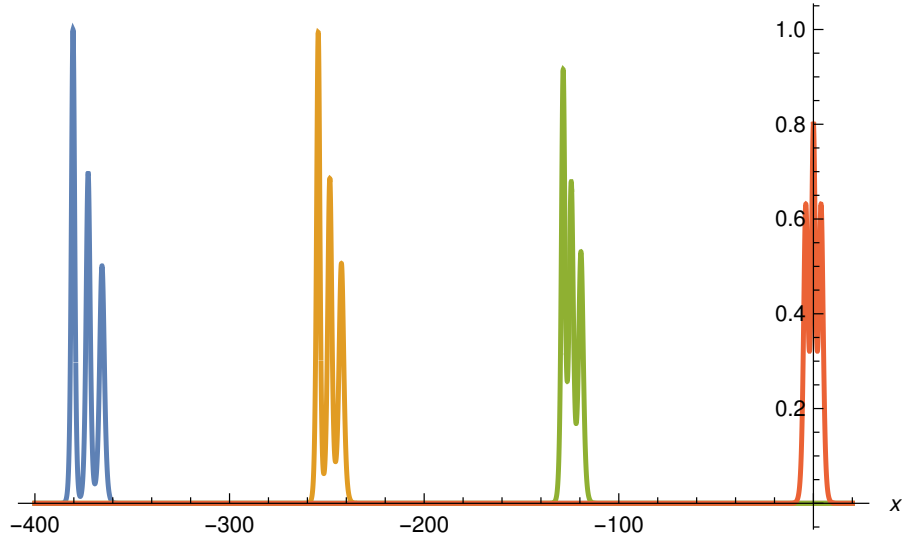
Fig. 3.4. Example of profiles of 3-soliton solution (3.63) for $\alpha = \beta = 0.1$ at time instants $t = -360, -240, -120$ and 0, respectively. The amplitudes of solitons are $A_1 = 0.5$, $A_2 = 0.7$ and $A_3 = 1$. For time instants $t = 120, 240, 360$ the corresponding profiles are symmetric to the displayed ones with respect to $x = 0$.

Then 3-soliton solution is expressed with (3.59)-(3.62) as

$$\eta(x,t) = A_1 \operatorname{sech}^2 \left[\Theta_1(x,t) \right] - 2(A_2 - A_3) \frac{X_1(x,t) + X_2(x,t)}{(X_3(x,t) - X_4(x,t))^2}. \qquad (3.63)$$

Remember that due to non-dimensionalization, the amplitude of the highest soliton is equal to 1.

Examples of 2-soliton (3.58) and 3-soliton (3.63) solutions are displayed in figures 3.3 and 3.4, respectively. Remember that (3.58) and (3.63) are solutions of KdV equation in fixed reference frame. In order to show more details of the soliton's collisions the motion of 2-soliton and 3-soliton solutions are also displayed in the moving reference frame in the figures 3.5 and 3.6.

Remark 3.1. Single soliton solutions (3.45) and periodic solutions(3.54) move with constant shapes and constant velocities. The velocity of KdV soliton depends on its amplitude. Therefore the different parts of multi-soliton solutions move with different velocities and the higher ones overcame the lower. During this 'collision' phase they change their shapes. However, when these parts are separated they move again without changes of their shapes with constant velocities.
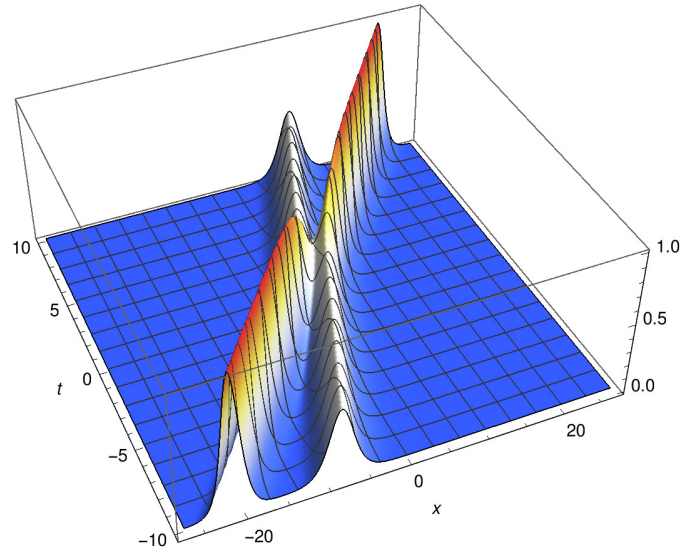
Fig. 3.5. 2-soliton motion corresponding to that shown in figure 3.3 displayed in a moving frame.
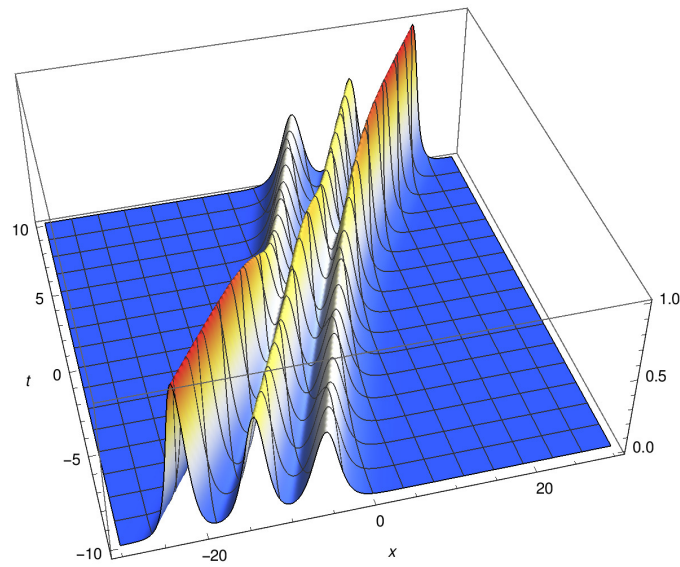
Fig. 3.6. 3-soliton motion corresponding to that shown in figure 3.4 presented in a moving frame.

4

Approximations: second order wave equations

4.1 Problem setting

In the standard approach to the shallow water wave problem, the fluid is assumed to be inviscid and incompressible and the fluid motion to be irrotational. Therefore a velocity potential ϕ is introduced. It satisfies the Laplace equation with appropriate boundary conditions. The Laplace equation must be valid for the whole volume of the fluid, whereas the equations for boundary conditions are valid at the surface of the fluid and at the impenetrable bottom. The system of equations for the velocity potential $\phi(x, y, z, t)$, including its derivation, can be found in many textbooks, for instance, see [127, Eqs. (5.2a-d)]. A standard procedure consists in introducing two small parameters $\alpha = a/H$ and $\beta = (H/L)^2$, where a is a typical amplitude of a surface wave η, H is the depth of the container and L is a typical wavelength of the surface waves. The parameters α, β are the same as the parameters ε, δ^2 in [127], respectively. In these notations, we follow the paper [24], where a systematic way for the derivation of wave equations of different orders is presented. In [78, 79] we introduced a third parameter $\delta = a_h/H$, where a_h is the amplitude of bottom variation. With this new parameter, we can consider the motion of surface waves over a non-flat bottom within the same perturbative approach as for derivation of KdV or higher-order KdV-like equations. In the following, we assume that all three parameters α, β, δ are small and of the same order.

In the following we limit our considerations to 2-dimensional flow, $\phi(x, z, t)$, $\eta(x, t)$, where x is the horizontal coordinate and z is the vertical one (this means translational symmetry with respect to y axis). The geometry of the problem is sketched in figure 4.1.
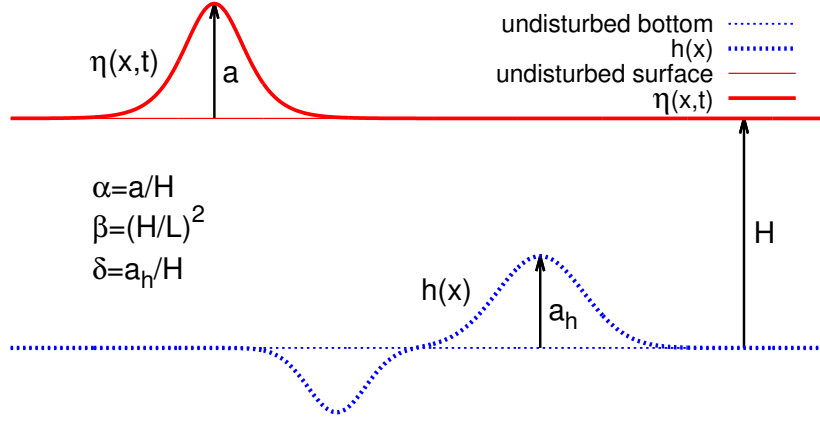
Fig. 4.1. Schematic view of the geometry of the shallow water wave problem for an uneven bottom.

Up to now, a generally small surface tension term has been neglected, but it can be taken into account. A third coordinate could also be included [72].

Like in the KdV case non-dimensional variables are introduced. Besides the standard non-dimensionalization of η, ϕ, x, z and t in (3.9) the bottom function has to be non-dimensionalized, as well. Then the non-dimensional variables are defined as follows

$$\tilde{\eta} = \eta/a, \quad \tilde{\phi} = \phi/(L\frac{a}{H}\sqrt{gH}), \quad \tilde{h} = h/H,$$
$$\tilde{x} = x/L, \quad \tilde{z} = z/H, \quad \tilde{t} = t/(L/\sqrt{gH}). \tag{4.1}$$

In this non-dimensional variables the set of hydrodynamic equations for 2-dimensional flow takes the following form (henceforth all tildes have been omitted)

$$\beta\phi_{xx} + \phi_{zz} = 0, \tag{4.2}$$

$$\eta_t + \alpha\phi_x\eta_x - \frac{1}{\beta}\phi_z = 0 \quad \text{for} \quad z = 1 + \alpha\eta, \tag{4.3}$$

$$\phi_t + \frac{1}{2}\alpha\phi_x^2 + \frac{1}{2}\frac{\alpha}{\beta}\phi_z^2 + \eta = 0 \quad \text{for} \quad z = 1 + \alpha\eta, \tag{4.4}$$

$$\phi_z - \beta\delta\left(h_x\,\phi_x\right) = 0 \quad \text{for} \quad z = \delta h(x). \tag{4.5}$$

The equations (4.2)-(4.4) are the same as (3.10)-(3.12). For the standard KdV case, the boundary condition at the bottom is $\phi_z = 0$. When the bottom varies,

this condition (in original variables) has to be replaced by $\phi_z = h_x \, \phi_x$, which in non-dimensional variables takes the form (4.5). However, in order to ensure that the perturbative approach makes sense, we assume that the derivatives of $h(x)$ are nowhere large.

Remark 4.1. We emphasize that the boundary condition for uneven bottom (4.5) is already second order expression with respect to small parameters. Therefore it is not possible to derive a wave equation containing terms from uneven bottom in first order perturbation approach.

4.2 Derivation of KdV2 - the extended KdV equations

The derivation of the nonlinear wave equation for the function $\eta(x, z, t)$ when the bottom is given by an arbitrary function $h(x)$ has been presented in [78]. This was done in two steps. In the first step, δ was set to zero and the *extended KdV equation (KdV2)* was obtained. The extended KdV equation, which is the second order equation for the flat bottom case was first derived by Marchant and Smyth [105] in 1990 from Luke's Lagrangian [103]. In the second step, we used relations obtained in the first step to find correction terms responsible for a variable bottom. Later, in the paper [79] we noticed that all second order terms, both related to flat and variable bottom can be derived in a single step. Below we describe this procedure in detail.

As in the standard first order approach, the velocity potential is approximated in the form of the series (3.14)

$$\phi(x, z, t) = \sum_{m=0}^{\infty} z^m \, \phi^{(m)}(x, t).$$

In our derivation (as in most) the velocity potential is limited to a polynomial with $m \leq 6$ and in the equations (4.2)-(4.5) only terms up to second order in small parameters α, β, δ are retained. the Laplace equation (4.2) allows us to express all $\phi^{(2m)}$ functions by the derivatives $\phi_{2mx}^{(0)}$ and $\phi^{(2m+1)}$ functions by the derivatives $\phi_{2mx}^{(1)}$. Insertion of the series (3.14) into the boundary condition at the bottom (4.5) yields

$$0 = \phi^{(1)} + \beta\delta \left(-h_x\phi_x^{(0)} - h\phi_{2x}^{(0)} \right) \tag{4.6}$$
$$+ \beta\delta^2 \left(-hh_x\phi_x^{(1)} - \frac{1}{2}h^2\phi_{2x}^{(1)} \right) + \beta^2\delta^3 \left(-\frac{1}{2}h^2 h_x\phi_{3x}^{(0)} + \frac{1}{6}h^3\phi_{4x}^{(0)} \right) + \dots$$

The full equation (4.6) gives very complicated relation between $\phi^{(1)}, \phi_x^{(0)}, h$ and their x-derivatives. However, limiting the boundary condition at the bottom (4.6) to the second order in small parameters, i.e. to

$$\phi^{(1)}(x,t) = \beta\delta\left(h_x\phi_x^{(0)} + h\phi_{2x}^{(0)}\right), \tag{4.7}$$

allows us to express all functions $\phi^{(m)}$ by $\phi^{(0)}, h$ and their derivatives. The resulting velocity potential is

$$\phi = \phi^{(0)} + z\beta\delta\left(h\phi_x^{(0)}\right)_x - \frac{1}{2}z^2\beta\,\phi_{2x}^{(0)} - \frac{1}{6}z^3\beta^2\delta\left(h\phi_x^{(0)}\right)_{3x}$$
$$+\frac{1}{24}z^4\beta^2\phi_{4x}^{(0)} + \frac{1}{120}z^5\beta^3\delta\left(h\phi_x^{(0)}\right)_{5x} + \frac{1}{720}z^6\beta^3\phi_{6x}^{(0)}. \tag{4.8}$$

In the next steps we insert $\phi(x,z,t)$ given by (4.8) into (4.3) and (4.4), then we neglect terms of order higher than second in small parameters α, β, δ. Equation (4.4) is then differentiated with respect to x and $w(x,t)$ is substituted in place of $\phi_x^{(0)}(x,t)$ in both equations. In this way a set of two coupled nonlinear differential equations is obtained which, in general, can be considered at different orders of the approximation.

Keeping only terms up to second order (to be consistent with the order of approximation used in the bottom boundary condition) one arrives at the second order Boussinesq's system

$$\eta_t + w_x + \alpha(\eta w)_x - \frac{1}{6}\beta w_{3x} - \frac{1}{2}\alpha\beta(\eta w_{2x})_x + \frac{1}{120}\beta^2 w_{5x} \tag{4.9}$$
$$-\delta(hw)_x + \frac{1}{2}\beta\delta(hw)_{3x} = 0,$$

$$w_t + \eta_x + \alpha w w_x - \frac{1}{2}\beta\,w_{2xt} + \frac{1}{24}\beta^2\,w_{4xt} + \beta\delta\,(hw_t)_{2x} \tag{4.10}$$
$$+\frac{1}{2}\alpha\beta\left[-2(\eta w_{xt})_x + w_x w_{2x} - w w_{3x}\right] = 0.$$

In (4.9), there are two terms depending on the variable bottom, the first order term $\delta(hw)_x$ and the second order term $\frac{1}{2}\beta\delta(hw)_{3x}$, whereas (4.10) contains only the second order term $\beta\delta(hw_t)_{2x}$. However, the bottom boundary condition (4.7), which is the source of these terms, is already second order in $\beta\delta$. Therefore we will treat all these terms on the same footing, as second order ones, i.e. replacing $\delta\,(hw)_x$ by $\beta\delta\,(hw)_x/b$, $b \neq 0$, during derivations and substituting $b = \beta$ in the final formulas. So, we consider equation (4.9) in a slightly reformulated form

$$\eta_t + w_x + \alpha\,(\eta w)_x - \frac{1}{6}\beta\,w_{3x} - \frac{1}{2}\alpha\beta\,(\eta w_{2x})_x + \frac{1}{120}\beta^2\,w_{5x}$$

$$+\frac{1}{2}\beta\delta\left(-\frac{2}{b}(hw)_x + (hw)_{3x}\right) = 0. \tag{4.11}$$

It is now time to eliminate one of the unknown functions, that is $w(x,t)$, in order to obtain a single equation for the wave profile $\eta(x,t)$. Note that keeping only first order terms one obtains Boussinesq's system for KdV (3.18)-(3.19). Burde and Sergyeyev [24] have shown how to proceed with approximations of higher order, assuming the case of the flat bottom. They showed how to eliminate sequentially the $w(x,t)$ function and obtain a single equation for $\eta(x,t)$ for the higher order perturbative approach. In principle, this method can be applied up to an arbitrary order and to cases when small parameters are not necessarily of the same order. It allows us to solve the problem in several ways. Corrections to the next order can be calculated either one by one for different small parameters in several steps or in a single step for all of them. Below we will present both of these cases.

The method consists in applying the known properties of solutions of lower order equations for w and η in derivations of corrections to equations in the next order. Therefore looking for wave equations of second order we make use of the Boussinesq's equations of first order, that is, eqs. (3.28)-(3.29).

4.2.1 KdV2 - second order equation for even bottom

In [78] we begun with flat bottom case, setting $\delta = 0$ in (4.9)-(4.10). Looking for consitent solutions of this system we took the second order trial function $w(x,t)$ in the following form

$$w(x,t) = \eta - \frac{1}{4}\alpha\,\eta^2 + \frac{1}{3}\beta\,\eta_{2x} + \alpha^2\,\mathrm{Q}^{(\alpha^2)}(x,t) + \beta^2\,\mathrm{Q}^{(\beta^2)}(x,t) + \alpha\beta\,\mathrm{Q}^{(\alpha\beta)}(x,t). \tag{4.12}$$

Note that in (4.12) terms up to first order are given by (3.28). Unknown $\mathrm{Q}^{(\alpha^2)}, \mathrm{Q}^{(\beta^2)}, \mathrm{Q}^{(\alpha\beta)}$ are second order corrections, functions of η and its x-derivatives. Then we insert (4.12) into (4.9)-(4.10) (with $\delta = 0$) and use η_t from first order solution

$$\eta_t = -\eta_x - \frac{3}{2}\alpha\,\eta\eta_x - \frac{1}{6}\beta\,\eta_{3x} \tag{4.13}$$

which causes reduction of terms up to first order. What leaves are equations for the correction functions

$$\alpha^2 \left(Q_x^{(\alpha^2)} - \frac{3}{4}\eta^2\eta_x \right) + \beta^2 \left(Q_x^{(\beta^2)} - \frac{17}{360}\eta_{5x} \right) \tag{4.14}$$

$$+ \alpha\beta \left(Q_x^{(\alpha\beta)} + \frac{1}{12}\eta_x\eta_{2x} - \frac{1}{12}\eta\eta_{3x} \right) = 0$$

and

$$\alpha^2 Q_t^{(\alpha^2)} + \beta^2 \left(Q_t^{(\beta^2)} + \frac{11}{72}\eta_{5x} \right) + \alpha\beta \left(Q_t^{(\alpha\beta)} + \frac{11}{6}\eta_x\eta_{2x} + \frac{11}{12}\eta\eta_{3x} \right) = 0. \tag{4.15}$$

Next, we substract these equations. Since parameters α, β are independent and arbitrary (within some intervals) then coefficients at α^2, β^2 and $\alpha\beta$ have to vanish simultaneously. This gives us three equations

$$-Q_t^{(\alpha^2)} + Q_x^{(\alpha^2)} - \frac{3}{4}\eta^2\eta_x = 0, \tag{4.16}$$

$$-Q_t^{(\beta^2)} + Q_x^{(\beta^2)} - \frac{1}{5}\eta_{5x} = 0, \tag{4.17}$$

$$-Q_t^{(\alpha\beta)} + Q_x^{(\alpha\beta)} - \frac{7}{4}\eta_x\eta_{2x} - \eta\eta_{3x} = 0. \tag{4.18}$$

For x- and t-derivatives of the second order correction functions we use the same arguments as for the first order ones (3.25) namely

$$Q_t^{(\alpha^2)} = -Q_x^{(\alpha^2)}, \qquad Q_t^{(\beta^2)} = -Q_x^{(\beta^2)}, \qquad Q_t^{(\alpha\beta)} = -Q_x^{(\alpha\beta)}. \tag{4.19}$$

This gives (4.16)-(4.18) in integrable form

$$Q_x^{(\alpha^2)} = \frac{3}{8}\eta^2\eta_x, \tag{4.20}$$

$$Q_x^{(\beta^2)} = \frac{1}{10}\eta_{5x}, \tag{4.21}$$

$$Q_x^{(\alpha\beta)} = \frac{7}{8}\eta_x\eta_{2x} + \frac{1}{2}\eta\eta_{3x}. \tag{4.22}$$

Integration yields

$$Q^{(\alpha^2)} = \frac{1}{8}\eta^3, \tag{4.23}$$

$$Q^{(\beta^2)} = \frac{1}{10}\eta_{4x}, \tag{4.24}$$

$$Q^{(\alpha\beta)} = \frac{3}{16}\eta_x^2 + \frac{1}{2}\eta\eta_{2x}. \tag{4.25}$$

So, finally we obtain $w(x,t)$ (4.12) as

$$w(x,t) = \eta - \frac{1}{4}\alpha\,\eta^2 + \frac{1}{3}\beta\,\eta_{2x} + \frac{1}{8}\alpha^2\eta^3 + \frac{1}{10}\beta^2\eta_{4x} + \alpha\beta \left(\frac{3}{16}\eta_x^2 + \frac{1}{2}\eta\eta_{2x} \right). \tag{4.26}$$

Substitution of this form into (4.10) and limitation up to second order terms gives the *extended KdV equation* [105] which we call **KdV2**

$$\eta_t + \eta_x + \frac{3}{2}\alpha\eta\eta_x + \frac{1}{6}\beta\eta_{3x} \tag{4.27}$$
$$+ \alpha^2\left(-\frac{3}{8}\eta^2\eta_x\right) + \alpha\beta\left(\frac{23}{24}\eta_x\eta_{2x} + \frac{5}{12}\eta\eta_{3x}\right) + \frac{19}{360}\beta^2\eta_{5x} = 0.$$

4.2.2 Uneven bottom - KdV2B

Now we can make the next step to derive corrections to KdV2 due to uneven bottom. Then we postulate the trial funtion $w(x,t)$ for the Boussinesq's set (4.10)-(4.11) adding a new correction term proportional to $\beta\delta$ to the solution (4.26), that is, in the form

$$w(x,t) = \eta - \frac{1}{4}\alpha\,\eta^2 + \frac{1}{3}\beta\,\eta_{2x} + \frac{1}{8}\alpha^2\eta^3 + \frac{1}{10}\beta^2\eta_{4x} + \alpha\beta\left(\frac{3}{16}\eta_x^2 + \frac{1}{2}\eta\eta_{2x}\right)$$
$$+ \beta\delta\,\mathrm{Q}^{(\beta\delta)}(x,t). \tag{4.28}$$

Insertion of this trial function into (4.10)-(4.11) supplies differential equations for the correction term. Again, substracting these equations, using the same relation between x- and t-derivatives, that is, $\mathrm{Q}_t^{(\beta\delta)} = -\mathrm{Q}_x^{(\beta\delta)}$ and integrating one obtains the correction term as

$$\mathrm{Q}^{(\beta\delta)}(x,t) = \frac{(h - bh_{2x})\eta}{4b} - h_x\eta_x - \frac{3}{4}h\eta_{2x}. \tag{4.29}$$

So, up to second order we have (restoring $b = \beta$)

$$w(x,t) = \eta - \frac{1}{4}\alpha\,\eta^2 + \frac{1}{3}\beta\,\eta_{2x} + \frac{1}{8}\alpha^2\eta^3 + \frac{1}{10}\beta^2\eta_{4x} + \alpha\beta\left(\frac{3}{16}\eta_x^2 + \frac{1}{2}\eta\eta_{2x}\right)$$
$$+ \beta\delta\left(\frac{(h - \beta\,h_{2x})\eta}{4\beta} - h_x\eta_x - \frac{3}{4}h\eta_{2x}\right) \tag{4.30}$$

and

$$\eta_t + \eta_x + \frac{3}{2}\alpha\eta\eta_x + \frac{1}{6}\beta\eta_{3x} - \frac{3}{8}\alpha^2\eta^2\eta_x + \alpha\beta\left(\frac{23}{24}\eta_x\eta_{2x} + \frac{5}{12}\eta\eta_{3x}\right) + \frac{19}{360}\beta^2\eta_{5x}$$
$$+ \beta\delta\left(-\frac{(h\eta)_x}{2\beta} - \frac{1}{4}(h\eta_{2x})_x + \frac{1}{4}(h_{2x}\eta)_x\right) = 0. \tag{4.31}$$

The equation (4.31) is the first KdV-type equation containing terms directly originating from the bottom topography in the lowest (second) order. We call

it **KdV2B** (B - from bottom). Note that by setting $\delta = 0$, that is, in the case of an even bottom this equation reduces to KdV2 (4.27). Neglection of all second order terms simplifies KdV2 and KdV2B to KdV equation.

It is not yet clear whether analytical solutions of (4.31) for some cases of the bottom function $h(x)$ can be found. On the other hand, numerical solutions for some particular initial conditions can be obtained relatively simply and they may inspire analytical studies, as happened in the past for the KdV case [48, 150].

In [79] we noticed that all second order corrections to KdV, including terms from bottom variation ($\delta \neq 0$) can be calculated in a single step. In order to obtain second order vave equation related to Boussinesq's system (4.9)-(4.9) we take the second order trial function $w(x,t)$ in the following form

$$w(x,t) = \eta - \frac{1}{4}\alpha\,\eta^2 + \frac{1}{3}\beta\,\eta_{2x} + \alpha^2\,Q^{(\alpha^2)}(x,t) + \beta^2\,Q^{(\beta^2)}(x,t)$$
$$+ \alpha\beta\,Q^{(\alpha\beta)}(x,t) + \beta\delta Q^{(\beta\delta)}(x,t), \qquad (4.32)$$

where $Q^{(\alpha^2)}, Q^{(\beta^2)}, Q^{(\alpha\beta)}, Q^{(\beta\delta)}$ are unknown functions of η, h and their derivatives. Insertion of the trial function (4.32) into (4.10) and (4.11), use of the properties of the first order equation (4.13) and rejection of higher order terms, yields a set of two equations containing derivatives of unknown functions. Both of them contain only second order terms, as lower order terms cancel . Then we substract these equations. Because we can treat small parameters as independent of each other, the coefficients in front of $\alpha^2, \beta^2, \alpha\beta, \beta\delta$ vanish separately. This procedure gives

$$-Q_t^{(\alpha^2)} + Q_x^{(\alpha^2)} - \frac{3}{4}\eta^2\eta_x = 0, \qquad (4.33)$$

$$-Q_t^{(\beta^2)} + Q_x^{(\beta^2)} - \frac{1}{5}\eta_{5x} = 0, \qquad (4.34)$$

$$-Q_t^{(\alpha\beta)} + Q_t^{(\alpha\beta)} - \frac{7}{4}\eta_x\eta_{2x} - \eta\eta_{3x} = 0, \qquad (4.35)$$

$$-Q_t^{(\beta\delta)}(x,t) + Q_x^{(\beta\delta)}(x,t) - \frac{(h\eta)_x}{b} + \frac{1}{2}h_{3x}\eta \qquad (4.36)$$

$$+\frac{5}{2}h_{2x}\eta_x + \frac{7}{2}h_x\eta_{2x} + \frac{3}{2}h\eta_{3x} = 0. \qquad (4.37)$$

Because the correction functions appear already in the second order, it is enough to use the zero order relation between their time and space derivatives. Therefore we use $Q_t = -Q_x$ (like $\eta_t = -\eta_x, w_t = -w_x$) in all equations (4.33)- (4.36), which allows us to integrate these equations and obtain analytic forms of all correction functions. This derivation of the correction term $Q^{(\beta\delta)}$

presented here differs from that in [78], where corrections $Q^{(\alpha^2)}, Q^{(\beta^2)}, Q^{(\alpha\beta)}$ where calculated first and $Q^{(\beta\delta)}$ was obtained in the next step. The final result is the same since differences only appear in third order.

So, finally we obtain (restoring $b = \beta$) the same equations (4.30) and (4.31).

Remark 4.2. For uneven bottom case, the full boundary condition at the bottom is given by (4.6). This equation admits expression of $\phi^{(1)}$ in terms of $\phi^{(0)}$ and its derivatives when perturbations are taken to the second order only. It is not possible for the third and higher orders. Therefore it is not possible to apply third order perturbation approach for the case of uneven bottom consistently.

4.3 Original derivation of KdV2 by Marchant and Smyth

Marchant and Smyth [105], in their derivation of the extended KdV equation, made use of variational principle for potential flow of incompressible and inviscid flows under gravity force. The appropriate variational principle was formulated by Luke in 1967 [103]. In dimensionless variables the Lagrangian density reads as

$$L = \int_0^{1+\alpha\eta} \left[\alpha \left(\frac{1}{2}\frac{\alpha}{\beta}\phi_z^2 + \frac{1}{2}\alpha\phi_x^2 + \phi_t \right) + z \right] dz. \qquad (4.38)$$

Integration of the last term with respect to z, rejection of the constant term and division by α gives an equivalent form suitable for next steps

$$L = \eta + \frac{1}{2}\alpha\eta^2 + \int_0^{1+\alpha\eta} \left(\frac{1}{2}\frac{\alpha}{\beta}\phi_z^2 + \frac{1}{2}\alpha\phi_x^2 + \phi_t \right) dz. \qquad (4.39)$$

Inserting the velocity potential (3.17) into (4.39) and retaining terms up to third order $O(\alpha^3, \alpha^2\beta, \alpha\beta^2)$ one gets

$$\begin{aligned}
L =\ & \phi_t^{(0)} + \alpha \left(\eta\phi_t^{(0)} + \frac{1}{2}\eta^2 + \frac{1}{2}\phi_x^{(0)2} \right) - \frac{1}{6}\beta\phi_{2xt}^{(0)} \\
& + \frac{1}{2}\alpha^2\eta\phi_x^{(0)2} + \frac{1}{120}\beta^2\phi_{4xt}^{(0)} + \alpha\beta\left(-\frac{1}{2}\eta\phi_{2xt}^{(0)} + \frac{1}{6}\phi_{2x}^{(0)2} - \frac{1}{6}\phi_x^{(0)}\phi_{3x}^{(0)} \right) \\
& + \alpha^2\beta\left(-\frac{1}{2}\eta^2\phi_{2xt}^{(0)} + \frac{1}{2}\eta\phi_{2x}^{(0)2} - \frac{1}{2}\eta\phi_x^{(0)}\phi_{3x}^{(0)} \right) \\
& + \alpha\beta^2\left(\frac{1}{24}\eta\phi_{4xt}^{(0)} + \frac{1}{40}\phi_{3x}^{(0)2} - \frac{1}{30}\phi_{2x}^{(0)}\phi_{4x}^{(0)} + \frac{1}{120}\phi_x^{(0)}\phi_{5x}^{(0)} \right).
\end{aligned} \qquad (4.40)$$

This is the equation (2.10) of [105]. The Lagrangian density (4.40) has the form $L\left(\eta, \phi_t^{(0)}, \phi_x^{(0)}, \phi_{2x}^{(0)}, \phi_{2xt}^{(0)}, \phi_{3x}^{(0)}, \phi_{4x}^{(0)}, \phi_{4xt}^{(0)}, \phi_{5x}^{(0)}\right)$. This is a functional depending on two unknown functions η and $\phi^{(0)}$ and derivatives of $\phi^{(0)}$ up to the fifth order. In general, when the Lagrangian is a functional of k unknown functions $f_1, f_2, \ldots, f_k$ of m variables $x_1, x_2, \ldots, x_m$ and their fractional derivatives up to n-th order

$$I[f_1, \ldots, f_k] =$$
$$\int L(x_1, \ldots, x_m; f_1, \ldots, f_k; f_{1,1}, \ldots, f_{k,m}; f_{1,11}, \ldots, f_{k,mm}; \ldots; f_{k,m\ldots m})d\boldsymbol{x},$$

where

$$f_{i,\nu} = \frac{\partial f_i}{\partial x_\nu}, \quad f_{i,\nu_1\nu_2} = \frac{\partial^2 f_i}{\partial x_{\nu_1}\partial x_{\nu_2}}, \ldots \qquad \nu_k = 1, 2, \ldots, m,$$

then the dynamics of the system is determined by the set of k Euler-Lagrange equations in the form [29]

$$\frac{\partial L}{\partial f_i} + \sum_{j=1}^{n}(-1)^j \frac{\partial^j}{\partial x_{\nu_1} \ldots \partial x_{\nu_j}}\left(\frac{\partial L}{\partial f_{i,\nu_1\ldots\nu_j}}\right) = 0. \qquad (4.41)$$

For the Lagrangian (4.40) the following set of two Euler-Lagrange equations results

$$0 = L_\eta, \qquad (4.42)$$

$$0 = L_{\phi_0} - \frac{\partial}{\partial t}L_{\phi_t^{(0)}} - \frac{\partial}{\partial x}L_{\phi_x^{(0)}} + \frac{\partial^2}{\partial x^2}L_{\phi_{2x}^{(0)}} - \frac{\partial^3}{\partial x^2 t}L_{\phi_{2xt}^{(0)}} - \frac{\partial^3}{\partial x^3}L_{\phi_{3x}^{(0)}} + \frac{\partial^4}{\partial x^4}L_{\phi_{4x}^{(0)}}$$
$$- \frac{\partial^5}{\partial x^4 t}L_{\phi_{4xt}^{(0)}} - \frac{\partial^5}{\partial x^5}L_{\phi_{5x}^{(0)}}. \qquad (4.43)$$

The explicit form of these equations is obtained by substituting into (4.42) and (4.43) the Lagrangian density (4.40) and retaining all terms up to second order in small parameters. Next we divide equations obtained from (4.42) and (4.43) by α and differentiate the first of them with respect to x. This yields the following set

$$\eta_x + \phi_{xt}^{(0)} - \frac{1}{2}\beta\phi_{3xt}^{(0)} + \alpha\phi_x^{(0)}\phi_{2x}^{(0)} \tag{4.44}$$

$$+ \alpha\beta\left(-\eta_x\phi_{2xt}^{(0)} - \eta\phi_{3xt}^{(0)} + \frac{1}{2}\phi_{2x}^{(0)}\phi_{3x}^{(0)} - \frac{1}{2}\phi_x^{(0)}\phi_{4x}^{(0)}\right) + \frac{1}{24}\beta^2\phi_{5xt}^{(0)} = 0,$$

$$\eta_t + \phi_{2x}^{(0)} + \alpha\left(\eta_x\phi_x^{(0)} + \eta\phi_{2x}^{(0)}\right) + \beta\left(-\frac{1}{2}\eta_{2xt} - \frac{2}{3}\phi_{4x}^{(0)}\right) + \beta^2\left(\frac{1}{24}\eta_{4xt} + \frac{2}{15}\phi_{6x}^{(0)}\right)$$

$$+ \alpha\beta\left(-\frac{5}{2}\eta_{2x}\phi_{2x}^{(0)} - \frac{1}{2}\eta_{3x}\phi_x^{(0)} - 4\eta_x\phi_{3x}^{(0)} - 2\eta_x\eta_{xt} - \eta_t\eta_{2x} - \eta\eta_{2xt} - d2\eta\phi_{4x}^{(0)}\right) = 0. \tag{4.45}$$

The above equations are up to first order in α an β identical with equations (3.18) i (3.19). Then it is possible to look for their solutions in the form $(w = \phi_x^{(0)})$

$$w(x,t) = \eta - \frac{1}{4}\alpha\,\eta^2 + \frac{1}{3}\beta\,\eta_{2x} + A_1\alpha^2\eta^3 + A_2\beta^2\eta_{4x} + \alpha\beta\left(A_3\eta_x^2 + A_4\eta\eta_{2x}\right) \tag{4.46}$$

and

$$\eta_t = -\eta_x - \frac{3}{2}\alpha\eta\eta_x - \frac{1}{6}\beta\eta_{3x} + B_1\alpha^2\,\eta^2\eta_x + B_2\beta^2\eta_{5x} + \alpha\beta\left(B_3\eta_x\eta_{2x} + B_4\eta\eta_{3x}\right). \tag{4.47}$$

Now equations (4.46) and (4.47) are substituted into (4.44) and (4.45) and terms of the order higher then the second are neglected. The obtained two equations for single uknown function $\eta(x,t)$ should be identical. This leads to the set of eight linear conditions on unknown constants $A_i, B_i, \; i = 1, \ldots, 4$,

$$-3A_1 + B_1 = 0, \qquad \frac{11}{72} - A_2 + B_2 = 0,$$

$$\frac{11}{6} - 2A_3 - A_4 + B_3 = 0, \qquad \frac{11}{12} - A_4 + B_4 = 0,$$

$$-\frac{3}{4} + 3A_1 + B_1 = 0, \qquad -\frac{17}{360} + A_2 + B_2 = 0, \tag{4.48}$$

$$\frac{1}{12} + 2A_3 + A_4 + B_3 = 0, \qquad -\frac{1}{12} + A_4 + B_4 = 0.$$

The set (4.48) has the following solution

$$A_1 = \frac{1}{8}, \qquad A_2 = \frac{1}{10}, \qquad A_3 = \frac{3}{16}, \qquad A_4 = \frac{1}{2},$$

$$B_1 = \frac{3}{8}, \qquad B_2 = -\frac{19}{360}, \qquad B_3 = \frac{23}{24}, \qquad B_4 = \frac{5}{12}.$$

This allows us to write (4.46) and (4.47) in the forms (4.26)

$$w(x,t) = \eta - \frac{1}{4}\alpha\,\eta^2 + \frac{1}{3}\beta\,\eta_{2x} + \frac{1}{8}\alpha^2\eta^3 + \frac{1}{10}\beta^2\eta_{4x} + \alpha\beta\left(\frac{3}{16}\eta_x^2 + \frac{1}{2}\eta\eta_{2x}\right)$$

and (4.27)

$$\eta_t = -\eta_x - \frac{3}{2}\alpha\eta\eta_x - \frac{1}{6}\beta\eta_{3x} + \alpha^2\frac{3}{8}\eta^2\eta_x - \alpha\beta\left(\frac{23}{24}\eta_x\eta_{2x} + \frac{5}{12}\eta\eta_{3x}\right) - \frac{19}{360}\beta^2\eta_{5x}.$$

These equations have been obtained by Marchant and Smyth [105] from Luke's Lagrangian. The same equations result from sequential solution of first order set of Boussinesq's equations and next solution of second order set according to Burde and Sergyeyev [24] or to papers by us and our co-workers [78, 79].

5

Analytic solitonic and periodic solutions to KdV2 - algebraic method

In this chapter we will show derivations of two kinds of exact solutions to the extended KdV equation (KdV2) presented already in Chapter 4 as (4.27).

For reader's convenience we rewrite this equation below

$$\eta_t + \eta_x + \frac{3}{2}\alpha\,\eta\eta_x + \frac{1}{6}\beta\,\eta_{3x} \tag{5.1}$$
$$-\frac{3}{8}\alpha^2\eta^2\eta_x + \alpha\beta\left(\frac{23}{24}\eta_x\eta_{2x} + \frac{5}{12}\eta\eta_{3x}\right) + \frac{19}{360}\beta^2\eta_{5x} = 0.$$

As we already stated, the KdV equation is *integrable*. This means that there exist solutions which can be obtained by direct integration, see, e.g., [36, 144] or Sect. 3.2. Integrability is related to the existence of a sufficient number of invariants (conservation laws) and reflects deep algebraic symmetry [122]. KdV equation has an infinite number of invariants.

Contrary to KdV, the KdV2 equation is *not integrable*. Therefore, the existence of analytic solutions was not expected. Not only is KdV2 nonintegrable, but it also has only one conservation law (volume or mass) [80, 132]. It is, however, possible to construct approximate invariants (called *adiabatic invariants*) which deviations from constant values are of the third order in small parameters. A simple derivation of adiabatically conserved quantities can be found in [82]. A detail presentation of adiabatic invariants for KdV2 is given in Chapter 9.

Although by some appropriate scaling KdV2 can be written in a simpler form (e.g., [93, 143]) we consider solutions to the KdV2 in the form (5.1) for the following reasons. KdV2 is a particular case of a more general equation, KdV2B (4.31), derived by our co-workers and us in the second order perturbation approach to the Euler equations for the shallow water problem with

uneven bottom [78, 79]. This equation (see, e.g., equation (35) in [78], equation (18) in [79] or equation (1) in [128]) contains direct terms from bottom changes and was derived in the second order perturbation approach with the assumption that the third small parameter δ is of the same order as α, β. This parameter is defined as the ratio of bottom function amplitude to the mean water depth. We prefer to use the KdV2 equation in the form (5.1) since we use the solutions to KdV2 as initial conditions to calculate the numerical evolution of waves entering the regions where bottom changes occur.

Many authors, e.g. [37–39, 45], argue that equations like (5.1) can be transformed to an asymptotically equivalent integrable form. The asymptotic equivalence means that solutions of these equations converge to the same solution when small parameters tend to zero. This approach was first introduced with *near-identity transformation* (NIT) by Kodama [94, 94] and then used and generalized by many others, e.g. [39, 56, 63]. However, NIT is an approximation in which terms of the higher order are neglected. Therefore, for finite values of small parameters (α, β), solutions of NIT-transformed integrable equation are not the same as **exact** solutions.

The KdV equation, despite its success, is not a law of nature. It is only an approximation of the first order perturbation approach to the set of the Euler equations. However, many authors seem to forget that applicability of KdV is limited to $\alpha \approx \beta \ll 1$ and improperly use it outside this range. Exact solutions to the KdV2 equation (5.1) are more suitable for larger values of α, β.

This chapter deals with two kinds of analytic solution to KdV2, single soliton solutions derived in [79] and periodic (cnoidal) solutions obtained in [70]. Both types of these solutions have been obtained by an algebraic method in which one assumes the functional form of the solution and solves the set of algebraic equations for the coefficients determining the solution. This set of algebraic equations results from the condition that the assumed form of the solution fulfills (5.1).

The chapter is organized as follows. In section 5.1 an algebraic approach to KdV is presented, and solitonic and periodic solutions to KdV are derived. In section 5.2 the exact soliton solution to KdV2 [79] is recalled. Exact periodic solutions to KdV2 in the form of cn^2 cnoidal functions are derived in section 5.3. Quite unexpectedly two branches of solutions are found. Numerical evolution of several examples of different solutions to KdV2 are presented in section 5.4.

5.1 Algebraic approach for KdV

Only as recently as in the last few years, it is known from the theory of nonlinear differential equations, see, e.g., [6, 7, 90–92], that for some classes of such equations exact solutions should exist in forms of either hyperbolic functions or Jacobi elliptic functions. It appears that both KdV and KdV2 equations belong to these classes. Therefore one can directly look for solutions of these equations assuming a particular form of the solution. Our main goal is to present exact solutions of KdV2 equation. In order to introduce the reader to the algebraic approach, we begin with much simpler KdV case.

5.1.1 Single soliton solution

Soliton solution is assumed as

$$\eta(x,t) = A\,\mathsf{sech}^2[B(x-vt)] = A\,\mathsf{sech}^2(By), \tag{5.2}$$

where $y = x - vt$. Substitution (5.2) into KdV (see, equation (3.29)) gives

$$-\frac{1}{3}AB\,\mathsf{tanh}(By)\,\mathsf{sech}^4(By)[G_0 + G_2\,\mathsf{cosh}(2By)] = 0. \tag{5.3}$$

Equation (5.3) is valid for any argument only when simultaneously

$$G_0 = 3 - 3v + 9\alpha A - 10\beta B^2 = 0, \tag{5.4}$$

$$G_2 = 3 - 3v + 2\beta B^2 = 0. \tag{5.5}$$

This gives immediately

$$B^2 = \frac{3}{4}\frac{\alpha}{\beta}A, \qquad v = 1 + \frac{\alpha}{2}A \tag{5.6}$$

and the solution coincides with (3.45).

Remark 5.1. It is clear from (5.6) that solutions exist for arbitrary parameters α, β, provided both are small. Since KdV imposes only two constraints on three coefficients A, B, v, there exists one parameter family of solutions. Usually, the amplitude A is considered arbitrary, until there is no contradiction with the condition that α is small.

5.1.2 Periodic solution

In this case solution is postulated in the form of cnoidal wave

$$\eta(x,t) = A \, \mathsf{cn}^2[B(x - vt), m] + D. \tag{5.7}$$

Equivalently, instead of Jacobi elliptic cn function, dn or sn Jacobi elliptic functions can be used.

Note, that the form (5.7) is identical with (3.53) when $A = \eta_1 + \eta_2$ and $D = -\eta_2$.

Then, substitution of (5.7) into KdV yields equation analogous to (5.3)

$$\frac{1}{3} AB \, \mathsf{cn} \, \mathsf{sn} \, \mathsf{dn} \left[G_0 + G_2 \, \mathsf{cn}^2 \right] = 0. \tag{5.8}$$

So, there must be

$$G_0 = 4\beta B^2 - 8\beta B^2 m - 9\alpha D + 6v - 6 = 0, \tag{5.9}$$

$$G_2 = 12\beta B^2 m - 9\alpha A = 0. \tag{5.10}$$

Equation (5.10) implies

$$B^2 = \frac{3}{4} \frac{\alpha}{\beta} \frac{A}{m}. \tag{5.11}$$

Volume conservation condition (details will be explained later) determines

$$D = -\frac{A}{m} \left[\frac{E(m)}{K(m)} + m - 1 \right]. \tag{5.12}$$

In (5.12), $E(m)$ and $K(m)$ are the complete elliptic integral and the complete elliptic integral of the first kind, respectively. Then from (5.9) one has

$$v = 1 + \frac{\alpha A}{2m} \left[2 - m - 3 \frac{E(m)}{K(m)} \right]. \tag{5.13}$$

Denoting

$$\mathrm{EK}(m) = 2 - m - 3 \frac{E(m)}{K(m)} \tag{5.14}$$

one obtains

$$D = \frac{A}{3m} \left[\mathrm{EK}(m) - 2m + 1 \right], \tag{5.15}$$

$$v = 1 + \frac{\alpha A}{2m} \mathrm{EK}(m). \tag{5.16}$$

The function $\mathrm{EK}(m)$ (see figure 5.1) is equal to zero for
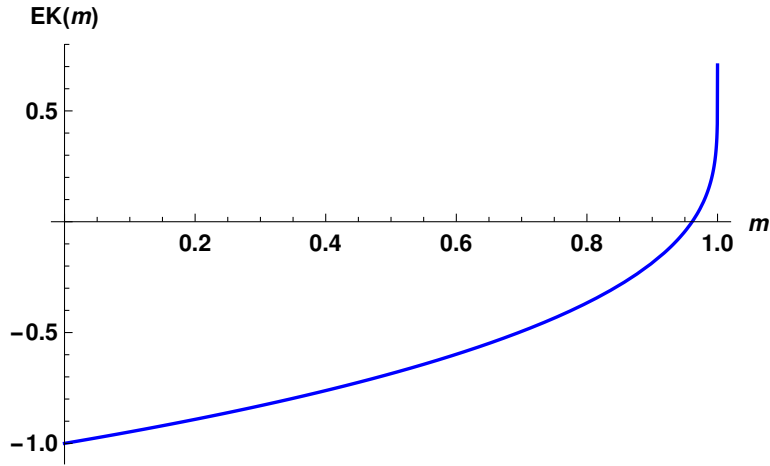
Fig. 5.1. Plot of the function EK(m) (5.14).
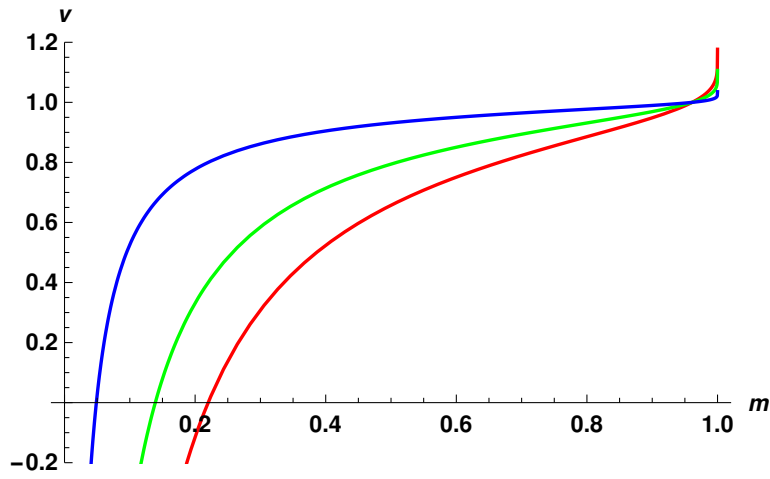
Fig. 5.2. Velocity (5.16) of KdV periodic solution (5.7) as function of m for $\alpha = 0.5, 0.3, 0.1$ plotted with red, green and blue lines, respectively. Coefficient $A = 1$.

$$m = m_s \approx 0.9611494753812$$

and reaches the value 1 for $m = 1$.

The limit $m \to 1$ gives the single soliton solution discussed in the previous subsection.

It is well known that cnoidal solutions of KdV are not a good approximation for short shallow water waves, see, e.g., [43, 44]. The limit $m \to 0$ preserves finite B (or finite wavelength $\sim 1/B$) in (5.11) when the amplitude A is proportional to m, only, that is, for infinitesimal waves. In reverse, if A

is finite then for $m \to 0$ or the wavelength tends to zero (since $B \to \infty$). At the same time velocity (5.16) tends to minus infinity, see figure 10.6.

Jacobi elliptic functions fulfil the following identities

$$\mathsf{cn}^2 + \mathsf{sn}^2 = 1, \qquad \mathsf{dn}^2 + m\,\mathsf{sn}^2 = 1.$$

Then one can express cn^2 in terms of sn^2 or dn^2

$$\mathsf{cn}^2 = 1 - \mathsf{sn}^2 \qquad \text{or} \qquad \mathsf{cn}^2 = \frac{1}{m}\,\mathsf{dn}^2 + 1 - \frac{1}{m}.$$

So, the solution (5.7) can be expressed as

$$A\,\mathsf{cn}^2(By, m) + D = A\left(1 - \mathsf{sn}^2(By, m)\right) + D = A_{\mathrm{sn}}\,\mathsf{sn}^2(By, m) + D_{\mathrm{sn}},$$

$$(5.17)$$

or

$$A\,\mathsf{cn}^2(By, m) + D = A\left(\frac{1}{m}\,\mathsf{dn}^2(By, m) + 1 - \frac{1}{m}\right) + D = A_{\mathrm{dn}}\,\mathsf{dn}^2(By, m) + D_{\mathrm{dn}},$$

$$(5.18)$$

where

$$A_{\mathrm{sn}} = -A \qquad \text{and} \qquad D_{\mathrm{sn}} = D + A, \tag{5.19}$$

$$A_{\mathrm{dn}} = \frac{A}{m} \qquad \text{and} \qquad D_{\mathrm{dn}} = D + 1 - \frac{1}{m}. \tag{5.20}$$

Therefore the cn^2 solutions are equivalent to sn^2 or dn^2 solutions with the same coefficients B, v but with A and D altered according to (5.19)-(5.20). This property applies to both KdV and KdV2 solutions.

Remark 5.2. In the case of cnoidal solutions, KdV with volume conservation condition supply three constraints on five parameters A, B, v, D, m. Then there is some freedom in allowable ranges of the coefficients. Usually, the amplitude A is considered arbitrary, until there is no contradiction with the condition that α is small. Then, for arbitrary A there exists an interval of permitted values of the elliptic parameter m.

5.2 Exact single soliton solution for KdV2

In [79] we found exact single solution for KdV2 assuming the same form of the solution as for KdV, that is (5.2). Below we briefly remind that result. Insertion of (5.2) into (5.1) gives (after some simplifications) equation analogous to (5.3)

$$C_0 + C_2 \operatorname{sech}^2(By) + C_4 \operatorname{sech}^4(By) = 0, \tag{5.21}$$

which supplies three conditions on parameters of solution formula

$$C_0 = (1 - v) + \frac{2}{3}B^2\beta + \frac{38}{45}B^4\beta^2 \qquad\qquad = 0, \tag{5.22}$$

$$C_2 = \frac{3\,A\alpha}{4} - B^2\beta + \frac{11}{4}A\alpha\,B^2\beta - \frac{19}{3}B^4\beta^2 \qquad = 0, \tag{5.23}$$

$$C_4 = -\left(\frac{1}{8}\right)(A\alpha)^2 - \frac{43}{12}A\alpha\,B^2\beta + \frac{19}{3}B^4\beta^2 \qquad = 0. \tag{5.24}$$

From (5.24), denoting $z = \dfrac{\beta B^2}{\alpha A}$ we obtain

$$\frac{19}{3}z^2 - \frac{43}{12}z - \frac{1}{8} = 0 \tag{5.25}$$

with roots

$$\begin{aligned}
z_1 &= \frac{43 - \sqrt{2305}}{152} \approx -0.033 < 0 \\
z_2 &= \frac{43 + \sqrt{2305}}{152} \approx 0.599 \quad > 0.
\end{aligned} \tag{5.26}$$

Inserting $\beta B^2 = \alpha A\,z$ into (5.23) we have

$$A = \frac{z - \frac{3}{4}}{\alpha\,z(\frac{11}{4} - \frac{19}{3}z)}. \tag{5.27}$$

Then

$$B = \sqrt{\frac{\alpha}{\beta}A\,z} = \sqrt{\frac{z - \frac{3}{4}}{\beta(\frac{11}{4} - \frac{19}{3}z)}}. \tag{5.28}$$

Now, (5.22) gives velocity as

$$v = 1 + \beta B^2\left(\frac{2}{3} + \frac{38}{45}\beta B^2\right) = 1 + \frac{z - \frac{3}{4}}{(\frac{11}{4} - \frac{19}{3}z)}\left(\frac{2}{3} + \frac{38}{45}\frac{z - \frac{3}{4}}{(\frac{11}{4} - \frac{19}{3}z)}\right). \tag{5.29}$$

Case $z = z_2$

Substitution $z = z_2$ into (5.27)-(5.68) yields

$$A = \frac{z_2 - \frac{3}{4}}{\alpha\,z_2(\frac{11}{4} - \frac{19}{3}z_2)} \approx \frac{0.242399}{\alpha} > 0, \tag{5.30}$$

$$B = \sqrt{\frac{\alpha}{\beta}A\,z_2} \approx \sqrt{\frac{0.145137}{\beta}}, \tag{5.31}$$

$$v \approx 1.11455. \tag{5.32}$$

These results are the same as in [79, Sec. 4].

Case $z = z_1$

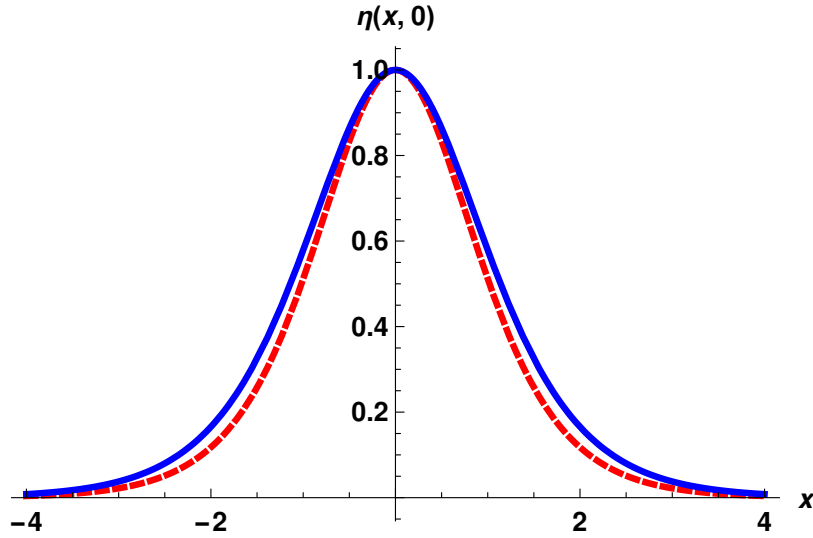Substitution $z = z_1$ into (5.27)-(5.68) results in

$$A = \frac{z_1 - \frac{3}{4}}{\alpha z_1(\frac{11}{4} - \frac{19}{3}z_1)} \approx \frac{8.02787}{\alpha} > 0, \qquad (5.33)$$

$$B^2 = \frac{\alpha}{\beta} A z_1 \approx -\frac{0.264625}{\beta} < 0, \qquad (5.34)$$

$$v = 0.882717. \qquad (5.35)$$

It is clear, that only the case $z = z_2$ supply physically relevant solutions, since in the case $z = z_2$ the coefficient $B^2 < 0$.

Fig. 5.3. Comparison of the profile of KdV soliton - red dashed line with KdV2 soliton - blue line. Both curves are obtained for the same value of the amplitude $A = 1$.

Comparing single soliton solutions for KdV and KdV2 we see the following differences.

- For KdV, $B = \sqrt{\frac{3}{4}\frac{\alpha}{\beta}}$, for KdV2, $B \approx \sqrt{0.6\frac{\alpha}{\beta}}$. This difference in B values means that the KdV2 soliton is a little wider than that of KdV (for the same parameters α, β), see figure 5.3.
- For KdV $\quad v = 1 + \frac{\alpha}{2} A$ depends on the amplitude, for KdV2 $\quad v \approx 1.11455$ is fixed.

- KdV admits a one parameter family of solutions (for instance A can be arbitrary). KdV2 imposes one more condition on coefficients of the solution; therefore parameters α, β of the equation, determine a single solution with coefficients given by (5.30)-(5.32). Such kind of fixed soliton solutions are sometimes called *embedded solitons* [93, 146].

5.3 Exact periodic solutions for KdV2

We look for periodic nonlinear wave solutions of KdV2 (5.1). Introduce $y = x - vt$. Then $\eta(x,t) = \eta(y)$, $\eta_t = -v\eta_y$ and equation (1) takes the form of an ODE

$$(1-v)\eta_y + \frac{3}{2}\alpha\,\eta\eta_y + \frac{1}{6}\beta\,\eta_{3y} - \frac{3}{8}\alpha^2\eta^2\eta_y \tag{5.36}$$
$$+ \alpha\beta\left(\frac{23}{24}\eta_y\eta_{2y} + \frac{5}{12}\eta\eta_{3y}\right) + \frac{19}{360}\beta^2\eta_{5y} = 0.$$

Now assume the periodic solution to be in the same form as corresponding solution of KdV

$$\eta(y) = A\,\mathsf{cn}^2(By, m) + D, \tag{5.37}$$

where A, B, D are yet unknown constants (m is the elliptic parameter). The constant D must ensure that the volume of water is the same for all m.

Now we calculate all derivatives η_{ny} entering (5.36). Using properties of Jacobi elliptic functions and their derivatives one can express them as functions of cn^2. So

$$\eta_y = 2AB\,\mathsf{cn}\left[-\mathsf{sn}\,\mathsf{dn}\right] = -2B\,\mathsf{cn}\,\mathsf{sn}\,\mathsf{dn}, \tag{5.38}$$
$$\eta_{2y} = 2AB^2[1 - m + (4m - 2)\,\mathsf{cn}^2 - 3m\,\mathsf{cn}^4], \tag{5.39}$$
$$\eta_{3y} = 8AB^3\,\mathsf{cn}\,\mathsf{dn}\,\mathsf{sn}[1 - 2m + 3m\,\mathsf{cn}^2], \tag{5.40}$$
$$\eta_{5y} = -16AB^5\,\mathsf{cn}\,\mathsf{dn}\,\mathsf{sn}[(2 - 17m + 17m^2) \tag{5.41}$$
$$+ (30m - 60m^2)\,\mathsf{cn}^2 + 45m^2\,\mathsf{cn}^4].$$

Denote (5.36) as

$$E_1 + E_2 + E_3 + E_4 + E_5 + E_6 + E_7 = 0, \tag{5.42}$$

where (common factor $\mathsf{CSD} = (-2AB\,\mathsf{cn}\,\mathsf{sn}\,\mathsf{dn})$)

$$E_1 = (1 - v)\eta_y = (1 - v)\,\mathsf{CSD}, \tag{5.43}$$

$$E_2 = \frac{3}{2}\alpha\,\eta\eta_y = \frac{3}{2}\alpha\,(\,\mathsf{cn}^2 + D)\,\mathsf{CSD}, \tag{5.44}$$

$$E_3 = \frac{1}{6}\beta\eta_{3x} = -\frac{2}{3}\beta\,B^2[1 - 2m + 3m\,\mathsf{cn}^2]\,\mathsf{CSD}, \tag{5.45}$$

$$E_4 = -\frac{3}{8}\alpha^2\eta^2\eta_y = -\frac{3}{8}\alpha^2(\,\mathsf{cn}^2 + D)^2\,\mathsf{CSD}, \tag{5.46}$$

$$E_5 = \frac{23}{24}\alpha\beta\,\eta_y\eta_{2y} \tag{5.47}$$

$$= \frac{23}{12}\alpha\beta\,B^2[1 - m + (4m - 2)\,\mathsf{cn}^2 - 3m\,\mathsf{cn}^4]\,\mathsf{CSD},$$

$$E_6 = \frac{5}{12}\alpha\beta\,\eta\eta_{3y} \tag{5.48}$$

$$= -\frac{5}{3}\alpha\beta\,B^2(\,\mathsf{cn}^2 + D)[1 - 2m + 3m\,\mathsf{cn}^2]\,\mathsf{CSD},$$

$$E_7 = \frac{19}{360}\beta^2\eta_{5x} = \frac{19}{45}\beta^2 B^4[(2 - 17m + 17m^2) \tag{5.49}$$

$$+ (30m - 60m^2)\,\mathsf{cn}^2 + 45m^2\,\mathsf{cn}^4]\,\mathsf{CSD}.$$

Then (5.42) becomes

$$(-2B\,\mathsf{cn}\,\mathsf{sn}\,\mathsf{dn})[F_0 + F_1\,\mathsf{cn}^2 + F_2\,\mathsf{cn}^4] = 0. \tag{5.50}$$

Equation (5.50) is valid for arbitrary argument of cn^2 when all three coefficients F_0, F_1, F_2 vanish simultaneously. This gives us a set of three equations for the coefficients v, B, D

$$F_0 = 690\alpha A\beta B^2(m-1) - (\beta B^2)^2(2584\,m(m-1) + 304)$$

$$+ 240\beta B^2(1 - 2m) - 60\alpha D\left(10\beta B^2(2m - 1) + 9\right)$$

$$+ 135(\alpha D)^2 + 360(v - 1) = 0, \tag{5.51}$$

$$F_1 = 90\alpha A\left[22\beta B^2(1 - 2m) + 3\alpha D - 6\right] \tag{5.52}$$

$$+ 120\beta B^2 m\left[38\beta B^2(2m - 1) + 15\alpha D + 6\right] = 0,$$

$$F_2 = 45\left(3\alpha^2 A^2 + 86\alpha A\beta B^2 m - 152\beta^2 B^4 m^2\right) = 0. \tag{5.53}$$

Equations (5.51)-(5.53), supplemented by the volume conservation law, allow us to find all unknowns as functions of the elliptic parameter m. Below we show these solutions explicitly.

Now, denote

$$z = \frac{B^2\,\beta}{A\,\alpha}m. \tag{5.54}$$

Then, equation (5.53) becomes identical with (5.25) and has the same roots (5.26).

5.3.1 Periodicity and volume conservation

In principle, exact periodic solutions of KdV2 with $D = 0$ exist. They make sense from a mathematical point of view. For KdV case the derivation of such periodic solutions is presented in Whitham's book [144]. The more careful derivation, presented by Dingemans [33], stresses that periodic solutions should have profile uplifts and depressions with respect to the undisturbed water level. Therefore the volume conservation condition is crucial for obtaining proper physical solutions.

Volume conservation determines the value of D. Here by mass conservation we mean that for each m the solution involves the same volume of water

$$\int_0^L \left(A\,\mathsf{cn}^2(By, m) + D \right) dy = 0.$$

Then

$$D = -\frac{A}{L} \int_0^L \mathsf{cn}^2(By, m)\,dy \equiv -\frac{A}{L} I(L), \tag{5.55}$$

where $L =$ is the wavelength. The periodicity condition implies

$$\mathsf{cn}^2(Bl, m) = \mathsf{cn}^2(0, m) \quad \Longrightarrow \quad L = \frac{2\,K(m)}{B}, \tag{5.56}$$

where $K(m)$ is the complete elliptic integral of the first kind. Hence

$$D = -\frac{A}{L} I(L) = -\frac{[E(\mathrm{am}(2K(m)|m)|m) + (m-1)K(m)]}{2mK(m)}, \tag{5.57}$$

where $E(\Theta|m)$ is the elliptic integral of the second kind and $\mathrm{am}(x|m)$ is the Jacobi elliptic function amplitude. Since

$$\frac{E(\mathrm{am}(2K(m)|m)|m))}{2\,K(m)} \equiv \frac{E(m)}{K(m)}, \tag{5.58}$$

where $E(m)$ is the complete elliptic integral, and (6.101) simplifies to

$$D = -\frac{A}{m} \left[\frac{E(m)}{K(m)} + m - 1 \right]. \tag{5.59}$$

The function $\left[\frac{E(m)}{K(m)} + m - 1 \right]$ is positive for $m \in (0, 1)$ and vanishes at $m = 0$ and $m = 1$. For $m \to 0$, D tends to $-\frac{A}{2}$ what is in agreement with sinusoidal (cosinusoidal) limit of the solution, whereas for $m \to 1$, D tends to 0, the solution becomes a soliton.

5.3.2 Coefficients of the exact solutions to KdV2

Without any assumptions on m, α, β, other than $0 \leq m \leq 1$ we obtained the set of four conditions (5.51)-(5.53) and (5.59) on A, B, D, v and m. Since equation (5.53) admits two values for z then we have to consider two different cases.

Case $z = z_2 = \dfrac{43 + \sqrt{2305}}{152}$

Solving the set (5.51)-(5.53) and (5.59) for $z = z_2$ one obtains

$$A = A(m, \alpha) = \frac{3\left(51 - \sqrt{2305}\right)m}{37\,\alpha\,\mathrm{EK}(m)} \approx \frac{0.2424}{\alpha}\,\frac{m}{\mathrm{EK}(m)}, \tag{5.60}$$

$$B = B(m, \beta) = \sqrt{\frac{3\left(-14 + \sqrt{2305}\right)}{703\,\beta\,\mathrm{EK}(m)}}, \tag{5.61}$$

$$D = D(m, \alpha) = \frac{\left(51 - \sqrt{2305}\right)}{37\,\alpha}\left(1 - \frac{2m - 1}{\mathrm{EK}(m)}\right), \tag{5.62}$$

$$v = v(m) = \frac{9439 - 69\sqrt{2305}}{5476} - \frac{\left(377197 - 7811\sqrt{2305}\right)\left(m^2 - m + 1\right)}{520220\,\mathrm{EK}(m)^2}$$

$$\approx 1.11875 - 0.00420523\,\frac{\left(m^2 - m + 1\right)}{\mathrm{EK}(m)^2}. \tag{5.63}$$

Hence, B is real-valued only when $\mathrm{EK}(m) > 0$ (see figure 5.1), that is for

$$m > m_s \approx 0.9611494753812. \tag{5.64}$$

Therefore, for this branch of solutions with $z = z_2$, the elliptic parameter $m \in (m_s, 1]$. For $m > m_s$, the amplitude $A > 0$.

Notice that the velocity depends only on m.

The dependence of A, B, D, v on m for several cases of α, β parameters is diplayed in figure 5.4.

Formulas (5.60)-(5.63) and figure 5.4 indicate that physically relevant solutions are obtained in a narrow range of m close to 1. Only for such m values of A are realistic (not very big). This conclusion is strengthen by the behavior of velocity as function of m. Velocity is positive for $m > m_{v=0}$, where $m_{v=0} \approx 0.97357$.

In figure 5.5 profiles of cnoidal KdV and KdV2 solutions are compared for m close to 1 assuming the same amplitude for both solutions.

It is worth to emphasize that in the limit $m \to 1$ coefficients of solutions (5.60)-(6.98) receive values known for single soliton KdV2 solutions given in [79].
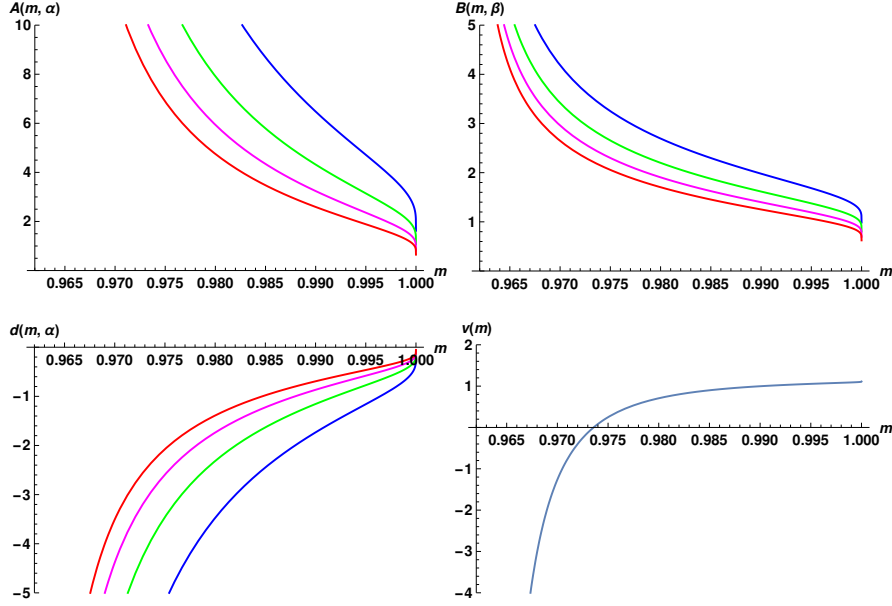
Fig. 5.4. Upper row: left - amplitude A (5.60), right - coefficient B (5.61) as functions of m for $\alpha = 0.2, 0.3, 0.4, 0.5$, represented by blue, green, magenta and red lines, respectively. Lower row: left - coefficient D (5.62), right - velocity v (6.98) as functions of m for the same parameters.

Case $z = z_1 = \dfrac{43 - \sqrt{2305}}{152}$

Now,

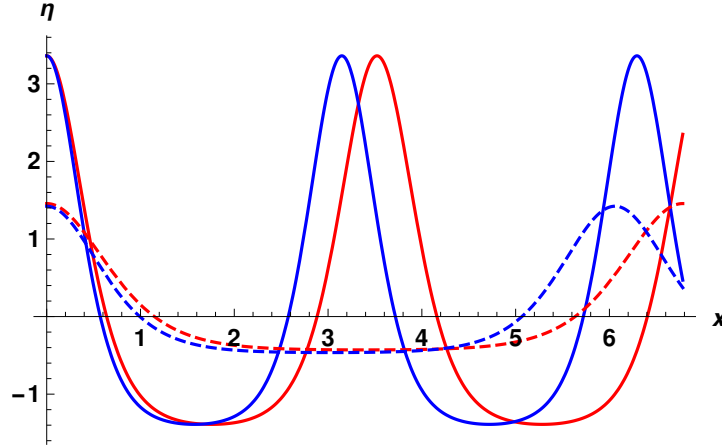$$A = A(m, \alpha) = \frac{3\left(51 + \sqrt{2305}\right)m}{37\,\alpha\,\mathrm{EK}(m)} \approx 8.02787\,\frac{m}{\alpha\,\mathrm{EK}(m)}, \tag{5.65}$$

$$B = B(m, \beta) = \sqrt{-\frac{3\left(14 + \sqrt{2305}\right)}{703\,\beta\,\mathrm{EK}(m)}}, \tag{5.66}$$

$$D = D(m, \alpha) = \frac{\left(51 + \sqrt{2305}\right)}{37\,\alpha}\left(1 - \frac{2m - 1}{\mathrm{EK}(m)}\right), \tag{5.67}$$

$$v = v(m) = \frac{9439 + 69\sqrt{2305}}{5476} - \frac{\left(377197 + 7811\sqrt{2305}\right)\left(m^2 - m + 1\right)}{520220\,\mathrm{EK}(m)^2}$$

$$\approx 2.32866 - 1.44594\,\frac{\left(m^2 - m + 1\right)}{\mathrm{EK}(m)^2}. \tag{5.68}$$

Figure 5.6 show the dependence of A, B, D, v on m for several cases of α, β parameters for this branch of KdV2 solutions.

Fig. 5.5. Profiles of KdV2 solutions (red) and KdV solutions (blue) for case $m = 0.98$ (solid) and $m = 0.995$ (dashed). All profiles are obtained with $\alpha = 0.5$ and $\beta = 0.4$. Amplitudes of KdV solutions are set to be equal to amplitudes of KdV2 solutions.

In this case physically reasonable values of $|A|$ occur only for m close to 0. Velocity stays positive for $m < m_{v=0}$, where $m_{v=0} \approx 0.50367$. It is worth to note that since $A < 0$, solutions are "**inverted**" cnoidal functions (with crests down and troughs up). This property is entirely unexpected, *new result*, since KdV admits only common cnoidal solutions.

These new solutions are, however, not much different from usual cosine waves. In figure 5.7 the profile of the inverted cnoidal wave, obtained in this branch with $\alpha = 0.3$, $\beta = 0.5$ and $m = 0.2$, is compared with the cosine wave of the same amplitude and wavelength.

5.4 Numerical evolution

In order to check our analytic results we followed the evolution of several cnoidal waves numerically. We used the finite difference (FDM) code developed for KdV2 in the fixed frame (5.1) in our papers [78,79]. In examples presented in this subsection we assume the initial wave to be the exact cnoidal wave $\eta(x,t) = A\,\mathsf{cn}^2[B(x-vt), m]+D$. The algorithm used was the Zabusky-Kruskal one [150], modified in order to include additional terms. The space derivatives of $\eta(x,t)$ were calculated numerically step by step from the grid values of the function and lower order derivatives by a nine-point central difference
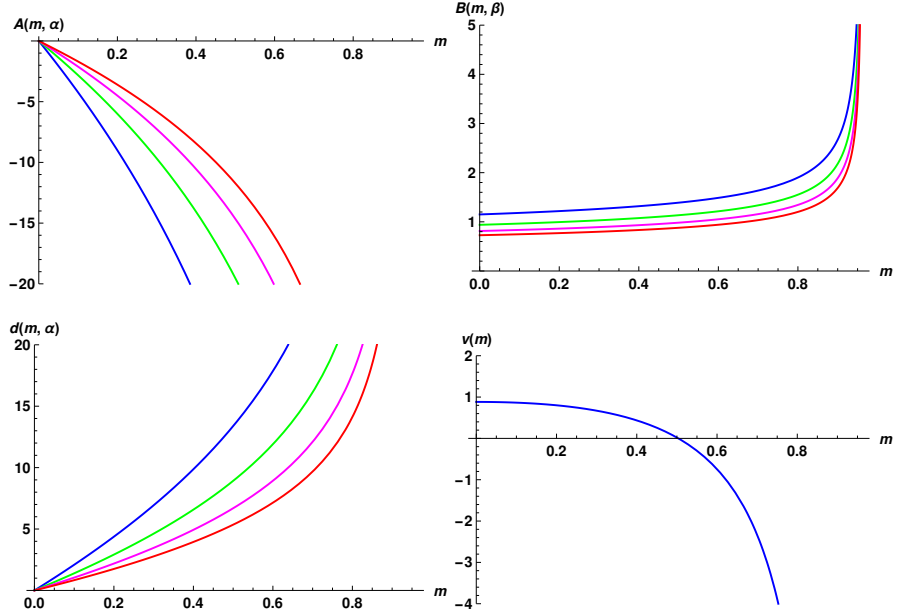
Fig. 5.6. Upper row: left - amplitude A (5.65), right - coefficient B (5.66) as functions of m for $\alpha = 0.2, 0.3, 0.4, 0.5$, represented by blue, green, magenta and red lines, respectively. Lower row: left - coefficient D (5.67), right - velocity v (5.68) as functions of m for the same parameters.

formula. Calculations were performed on the interval $x \in [0, \lambda]$ with periodic boundary conditions of N grid points. The time step Δt was chosen as in [150], i.e., $\Delta t \leq (\Delta x)^3/4$. The calculations shown in this section used grids with $N = 200$. In calculations presented below the number of time steps reached $10^7 - 10^8$. In all cases, the algorithm secures volume (mass) conservation up to 10-11 decimal digits. The precision of our model was confirmed in our studies with the finite element method (FEM) [83, 84].

An example of the motion of the normal cnoidal wave, the solution of the KdV2 equation, obtained with numerical evolution for $\alpha = 0.5$, $\beta = 0.4$, $m = 0.995$ is shown in figure 5.8. This is the same wave as that shown in figure 5.5 with the red dashed line.

The numerical solutions of normal cnoidal waves obtained for the $z = z_1$ branch are stable. The profile shown by the open symbols in figure 5.8, obtained after $2.4 \cdot 10^7$ time steps deviates from the analytic result by less than 10^{-5}. Other tests made with initially perturbed solutions confirm their numerical stability. In these tests, analytic solutions (5.37) were perturbed
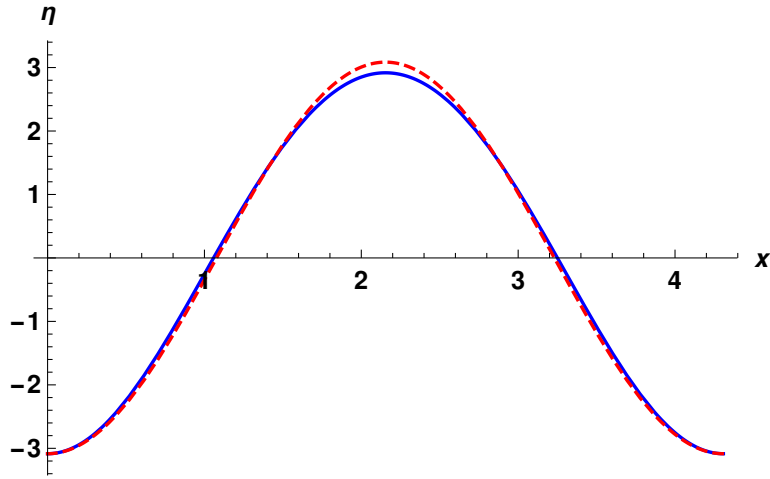
Fig. 5.7. Profiles of KdV2 solution (blue line) with the cosine wave of the same amplitude and wavelength (red, dashed line). The KdV2 solution corresponds to the case $\alpha = 0.3$, $\beta = 0.5$ and $m = 0.2$.
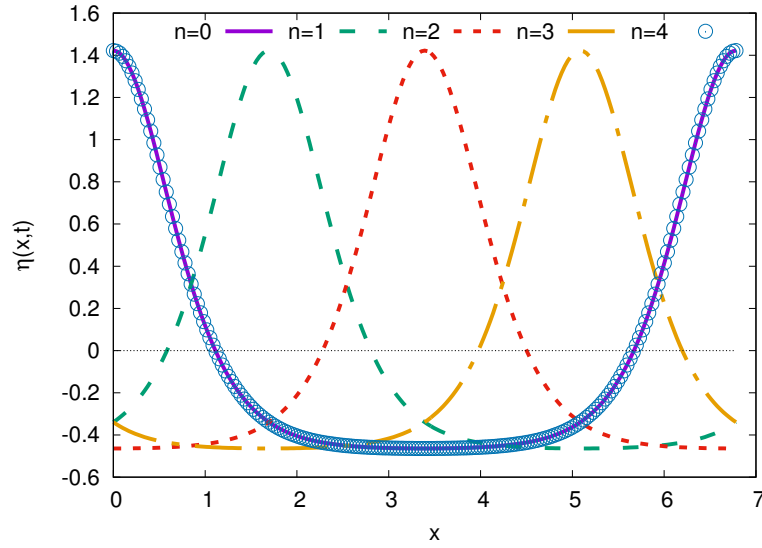
Fig. 5.8. Time evolution of the normal cnoidal wave for the case of parameters $\alpha = 0.5$, $\beta = 0.4$, $m = 0.995$. Profiles are displayed at time instants $t_n = n\,dt$, where $dt = \frac{1}{4}T$.
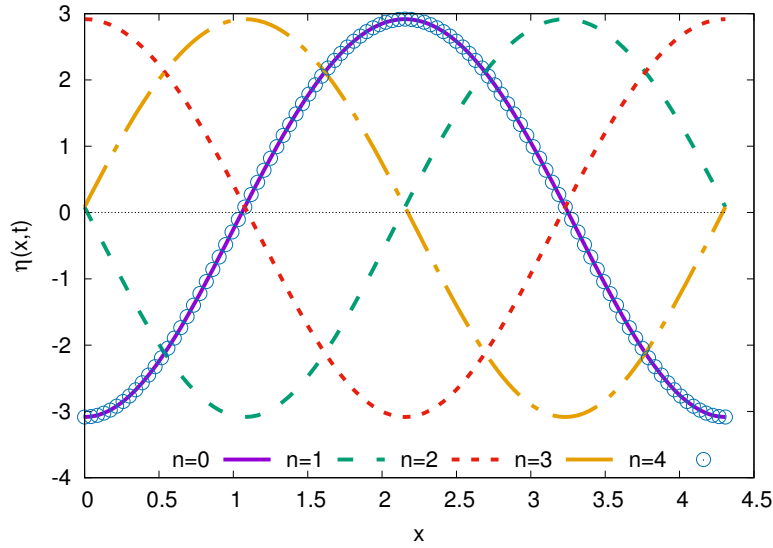
Fig. 5.9. Time evolution of the inverted cnoidal wave i for the case $\alpha = 0.3$, $\beta = 0.5$ and $m = 0.2$. Profiles are displayed at time instants $t_n = n\,dt$, where $dt = \frac{1}{4}T$.

by a cosine wave with the amplitude of 1% of the cnoidal wave amplitude. Profiles obtained after one period overlapped the initial profiles within the line width. Numerical solutions are stable for much longer time intervals, as well.

The same stability of numerical solutions is obtained for inverted cnoidal waves. An example of the motion of the inverted cnoidal solution to the KdV2 for $z = z_1$ branch, obtained by numerical evolution, is presented in figure 5.9. The displayed case corresponds to the wave with $\alpha = 0.3$, $\beta = 0.5$ and $m = 0.2$. This is the same wave as that displayed with the solid line in figure 5.7. The deviations of the profile obtained by the numerical evolution of the inverted cnoidal solution after one period from the analytic solution are again less than 10^{-5}. Similarly to solutions belonging to the branch with $z = z_2$ the inverted cnoidal solutions belonging to the $z = z_1$ branch are resistant to small perturbations of the initial conditions. The motion is numerically stable for periods much longer than T, as well.

5.4.1 Comments

From the study presented in this chapter, the following conclusions can be drawn.

- For extended Korteweg - de Vries equation exact solutions, both solitonic and periodic exist. These solutions have the same form as the corresponding solutions of KdV equations but with coefficients altered.
- KdV2 equation imposes severe limitations on its exact solutions. Physically relevant periodic solutions of KdV2 are related to two narrow intervals of the m parameter. For m very close to 1, regular cnoidal waves are obtained. For m very close to 0, inverted cnoidal waves are found. This is the entirely **new result** specific for KdV2. First, since KdV fails for small m values. Second, since KdV does not admit inverted cnoidal solutions. However, wave profiles of these inverted cnoidal solutions to KdV2 are not much different from a cosine function.

6

Superposition solutions to KdV and KdV2

Recently, Khare and Saxena [90–92] demonstrated that for several nonlinear equations which admit solutions in terms of elliptic functions $\mathsf{cn}(x, m)$, $\mathsf{dn}(x, m)$ there exist solutions in terms of superpositions $\mathsf{cn}(x, m) \pm \sqrt{m}\, \mathsf{dn}(x, m)$. They also showed that KdV which admits solutions in terms of $\mathsf{dn}^2(x, m)$ also admits solutions in terms of superpositions $\mathsf{dn}^2(x, m) \pm \sqrt{m}\, \mathsf{cn}(x, m)\, \mathsf{dn}(x, m)$. Since then we found analytic solutions to KdV2 in terms of $\mathsf{cn}^2(x, m)$ [70] the results of Khare and Saxena [90–92] inspired us to look for solutions to KdV2 in a similar form.

6.1 Mathematical solutions to KdV

First, we recall shortly the results obtained by Khare and Saxena [90] for the KdV equation. Let us note that the authors of the papers [90–92] were mainly interested in the mathematical properties of solutions mostly disregarding physical context.

Let us follow the approach used in [90] but formulating it in a fixed frame, that is, for the equation (3.29)

$$\eta_t + \eta_x + \frac{3}{2}\alpha\,\eta\eta_x + \frac{1}{6}\beta\,\eta_{3x} = 0. \tag{6.1}$$

Introduce $y = x - vt$. Then $\eta(x, t) = \eta(y)$, $\eta_t = -v\eta_y$ and equation (6.1) takes the form of an ODE

$$(1 - v)\eta_y + \frac{3}{2}\alpha\,\eta\eta_y + \frac{1}{6}\beta\,\eta_{3y} = 0. \tag{6.2}$$

6.1.1 Single dn^2 solution

Assuming solution in the form

$$\eta(x,t) = A\,\mathsf{dn}^2[B(x-vt),m] \equiv A\,\mathsf{dn}^2[By,m] \tag{6.3}$$

and substituting (6.3) into (6.2) one obtains after some simplifications

$$\frac{1}{3}ABm\,\mathsf{cn}[By,m]\,\mathsf{dn}[By,m]\,\mathsf{sn}[By,m]\left(C_0 + C_2\,\mathsf{cn}^2[By,m]\right). \tag{6.4}$$

Equation (6.4) is satisfied when

$$C_0 = -6 + 6v - 9A\alpha + 9Am\alpha + 4B^2\beta - 8B^2m\beta = 0 \tag{6.5}$$

$$C_2 = -9Am\alpha + 12B^2m\beta = 0. \tag{6.6}$$

This implies

$$B = \sqrt{\frac{3\alpha}{4\beta}A} \qquad \text{and} \qquad v = 1 + \frac{\alpha}{2}A(2-m). \tag{6.7}$$

From mathematical point of view the amplitude A can be arbitrary.

6.1.2 Superposition solution

Next, the authors [90] studied superpositions

$$\eta_\pm(x,t) = \frac{1}{2}A\left(\mathsf{dn}^2[B(x-vt),m] \pm \sqrt{m}\,\mathsf{cn}[B(x-vt),m]\,\mathsf{dn}[B(x-vt),m]\right)$$

$$= \frac{1}{2}A\left(\mathsf{dn}^2[By,m] \pm \sqrt{m}\,\mathsf{cn}[By,m]\,\mathsf{dn}[By,m]\right). \tag{6.8}$$

Substitution of (6.8) into (6.2) leads to equation analogous to (6.4)

$$CF\left(C_0{}^s + C_2{}^s\,\mathsf{cn}^2[By,m] + C_{11}\,\mathsf{cn}\,\mathsf{dn}\right), \tag{6.9}$$

where the common factor CF is

$$CF = \frac{1}{24}AB\sqrt{m}\left(\mathsf{dn}[By,m] \pm \sqrt{m}\,\mathsf{cn}[By,m]\right)^2\mathsf{sn}[By,m]. \tag{6.10}$$

The conditions for coefficients C_0^s, C_2^s, C_{11} have in this case the form

$$C_0{}^s = 9\alpha A - 9\alpha Am - 2\beta B^2 + 10\beta B^2 m - 12v + 12 = 0, \tag{6.11}$$

$$C_2{}^s = m(9A\alpha - 12B^2\beta) = 0, \tag{6.12}$$

$$C_{11} = \sqrt{m}(9A\alpha - 12B^2\beta) = 0. \tag{6.13}$$
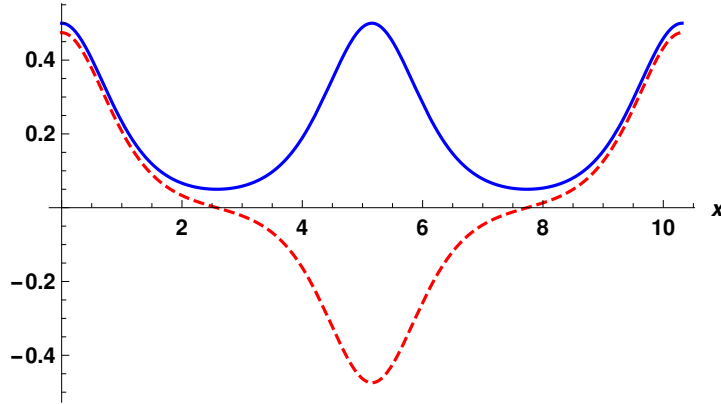
Fig. 6.1. Profiles of functions $\frac{A}{2}\mathsf{dn}^2(x,m)$ - blue solid line and $\frac{A}{2}\sqrt{m}\,\mathsf{cn}(x,m)\,\mathsf{dn}(x,m)$ - red dashed line.

The equations (6.12) and (6.13) are equivalent and the same as (6.6). Therefore the relation $B = \sqrt{\frac{3\alpha}{4\beta}}A$ remains the same as in (6.7). The equation (6.11) implies that the velocity for both solutions $\eta_\pm$ (6.8) is

$$v = 1 + \frac{\alpha}{8}A(5-m). \tag{6.14}$$

In both cases of periodic solutions to KdV, that is, in the single dn^2 solution (6.3) and the superposition solution (6.8) the KdV equation imposes only two conditions on three coefficients A, B, v. Therefore one of them is arbitrary. The usual choice is the amplitude A.

Superpositions $\eta_\pm$ (6.8) are the sum or the difference of two functions: $\frac{A}{2}\mathsf{dn}^2[(x-vt),m]$ and $\frac{A}{2}\sqrt{m}\,\mathsf{cn}[(x-vt),m]\,\mathsf{dn}[(x-vt),m]$. Profiles of these functions are displayed in figure 6.1 for $A = B = 1$, $t = 0$ and $m = 0.9$ on the interval $x \in [0, L]$, where $L = 4K(m)$ is the space period of $\eta_\pm$ [$K(m)$ is the complete elliptic integral of the first kind]. It is clear that the wavelength of $\eta_\pm$ is twice of the wavelength of single function solution $A\,\mathsf{dn}^2[(x-vt),m]$.

Profiles of solutions η_+ and η_- are presented in figure 6.2 for the same coefficients. It is well seen that both solutions represent the same wave only shifted by $L/2 = 2K(m)$. This value $2K(m)$ is the wavelength of the single dn^2 solution which is the sum $\eta_+ + \eta_-$.

6.2 Mathematical solutions to KdV2

Now, we look for periodic nonlinear wave solutions to KdV2 (5.1). After substitution $y = x - vt$ the equation (5.1) takes the form of an ODE
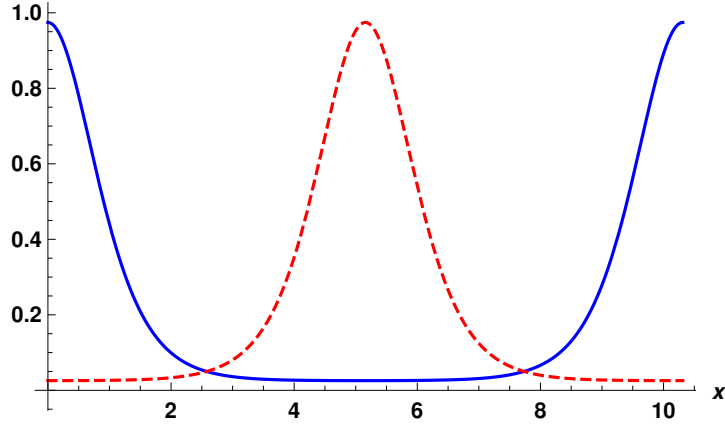
Fig. 6.2. Profiles of functions η_+ - blue solid line and η_- - red dashed line.

$$(1-v)\eta_y + \frac{3}{2}\alpha\,\eta\eta_y + \frac{1}{6}\beta\,\eta_{3y} - \frac{3}{8}\alpha^2\eta^2\eta_y \qquad (6.15)$$
$$+ \alpha\beta\left(\frac{23}{24}\eta_y\eta_{2y} + \frac{5}{12}\eta\eta_{3y}\right) + \frac{19}{360}\beta^2\eta_{5y} = 0.$$

6.2.1 Single periodic solution

First, we recall some properties of the Jacobi elliptic functions (arguments are omitted)

$$\mathsf{sn}^2 + \mathsf{cn}^2 = 1, \quad \mathsf{dn}^2 + m\,\mathsf{sn}^2 = 1. \qquad (6.16)$$

Their derivatives are

$$\frac{d\,\mathsf{sn}}{dy} = \mathsf{cn}\,\mathsf{dn}, \quad \frac{d\,\mathsf{cn}}{dy} = -\,\mathsf{sn}\,\mathsf{dn}, \quad \frac{d\,\mathsf{dn}}{dy} = -m\,\mathsf{sn}\,\mathsf{cn}. \qquad (6.17)$$

Assume a solution of (5.1) in the same form as KdV solution (6.3). Insertion of (6.3) into (6.15) yields

$$\frac{ABm}{180}\,\mathsf{cn}\,\mathsf{dn}\,\mathsf{sn}\left(F_0 + F_2\,\mathsf{cn}^2 + F_4\,\mathsf{cn}^4\right) = 0. \qquad (6.18)$$

Equation (6.18) holds for arbitrary arguments when F_0, F_2, F_4 vanish simultaneously. The explicit form of this set of equations is following

$$F_0 = 135\alpha^2 A^2 (m-1)^2 + 30\alpha A(m-1)\left(\beta B^2 (63m-20)+18\right)$$
$$- 8\left(19\beta^2 B^4\left(17m^2-17m+2\right)+30\beta B^2(2m-1)+45\right)$$
$$+ 360v = 0, \tag{6.19}$$

$$F_2 = -30m\left[9\alpha^2 A^2(m-1)+6\alpha A\left(\beta B^2(32m-21)+3\right)\right.$$
$$\left. -8\beta B^2\left(19\beta B^2(2m-1)+3\right)\right] = 0, \tag{6.20}$$

$$F_4 = 45m^2\left(3\alpha^2 A^2 + 86\alpha A\beta B^2 - 152\beta^2 B^4\right) = 0. \tag{6.21}$$

Equation (6.21) is equivalent to the [79, equation (26)] obtained for solitonic solutions to KdV2. Denoting $z = \frac{B^2\beta}{A\alpha}$ one obtains from (6.21) two possible solutions

$$z_1 = \frac{43 - \sqrt{2305}}{152} < 0 \quad \text{and} \quad z_2 = \frac{43 + \sqrt{2305}}{152} > 0. \tag{6.22}$$

Then the corresponding amplitudes A are

$$A_1 = \frac{-43 - \sqrt{2305}}{3}\frac{B^2\beta}{\alpha} < 0 \qquad \text{and}$$
$$A_2 = \frac{-43 + \sqrt{2305}}{3}\frac{B^2\beta}{\alpha} > 0. \tag{6.23}$$

Inserting this into (6.78) yields

$$B_1^{\;2} = \frac{3\left(47 + \sqrt{2305}\right)}{\left(549 + 11\sqrt{2305}\right)\beta(m-2)} \qquad \text{and}$$
$$B_2^{\;2} = \frac{3\left(-47 + \sqrt{2305}\right)}{\left(-549 + 11\sqrt{2305}\right)\beta(m-2)}. \tag{6.24}$$

Finally, from (6.77) one obtains

$$v_{1/2} = \left\{\left(2561482 \pm 53302\sqrt{2305}\right)m^2\right.$$
$$\mp\left(22827517 \pm 475267\sqrt{2305}\right)(m-1)\Big\} / \tag{6.25}$$
$$\left\{10\left(290153 + 6039\sqrt{2305}\right)(m-2)^2\right\}.$$

Despite the same form of solutions to KdV and KdV2 there is a fundamental difference. For given m, KdV imposes only two conditions on coefficients A, B, v, so there is one parameter freedom. This is no longer the case for KdV2.

Remark 6.1. Solutions $\eta_1(x,t) = A_1 \, \mathsf{dn}^2[B_1(x - v_1 t), m]$, *belonging to the branch* $z = z_1$, *are unphysical. Since* $m \in [0,1]$, *then* $B_1^{\;2} < 0$. *Then* B_1 *is*

purely imaginary, $B_1 = i\bar{B}_1$. Jacobi elliptic functions dn *of imaginary arguments can be expressed in terms of Jacobi elliptic functions of real arguments*

$$\mathsf{dn}(iq, m) = \frac{\mathsf{cn}(q, 1-m)\,\mathsf{dn}(q, 1-m)}{1 - \mathsf{sn}^2(q, 1-m)}. \tag{6.26}$$

Since $\mathsf{sn}^2 \in [0, 1]$, *when* $\mathsf{sn}^2 = 1$, *the denominator becomes zero, therefore the solution* $\eta_1(x, t)$ *is singular for some arguments.*

So, in the case of single dn^2 (6.3) solutions to KdV2 only z_2 root (6.22) has physical relevance. Finally, the coefficients of the solution are

$$A = \frac{3(51 - \sqrt{2305})}{37(2-m)\alpha} \approx \frac{0.2424}{(2-m)\alpha} \tag{6.27}$$

$$B = \sqrt{\frac{3(-14 + \sqrt{2305})}{703(2-m)\beta}} \approx \sqrt{0.145(2-m)\beta} \tag{6.28}$$

$$v = \frac{4\left(314\sqrt{2305} + 129877\right)m^2 + \left(18409\sqrt{2305} - 3209623\right)(m-1)}{520220(2-m)^2}$$

$$\approx \frac{1.11455\,m^2 - 4.4708(m-1)}{(2-m)^2} \tag{6.29}$$

The velocity given by (6.29) is almost constant as function of m. It decreases slowly from $v(0) \approx 1.1177$ to $v(1) \approx 1.11455$.

Comparison of KdV and KdV2 dn^2 solutions (6.3)

Is a dn^2 solution of KdV2 much different from the KdV solution for the same m? In order to compare solutions of both equations, remember that the set of three equations (6.77)-(6.21) fixes all A, B, v coefficients for KdV2 for given m. In the case of KdV, the equation analogous to (6.18) imposes only two conditions on three parameters. Therefore one parameter, say amplitude A, can be chosen arbitrarily. Then we compare coefficients of solutions to KdV2 and KdV chosing the same value of A, that is, A_{KdV2}. Such comparison is displayed in figure 6.3 for $\alpha = \beta = \frac{1}{10}$.

It is clear that v_{KdV2} and v_{KdV} are very similar. We have the following relations: for KdV $\frac{B^2}{A} = \frac{3}{4}\frac{\alpha}{\beta}$, whereas for KdV2 $\frac{B^2}{A} = \frac{\alpha}{\beta}z_2$. Since $z_2 \approx 0.6$, $B_{\mathrm{KdV}}/B_{\mathrm{KdV}} = \sqrt{\frac{3}{4z_2}} \approx 1.12$ for $\alpha = \beta$. The same relations hold between KdV2 and KdV coefficients for superposition solutions shown in figure 6.4.
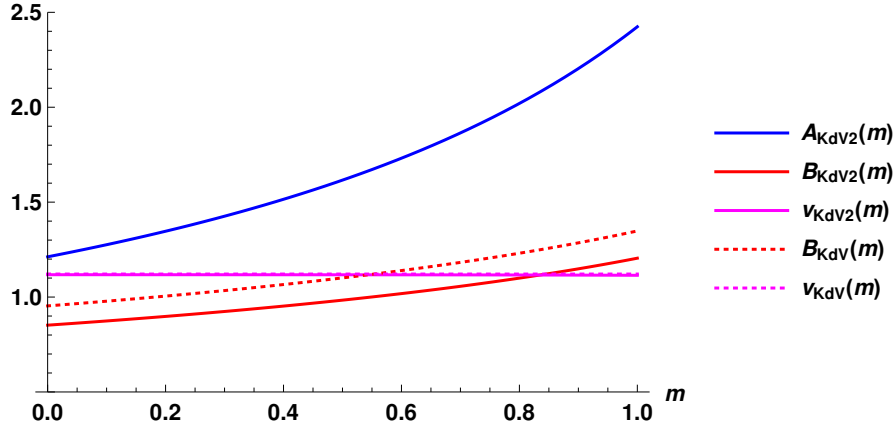
Fig. 6.3. Comparison of the coefficients $A, B, v, (z = z_2)$ as functions of m for the periodic dn^2 solutions (6.3) to KdV and KdV2. Solid blue, red and magenta lines represent KdV2 coefficients $(A, B, v$ - respectively), dotted lines KdV coefficients. For this comparison the coefficient A_{KdV} (for KdV) is chosen to be equal to A_{KdV2}. In this example $\alpha = \beta = 0.1$.

6.2.2 Superposition "$\mathsf{dn}^2 + \sqrt{m}\,\mathsf{cn}\,\mathsf{dn}$"

Now assume the periodic solution to be in the same form as the corresponding superposition solution of KdV [90]

$$\eta_+(y) = \frac{1}{2}A\left[\,\mathsf{dn}^2(By, m) + \sqrt{m}\;\mathsf{cn}(By, m)\,\mathsf{dn}(By, m)\right], \qquad (6.30)$$

where A, B, v are yet unknown constants (m is the elliptic parameter). We will need

$$\eta_y = -\frac{1}{2}AB\,\sqrt{m}\left(\sqrt{m}\,\mathsf{cn} +\,\mathsf{dn}\right)^2\,\mathsf{sn}, \qquad (6.31)$$

$$\eta_{2y} = \frac{1}{2}AB^2\,\sqrt{m}\left(\sqrt{m}\,\mathsf{cn} +\,\mathsf{dn}\right)^2\!\left(-\mathsf{cn}\,\mathsf{dn} + 2\sqrt{m}\,\mathsf{sn}^2\right), \qquad (6.32)$$

$$\eta_{3y} = \frac{1}{2}AB^3\,\sqrt{m}\left(\sqrt{m}\,\mathsf{cn} +\,\mathsf{dn}\right)^2 \qquad (6.33)$$
$$\times\,\mathsf{sn}\left(m\,\mathsf{cn}^2 + 6\sqrt{m}\,\mathsf{cn}\,\mathsf{dn} +\,\mathsf{dn}^2 - 4m\,\mathsf{sn}^2\right),$$

$$\eta_{5y} = -\frac{1}{2}AB^5\,\sqrt{m}\left(\sqrt{m}\,\mathsf{cn} +\,\mathsf{dn}\right)^2$$
$$\times\,\mathsf{sn}\left[m^2\,\mathsf{cn}^4 + 30m^{3/2}\,\mathsf{cn}^3\,\mathsf{dn} +\,\mathsf{dn}^4 - 44\,\mathsf{dn}^2\,\mathsf{sn}^2\right. \qquad (6.34)$$
$$+\,16m^2\,\mathsf{sn}^4 - 30\sqrt{m}\,\mathsf{cn}\,\mathsf{dn}\left(-\,\mathsf{dn}^2 + 4m\,\mathsf{sn}^2\right)$$
$$\left.+\,\mathsf{cn}^2\left(74m\,\mathsf{dn}^2 - 44m^2\,\mathsf{sn}^2\right)\right].$$

Denote (6.15) as

$$E_1 + E_2 + E_3 + E_4 + E_5 + E_6 + E_7 = 0, \tag{6.35}$$

where

$$E_1 = (1-v)\eta_y = -\frac{1}{2}AB(1-v)\sqrt{m}\left(\sqrt{m}\,\mathsf{cn} + \mathsf{dn}\right)^2\mathsf{sn}, \tag{6.36}$$

$$E_2 = \frac{3}{2}\alpha\,\eta\eta_y = -\frac{3}{8}\alpha\,A^2B\,\sqrt{m}\left(\sqrt{m}\,\mathsf{cn} + \mathsf{dn}\right)^3\mathsf{sn}\,\mathsf{dn}, \tag{6.37}$$

$$E_3 = \frac{1}{6}\beta\eta 3y = \frac{1}{12}\beta\,AB^3\,\sqrt{m}\left(\sqrt{m}\,\mathsf{cn} + \mathsf{dn}\right)^2\mathsf{sn}$$
$$\left(m\,\mathsf{cn}^2 + 6\sqrt{m}\,\mathsf{cn}\,\mathsf{dn} + \mathsf{dn}^2 - 4m\,\mathsf{sn}^2\right), \tag{6.38}$$

$$E_4 = -\frac{3}{8}\alpha^2\eta^2\eta_y = \frac{3}{64}\alpha^2A^3B\sqrt{m}\,\mathsf{dn}^2\left(\sqrt{m}\,\mathsf{cn} + \mathsf{dn}\right)^4\mathsf{sn}, \tag{6.39}$$

$$E_5 = \frac{23}{24}\alpha\beta\,\eta_y\eta_{2y} = -\frac{23}{96}\alpha\beta\,A^2B^3\,m\,\left(\sqrt{m}\,\mathsf{cn} + \mathsf{dn}\right)^4\mathsf{sn}$$
$$\left(-\mathsf{cn}\,\mathsf{dn} + 2\sqrt{m}\,\mathsf{sn}^2\right), \tag{6.40}$$

$$E_6 = \frac{5}{12}\alpha\beta\,\eta\eta_{3y} = \frac{5}{48}\alpha\beta\,A^2B^3\,\sqrt{m}\,\mathsf{dn}\left(\sqrt{m}\,\mathsf{cn} + \mathsf{dn}\right)^3\mathsf{sn}$$
$$\left(m\,\mathsf{cn}^2 + 6\sqrt{m}\,\mathsf{cn}\,\mathsf{dn} + \mathsf{dn}^2 - 4m\,\mathsf{sn}^2\right), \tag{6.41}$$

$$E_7 = \frac{19}{360}\beta^2\eta_{5y} = -\frac{19}{720}\beta^2AB^5\,\sqrt{m}\left(\sqrt{m}\,\mathsf{cn} + \mathsf{dn}\right)^2\mathsf{sn}$$
$$\left[m^2\,\mathsf{cn}^4 + 30m^{3/2}\,\mathsf{cn}^3\,\mathsf{dn} + \mathsf{dn}^4 - 44\,\mathsf{dn}^2\,\mathsf{sn}^2\right.$$
$$+ 16m^2\,\mathsf{sn}^4 - 30\sqrt{m}\,\mathsf{cn}\,\mathsf{dn}\left(-\mathsf{dn}^2 + 4m\,\mathsf{sn}^2\right) \tag{6.42}$$
$$\left.+ \mathsf{cn}^2\left(74m\,\mathsf{dn}^2 - 44m^2\,\mathsf{sn}^2\right)\right].$$

Then (6.35) becomes

$$\frac{1}{2}AB\,\sqrt{m}\left(\sqrt{m}\,\mathsf{cn} + \mathsf{dn}\right)^2\mathsf{sn} \tag{6.43}$$
$$\times\left(F_0 + F_{cd}\,\mathsf{cn}\,\mathsf{dn} + F_{c^2}\,\mathsf{cn}^2 + F_{c^3d}\,\mathsf{cn}^3\,\mathsf{dn} + F_{c^4}\,\mathsf{cn}^4\right) = 0.$$

Equation (6.43) is valid for arbitrary arguments when all coefficients $F_0, F_{cd}, F_{c^2}, F_{c^3d}, F_{c^4}$ vanish simultaneously. This gives us a set of equations for the coefficients A, B, v

$$F_0 = -1440v - 135\alpha^2 A^2 (m-1)^2$$
$$- 60\alpha A(m-1)\left[\beta B^2(48m-5)+18\right] \tag{6.44}$$
$$+ 4\left[19\beta^2 B^4 \left(61m^2 - 46m + 1\right)\right.$$
$$\left. + 60\beta B^2(5m-1) + 360\right] = 0,$$

$$F_{cd} = 30\sqrt{m}\left[9\alpha^2 A^2(m-1) + 3\alpha A\left(\beta B^2(75m-31)+12\right)\right.$$
$$\left. -4\beta B^2\left(19\beta B^2(5m-1)+12\right)\right] = 0, \tag{6.45}$$

$$F_{c^2} = 15m\left(27\alpha^2 A^2(m-1) + 12\alpha A\left(\beta B^2(59m-37)+6\right)\right.$$
$$\left. -32\beta B^2\left(19\beta B^2(2m-1)+3\right)\right) = 0, \tag{6.46}$$

$$F_{c^3 d} = -90m^{3/2}\left(3\alpha^2 A^2 + 86\alpha A\beta B^2 - 152\beta^2 B^4\right) = 0, \tag{6.47}$$

$$F_{c^4} = -90m^2\left(3\alpha^2 A^2 + 86\alpha A\beta B^2 - 152\beta^2 B^4\right) = 0. \tag{6.48}$$

Equations (6.47) and (6.48) are equivalent and give the same condition as (6.21). Solving (6.47) with respect to B^2, we obtain the same relations as in [79, equation (28)]

$$(B_{1/2})^2 = \frac{A\alpha}{\beta}\left(\frac{43 \mp \sqrt{2305}}{152}\right). \tag{6.49}$$

Denote

$$z_1 = \frac{43 - \sqrt{2305}}{152} \qquad \text{and} \qquad z_2 = \frac{43 + \sqrt{2305}}{152}. \tag{6.50}$$

It is clear that $z_1 < 0$ and $z_2 > 0$. B has to be real-valued. This is possible for the case $z = z_1$ if $A < 0$, and for $z = z_2$ if $A > 0$. The value of z_2 is the same as that found for the exact soliton solution in [79, equation (28)]. In general

$$B^2 = \frac{A\alpha}{\beta} z. \tag{6.51}$$

Now, we insert (6.51) into (6.44),(6.45) and (6.46). Besides a trivial solution with $A = 0$ we obtain

$$1440(1-v) + A\alpha(1-m)\left[1080 - 135A\alpha(1-m)\right] \tag{6.52}$$
$$-240A\alpha(1-5m) - 30(A\alpha)^2(10 - 109m + 96m^2)\,z$$
$$+4(A\alpha)^2(19 - 847m + 1159m^2)\,z^2 = 0,$$

$$9[A\alpha(m-1)+4] + 3[A\alpha(75m-31)-16]\,z \tag{6.53}$$
$$-76A\alpha(5m-1)\,z^2 = 0,$$

$$9(3A\alpha(m-1)+8) + 12(A\alpha(59m-37)-8)\,z \tag{6.54}$$
$$-608A\alpha(2m-1)\,z^2 = 0.$$

From (6.53) we find

$$A = -\frac{12(4z - 3)}{\alpha\left[76z^2(5m - 1) - z(225m - 93) - 9(m - 1)\right]} \tag{6.55}$$

but from (6.54) it follows that

$$A = -\frac{24(4z - 3)}{\alpha\left[608z^2(2m-1)-4z(177m-111)-27(m-1)\right]}. \tag{6.56}$$

This looks like a contradiction, but substitution $z = z_1 = (43 - \sqrt{2305})/152$ in both (6.55) and (6.56) gives the same result

$$A_1 = \frac{24\left(71 + \sqrt{2305}\right)}{\left(-329 + 5\sqrt{2305}\right)\alpha\,(m - 5)}. \tag{6.57}$$

For $z = z_2 = (43 + \sqrt{2305})/152$ the common result is

$$A_2 = \frac{24\left(-71 + \sqrt{2305}\right)}{\left(329 + 5\sqrt{2305}\right)\alpha\,(m - 5)}. \tag{6.58}$$

Now, using $z = z_1$ and A_1 given by (6.57) we obtain from (6.52)

$$v_1 = \frac{\mathrm{vnum}_-(m)}{\mathrm{vden}_-(m)} \tag{6.59}$$

and with $z = z_2$ and A_2 given by (6.58)

$$v_2 = \frac{\mathrm{vnum}_+(m)}{\mathrm{vden}_+(m)}, \tag{6.60}$$

where

$$\mathrm{vnum}_\mp(m) = 6\left\{\left(2912513 \mp 58361\sqrt{2305}\right)m^2\right.$$
$$- 54\left(584397 \mp 10069\sqrt{2305}\right)m$$
$$\left. +75245133 \mp 1419141\sqrt{2305}\right\}$$

and

$$\mathrm{vden}_\mp(m) = 95\left(329 \mp 5\sqrt{2305}\right)^2(m - 5)^2.$$

Discussion of mathematical solutions in the form (6.30)

From strictly mathematical point of view we found two families of solutions determined by coefficients A, B, v as functions of the elliptic parameter m. There are two cases.

- **Case 1.** $z = z_1 = \dfrac{43 - \sqrt{2305}}{152} \approx -0.0329633 < 0$. Then

$$A_1 = -\frac{12\left(51 + \sqrt{2305}\right)}{37\,\alpha\,(5 - m)} < 0, \tag{6.61}$$

$$B_1 = i\sqrt{\frac{12(14 + \sqrt{2305})}{703(5 - m)\beta}} \equiv i\,B_1' \tag{6.62}$$

and v_1 is given by (6.59). Note that $B_1^2 < 0$, so B_1 is imaginary. Jacobi elliptic functions of imaginary arguments can be expressed as real-valued functions of real arguments, since

$$\mathsf{cn}(i\,q, m) = \frac{1}{\mathsf{cn}(q, (1{-}m))}, \quad \mathsf{dn}(i\,q, m) = \frac{\mathsf{dn}(q, (1{-}m))}{\mathsf{cn}(q, (1{-}m))}.$$

Then solution (6.30) reads

$$\begin{aligned}
\eta_1(x - v_1 t, m) &= \frac{1}{2} A_1 \left[\, \mathsf{dn}^2(B_1(x - v_1 t), m)\right.\\
&\qquad\left. + \sqrt{m}\,\mathsf{cn}(B_1(x - v_1 t), m)\,\mathsf{dn}(B_1(x - v_1 t), m)\right]\\
&= \frac{1}{2} A_1 \left[\frac{\mathsf{dn}^2(B_1'(x - v_1 t), (1 - m))}{\mathsf{cn}^2(B_1'(x - v_1 t), (1 - m))}\right.\\
&\qquad\left. + \sqrt{m}\,\frac{\mathsf{dn}(B_1'(x - v_1 t), (1 - m))}{\mathsf{cn}^2(B_1'(x - v_1 t), (1 - m))}\right].
\end{aligned} \tag{6.63}$$

This form of solutions appears, to our best knowledge, for the first time in the literature. Unfortunately, this solution becomes singular when cn crosses zero and therefore has no physical relevance.
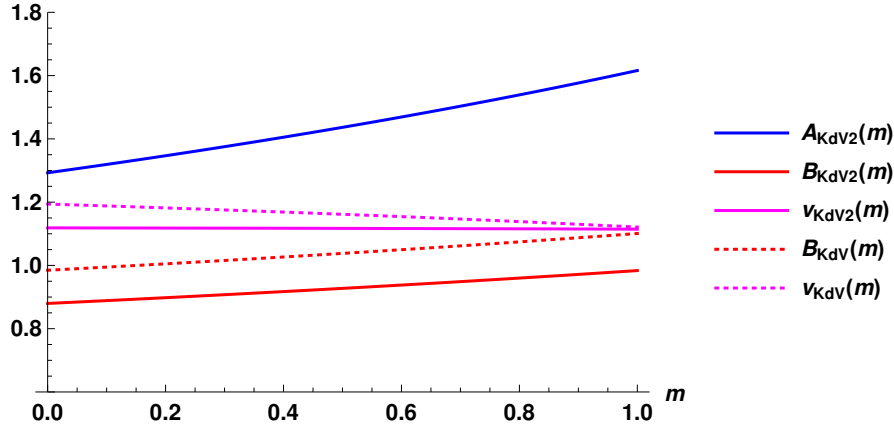
Remark 6.2. Absolute values of coefficients A_1 are large for all $m \in [0, 1]$. One can argue that this is in contradiction with regime of validity of assumptions necessary to derive the equation (5.1).

- **Case 2.** $z = z_2 = \dfrac{43 + \sqrt{2305}}{152} \approx 0.598753 > 0$. Then

$$A_2 = \frac{12\left(51 - \sqrt{2305}\right)}{37\,\alpha\,(5 - m)} \approx \frac{0.9696}{\alpha\,(5 - m)} > 0, \tag{6.64}$$

$$B_2 = \sqrt{\frac{12(-14 + \sqrt{2305})}{703(5 - m)\beta}} \approx \sqrt{\frac{0.58055}{(5 - m)\beta}} > 0, \tag{6.65}$$

$$v_2 \approx \frac{1.11455\,m^2 - 11.2464\,m + 27.9646}{(m - 5)^2}. \tag{6.66}$$

Fig. 6.4. The same as in figure 6.3 but for superposition solutions η_+ (6.30) and η_- (6.68). In this example $\alpha = \beta = 0.15$.

The formula (6.66) for v_2 is obtained by simplification of (6.60). Since $m \in [0,1]$, $(5-m) > 0$ then B_2 is real. The solution in this case is

$$\eta_2(x - v_2 t, m) = \frac{1}{2} A_2 \left[\mathsf{dn}^2(B_2(x - v_2 t), m) \right. \tag{6.67}$$
$$\left. + \sqrt{m}\, \mathsf{cn}(B_2(x - v_2 t), m)\, \mathsf{dn}(B_2(x - v_2 t), m) \right].$$

Coefficients A_2, B_2, v_2 of superposition solutions (6.30) to KdV2 as functions of m are presented in figure 6.4 for $\alpha = \beta = 0.15$ and compared to corresponding solutions to KdV. Here, similarly as in figure 6.3, we assume that $A_{\mathrm{KdV}} = A_{\mathrm{KdV2}}$.

6.2.3 Superposition "$\mathsf{dn}^2 - \sqrt{m}\,\mathsf{cn}\,\mathsf{dn}$"

Now we check the alternative superposition "$\mathsf{dn}^2 - \sqrt{m}\,\mathsf{cn}\,\mathsf{dn}$"

$$\eta_-(y) = \frac{1}{2} A \left[\mathsf{dn}^2(By, m) - \sqrt{m}\, \mathsf{cn}(By, m)\, \mathsf{dn}(By, m) \right]. \tag{6.68}$$

In this case the derivatives are given by formulas similar to (6.31)-(6.34) with some signs altered. Analogous changes occure in formulas (6.36)-(6.42). Then (6.35) has a similar form like (6.43)

$$\frac{1}{2} AB \sqrt{m} \left(-\sqrt{m}\, \mathsf{cn} + \mathsf{dn} \right)^2 \mathsf{sn} \tag{6.69}$$
$$\times \left(F_0 + F_{cd}\, \mathsf{cn}\,\mathsf{dn} + F_{c^2}\, \mathsf{cn}^2 + F_{c^3 d}\, \mathsf{cn}^3\, \mathsf{dn} + F_{c^4}\, \mathsf{cn}^4 \right) = 0.$$

Equation (6.69) is valid for arbitrary arguments when all coefficients F_0, F_{cd}, F_{c^2}, F_{c^3d}, F_{c^4} vanish simultaneously. This gives us a set of equations for the coefficients v, A, B. Despite some changes in signs on the way to (6.69) this set is the same as for "$\mathsf{dn}^2 + \sqrt{m}\,\mathsf{cn}\,\mathsf{dn}$" superposition (6.44)–(6.48). Then the coefficients A, B, v for superposition "$\mathsf{dn}^2 - \sqrt{m}\,\mathsf{cn}\,\mathsf{dn}$" are the same as for superposition "$\mathsf{dn}^2 + \sqrt{m}\,\mathsf{cn}\,\mathsf{dn}$" given above. This property for KdV2 is the same as for KdV, see [90]. It follows from periodicity of the Jacobi elliptic functions. From

$$\mathsf{cn}(y+2K(m), m) = -\,\mathsf{cn}(y, m), \quad \mathsf{dn}(y+2K(m), m) = \mathsf{dn}(y, m)$$

it follows that

$$\mathsf{dn}^2(y+2K(m), m) + \sqrt{(m)}\,\mathsf{cn}(x+2K(m), m)\,\mathsf{dn}(x+2K(m), m)$$
$$= \mathsf{dn}^2(x, m) - \sqrt{(m)}\,\mathsf{cn}(x, m)\,\mathsf{dn}(x, m). \tag{6.70}$$

So, both superpositions η_+ (6.30) and η_- (6.68) represent the same solution, but shifted by the period of the Jacobi elliptic functions. This property is well seen in figures 6.5-6.7.
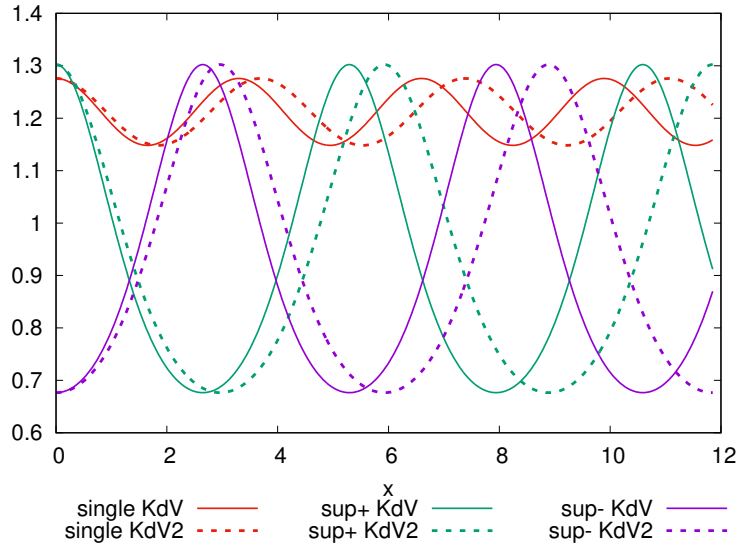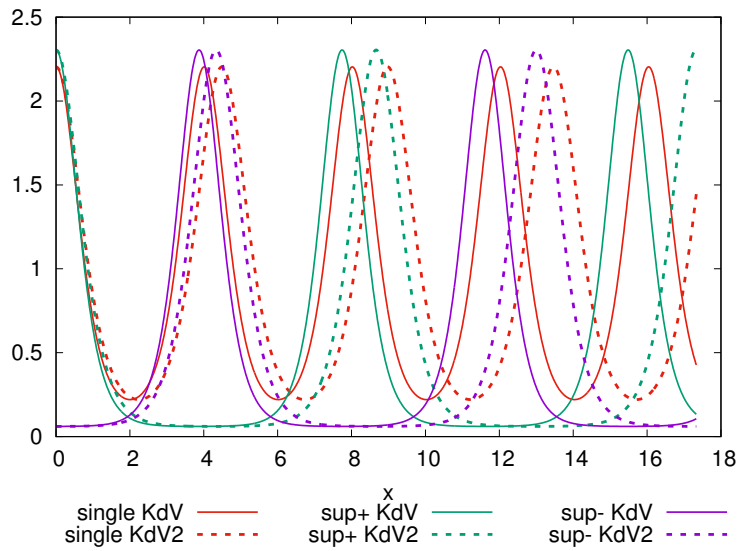

Fig. 6.5. Profiles of KdV and KdV2 waves for $m = 0.1$.

6.2.4 Examples

Below, some examples of wave profiles for both KdV and KdV2 are presented. We know from section 6.1 that for a given m, the coefficients A, B, v of KdV2 solutions are fixed. As we have already written, this is not the case for A, B, v of KdV solutions. So, there is one free parameter. In order to compare KdV2 solutions to those of KdV for identical m, we set $A_{\mathrm{KdV}} = A_{\mathrm{KdV2}}$. In figures 6.5-6.7, KdV solutions of the forms (6.3), (6.30) and (6.68) are drawn with solid red, green and blue lines, respectively. For KdV2 solutions the same color convention is used, but with dashed lines.

Fig. 6.6. Profiles of KdV and KdV2 waves for $m = 0.9$.

Comparison of wave profiles for different m suggests several observations. For small m, solutions given by the single formula (6.3) differ substantially from those given by superpositions (6.30) and (6.68). Note that (6.3) is equal to the sum of both superpositions and when $m \to 1$ the distance between crests of η_+ and η_- increases to infinity (in the $m = 1$ limit). All three solutions converge to the same soliton.
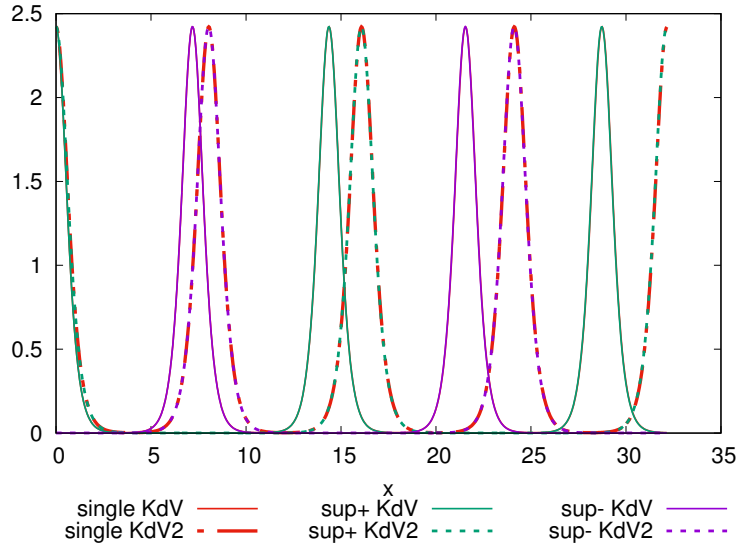
Fig. 6.7. Profiles of KdV and KdV2 waves for $m = 0.99$.

6.2.5 Comments

It is shown that several kinds of analytic solutions of KdV2 have the same forms as the corresponding solutions to KdV but with different coefficients. This statement is true for our single solitonic solutions [79], periodic solutions in the form of single Jacobi elliptic functions cn^2 [70] or dn^2, and for periodic solutions in the form of superpositions $\mathsf{dn}^2 \pm \sqrt{m}\,\mathsf{cn}\,\mathsf{dn}$ [129]. Coefficients A, B, v of these solutions to KdV2 are fixed by coefficients of the equation, that is by values of α, β parameters. This property of KdV2 is different from the KdV case where one coefficient (chosen usually as A) is arbitrary.

6.3 Physical constraints on periodic solutions to KdV and KdV2

Solutions to KdV and KdV2 discussed in Sections 6.1 and 6.2 are correct from the mathematical point of view. However, they do not take into account the fact that the volume of the fluid has to be the same for any amplitudes of the excited waves. This requirement can be fulfilled by the presence of the appropriate coefficient D in the wave profiles (6.71) or (6.75) which depends on the amplitude of the wave.

6.3.1 Constraints on solutions to KdV

Single dn^2 solutions

First, consider periodic solutions in the form of single function dn^2.

Assume solutions to KdV as

$$\eta(x,t) = A\,\mathsf{dn}^2[B(x-vt),m] + D \quad \text{or} \quad \eta(y) = A\,\mathsf{dn}^2[By,m] + D. \quad (6.71)$$

Then substitution of (6.71) into (6.2) yields equation analogous to (6.4). Solution requires vanishing of coefficients C_0 and C_2. Condition $C_2 = 0$ is in this case identical with (6.6) implying the same relation between B and A, that is,

$$B = \sqrt{\frac{3\alpha}{4\beta}}A.$$

The condition $C_0 = 0$, due to nonzero D takes now the form

$$9\alpha A - 9\alpha Am - 4\beta B^2 + 8\beta B^2 m + 9\alpha D - 6v + 6 = 0. \quad (6.72)$$

Then periodicity condition for dn^2 function and volume conservation condition give

$$L = \frac{2K(m)}{B} \qquad \text{and} \qquad D = -\frac{A}{2}\frac{E(m)}{K(m)} \quad (6.73)$$

and from (6.72)

$$v = 1 + \frac{\alpha}{2}A\left(2 - m - \frac{3E(m)}{2K(m)}\right). \quad (6.74)$$

The velocity given by (6.74) is sligtly different (by the last term in the bracket) from that in (6.7). As always for KdV, the amplitude coefficient A can be arbitrary.

Superposition solutions $\eta_\pm$

Assume solutions to KdV in the form analogous to (6.8) with $y = x - vt$

$$\eta_\pm(y) = \frac{A}{2}\left[\mathsf{dn}^2(By,m) \pm \sqrt{m}\,\mathsf{cn}(By,m)\,\mathsf{dn}(By,m)\right] + D, \quad (6.75)$$

where A, B, D, v are yet unknown constants (m is the elliptic parameter) which have the same meaning as in a single dn^2 solution. Coefficient D is necessary in order to maintain, for arbitrary m, the same volume for a wave's elevations and depressions with respect to the undisturbed water level.

Insertion of (6.75) into (6.2) gives equation anlogous to (6.9)

$$CF\left(F_0 + F_2\,\mathsf{cn}^2 + F_{11}\,\mathsf{cn}\,\mathsf{dn}\right) = 0, \tag{6.76}$$

where common factor is $CF = AB\sqrt{m}\left(\sqrt{m}\,\mathsf{cn} + \mathsf{dn}\right)^2\mathsf{sn}$. Then there are three conditions on the solution

$$F_0 = 9\alpha A - 9\alpha Am - 2\beta B^2 + 10\beta B^2 m + 18\alpha D - 12v + 12 = 0, \tag{6.77}$$

$$F_2 = 9\alpha Am - 12\beta B^2 m = 0, \tag{6.78}$$

$$F_{11} = 9\alpha A\sqrt{m} - 12\beta B^2\sqrt{m} = 0. \tag{6.79}$$

Equations (6.78) and (6.79) are equivalent and yield the same

$$B = \sqrt{\frac{3\alpha}{4\beta}}\,A. \tag{6.80}$$

Insertion this into (6.77) gives

$$\alpha A(m - 5) - 4(3\alpha D + 2) + 8v = 0. \tag{6.81}$$

Periodicity condition implies

$$L = \frac{4K(m)}{B}. \tag{6.82}$$

Note that the space period L is for $\eta_\pm$ solutions two times larger than that of dn^2 or cn^2 solutions for the same elliptic parameter m. Then volume conservation condition determines D as

$$D = -\frac{A}{2}\frac{E(m)}{K(m)}. \tag{6.83}$$

Finally insertion of D into (6.81) gives velocity as

$$v = 1 + \frac{\alpha A}{8}\left[5 - m - 6\frac{E(m)}{K(m)}\right] \equiv 1 + \frac{\alpha A}{8}\,\mathrm{fEK}(m). \tag{6.84}$$

Note that the velocity (6.84) is different from (6.14) only by the last term in the square bracket.

$K(m)$ and $E(m)$ which appear in (6.73)-(6.74) and (6.82)-(6.84) are the complete elliptic integral of the first kind and the complete elliptic integral, respectively.

Equations (6.80), (6.83) and (6.84) express coefficients B, D, v of the superposition solution (6.75) as functions of the amplitude A, elliptic parameter $m \in [0, 1]$ and parameters α, β of the KdV equation. In principle, these equations admit arbitrary amplitude A of KdV solution in the form (6.75).

EK(*m*)
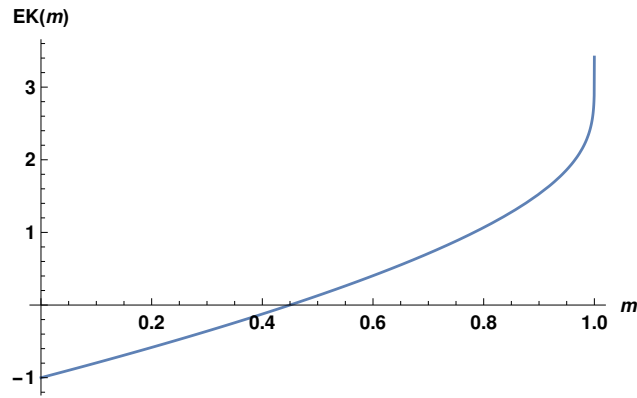
Fig. 6.8. Function fEK(m) given by (6.85).

Coefficients B, D, v and the wavelength L obtained above for solution (6.75) are different form coefficients of usual cnoidal solutions in the form (11.6). In particular, since the function

$$\text{fEK}(m) = \left[5 - m - 6\,\frac{E(m)}{K(m)}\right] \tag{6.85}$$

changes its sign at $m \approx 0.449834$ the velocity dependence of the wave (6.75) is much different than that of the cn^2 wave [For cn^2 wave $v = 1 + \frac{\alpha A}{2m}\left(2 - m - 3\,\frac{E(m)}{K(m)}\right)$], see, [70, equation (24)]. Examples of m dependence of the velocity (6.84) are displayed in figure 6.9.
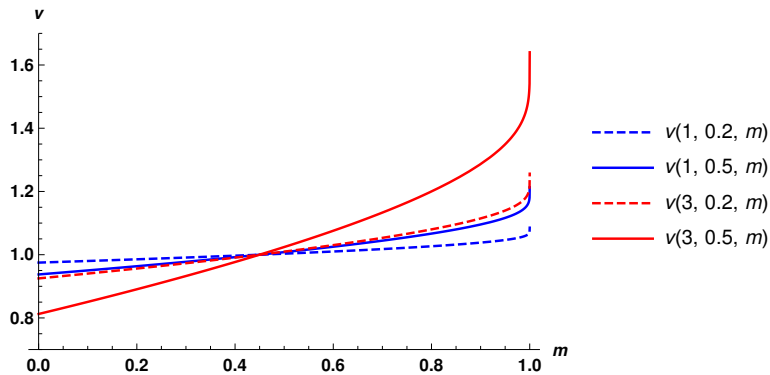
Fig. 6.9. Velocity $v(A, \alpha, m)$ (6.84) of the solution (6.75) for different A and α.

6.3.2 Constrains on superposition solutions to KdV2

Now, we look for solutions to KdV2 (5.1) in the same form (6.75) as solutions to KdV. In this case, the corresponding ODE takes the form (6.15).

Assume solutions to KdV2 in the form (6.75), that is,

$$\eta_\pm(y) = \frac{A}{2} \left[\mathsf{dn}^2(By, m) \pm \sqrt{m}\, \mathsf{cn}(By, m)\, \mathsf{dn}(By, m) \right] + D,$$

where A, B, D, v are yet unknown constants (m is the elliptic parameter) which have the same meaning as previously.

Insertion of (6.75) to (6.15) yields

$$CF\left(F_0 + F_2\, \mathsf{cn}^2 + F_4\, \mathsf{cn}^4 + F_{11}\, \mathsf{cn}\, \mathsf{dn} + F_{31}\, \mathsf{cn}^3\, \mathsf{dn}\right) = 0, \tag{6.86}$$

where common factor is

$$CF = AB\sqrt{m}\left(\sqrt{m}\, \mathsf{cn} + \, \mathsf{dn}\right)^2 \mathsf{sn}.$$

Equation (6.86) is satisfied for arbitrary arguments when all coefficients $F_0, \ldots, F_{31}$ vanish simultaneously. This imposes five conditions on parameters

$$
\begin{aligned}
F_0 &= 135\alpha^2 A^2(m-1)^2 + 60\alpha A(m-1)\left(\beta B^2(48m-5) - 9\alpha D + 18\right) \\
&\quad - 4\left[19\beta^2 B^4\left(61m^2 - 46m + 1\right) + 30\alpha D\left(5\beta B^2(5m-1) + 18\right)\right. \\
&\quad \left. + 60\beta B^2(5m-1) - 135\alpha^2 D^2 + 360\right] + 1440v = 0, \tag{6.87}
\end{aligned}
$$

$$
\begin{aligned}
F_2 &= -15m\left[27\alpha^2 A^2(m-1) - 12\alpha A\left(\beta B^2(37-59m) + 3\alpha D - 6\right)\right. \tag{6.88} \\
&\quad \left. - 16\beta B^2\left(38\beta B^2(2m-1) + 15\alpha D + 6\right)\right] = 0,
\end{aligned}
$$

$$F_4 = 90m^2\left(3\alpha^2 A^2 + 86\alpha A\beta B^2 - 152\beta^2 B^4\right) = 0, \tag{6.89}$$

$$
\begin{aligned}
F_{11} &= -30\sqrt{m}\left[9\alpha^2 A^2(m-1) - 3\alpha A\left(\beta B^2(31-75m) + 6\alpha D - 12\right)\right. \tag{6.90} \\
&\quad \left. - 4\beta B^2\left(19\beta B^2(5m-1) + 30\alpha D + 12\right)\right] = 0,
\end{aligned}
$$

$$F_{31} = 90m^{3/2}\left(3\alpha^2 A^2 + 86\alpha A\beta B^2 - 152\beta^2 B^4\right) = 0. \tag{6.91}$$

As stated in [130], equations (6.89) and (6.91) are equivalent.

Denote $z = \dfrac{\beta B^2}{\alpha A}$. Then z roots of (6.91) are the same as for solitonic solutions [79], cn^2 solutions [70] and $\mathsf{dn}^2 \pm \mathsf{cn}\, \mathsf{dn}$ solutions [129], that is,

$$z_{1/2} = \frac{43 \mp \sqrt{2305}}{152}. \tag{6.92}$$

In principle we should discuss both cases.

Express equations (6.87), (6.88) and (6.90) through z by substituting

$$B = \sqrt{\frac{A\alpha z}{\beta}}. \tag{6.93}$$

This gives

$$608\alpha A(2m-1)z^2 + 12z(\alpha A(37-59m) + 20\alpha D + 8) \tag{6.94}$$
$$-9(3\alpha A(m-1) - 4\alpha D + 8) = 0,$$

$$9A(\alpha - \alpha m) + 76\alpha A(5m-1)z^2 + 3\alpha A(31 - 75m)z \tag{6.95}$$
$$+18\alpha D + 24z(5\alpha D + 2) - 36 = 0$$

from (6.88) and (6.90), respectively, and

$$v = 1 - \frac{\alpha}{1440}\left\{\alpha A^2\left[m^2\left(-4636z^2 + 2880z + 135\right) + m\left(3496z^2 - 3180z - 270\right)\right.\right.$$
$$-76z^2 + 300z + 135\right] - 60A\left[-9\alpha D + m(9\alpha D + 50\alpha Dz + 20z - 18)\right.$$
$$\left.-2z(5\alpha D + 2) + 18\right] + 540D(\alpha D - 4)\right\} \tag{6.96}$$

from (6.87). Equations (6.94) and (6.95) are, in general, not equivalent for arbitrary z. However, in both cases when $z = z_1$ or $z = z_2$, required by (6.89) and (6.91), they express the same condition. This shows that equations (6.88) and (6.90) are equivalent, just as (6.89) and (6.91) are, so equations (6.87)-(6.91) supply only three independent conditions.

Solving (6.94) for D yields

$$D = \left[-27\alpha A + 27\alpha Am - 1216\alpha Amz^2 + 708\alpha Amz + 608\alpha Az^2\right.$$
$$\left.-444\alpha Az - 96z + 72\right] \times \left[12\alpha(20z + 3)\right]^{-1}. \tag{6.97}$$

Substitution of B and D into (6.96) gives a long formula for the wave's velocity

$$v = -\left\{\alpha^2 A^2\left[24320(m(1607m - 1382) + 323)z^4\right.\right.$$
$$-3840(m(7703m - 7368) + 1791)z^3 + 576(m(5919m - 7324) + 2044)z^2$$
$$\left.+4320(m-1)(42m - 19)z + 1215(m-1)^2\right]$$
$$+69120\alpha A(2m-1)z(2z(76z - 43) - 3) - 2880(8z(34z + 75) + 45)\right\}$$
$$\times \left[5760(20z + 3)^2\right]^{-1}. \tag{6.98}$$

The explicit form of (6.98) will be presented in the next section, after specifying the branch of z and taking into account conditions implied by periodicity and volume conservation.

Periodicity and volume conservation conditions

Denote $\quad u(By, m) = \mathsf{dn}^2(By, m) \pm \sqrt{m}\,\mathsf{cn}(By, m)\,\mathsf{dn}(By, m)$.
The periodicity condition implies

$$u\,(BL, m) = u(0, m) \quad \Longrightarrow \quad L = \frac{4\,K(m)}{B}, \tag{6.99}$$

where $K(m)$ is the complete elliptic integral of the first kind. Note that the wavelength L given by (6.99) is two times greater than that for a single cn^2 periodic solution (5.56) (see also [70]).

Then volume conservation requires

$$\int_0^L \eta_\pm(By, m)\,dy = \frac{A}{2}\int_0^L u(By, m)\,dy + D\,L = 0. \tag{6.100}$$

Volume conservation means that elevated and depressed (with respect to the mean level) volumes are the same over the period of the wave.

From properties of elliptic functions

$$\int_0^L u(By, m)\,dy = \frac{E(\mathrm{am}(4K(m)|m)|m)}{B} = \frac{4\,E(m)}{B}, \tag{6.101}$$

where $\quad E(\Theta|m)$ is the elliptic integral of the second kind, $\mathrm{am}(x|m)$ is the Jacobi elliptic function amplitude and $E(m)$ is the complete elliptic integral.

Then from (6.100)-(6.101) one obtains D in the form

$$D = -\frac{A\,E(m)}{2\,K(m)}. \tag{6.102}$$

In order to obtain explicit expressions for coefficients A, B, D, v, one has to specify z. Choose the positive root first.

**Case $\ \ \mathbf{z = z_2} = \frac{43 + \sqrt{2305}}{152} \approx 0.59875.$**

With this choice $A > 0$ and the cnoidal wave has crests elevation larger than troughs depression with respect to still water level.

Substitution of z_2 into equation (6.94) (or equivalently (6.95)) supplies another relation between A and D, giving

$$D = -\frac{12(-51 + \sqrt{2305}) + 37(5 - m)\alpha A}{444\,\alpha}. \tag{6.103}$$

Equating (6.102) with (6.103) one obtains (fEK(m) is given by (6.85))

$$A = \frac{12\left(51 - \sqrt{2305}\right)}{37\alpha\,\mathrm{fEK}(m)}, \tag{6.104}$$
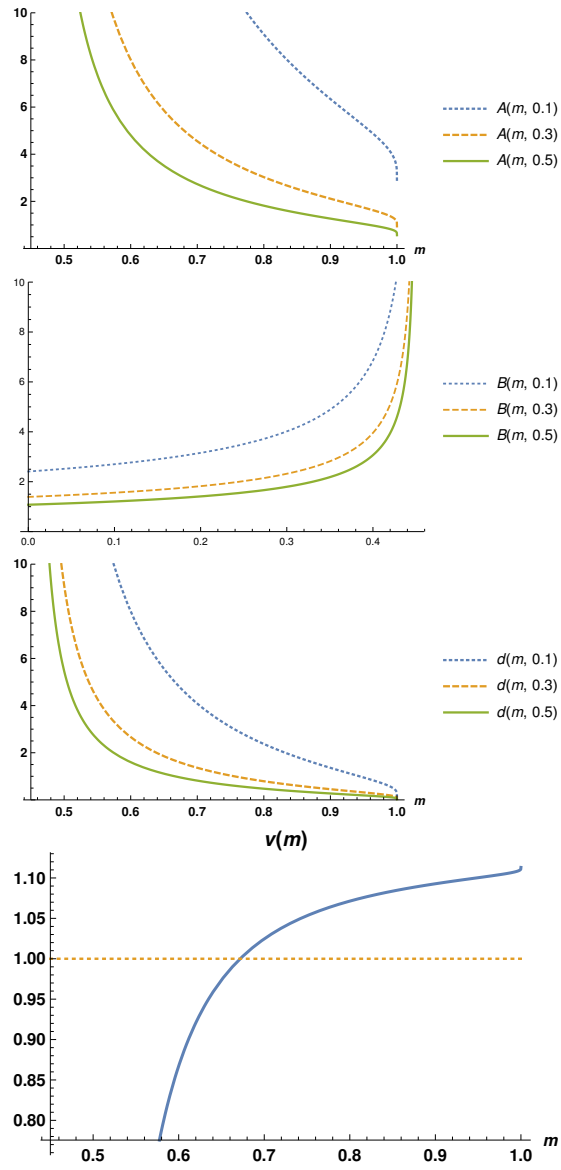
Fig. 6.10. From top to bottom: amplitude $A(m, \alpha)$ (6.104), coefficient B (6.105), coefficient $D(m, \alpha)$ (6.106) and velocity $v(m)$ (6.107) of the solution (6.75) as functions of m for $\alpha = 0.1, 0.3, 0.5$.

$$B = \sqrt{\frac{12(\sqrt{2305} - 14)}{703\beta \,\mathrm{fEK}(m)}}, \tag{6.105}$$

$$D = -\frac{6\left(51 - \sqrt{2305}\right)}{37\alpha \,\mathrm{fEK}(m)} \frac{E(m)}{K(m)}. \tag{6.106}$$

Velocity formula (6.98) simplifies to

$$v = \frac{9439 - 69\sqrt{2305}}{5476} + \left(\frac{7811\sqrt{2305} - 377197}{520220}\right) \frac{\left(m^2 + 14m + 1\right)}{[\mathrm{fEK}(m)]^2} \tag{6.107}$$

$$\approx 1.11875 - 0.00420523 \,\frac{\left(m^2 + 14m + 1\right)}{[\mathrm{fEK}(m)]^2}.$$

In general, as stated in previous papers [70, 79, 129] the KdV2 equation imposes one more condition on coefficients of solutions than KdV. Let us discuss obtained results in more detail. Coefficients A, B, D, v are related to the function $\mathrm{fEK}(m)$. This function is plotted in figure 6.8.

It is clear that for real-valued B the amplitude A has to be positive, and therefore m must be greater than ≈ 0.45. Since B depends on m this condition imposes restricts on wavenumbers. The m-dependence of coefficients A, B, D and velocity v (6.104)-(6.107) are displayed in figure 6.10. Note, that v given by (6.107) contrary to KdV case (6.84) depends only on m.

For m close to 1 the wave height, that is the difference between the crest's and trough's level is almost equal to $A/2$. It is clear from figure 6.10 that the wave height is reasonably small for m close to 1.

Case $\mathbf{z = z_1} = \frac{43 - \sqrt{2305}}{152} \approx -0.0329633.$

$$A = \frac{12\left(\sqrt{2305} + 51\right)}{37\alpha \,\mathrm{fEK}(m)}, \tag{6.108}$$

$$B = \sqrt{-\frac{12(\sqrt{2305} + 14)}{703\beta \,\mathrm{fEK}(m)}}, \tag{6.109}$$

$$D = -\frac{6\left(\sqrt{2305} + 51\right)}{37\alpha \,\mathrm{fEK}(m)} \frac{E(m)}{K(m)}. \tag{6.110}$$

Velocity formula (6.98) simplifies to

$$v = -\frac{9439 + 69\sqrt{2305}}{5476} + \left(\frac{7811\sqrt{2305} + 377197}{520220}\right) \frac{\left(m^2 + 14m + 1\right)}{[\mathrm{fEK}(m)]^2} \tag{6.111}$$

$$\approx -2.32866 + 1.44594 \,\frac{\left(m^2 + 14m + 1\right)}{[\mathrm{fEK}(m)]^2}.$$
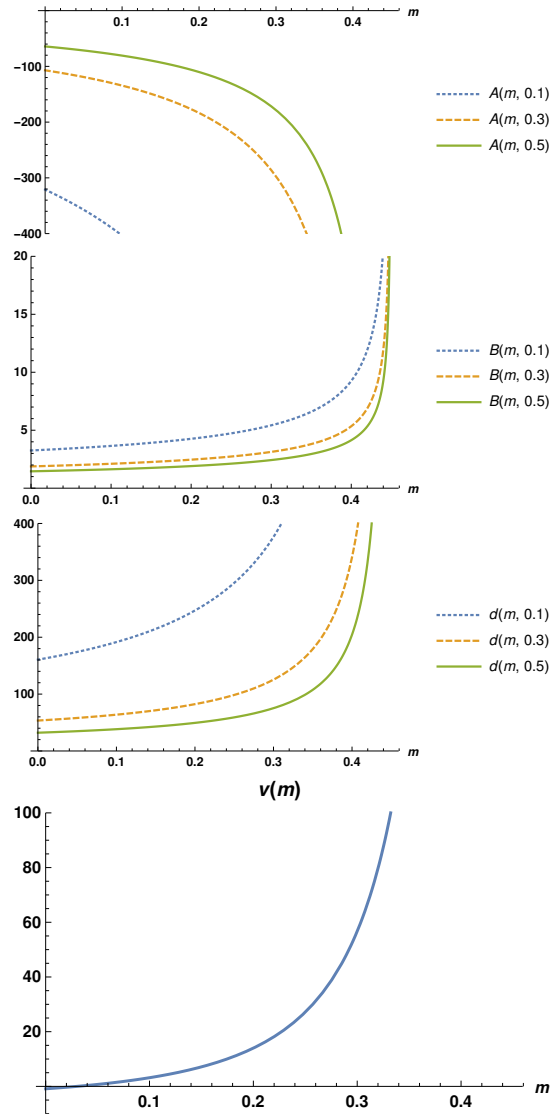
Fig. 6.11. From top to bottom: amplitude $A(m,\alpha)$ (6.108), coefficient $B(m,\beta)$ (6.109), coefficient $D(m,\alpha)$ (6.110) and velocity $v(m)$ (6.111) of the solution (6.75) as functions of m for $\alpha = 0.1, 0.3, 0.5$.

In this case B is real-valued when fEK(m) is negative, that is for m less that ≈ 0.45 (see, e.g, figure 6.8). But this means that A is negative, that is the cnoidal wave has an inverted shape (crests down, troughs up). The following

figure 6.11 illustrates examples of m-dependence of coefficients A, B, D, v for $m < 0.449$.

6.3.3 Examples, numerical simulations

Table 6.1 contains several examples of coefficients A, B, D, v and the wavelength L of superposition solutions to KdV2 for some particular values of α, β and m for the branch $z = z_2$.

Table 6.1. Examples of values of A, B, D, v and L for $z = z_2$ case.

| α	β	m	A	B	D	v	L
0.10	0.10	0.99	4.108	1.5683	-0.5646	1.107	9.426
0.30	0.30	0.99	1.369	0.9054	-0.1882	1.107	16.33
0.50	0.50	0.99	0.822	0.7013	-0.1129	1.107	21.08
0.30	0.30	0.80	3.028	1.3465	-0.7904	1.071	6.706
0.50	0.50	0.80	1.817	1.0430	-0.4743	1.071	8.657

Figure 6.12 displays a comparison of a solution of KdV2 to solution of KdV. For comparison, parameters α, β of the equations were chosen to be $\alpha = \beta = 0.3$. Compared are waves corresponding to $m = 0.99$. Coefficients A, B, D, v of KdV2 solution are given in the second raw of Table 6.1. For comparison KdV solution is chosen with the same A but B, D, v are given by (6.80), (6.83) and (6.84), respectively.

Table 6.2 gives two examples of coefficients A, B, D, v and the wavelength L of superposition solutions to KdV2 for some particular values of α, β and small m for the branch $z = z_1$.

Table 6.2. Examples of values of A, B, D, v and L for $z = z_1$ case.

α	β	m	A	B	D	v	L
0.30	0.30	0.10	-134.5	2.105	63.83	3.170	3.064
0.50	0.50	0.05	-71.44	1.535	34.82	0.717	4.147

In figure 6.13 profiles of the solution to KdV2 for the case $\alpha, \beta = 0.5$ and $m = 0.05$ are displayed for $t = 0, T/3, 2T/3, T$. In this case, we obtain an inverted cnoidal shape, with crest depression equals to -8.885 and trough elevation equals 7.088.
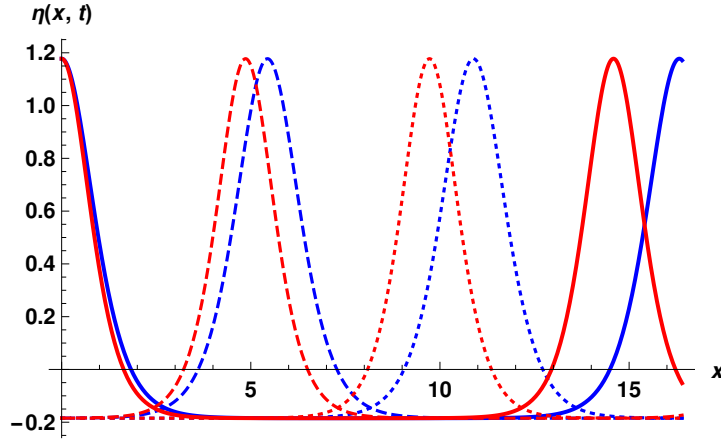
Fig. 6.12. Profiles of the KdV2 (blue lines) and KdV solutions (red lines) for $\alpha = \beta = 0.3$ and $m = 0.99$. Solid lines correspond to $t = 0, T$, dashed lines to $t = T/3$ and dotted lines to $t = 2T/3$, respectively (T is the wave period).

In the case $\alpha, \beta = 0.3$ and $m = 0.1$ the corresponding values of crest and trough are -24.67 and 17.85, respectively.

For m close to 1 the wave height is much smaller than the coefficient A and there exist an interval of small m where the wave height is physically relevant.

Numerical calculations of the time evolution of superposition solutions performed with the finite difference code as used in previous papers [70,78,79, 129] confirm the analytic results. Numerical evolution of any of the presented solution shows their uniform motion with perfectly preserved shapes. The case corresponding to $z = z_2$ branch, with parameters listed in the second row of Table 6.1, is illustrated in figure 6.14. This is the same wave as that displayed in figure 6.12 (blue lines).

The case corresponding to $z = z_1$ branch, with parameters listed in the first row of Table 6.2, is illustrated in figure 6.15. This is the same wave as that displayed in figure 6.13 (blue lines).

Remark 6.3. From periodicity of the Jacobi elliptic functions it follows that

$$\eta_+(x,t) = \eta_-(x \pm L/2, t). \tag{6.112}$$

This means that both $\eta_+(x,t)$ and $\eta_-(x,t)$ represent the same wave, but shifted by half of the wavelength with respect to one another.
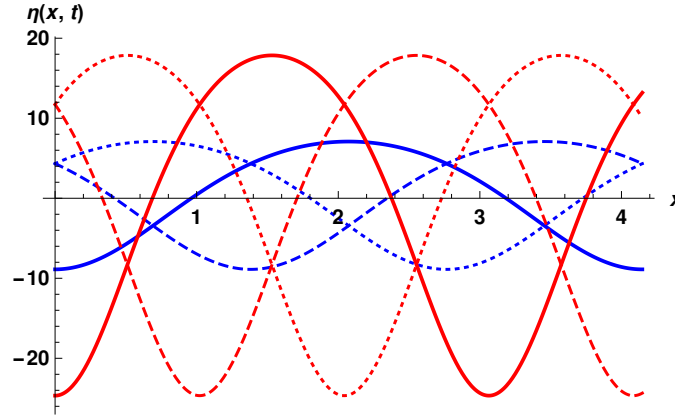
Fig. 6.13. Profiles of the KdV2 solutions for $\alpha = \beta = 0.5$ and $m = 0.05$ (blue lines) and for $\alpha = \beta = 0.3$ and $m = 0.1$ (red lines). Solid lines correspond to $t = 0, T$, dashed lines to $t = T/3$ and dotted lines to $t = 2T/3$, respectively (T is the wave period corresponding to the case).

Conclusions

From the studies on the KdV2 equation presented in this chapter and in $[70, 79, 129, 130]$ one can draw the following conclusions.

- There exist several classes of exact solutions to KdV2 which have the same form as the corresponding solutions to KdV but with slightly different coefficients. These are solitary waves of the form $A\,\text{cn}^2$ [79], cnoidal waves $A\,\text{cn}^2 + D$ [70] and periodic waves in the form (6.75), that is, $\frac{A}{2}[\text{dn}^2 \pm \sqrt{m}\,\text{cn}\,\text{dn}] + D$ studied in $[129, 130]$.
- KdV2 imposes one more condition on coefficients of the exact solutions than KdV.
- Periodic solutions for KdV2 can appear in two forms. The first form, $A\,\text{cn}^2 + D$, is, as pointed out in [70], physically relevant in two narrow intervals of m, one close to $m = 0$, another close to $m = 1$. The second form, given by (6.75) gives physically relevant periodic solutions in similar intervals. However, for m close to 1 the superposition solution (6.75) forms a wave similar to $A\,\text{cn}^2 + D$, whereas for small m this wave has inverted cnoidal shape.
- All the above-mentioned solutions to KdV2 have the same function form as the corresponding KdV solutions but with slightly different coefficients.
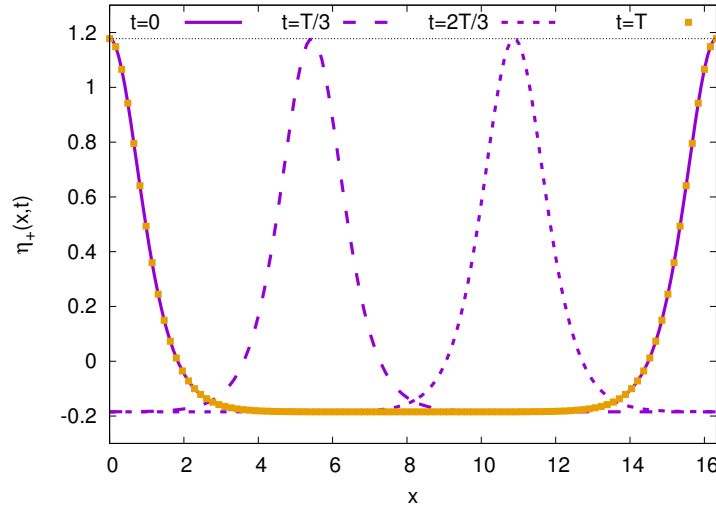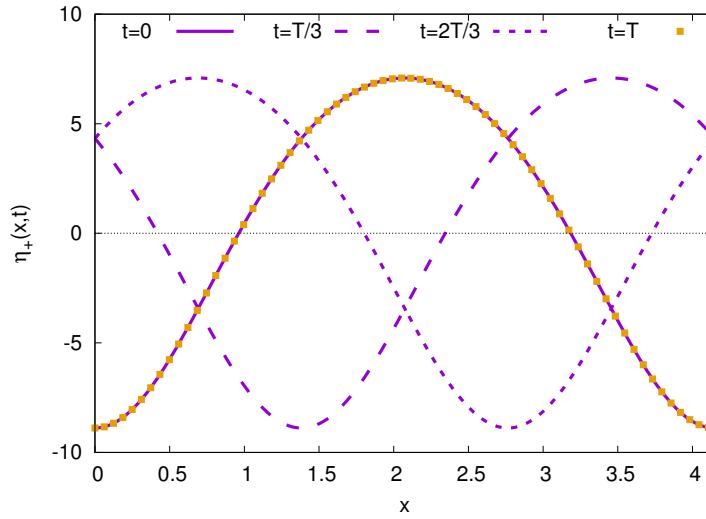
Fig. 6.14. Time evolution of the superposition solution $\eta_+(x,t)$ for $\alpha = \beta = 0.3$ and $m = 0.99$ obtained in numerical simulations. Profiles of the wave at $t = 0, T/3, 2T/3, T$ are shown, where T is the period. The x interval is equal to the wavelength.

Besides having single solitonic and periodic solutions, KdV also possesses multi-soliton solutions. The question whether exact multi-soliton solutions for KdV2 exist is still open. However, numerical simulations presented in the subsection 6.3.4, in line with the Zabusky-Kruskal numerical experiment [150] suggest such a possibility.

### 6.3.4 Do multi-soliton solutions to KdV2 exist?

For KdV there exist multi-soliton solutions which can be obtained, e.g. using the inverse scattering method [2, 48], nonlinear superposition principle based on auto-Backlund transformations [142] or the Hirota direct method [65]. The fact that KdV2 is nonintegrable would seem to exclude the existence of multi-soliton solutions to KdV2. On the other hand, numerical simulations demonstrate, that for some initial conditions a train of KdV2 solitons, almost the same as of KdV solitons emerges from the cosine wave as in Zabusky and Kruskal [150] numerical simulation. Below we describe such numerical simulations with results displayed in figure 6.16.

Fig. 6.15. Time evolution of the superposition solution $\eta_+(x,t)$ for $\alpha = \beta = 0.3$ and $m = 0.05$ obtained in numerical simulations. Profiles of the wave at $t = 0, T/3, 2T/3, T$ are shown, where T is the period. The x interval is equal to the wavelength.

Initial conditions for both simulations were chosen as a hump $\eta(x,0) = A\cos(\frac{\pi}{40}(x+20))$ for $0 \leq x \leq 40$ and $\eta(x,0) = 0$ for $x > 40$ moving to the right. Then such a wave was evolved by a finite difference method code developed in [78–80]. There is a surprising similarity of trains of solitons obtained in evolutions with KdV and KdV2. This behavior might suggest the possible existence of multi-soliton KdV2 solutions.

In a multi-soliton solution of KdV, each soliton has a different amplitude. Otherwise, these amplitudes are arbitrary. KdV2 always imposes one more condition on coefficients of the solutions than does KdV. Therefore if multi-soliton solutions to KdV2 exist, we would expect some restrictions on these amplitudes.
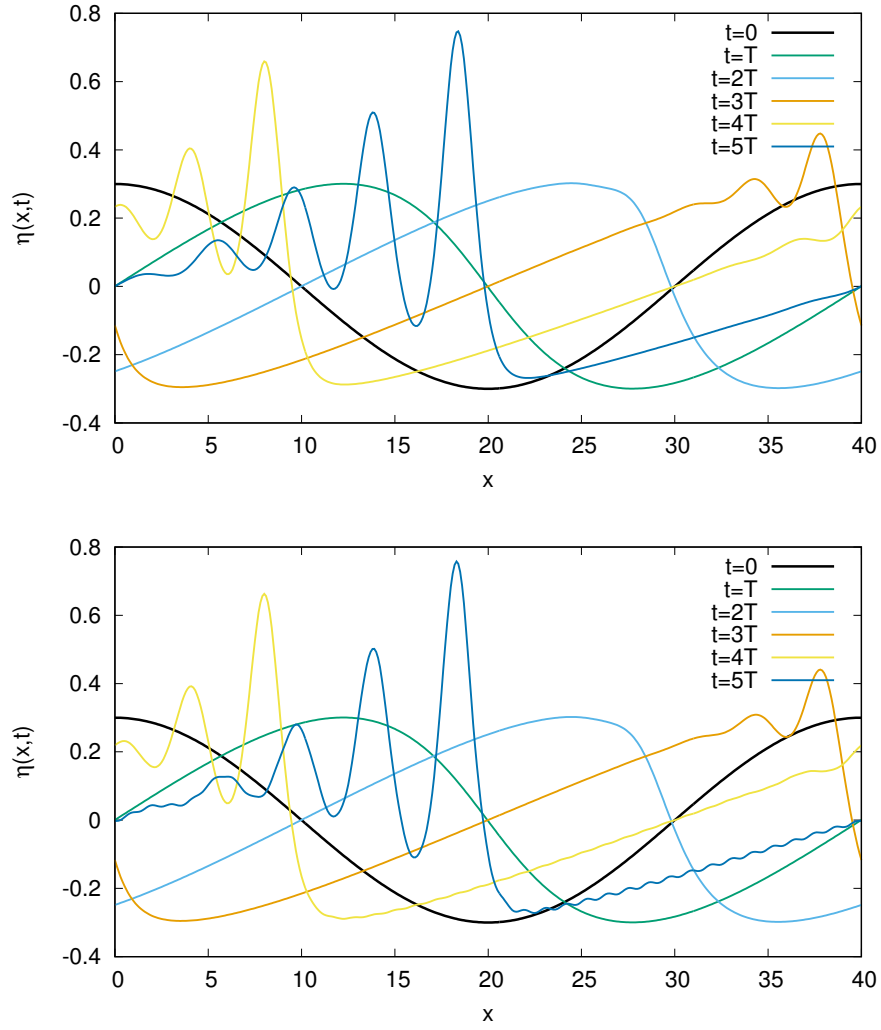
Fig. 6.16. Top: Emergence of soliton trains according to KdV from initial cosine wave. $A = 0.3$, $T = 50$. Bottom: The same according to KdV2.

7

Approximate analytic solutions to KdV2 equation for uneven bottom

The ubiquitous Korteweg–de Vries equation [96] is a common approximation for several problems in nonlinear physics. One of these problems is the *shallow water wave problem* extensively studied during the last fifty years and described in many textbooks and monographs (see, e.g., [2, 36, 66, 72, 117, 123, 127, 144]). The KdV equation corresponds to the case when the water depth is constant. There have been numerous attempts to study nonlinear waves in the case of a non-flat bottom. One of the first attempts to incorporate bottom topography is due to Mei and Le Méhauté [111]. However, the authors did not obtain any simple KdV-type equation. Among the first papers treating a slowly varying bottom is Grimshaw's paper [53]. He obtained an asymptotic solution describing a slowly varying solitary wave above a slowly varying bottom. For small amplitudes, the wave amplitude varies inversely as the depth. Djordjević and Redekopp [34] studied the development of packets of surface gravity waves moving over an uneven bottom. They derived the variable coefficient nonlinear Schrödinger equation (NLS) for such waves and using expansion in a single small parameter they found fission of an envelope soliton. Benilov and Howlin [11] later developed a similar approach. This fission from the NLS has also been found in other physical contexts [11, 72].

We point out papers [57, 116, 124] as examples of approaches which combine linear and nonlinear theories. For instance, in [116] the authors study long-wave scattering by piecewise-constant periodic topography for solitary-like wave pulses and KdV solitons. Another extensively investigated approach is the Gardner equation (sometimes called the forced KdV equation) [58, 77, 134]. Van Groeasen and Pudjaprasetya [?, 126] within a Hamiltonian approach. For a slowly varying bottom, they obtained a forced KdV-type equation. The dis-

cussion of that equation gives an increase of the amplitude and decrease of the wavelength when a solitary wave enters a shallower region. The Green-Naghdi equations follow when taking an appropriate average of vertical variables [50, 89, 115]. Another study of long wave propagation over a submerged 2-dimensional bump was recently presented in [118], albeit according to linear long-wave theory.

An interesting numerical study of solutions to the free-surface Euler equations in the conformal-mapping formulation has been published by the team working within the MULTIWAVE project [114]. The authors illustrate that approach by numerical results for soliton fission over a submerged step and supercritical stream over a submerged obstacle [140].

In this chapter, we briefly summarize the derivation of a KdV-type equation, second order in small parameters, containing terms from the bottom function, derived by us in [78]. Next, we present some examples of the evolution of a KdV soliton according to that equation, obtained in numerical simulations, stressing changes of soliton's velocity and amplitude when the wave passes over an extended obstacle or hole. It is worth noting that the equation derived in [78] is a KdV-like equation of the second order, a single evolution equation for surface waves which contains terms for a bottom variation. In this context see a paper by Kichenassamy and Olver "Existence and nonexistence of solitary wave solutions to higher-order model evolution equations" [88]. The authors claimed *for most of the higher-order models, but only those which reduce to KdV solitary waves in an appropriate scaling limit, solitary wave solutions of the appropriate form do not exist!* On the other hand, Burde [23] presents solitary wave solutions of the higher-order KdV models for bi-directional water waves.

Recently, with E. Infeld and G. Rowlands, we found exact solitonic [79] and periodic [70] wave solutions for water waves moving over a smooth riverbed. Amazingly they were simple, though governed by a more exact expansion of the Euler equations with several new terms as compared to KdV [24, 78, 79, 105]. Our next step is to consider how a rough river or ocean bottom modifies these results. We start with a simple case. The geometry is one space dimensional, and the wave is a soliton.

Here we consider the KdV2B equation (4.31) (introduced in section 4.2) governing the elevation of the water surface η/H above a flat equilibrium at the surface. For reader's convenience it is rewritten below

$$\eta_t + \eta_x + \alpha\frac{3}{2}\eta\eta_x + \beta\frac{1}{6}\eta_{3x}$$

$$+ \alpha^2\left(-\frac{3}{8}\eta^2\eta_x\right) + \alpha\beta\left(\frac{23}{24}\eta_x\eta_{2x} + \frac{5}{12}\eta\eta_{3x}\right) + \beta^2\frac{19}{360}\eta_{5x} \qquad (7.1)$$

$$+ \beta\delta\frac{1}{4}\left(-\frac{2}{\beta}(h\eta)_x + (h_{2x}\eta)_x - (h\eta_{2x})_x\right) = 0.$$

The last three terms are due to a bottom profile. We emphasize, that (7.1) was derived in [78, 79] under the assumption that α, β, δ are small (positive by definition) and of the same order. The details of the derivation of KdV2B equation are contained in section 4.2.

This chapter presents an attempt, made in [128], to describe dynamics of the exact KdV2 soliton when it approaches a finite interval of an uneven bottom. We will use the reductive perturbation method introduced by Taniuti and Wei [137]. Using two space scales allows us to transform equation for the uneven bottom (7.1) into KdV2 equation with some coefficients altered, that is, the equation for the flat bottom. This transformation is approximate, but the analytic solution of the resulted equation is known. This approximate analytic description will be compared with 'exact' numerical calculations.

As already described in section 5.2 the exact single soliton solution of the KdV2 equation (4.27) (which is also equivalent to (7.1) with $\delta = 0$, or $h = 0$) has the same form as the KdV soliton

$$\eta(x,t) = A\,\mathsf{sech}[B(x - vt)]^2. \qquad (7.2)$$

However, coefficients A, B, v of the KdV2 soliton given in equations (5.30)-(5.32), are slightly different than those for the KdV soliton, see their comparison in section 5.2. Let us remind that on the way to the derivation of the solution three intermediate conditions for the coefficients have been obtained (5.22)-(5.24). These three conditions are as follows

$$(1 - v) + \frac{2}{3}B^2\beta + \frac{38}{45}B^4\beta^2 = 0, \qquad (7.3)$$

$$\frac{3A\alpha}{4} - B^2\beta + \frac{11}{4}A\alpha B^2\beta - \frac{19}{3}B^4\beta^2 = 0, \qquad (7.4)$$

$$-\left(\frac{1}{8}\right)(A\alpha)^2 - \frac{43}{12}A\alpha B^2\beta + \frac{19}{3}B^4\beta^2 = 0. \qquad (7.5)$$

Denoting $z = \dfrac{\beta B^2}{\alpha A}$ one obtains (7.5) as quadratic equation with respect to z with solutions

$$z_1 = \frac{43 - \sqrt{2305}}{152} \approx -0.033 < 0 \quad \text{and} \quad z_2 = \frac{43 + \sqrt{2305}}{152} \approx 0.599 > 0. \quad (7.6)$$

Since $B = \sqrt{\frac{\alpha}{\beta} z A}$, only z_2 provides real B value. Equations (7.4) and (7.5) are consistent only when $\alpha = \alpha_s = \dfrac{3(51 - \sqrt{2305})}{37} \approx 0.242399$. Then (7.3) determines velocity

$$v = 1 + \frac{2}{3} \alpha_s z_2 + \frac{38}{45} (\alpha_s z_2)^2 \approx 1.114546. \tag{7.7}$$

7.1 Approximate analytic approach to KdV2B equation

Equation (7.1) can be written in the form

$$\frac{\partial \eta}{\partial t} + \frac{\partial}{\partial x} f(\eta, h) = 0, \tag{7.8}$$

where $f(\eta, h)$ is given by

$$f(\eta, h) = \eta + \frac{3\alpha}{4} \eta^2 - \frac{\alpha^2}{8} \eta^3 + \alpha\beta \left[\frac{13}{48} \left(\frac{\partial \eta}{\partial x} \right)^2 + \frac{5}{12} \eta \frac{\partial^2 \eta}{\partial x^2} \right] + \frac{\beta}{6} \frac{\partial^2 \eta}{\partial x^2}$$
$$+ \frac{19}{360} \beta^2 \frac{\partial^4 \eta}{\partial x^4} + \beta\delta \left[-\frac{2}{\beta} h\eta + \frac{\partial^2 h}{\partial x^2} \eta - h \frac{\partial^2 \eta}{\partial y^2} \right]. \tag{7.9}$$

We treat h as slowly varying and introduce two space scales x and $x_1 (= \epsilon x)$ which are treated as independent until the end of calculation [137]

$$h = h(\epsilon x) = h(x_1), \qquad \epsilon \ll 1. \tag{7.10}$$

We also introduce

$$y = \int_0^x a(\epsilon x) dx - t, \tag{7.11}$$

where a is as yet undefined. To first order in ϵ

$$\eta = \eta_0(y, x_1) + \epsilon \eta_1(y, x_1) + \dots \tag{7.12}$$

$$\frac{\partial \eta}{\partial t} = -\frac{\partial \eta_0}{\partial y} - \epsilon \frac{\partial \eta_1}{\partial y} + \dots \tag{7.13}$$

$$\frac{\partial \eta}{\partial x} = a(x_1) \frac{\partial \eta_0}{\partial y} + \epsilon \frac{\partial \eta_0}{\partial x_1} + \epsilon a(x_1) \frac{\partial \eta_1}{\partial y} + \dots \tag{7.14}$$

$$\frac{\partial^2 \eta}{\partial x^2} = a^2 \frac{\partial^2 \eta_0}{\partial y^2} + \epsilon \left(\frac{\partial a}{\partial x_1} \frac{\partial \eta_0}{\partial y} + 2a \frac{\partial^2 \eta_0}{\partial y \partial x_1} + a^2 \frac{\partial^2 \eta_0}{\partial y^2} \right) + \dots \tag{7.15}$$

Now

$$\frac{\partial^n \eta}{\partial x^n} = a^n \frac{\partial^n \eta_0}{\partial y^n} + O(\epsilon). \tag{7.16}$$

We have

$$f(\eta, h) = \eta_0 + \frac{3\alpha}{4}\eta_0^2 - \frac{\alpha^2}{8}\eta_0^3 + \alpha\beta\left[\frac{13}{48}a^2\left(\frac{\partial\eta_0}{\partial y}\right)^2 + \frac{5}{12}\eta_0 a^2\frac{\partial^2\eta_0}{\partial y^2}\right]$$

$$+ \frac{\beta}{6}a^2\frac{\partial^2\eta_0}{\partial y^2} + \frac{19}{360}\beta^2 a^4\frac{\partial^4\eta_0}{\partial y^4} \tag{7.17}$$

$$+ \beta\delta\left[-\frac{h(x_1)\eta_0}{2\beta} - a^2 h(x_1)\frac{\partial^2\eta_0}{\partial y^2}\right] + O(\epsilon) = f_0(\eta_0, h) + O(\epsilon).$$

From (7.8), (7.13) and (7.17) to lowest order we have

$$-\frac{\partial\eta_0}{\partial y} + a\frac{\partial}{\partial y}\left[f_0(\eta_0, h)\right] = 0 \tag{7.18}$$

and, since $a = a(x_1)$, we obtain

$$\frac{\partial}{\partial y}(\eta_0 - af_0) = 0. \tag{7.19}$$

We restrict consideration to a single soliton, so $\eta_0 \to 0$ as $y \to \pm\infty$ and so does f_0. Integration of (7.19) yields to the lowest order

$$\eta_0 - a(x_1)f_0 = 0. \tag{7.20}$$

Introduce $\zeta = y/a(x_1)$ which is constant in our approximation. Now

$$\frac{\partial\eta_0}{\partial y} = \frac{1}{a}\frac{\partial\eta_0}{\partial\zeta} \tag{7.21}$$

and from (7.20), (7.17), (7.21) we obtain

$$(1 - a(x_1))\eta_0 - \frac{3\alpha}{4}\eta_0^2\, a + \frac{\alpha^2}{8}\eta_0^3\, a - \alpha\beta\left[\frac{13}{48}\left(\frac{\partial\eta_0}{\partial\zeta}\right)^2 + \frac{5}{12}\eta_0\frac{\partial^2\eta_0}{\partial\zeta^2}\right]a \quad (7.22)$$

$$- \frac{19}{360}\beta^2\frac{\partial^4\eta_0}{\partial\zeta^4}\, a + \beta\delta\, h(x_1)\left[\frac{\eta_0}{2\beta} + \frac{\partial^2\eta_0}{\partial\zeta^2}\right]a - \frac{\beta}{6}\frac{\partial^2\eta_0}{\partial\zeta^2}\, a = 0.$$

Dividing by $(-a)$ yields

$$\left(1 - \frac{\delta\, h}{2} - \frac{1}{a}\right)\eta_0 + \frac{3\alpha}{4}\eta_0^2 - \frac{\alpha^2}{8}\eta_0^3 + \alpha\beta\left[\frac{13}{48}\left(\frac{\partial\eta_0}{\partial\zeta}\right)^2 + \frac{5}{12}\eta_0\frac{\partial^2\eta_0}{\partial\zeta^2}\right]$$

$$+ \frac{19}{360}\beta^2\frac{\partial^4\eta_0}{\partial\zeta^4} + \frac{\beta}{6}\left(1 - 6\,\delta\, h\right)\frac{\partial^2\eta_0}{\partial\zeta^2} = 0. \tag{7.23}$$

This should be compared to (4.27) or [79, equation (22)]. Remember that at this stage $\delta\, h(x_1)$ is to be treated as constant with respect to inegration over

ζ. The only difference is that $v = \left(\dfrac{\delta h}{2} + \dfrac{1}{a}\right)$ and $(1 - 6\,\delta\,h)$ instead of 1 appear in the last term.

Following [79] we obtain

$$\eta_0 = A\operatorname{sech}^2(B\,\zeta), \qquad \zeta = \frac{1}{a(x_1)}\left[\int_0^x a(x_1)dx - t\right]. \qquad (7.24)$$

In equations (7.3)-(7.4) [(24),(25) and (20) of [79]] we replace $\beta\,B^2$ (but not $\beta^2 B^4$ or $\alpha\beta AB^2$ since we modify only first order terms) by

$$\beta\,(1 - 6\,\delta\,h)\,B^2. \qquad (7.25)$$

Now $z = z_2 = \frac{43+\sqrt{2305}}{152}$ is as in (7.6). We obtain

$$\eta_0 = \bar{A}\operatorname{sech}^2\left[\frac{\bar{B}}{a(x_1)}\left(\int_0^x a(x_1)dx - t\right)\right] \qquad (7.26)$$

with

$$\frac{1}{a} + \frac{\delta\,h}{2} = v - \beta\delta h, \qquad q = \frac{b}{B^2}, \qquad b = \frac{3z}{\frac{76}{3}z - 11} \qquad (7.27)$$

and

$$\bar{A} = A(1 + q\delta h), \qquad \bar{B} = B(1 + q\delta\,h/2),$$

where A, B, v are given by eqs. (30)-(32) in [79]. Thus

$$\frac{1}{a} = v - \left(\frac{1}{2} + \beta\right)\delta h. \qquad (7.28)$$

At this stage we take $x_1 = \epsilon\,x$ and $\delta h = \delta h(x)$. So

$$\int_0^x a(x)\,dx = \int_0^x \frac{dx}{v - \left(\frac{1}{2} + \beta\right)\delta h(x)}. \qquad (7.29)$$

Assume $\delta h(x)$ is nonzero only in interval $x \in [L_1, L_2]$.

For $x < L_1$, $\quad \eta_0 = A\operatorname{sech}^2(B(x - vt))$, $\quad \delta h \equiv 0$, $\frac{1}{a} = v$.

For $x > L_2$, $\quad \delta h \equiv 0$, $\frac{1}{a} = v$ and

$$\eta_0 = A\operatorname{sech}^2\left[B\left(v\int_{L_1}^{L_2} a(x)dx + (x - vt)\right)\right]. \qquad (7.30)$$

There is a change of phase as the pulse passes through the region where $\delta h \neq 0$. The alteration in the phase is given by

$$\int_{L_1}^{L_2} dx\left[\frac{1}{1 - \frac{(1/2+\beta)\delta h}{v}} - 1\right] \approx \frac{\beta + 1/2}{v}\int_{L_1}^{L_2}\delta\,h(x)\,dx. \qquad (7.31)$$

If this integral is zero phase is unaltered. This can happen if a deeper region is followed by a shallower region of appropriate shape or vice versa.

7.2 Numerical tests

In the following figures, we present time evolution of the approximate analytic solution (7.26) to KdV2 equation with the uneven bottom (7.1) for several values of parameters of the system. These evolutions are compared with 'exact' numerical solutions of (7.1). In both cases, initial conditions were the exact solutions of KdV2 equation. Therefore in all presented examples $\alpha = \alpha_s$ and the amplitude of initial soliton is equal to 1.
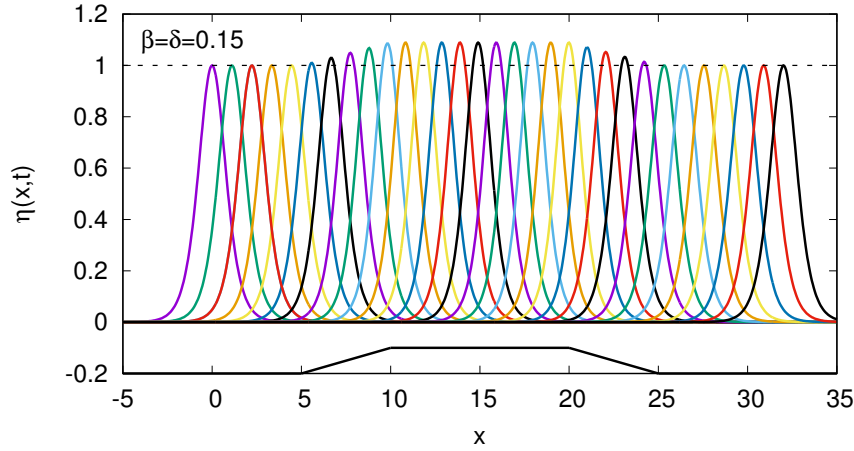
Fig. 7.1. Profiles of the soliton as given by (7.26). The shape of the trapezoidal bottom is shown (not in scale). Consecutive times are $t_n = n, \ n = 0, 1, 2, 3, \ldots, 32$.

In figure 7.1 we present the approximate solution (7.26) for the case when soliton moves over a trapezoidal elevation with $L_1 = 5$ and $L_2 = 25$. We took $\beta = \delta = 0.15$. For smaller δ the effects of uneven bottom are very small, for larger δ second order effects (not present in analytic approximation) cause stronger overlaps of different profiles.

We compare this approximate solution of (7.1) to a numerical simulation obtained with the same initial condition. The evolution is shown in figure 7.2. We see that the approximate solution has the main properties of the soliton motion as governed by equation (7.1). However, since the numerical solution contains higher order terms depending on the shape of h the exact motion as obtained from numerics shows additional small amplitude structures known from earlier papers, for example, [78,79]. This is clearly seen in figure 7.3 where
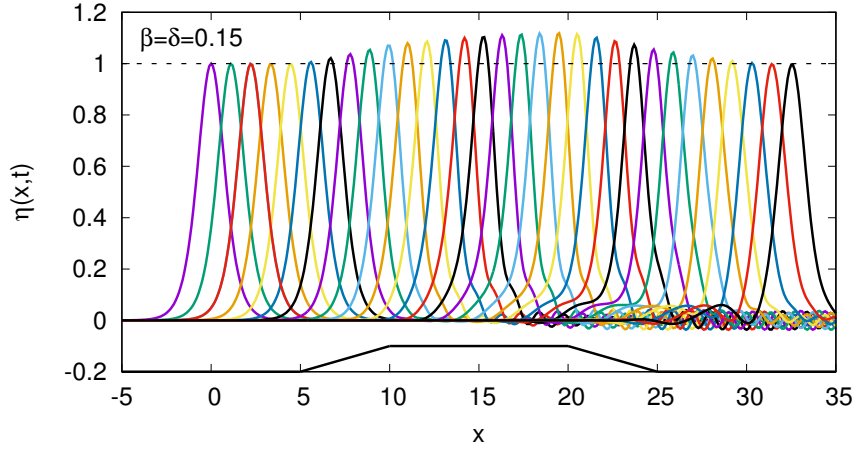
Fig. 7.2. Profiles of numerical solution of the equation (7.1) obtained with the same initial condition. Time instants the same as in figure 7.1.

profiles obtained in analytic and numeric calculations are compared at time instants $t = 0, 5, 10, 15, 20, 25, 30$ on wider interval of x. All numerical results were obtained with calculations performed on wider interval $x \in [-30, 70]$ with periodic boundary conditions. Details of numerics was described in [70,78,79].

In figures 7.4-7.6 we present results analogous to those presented in figures 7.1-7.3 but with a different shape of the bottom bump and larger values of $\beta = \delta = 0.2$. In this case the bump is chosen as an arc of parabola $h(x) = 1 - (x - 15)^2/100$ between the same $L_1 = 5$ and $L_2 = 24$ as in trapezoidal case.

In approximate analytic solution, KdV2 soliton changes its amplitude and velocity only over bottom fluctuation. When the bottom bump is passed it comes back to initial shape (phase only may be changed). This is not the case for 'exact' numerical evolution of the same initial KdV2 soliton when it evolves according to the second order equation (7.1). This is clearly visible in figures 7.3 and 7.6. What is this motion for much larger times? In order to answer this question, one has to perform numerical calculations on a much wider interval of x. Such results are presented in figure 7.7. The interaction of soliton with the bottom bump creates two wave packets of small amplitudes. First moves with higher frequency faster than the soliton and is created when soliton enters the bump, second moves slower with lower frequency and appears when soliton leaves it. After some time both are separated from the main wave. Since
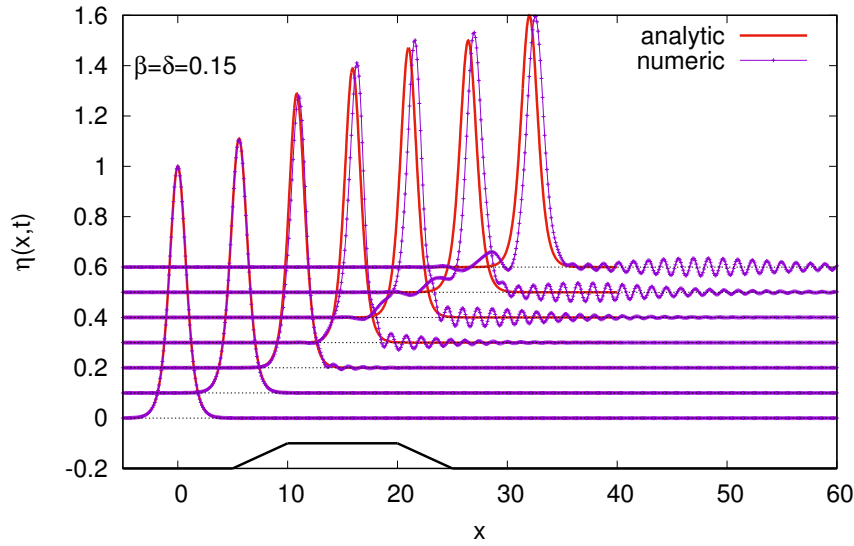
Fig. 7.3. Comparison of +48 68 3282 909wave profiles shown if figures 7.1 and 7.2 for time instants $t = 0, 5, 10, 15, 20, 25, 30$. Consecutive profiles are vertically shifted by 0.1.

periodic boundary conditions were used in the numerical algorithm, the head of the wave packet, radiated forward, traveled for $t = 152$ larger distance than the interval chosen for calculation and is seen at the left side of the wave profile.

We have to emphasize that this behavior is generic, it looks similar for different shapes of bottom bumps and different values of β, δ parameters. It was observed in our earlier papers [79, 80, 82] in which initial conditions were in the form of KdV soliton.

We have derived a simple formula describing approximately a soliton encountering an uneven riverbed. The model reproduces the known increase in amplitude when passing over a shallower region, as well as the change in phase. However, the full dynamics of the soliton motion is much richer, the uneven bottom causes low amplitude soliton radiation both ahead and after the main wave. This behavior was observed in our earlier papers [79, 80, 82] in which initial conditions were in the form of KdV soliton, whereas in the present cases the KdV2 soliton, that is, the exact solution of the KdV2 equation was used.
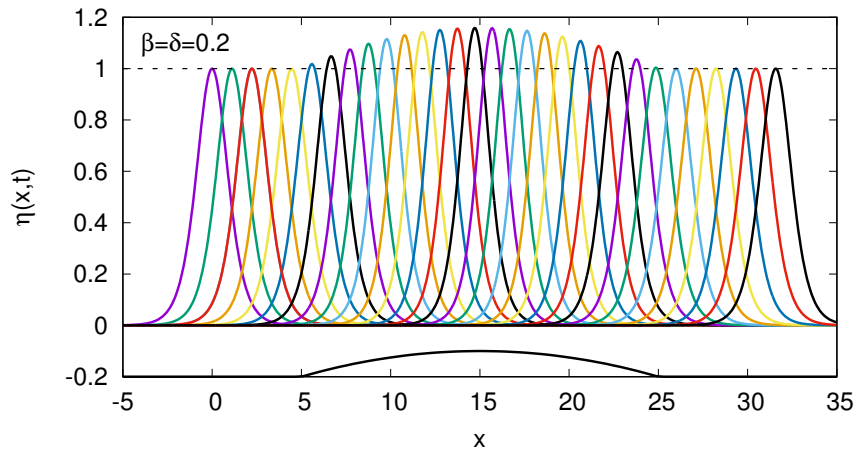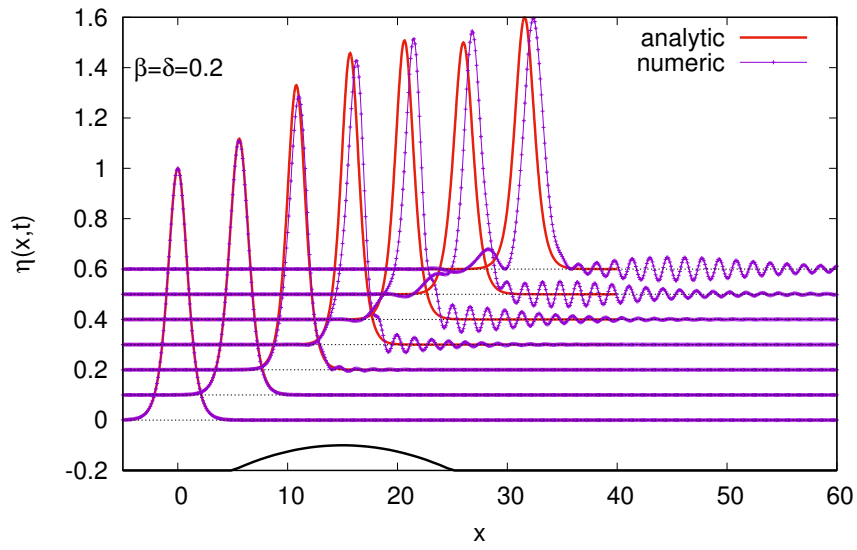
Fig. 7.4. Profiles of the soliton as given by (7.26). The shape of the trapezoidal bottom is shown (not in scale). Consecutive times are $t_n = n, \ \ n = 0, 1, 2, 3, \ldots, 32$.
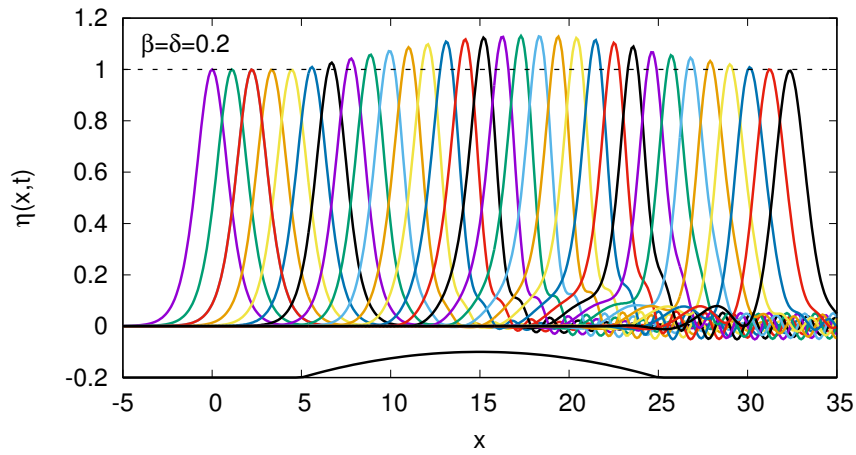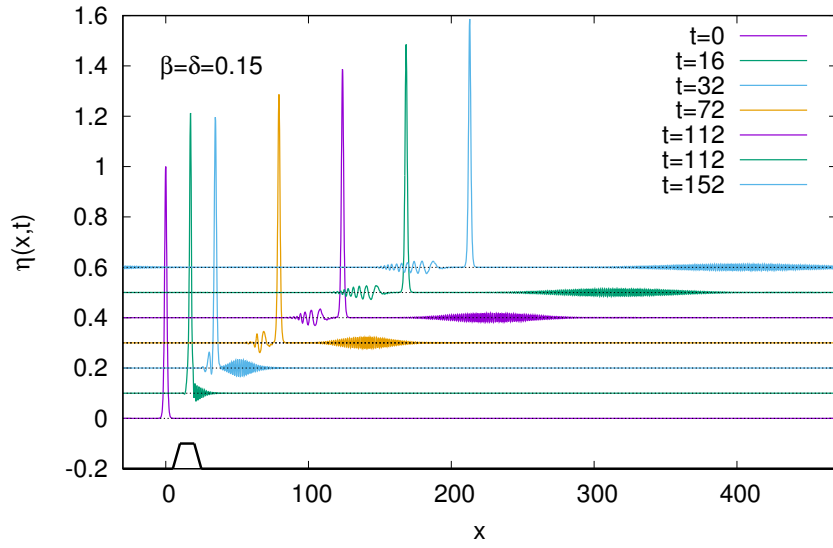

Fig. 7.5. Profiles of numerical solution of the equation (7.1) obtained with the same initial condition. Time instants the same as in figure 7.4.

Fig. 7.6. Comparison of wave profiles shown if figures 7.4 and 7.5 for time instants $t = 0, 5, 10, 15, 20, 25, 30$.

Fig. 7.7. Long time numerical evolution with trapezoidal bottom bump for $\beta = \delta = 0.15$.

8

Conservation laws

It is well known, see, e.g., $[36, 112, 113, 117]$, that for the KdV equation there exists an infinite number of invariants, that is, integrals over space of functions of the wave profile and its derivatives, which are constants in time. Looking for analogous invariants for the second order KdV equation we met with some problems even for the standard KdV equation (which is first order in small parameters). This problem appears when energy conservation is considered.

In this chapter, we reconsider invariants of the KdV equation and formulas for the total energy in several different approaches and different frames of reference (fixed and moving ones). We find that the invariant $I^{(3)}$, sometimes called the energy invariant, does not always have that interpretation. We also give a proof that for the second order KdV equation, obtained in $[24, 78, 79, 105]$, $\int_{-\infty}^{\infty} \eta^2 dx$ is not an invariant of motion.

There are many papers considering higher-order KdV type equations. Among them we would like to point out works of Byatt-Smith [25], Kichenassamy and Olver [88], Marchant [105–109], Zou and Su [153], Tzirtzilakis *et.al.* [139] and Burde [23]. It was shown that if some coefficients of the second order equation for shallow water problem (4.27) are different or zero then there exists a hierarchy of soliton solutions. Kichenassamy and Olver [88] even claimed that for second order KdV equation solitary solutions of appropriate form cannot exist. This claim was falsified in our paper [79] where the analytic soliton solution of the extended KdV equation (4.27) was found and next in $[70, 129, 130]$ where several types of analytic periodic solutions were derived. Concerning the energy conservation, there are indications that collisions of solitons $[64, 66]$ which are solutions of higher order equations of KdV type can be inelastic $[139, 153]$.

8.1 KdV and KdV2 equations

As already presented in Section 3.1, the KdV equation, derived in scaled variables, in a fixed reference frame according to the first order perturbation approach with respect to two small parameters, has the form (3.29), that is,

$$\eta_t + \eta_x + \alpha\,\frac{3}{2}\eta\eta_x + \beta\,\frac{1}{6}\eta_{3x} = 0. \tag{8.1}$$

Small parameters α, β are defined by ratios of the wave amplitude a, the average water depth h and mean wavelength l as $\alpha = \frac{a}{h}$ and $\beta = \left(\frac{h}{l}\right)^2$. (For reader's convenience we repeat several equations from Section 3.1 with new numeration).

Reminder: The scaling of variables leading to dimensionless variables in the fixed reference frame is given by (3.9).

Transformation to a *moving frame* in the form

$$\bar{x} = (x - t), \qquad \bar{t} = t, \qquad \bar{\eta} = \eta, \tag{8.2}$$

allows us to remove the term η_x in the KdV equation in a frame moving with the velocity of sound $\sqrt{g\bar{h}}$

$$\bar{\eta}_{\bar{t}} + \alpha\,\frac{3}{2}\bar{\eta}\bar{\eta}_{\bar{x}} + \beta\,\frac{1}{6}\bar{\eta}_{3\bar{x}} = 0. \tag{8.3}$$

The simplest, *mathematical* form of the KdV equation is obtained from (8.1) by passing to the moving frame with additional scaling

$$\hat{x} = \sqrt{\frac{3}{2}}(x - t), \qquad \text{and} \qquad \hat{t} = \frac{1}{4}\sqrt{\frac{3}{2}}\,\alpha\,t, \tag{8.4}$$

which gives a standard, *mathematical* form of the KdV equation

$$\eta_{\hat{t}} + 6\,\eta\,\eta_{\hat{x}} + \frac{\beta}{\alpha}\eta_{\hat{x}\hat{x}\hat{x}} = 0 \quad \text{or}$$

$$\eta_{\hat{t}} + 6\,\eta\,\eta_{\hat{x}} + \eta_{\hat{x}\hat{x}\hat{x}} = 0 \quad \text{for} \quad \beta = \alpha. \tag{8.5}$$

Equations (8.5), particularly with $\beta = \alpha$ are favored by mathematicians, see, e.g., [98]. This form of KdV is the most convenient for ISM (the Inverse Scattering Method, see, e.g., [2, 5, 48]) used for construction of multi-soliton solutions.

Problems with mass, momentum and energy conservation in the KdV equation were discussed by Ali and Kalisch in [8]. In this paper the authors

considered the KdV equations in the original dimensional variables. Then the KdV equations are

$$\eta_t + c\eta_x + \frac{3}{2}\frac{c}{h}\eta\eta_x + \frac{ch^2}{6}\eta_{xxx} = 0 \tag{8.6}$$

in a fixed frame of reference and

$$\eta_t + \frac{3}{2}\frac{c}{h}\eta\eta_x + \frac{ch^2}{6}\eta_{xxx} = 0 \tag{8.7}$$

in a moving frame. In both equations, $c = \sqrt{gh}$ and (8.7) is obtained from (8.6) by setting $x' = x - ct$ and dropping the prime sign.

In this chapter we discuss the energy formulas obtained both in fixed and moving frames of reference for KdV (8.1), (8.3), (8.5)-(8.7). There seem to be some contradictions in the literature because the form of some invariants and the energy formulas are not the same in different sources, sometimes because of using different reference frames and/or not the same scalings. In this chapter we address these problems.

The second goal is to present some invariants for the extended KdV equation (4.27), that is, the equation obtained from the set of hydrodynamic equations (4.2)-(4.5) in the second order perturbation approach.

8.2 Invariants of KdV type equations

What invariants can be attributed to equations (8.1), (8.3), (8.5)-(8.7)?

It is well known, see, e.g. [36, Ch. 5], that an equation of the form (an analog to continuity equation $\frac{\partial \varrho}{\partial t} + \frac{\partial(\varrho v)}{\partial x} = 0$)

$$\frac{\partial T}{\partial t} + \frac{\partial X}{\partial x} = 0, \tag{8.8}$$

where neither T (an analog to density) nor X (an analog to flux) contain partial derivatives with respect to t, corresponds to some *conservation law*. It can be applied, in particular, to KdV equations (where there exist an infinite number of such conservation laws) and to the equations of KdV type like (4.27). Functions T and X may depend on $x, t, \eta, \eta_x, \eta_{2x}, \ldots, h, h_x, \ldots$, but not on η_t. If both functions T and X_x are integrable on $(-\infty, \infty)$ and $\lim_{x \to \pm\infty} X = $ const (soliton solutions), then integration of equation (8.8) yields

$$\frac{\mathrm{d}}{\mathrm{d}t}\left(\int_{-\infty}^{\infty} T\, dx\right) = 0 \qquad \text{or} \qquad \int_{-\infty}^{\infty} T\, dx = \text{const.} \tag{8.9}$$

since

$$\int_{-\infty}^{\infty} X_x \, dx = X(\infty, t) - X(-\infty, t) = 0. \tag{8.10}$$

The same conclusion applies for periodic solutions (cnoidal waves), when in the integrals (8.9), (8.10) limits of integration $(-\infty, \infty)$ are replaced by (a, b), where $b - a = L$ is the space period of the cnoidal wave (the wave length).

8.2.1 Invariants of the KdV equation

For the KdV equation (8.1) the two first invariants can be obtained easily. Writing (8.1) in the form

$$\frac{\partial \eta}{\partial t} + \frac{\partial}{\partial x} \left(\eta + \frac{3}{4} \alpha \eta^2 + \frac{1}{6} \beta \eta_{xx} \right) = 0 \tag{8.11}$$

one immediately obtains the conservation of mass (volume) law

$$I^{(1)} = \int_{-\infty}^{\infty} \eta \, dx = \text{const.} \tag{8.12}$$

Similarly, multiplication of (8.1) by η gives

$$\frac{\partial}{\partial t} \left(\frac{1}{2} \eta^2 \right) + \frac{\partial}{\partial x} \left(\frac{1}{2} \eta^2 + \frac{1}{2} \alpha \eta^3 - \frac{1}{12} \beta \eta_x^2 + \frac{1}{6} \beta \eta \eta_{xx} \right) = 0 \tag{8.13}$$

resulting in the invariant of the form

$$I^{(2)} = \int_{-\infty}^{\infty} \eta^2 \, dx = \text{const.} \tag{8.14}$$

In the literature of the subject, see, e.g., [8,36], $I^{(2)}$ is attributed to momentum conservation.

Invariants $I^{(1)}, I^{(2)}$ have the same form for all KdV equations (8.1), (8.3), (8.5), (8.6), (8.7).

Denote the left hand side of (8.1) by $\text{KDV}(x, t)$ and take

$$3\eta^2 \times \text{KDV}(x, t) - \frac{2}{3} \frac{\beta}{\alpha} \eta_x \times \frac{\partial}{\partial x} \text{KDV}(x, t). \tag{8.15}$$

The result, after simplifications is

$$\frac{\partial}{\partial t} \left(\eta^3 - \frac{1}{3} \frac{\beta}{\alpha} \eta_x^2 \right) + \frac{\partial}{\partial x} \left(\frac{9}{8} \alpha \eta^4 + \frac{1}{2} \beta \eta_{2x} \eta^2 \right. \tag{8.16}$$

$$\left. - \beta \eta_x^2 \eta + \eta^3 + \frac{1}{18} \frac{\beta^2}{\alpha} \eta_{2x}^2 - \frac{1}{9} \frac{\beta^2}{\alpha} \eta_x \eta_{3x} - \frac{1}{3} \frac{\beta}{\alpha} \eta_x^2 \right) = 0.$$

Then the next invariant for KdV in the fixed reference frame (8.1) is

$$I_{\text{fixed frame}}^{(3)} = \int_{-\infty}^{\infty} \left(\eta^3 - \frac{1}{3}\frac{\beta}{\alpha}\eta_x^2 \right) dx = \text{const.} \qquad (8.17)$$

The same construction like (8.15) but for the equation (8.3) in moving frame results in

$$\frac{\partial}{\partial t}\left(\eta^3 - \frac{1}{3}\frac{\beta}{\alpha}\eta_x^2 \right) + \frac{\partial}{\partial x}\left(\frac{9}{8}\alpha\eta^4 + \frac{1}{2}\beta\eta_{2x}\eta^2 \right. \qquad (8.18)$$

$$\left. -\beta\eta_x^2\eta + \eta^3 + \frac{1}{18}\frac{\beta^2}{\alpha}\eta_{2x}^2 - \frac{1}{9}\frac{\beta^2}{\alpha}\eta_x\eta_{3x} \right) = 0.$$

Then the next invariant for KdV equation in moving reference frame (8.3) is

$$I_{\text{moving frame}}^{(3)} = \int_{-\infty}^{\infty} \left(\eta^3 - \frac{1}{3}\frac{\beta}{\alpha}\eta_x^2 \right) dx = \text{const.} \qquad (8.19)$$

The procedure similar to those described above leads to the same invariants for both equations (8.6) and (8.7) where KdV equations are written in dimensional variables. To see this, it is enough to take $\;3\eta^2 \times kdv(x,t) - \frac{2}{3}h^3\frac{\partial}{\partial x}kdv(x,t) = 0$, where $\;kdv(x,t)$ is the l.h.s. either of (8.6) or (8.7). For equation (8.6) the conservation law is

$$\frac{\partial}{\partial t}\left(\eta^3 - \frac{h^3}{3}\eta_x^2 \right) + \frac{\partial}{\partial x}\left(c\eta^3 - \frac{9c}{8h}\eta^4 - \frac{1}{3}ch^3\eta_x^2 \right. \qquad (8.20)$$

$$\left. -ch^2\eta\eta_x^2 + \frac{1}{2}ch^2\eta^2\eta_{xx} + \frac{1}{18}ch^5\eta_{xx}^2 - \frac{1}{9}ch^5\eta_x\eta_{xxx} \right) = 0,$$

whereas for equation (8.7) the flux term is different

$$\frac{\partial}{\partial t}\left(\eta^3 - \frac{h^3}{3}\eta_x^2 \right) + \frac{\partial}{\partial x}\left(\frac{9c}{8h}\eta^4 - ch^2\eta\eta_x^2 \right. \qquad (8.21)$$

$$\left. +\frac{1}{2}ch^2\eta^2\eta_{xx} + \frac{1}{18}ch^5\eta_{xx}^2 - \frac{1}{9}ch^5\eta_x\eta_{xxx} \right) = 0.$$

But in both cases the same $I^{(3)}$ invariant is obtained as

$$I_{\text{dimensional}}^{(3)} = \int_{-\infty}^{\infty} \left(\eta^3 - \frac{h^3}{3}\eta_x^2 \right) dx = \text{const.} \qquad (8.22)$$

For the moving reference frame, in which the KdV equation has a standard (mathematical) form (8.5), invariants $I^{(1)}$ and $I^{(2)}$ have the same form, but

the invariant $I^{(3)}$ is slightly different. To see this difference denote the l.h.s. of (8.5) by $\mathrm{KDVm}(x,t)$ and construct

$$3\eta^2 \times \mathrm{KDVm}(x,t) - \frac{\beta}{\alpha}\eta_x \times \frac{\partial}{\partial x}\mathrm{KDVm}(x,t) = 0.$$

Then after simplifications one obtains

$$\frac{\partial}{\partial t}\left(\eta^3 - \frac{1}{2}\frac{\beta}{\alpha}\eta_x^2\right) + \frac{\partial}{\partial x}\left[\frac{9}{2}\eta^4 - 6\frac{\beta}{\alpha}\eta\eta_x^2\right. \tag{8.23}$$
$$\left. +3\frac{\beta}{\alpha}\eta^2\eta_{xx} - \frac{1}{2}\left(\frac{\beta}{\alpha}\eta_{xx}\right)^2 + \left(\frac{\beta}{\alpha}\right)^2\eta_x\eta_{xxx}\right] = 0,$$

which implies the invariant $I^{(3)}$ in the following form

$$I^{(3)}_{\text{moving frame}} = \int_{-\infty}^{\infty}\left(\eta^3 - \frac{1}{2}\frac{\beta}{\alpha}\eta_x^2\right)dx = \text{const} \quad \text{or} \tag{8.24}$$
$$I^{(3)}_{\text{moving frame}} = \int_{-\infty}^{\infty}\left(\eta^3 - \frac{1}{2}\eta_x^2\right)dx = \text{const} \quad \text{for} \quad \beta = \alpha.$$

We see, however, that the difference between (8.24) and (8.19) is caused by additional scaling.

Conclusion *Invariants $I^{(3)}$ have the same form for fixed and moving frames of reference when the transformation from fixed to moving frame scales x and t in the same way (e.g. $x' = x - t$ and $t' = t$). When scaling factors are different, like in (8.4), then the form of $I^{(3)}$ in the moving frame differs from the form in the fixed frame.*

For those solutions of KdV which preserve their shapes during the motion, that is, for cnoidal solutions and single soliton solutions, integrals of any power of $\eta(x,t)$ and any power of arbitrary derivative of the solution with respect to x are invariants. That is,

$$I^{(a,n)} = \int_{-\infty}^{\infty}(\eta_{nx})^a dx = \text{const}, \tag{8.25}$$

where $n = 0, 1, 2, \ldots$, and $a \in \mathbb{R}$ is an arbitrary real number. Then an arbitrary linear combination of $I^{(a,n)}$ is an invariant, as well. Therefore for such KdV solutions the particular form of the $I^{(3)}$ invariant, i.e. (8.17), (8.24) or (8.22) is not important because each term is an invariant, separately. Differences, however, can show up for multi-soliton solutions during soliton collisions when different scaling is used.

8.2.2 Invariants of the second order equations

Can we construct invariants for the extended KdV equation (KdV2)? Let us try to take $T = \eta$ for equation (4.27). Then we find that all terms, except η_t, can be written as X_x, as

$$\int \left[\eta_x + \alpha \frac{3}{2} \eta \eta_x + \beta \frac{1}{6} \eta_{3x} + \alpha^2 \left(-\frac{3}{8} \eta^2 \eta_x \right) \right.$$

$$\left. + \alpha\beta \left(\frac{23}{24} \eta_x \eta_{2x} + \frac{5}{12} \eta \eta_{3x} \right) + \beta^2 \frac{19}{360} \eta_{5x} \right] dx \qquad (8.26)$$

$$= \quad \eta + \frac{3}{4} \alpha \eta^2 + \frac{1}{6} \beta \eta_{2x} - \frac{1}{8} \alpha^2 \eta^3 + \alpha\beta \left(\frac{13}{48} \eta_x^2 + \frac{5}{12} \eta \eta_{2x} \right) + \frac{19}{360} \beta^2 \eta_{4x}.$$

As (8.26) depends on η and space derivatives and also since all those functions vanish when $x \to \pm\infty$, the conservation law for mass (volume)

$$\int_{-\infty}^{\infty} \eta(x, t)\, dx = \text{const.} \qquad (8.27)$$

holds for the second order equation. (Conservation law (8.27) holds for the equation with an uneven bottom (4.31), as well.)

Until now we did not find any other invariants for the second order equations. Moreover, we can show that the integral $I^{(2)}$ (8.14) **is no longer** an invariant of the second order KdV equation (4.27).

Upon multiplication of the equation (4.27) by η one obtains

$$\frac{\partial}{\partial t} \left(\frac{1}{2} \eta^2 \right) + \frac{\partial}{\partial x} \left[\frac{1}{2} \eta^2 + \frac{1}{2} \alpha \eta^3 + \frac{1}{6} \beta \left(-\frac{1}{2} \eta_x^2 + \eta \eta_{2x} \right) - \frac{3}{32} \alpha^2 \eta^4 \right. \qquad (8.28)$$

$$\left. + \frac{19}{360} \beta^2 \left(\frac{1}{2} \eta_{xx}^2 - \eta_x \eta_{3x} + \eta \eta_{4x} \right) + \frac{5}{12} \alpha\beta\, \eta^2 \eta_{2x} \right] + \frac{1}{8} \alpha\beta\, \eta \eta_x \eta_{2x} = 0.$$

The last term in (8.28) can not be expressed as $\frac{\partial}{\partial x} X(\eta, \eta_x, \ldots)$. Therefore $\int_{-\infty}^{+\infty} \eta^2 dx$ is not a conserved quantity. The same conclusion holds for the second order equation with an uneven bottom (4.31).

Since besides $I^{(2)}$, there are no exact invariants for KdV2 (4.31) one can look for adiabatic (approximate) invariants. This problem is described in Chapter 9.

8.3 Energy

The invariant $I^{(3)}$ is, in the literature, usually referred to as the energy invariant. Is this really the case?

8.3.1 Energy in a fixed frame as calculated from the definition

The hydrodynamic equations for an incompressible, inviscid fluid, in irrotational motion and under gravity in a fixed frame of reference, lead to a KdV equation (3.29)

$$\tilde{\eta}_{\tilde{t}} + \tilde{\eta}_{\tilde{x}} + \alpha \frac{3}{2}\tilde{\eta}\tilde{\eta}_{\tilde{x}} + \beta \frac{1}{6}\tilde{\eta}_{3\tilde{x}} = 0 \tag{8.29}$$

with accompanying equation (3.28) for velocity potential (below $w = f_x$)

$$\tilde{f}_{\tilde{x}} = \tilde{\eta} - \frac{1}{4}\alpha\tilde{\eta}^2 + \frac{1}{3}\beta\tilde{\eta}_{\tilde{x}\tilde{x}} \tag{8.30}$$

allows us to calculate the total energy of the fluid (in dimensionless quantities) from the definition.

The total energy is the sum of potential and kinetic energy. In our two-dimensional system the energy in original (dimensional coordinates) is

$$E = T + V = \int_{-\infty}^{+\infty}\left(\int_0^{h+\eta}\frac{\rho v^2}{2}dy\right)dx + \int_{-\infty}^{+\infty}\left(\int_0^{h+\eta}\rho g y\, dy\right)dx\,. \tag{8.31}$$

Equations (8.29) and (8.30) are obtained after scaling [24, 78, 79]. We now have dimesionless variables, according to (3.9)

$$\tilde{\phi} = \frac{h}{La\sqrt{gh}}\phi, \quad \tilde{x} = \frac{x}{L}, \quad \tilde{\eta} = \frac{\eta}{a}, \quad \tilde{y} = \frac{y}{h}, \quad \tilde{t} = \frac{t}{L/\sqrt{gh}}, \tag{8.32}$$

and

$$V = \rho g h^2 L \int_{-\infty}^{+\infty}\int_0^{1+\alpha\tilde{\eta}}\rho\,\tilde{y}\,d\tilde{y}\,d\tilde{x}, \tag{8.33}$$

$$T = \frac{1}{2}\rho g h^2 L \int_{-\infty}^{+\infty}\int_0^{1+\alpha\tilde{\eta}}\left(\alpha^2\tilde{\phi}_{\tilde{x}}^2 + \frac{\alpha^2}{\beta}\tilde{\phi}_{\tilde{y}}^2\right)d\tilde{y}\,d\tilde{x}. \tag{8.34}$$

Note, that the factor in front of the integrals has the dimension of energy.

In the following, we omit signs $\sim$, having in mind that we are working in dimensionless variables. Integration in (8.33) with respect to y yields

$$V = \frac{1}{2}gh^2 L\rho \int_{-\infty}^{\infty}\left(\alpha^2\eta^2 + 2\alpha\eta + 1\right)dx \tag{8.35}$$

$$= \frac{1}{2}gh^2 L\rho\left[\int_{-\infty}^{\infty}\left(\alpha^2\eta^2 + 2\alpha\eta\right)dx + \int_{-\infty}^{\infty}dx\right].$$

After renormalization (substraction of constant term $\int_{-\infty}^{\infty}dx$) one obtains

$$V = \frac{1}{2}gh^2 L\rho \int_{-\infty}^{\infty}\left(\alpha^2\eta^2 + 2\alpha\eta\right)dx. \tag{8.36}$$

In kinetic energy we use the velocity potential expressed in the lowest (first) order

$$\phi_x = f_x - \frac{1}{2}\beta y^2 f_{xxx} \quad \text{and} \quad \phi_y = -\beta y f_{xx},\tag{8.37}$$

where f_x was defined in (8.30). Now the bracket in the integral (8.34) is

$$\left(\alpha^2 \phi_x{}^2 + \frac{\alpha^2}{\beta}\phi_y{}^2\right) = \alpha^2\left(f_x^2 + \beta y^2(-f_x f_{xxx} + f_{xx}^2)\right).\tag{8.38}$$

Inegration with respect to the vertical coordinate y gives, up to the same order,

$$T = \frac{1}{2}\rho g h^2 L \int_{-\infty}^{+\infty}\alpha^2\left[f_x^2(1+\alpha\eta) + \beta(-f_x f_{xxx} + f_{xx}^2)\frac{1}{3}(1+\alpha\eta)^3\right]dx$$

$$= \frac{1}{2}\rho g h^2 L \int_{-\infty}^{+\infty}\alpha^2\left[f_x^2 + \alpha f_x^2\eta + \frac{1}{3}\beta\left(f_{xx}^2 - f_x f_{xxx}\right)\right]dx.\tag{8.39}$$

In order to express energy through the elevation function η we use (8.30). We then substitute $f_x = \eta$ in terms of the third order and $f_x^2 = \eta^2 - \frac{1}{2}\alpha\eta^3 + \frac{2}{3}\beta\eta\eta_{xx}$ in terms of the second order

$$T = \frac{1}{2}\rho g h^2 L \int_{-\infty}^{+\infty}\alpha^2\left[\left(\eta^2 - \frac{1}{2}\alpha\eta^3 + \frac{2}{3}\beta\eta\eta_{xx}\right) + \alpha\eta^3 + \frac{1}{3}\beta\left(\eta_x^2 - \eta\eta_{xx}\right)\right]dx$$

$$= \frac{1}{2}\rho g h^2 L \alpha^2\left[\int_{-\infty}^{+\infty}\left(\eta^2 + \frac{1}{2}\alpha\eta^3\right)dx + \int_{-\infty}^{+\infty}\frac{1}{3}\beta\left(\eta_x^2 + \eta\eta_{xx}\right)dx\right].\tag{8.40}$$

The last term vanishes as

$$\int_{-\infty}^{+\infty}\left(\eta_x^2 + \eta\eta_{xx}\right)dx = \int_{-\infty}^{+\infty}\eta_x^2 dx + \eta\eta_x|_{-\infty}^{+\infty} - \int_{-\infty}^{+\infty}\eta_x^2 dx = 0.\tag{8.41}$$

Therefore the total energy in the fixed frame is given by

$$E_{\text{tot}} = T + V = \rho g h^2 L \int_{-\infty}^{\infty}\left(\alpha\eta + (\alpha\eta)^2 + \frac{1}{4}(\alpha\eta)^3\right)dx.\tag{8.42}$$

The energy (8.42) in a fixed frame of reference does not contain the $I^{(3)}$ invariant

$$E_{\text{tot}} = T + V = \rho g h^2 L \int_{-\infty}^{\infty}\left(\alpha\eta + (\alpha\eta)^2 + \frac{1}{4}(\alpha\eta)^3\right)dx$$

$$= \rho g h^2 L \left(\alpha I^{(1)} + \alpha^2 I^{(2)} + \frac{1}{4}\alpha^2 I^{(3)} + \frac{1}{12}\alpha^2\beta\int_{-\infty}^{\infty}\eta_x^2 dx\right).\tag{8.43}$$

The energy (8.42), (8.43) in a fixed frame of reference **has noninvariant form**. The last term in (39) results in small deviations from energy conservation only when η_x changes in time in soliton's reference frame, what occurs

only during soliton collision. This deviations are discussed and illustrated in Section 8.5.

The result (8.42) gives the energy in powers of η only. The same structure of powers in η was obtained by the authors of [8], who work in dimensional KdV equations (8.6) and (8.7). On page 122 they present a non-dimensional energy density E in a frame moving with the velocity U. Then, if $U = 0$ is set, the energy density in a fixed frame is proportional to $\alpha\eta + \alpha^2\eta^2$ as the formula is obtained up to second order in α. However, the third order term is $\frac{1}{4}\alpha^3\eta^3$, so the formula up to the third order in α becomes

$$E \sim \alpha\eta + \alpha^2\eta^2 + \frac{1}{4}\alpha^3\eta^3. \tag{8.44}$$

This energy density contains the same terms like (8.42) and does not contain the term η_x^2, as well.

Energy calculated from the definition does not contain a proper invariant of motion.

8.3.2 Energy in a moving frame

Now, we consider the total energy according to (28) calculated in a frame moving with the velocity of sound $c = \sqrt{gh}$. Using the same scaling (29) to dimensionless variables we note that in these variables $c = 1$. As pointed by Ali and Kalisch [8, Sect. 3], working with such system one has to replace ϕ_x by the horizontal velocity in a moving frame, that is by $\tilde{\phi}_{\tilde{x}} - \frac{1}{\alpha} = \alpha\tilde{\eta} - \frac{1}{4}\alpha\tilde{\eta}^2 + \beta\left(\frac{1}{3} - \frac{y^2}{2}\right)\tilde{\eta}_{\tilde{x}\tilde{x}} - \frac{1}{\alpha}$. Then repeating the same steps as in the previous subsection yields the energy expressed by invariants

$$E_{\text{tot}} = \rho g h^2 L \int_{-\infty}^{\infty} \left[-\frac{1}{2}\alpha\tilde{\eta} + \frac{1}{4}(\alpha\tilde{\eta})^2 + \frac{1}{2}\alpha^3\left(\tilde{\eta}^3 - \frac{1}{3}\frac{\beta}{\alpha}\tilde{\eta}_{\tilde{x}}^2\right) \right] d\tilde{x}$$

$$= \rho g h^2 L \left(-\frac{1}{2}\alpha I^{(1)} + \frac{1}{4}\alpha^2 I^{(2)} + \frac{1}{2}\alpha^3 I^{(3)} \right). \tag{8.45}$$

The crucial term $-\frac{1}{6}\alpha^2\beta\,\tilde{\eta}_{\tilde{x}}^2$ in (8.45) appears due to integration over vertical variable of the term $\frac{\beta}{\alpha}\tilde{\eta}_{\tilde{x}\tilde{x}}$ supplied by $(\tilde{\phi}_{\tilde{x}} - \frac{1}{\alpha})^2$.

8.4 Variational approach

8.4.1 Lagrangian approach, potential formulation

Some attempts at the variational approach to shallow water problems are summarized in Whitham's book [144, Sect 16.14].

For KdV as it stands, we can not write a variational principle directly. It is necessary to introduce a velocity potential. The simplest choice is to take $\eta = \varphi_x$. Then equation (8.1) in the fixed frame takes the form

$$\varphi_{xt} + \varphi_{xx} + \frac{3}{2}\alpha\varphi_x\varphi_{xx} + \frac{1}{6}\beta\varphi_{xxxx} = 0\,. \tag{8.46}$$

The appropriate Lagrangian density is

$$\mathcal{L}_{\text{fixed frame}} = -\frac{1}{2}\varphi_t\varphi_x - \frac{1}{2}\varphi_x^2 - \frac{\alpha}{4}\varphi_x^3 + \frac{\beta}{12}\varphi_{xx}^2\,. \tag{8.47}$$

Indeed, the Euler–Lagrange equation obtained from Lagrangian (8.47) is just (8.46).

For our moving reference frame the substitution $\eta = \varphi_x$ into (8.3) gives

$$\varphi_{xt} + \frac{3}{2}\alpha\varphi_x\varphi_{xx} + \frac{1}{6}\beta\varphi_{xxxx} = 0\,. \tag{8.48}$$

So, the appropriate Lagrangian density is

$$\mathcal{L}_{\text{moving frame}} = -\frac{1}{2}\varphi_t\varphi_x - \frac{\alpha}{4}\varphi_x^3 + \frac{\beta}{12}\varphi_{xx}^2\,. \tag{8.49}$$

Again, the Euler-Lagrange equation obtained from Lagrangian (8.49) is just (8.48).

8.4.2 Hamiltonians for KdV equations in the potential formulation

The Hamiltonian for the KdV equation in a fixed frame (8.1) can be obtained in the following way [28]. Defining generalized momentum $\pi = \dfrac{\partial\mathcal{L}}{\partial\varphi_t}$, where $\mathcal{L}$ is given by (8.47), one obtains

$$\begin{aligned}
H &= \int_{-\infty}^{\infty} [\pi\dot{\varphi} - \mathcal{L}]\,dx = \int_{-\infty}^{\infty} \left[\frac{1}{2}\varphi_x^2 + \frac{\alpha}{4}\varphi_x^3 - \frac{\beta}{12}\varphi_{xx}^2\right] dx \\
&= \int_{-\infty}^{\infty} \left[\frac{1}{2}\eta^2 + \frac{1}{4}\alpha\left(\eta^3 - \frac{\beta}{3\alpha}\eta_x^2\right)\right] dx\,.
\end{aligned} \tag{8.50}$$

The energy is expressed by invariants $I^{(2)}$, $I^{(3)}$ so it is a constant of motion.

The same procedure for KdV in a moving frame (8.3) gives

$$\begin{aligned}
H &= \int_{-\infty}^{\infty} [\pi\dot{\varphi} - \mathcal{L}]\,dx = \int_{-\infty}^{\infty} \left[\frac{\alpha}{4}\varphi_x^3 - \frac{\beta}{12}\varphi_{xx}^2\right] dx \\
&= \frac{1}{4}\alpha \int_{-\infty}^{\infty} \left(\eta^3 - \frac{\beta}{3\alpha}\eta_x^2\right) dx\,.
\end{aligned} \tag{8.51}$$

The Hamiltonian (8.51) only consists $I^{(3)}$.

The constant of motion in a moving frame is

$$E = \frac{1}{4}I^{(3)} = \text{const.} \qquad (8.52)$$

The potential formulation of the Lagrangian, described above, is succesful for deriving KdV equations both for fixed and moving reference frames. It fails, however, for the extended KdV equation (4.27). We proved that there exists a nonlinear expression of $\mathcal{L}(\varphi_t, \varphi_x, \varphi_{xx}, \ldots)$, such that the resulting Euler–Lagrange equation differs very little from equation (4.27). The difference lies only in the value of one of the coefficients in the second order term $\alpha\beta \left(\frac{23}{24}\eta_x\eta_{2x} + \frac{5}{12}\eta\eta_{3x} \right)$. Particular values of coefficients in this term cause the lack of the $I^{(2)}$ invariant for second order KdV equation, (see (8.28)) and admit for adiabatic invariants only. A more detailed discussion on this point is given in Chapter 9.

8.5 Luke's Lagrangian and KdV energy

The full set of Euler equations for the shallow water problem, as well as KdV equations (8.1), (8.5), and the extended KdV equation (4.27) can be derived from Luke's Lagrangian [103], see, e.g. [105]. Luke points out, however, that his Lagrangian is not equal to the difference of kinetic and potential energy. Euler-Lagrange equations obtained from $\mathscr{L} = T - V$ do not have the proper form at the boundary. Instead, Luke's Lagrangian is the sum of kinetic and potential energy supplemented by the ϕ_t term which is necessary for dynamical boundary condition.

8.5.1 Derivation of KdV energy from the original Euler equations according to [72]

In Chapter 5.2 of [72], Infeld and Rowlands present a derivation of the KdV equation from the Euler (hydrodynamic) equations using a single small parameter ε. Moreover, they show that the same method allows us to derive the Kadomtsev-Petviashvili (KP) equation [76] for water waves [12, 67, 68, 102] and also nonlinear equations for ion-acoustic waves in a plasma [69, 71]. The authors first derive equations of motion, then construct a Lagrangian and look for constants of motion. For the purpose of this paper and for comparison to results obtained in the next subsections it is convenient to present their results

starting from Luke's Lagrangian density. That density can be written as (here $g = 1$)

$$\mathcal{L} = \int_0^{1+\eta} \left[\phi_t + \frac{1}{2}(\phi_x^2 + \phi_z^2) + z \right] dz \,. \tag{8.53}$$

In Chapter 5.2.1 of [72] the authors introduce scaled variables in a movimg frame (ε plays a role of small parameter and if $\varepsilon = \alpha = \beta$, then KdV equation is obtained).

Then (for details, see [72, Chapter 5.2])

$$\phi_z = -\varepsilon^{\frac{3}{2}} z f_{\xi\xi}, \qquad \phi_x = \varepsilon f_\xi - \varepsilon^2 \frac{z^2}{2} f_{\xi\xi\xi},$$

$$\phi_t = -\varepsilon f_\xi + \varepsilon^2 \left(f_\tau + \frac{z^2}{2} f_{\xi\xi\xi} \right) - \varepsilon^3 \frac{z^2}{2} f_{\xi\xi\tau}. \tag{8.54}$$

Substitution of the above formulas into the expression [ ] under the integral in (8.53) gives

$$[\,] = z - \varepsilon f_\xi + \varepsilon^2 \left(f_\tau + \frac{1}{2} f_\xi^2 + \frac{z^2}{2} f_{\xi\xi\xi} \right) \tag{8.55}$$

$$+ \varepsilon^3 \frac{z^2}{2} \left[-f_{\xi\xi\tau} + (f_{\xi\xi}^2 - f_\xi f_{\xi\xi\xi}) \right] + O(\varepsilon^4).$$

Remark 8.1. The full Lagrangian is obtained by integration of the Lagrangian density (8.53) with respect to x. Integration limits are $(-\infty, \infty)$ for a soliton solutions, or $[a, b]$, where $b - a = L$ the wave length (space period) for cnoidal solutions. Integration by parts and properties of the solutions at the limits, see (8.10), allow us to use the equivalence $\int_{-\infty}^{\infty} (f_{\xi\xi}^2 - f_\xi f_{\xi\xi\xi}) d\xi = \int_{-\infty}^{\infty} 2 f_{\xi\xi}^2 d\xi$.

Therefore

$$[\,] = z - \varepsilon f_\xi + \varepsilon^2 \left(f_\tau + \frac{1}{2} f_\xi^2 + \frac{z^2}{2} f_{\xi\xi\xi} \right) + \varepsilon^3 \frac{z^2}{2} \left[-f_{\xi\xi\tau} + 2 f_{\xi\xi}^2 \right] + O(\varepsilon^4). \tag{8.56}$$

Integration over y gives (note that $1 + \eta \Longrightarrow 1 + \varepsilon\eta$)

$$\mathcal{L} = \frac{1}{2}(1 + \varepsilon\eta)^2 + (1 + \varepsilon\eta) \left[-\varepsilon f_\xi + \varepsilon^2 \left(f_\tau + \frac{1}{2} f_\xi^2 \right) \right]$$

$$+ \frac{1}{3}(1 + \varepsilon\eta)^3 \left[\frac{1}{2} \varepsilon^2 f_{\xi\xi\xi} - \frac{1}{2} \varepsilon^3 f_{\xi\xi\tau} + \varepsilon^3 f_{\xi\xi}^2 \right]. \tag{8.57}$$

Write (8.57) up to third order in ε

$$\mathcal{L} = \mathcal{L}^{(0)} + \varepsilon \mathcal{L}^{(1)} + \varepsilon^2 \mathcal{L}^{(2)} + \varepsilon^3 \mathcal{L}^{(3)} + O(\varepsilon^4) \,.$$

It is easy to show, that

$$\mathcal{L}^{(0)} = \frac{1}{2}, \qquad \mathcal{L}^{(1)} = \eta - f_\xi,$$

$$\mathcal{L}^{(2)} = f_\tau + \frac{1}{2}\eta^2 - \eta f_\xi + \frac{1}{2}f_\xi^2 + \frac{1}{6}f_{\xi\xi\xi},$$

$$\mathcal{L}^{(3)} = \eta f_\tau + \frac{1}{2}\eta f_\xi^2 + \frac{1}{2}\eta f_{\xi\xi\xi} - \frac{1}{6}f_{\xi\xi\tau} + \frac{1}{3}f_{\xi\xi}^2.$$

(8.58)

The Hamiltonian density reads as

$$H = f_\tau \frac{\partial \mathcal{L}}{\partial f_\tau} + f_{\xi\xi\tau} \frac{\partial \mathcal{L}}{\partial f_{\xi\xi\tau}} - \mathcal{L}$$

(8.59)

$$= -\left[\frac{1}{2} + \varepsilon\,(\eta - f_\xi) + \varepsilon^2 \left(\frac{1}{2}\eta^2 - \eta f_\xi + \frac{1}{2}f_\xi^2 + \frac{1}{6}f_{\xi\xi\xi}\right)\right.$$

$$\left. + \varepsilon^3 \left(\frac{1}{2}\eta f_\xi^2 + \frac{1}{2}\eta f_{\xi\xi\xi} + \frac{1}{3}f_{\xi\xi}^2\right)\right].$$

Dropping the constant term one obtains the total energy as

$$\mathcal{E} = \int_{-\infty}^{\infty} \left[\varepsilon\,(\eta - f_\xi) + \varepsilon^2 \left(\frac{1}{2}\eta^2 - \eta f_\xi + \frac{1}{2}f_\xi^2 + \frac{1}{6}f_{\xi\xi\xi}\right)\right.$$

$$\left. + \varepsilon^3 \left(\frac{1}{2}\eta f_\xi^2 + \frac{1}{2}\eta f_{\xi\xi\xi} + \frac{1}{3}f_{\xi\xi}^2\right)\right] d\xi.$$

(8.60)

Now, we need to express f_ξ and its derivatives by η and its derivatives. We use (8.30) replacing α and β by ε, that is,

$$f_\xi = \eta - \frac{1}{4}\varepsilon\eta^2 + \frac{1}{3}\varepsilon\eta_{\xi\xi}.$$

(8.61)

Then the total energy in a moving frame is expressed in terms of the second and the third invariants

$$\mathcal{E} = -\left[\varepsilon^2 \frac{1}{4}\int_{-\infty}^{\infty} \eta^2\,dx + \varepsilon^3 \frac{1}{2}\int_{-\infty}^{\infty}\left(\eta^3 - \frac{1}{3}\eta_\xi^2\right)dx\right].$$

(8.62)

Note that the term $\frac{1}{3}\eta_\xi^2$ occuring in the third order invariant originates from three terms appearing in ϕ_z^2, ϕ_x^2 and ϕ_t (see terms $f_{\xi\xi}$ and $f_{\xi\xi\xi}$ in (8.54)).

8.5.2 Luke's Lagrangian

The original Lagrangian density in Luke's paper [103] is

$$\mathcal{L} = \int_0^{h(x)} \rho\left[\phi_t + \frac{1}{2}(\phi_x^2 + \phi_y^2) + gy\right] dy.$$

(8.63)

After scaling as in $[24, 78, 79]$

$$\tilde{\phi} = \frac{h}{La\sqrt{gh}}\phi, \quad \tilde{x} = \frac{x}{L}, \quad \tilde{\eta} = \frac{\eta}{a}, \quad \tilde{y} = \frac{y}{h}, \quad \tilde{t} = \frac{t}{L/\sqrt{gh}}, \tag{8.64}$$

we obtain

$$\phi_t = gh\alpha\,\tilde{\phi}_{\tilde{t}}, \qquad \phi_x^2 = gh\alpha^2\,\tilde{\phi}_{\tilde{x}}^2, \qquad \phi_y^2 = gh\frac{\alpha^2}{\beta}\,\tilde{\phi}_{\tilde{y}}^2. \tag{8.65}$$

The Lagrangian density in scaled variables becomes $(dy = hd\tilde{y})$

$$\mathcal{L} = \rho gha \int_0^{1+\alpha\eta} \left[\tilde{\phi}_{\tilde{t}} + \frac{1}{2}\left(\tilde{\phi}_{\tilde{x}}^2 + \frac{\alpha^2}{\beta}\,\tilde{\phi}_{\tilde{y}}^2\right)\right] d\tilde{y} + \frac{1}{2}\rho gh^2(1+\alpha\eta)^2. \tag{8.66}$$

So, in dimensionless quantities

$$\frac{\mathcal{L}}{\rho gha} = \int_0^{1+\alpha\eta} \left[\tilde{\phi}_{\tilde{t}} + \frac{1}{2}\left(\alpha\tilde{\phi}_{\tilde{x}}^2 + \frac{\alpha}{\beta}\,\tilde{\phi}_{\tilde{y}}^2\right)\right] d\tilde{y} + \frac{1}{2}\alpha\eta^2, \tag{8.67}$$

where the constant term and the term proportional to η in the expansion of $(1+\alpha\eta)^2$ are omitted. The form (8.67) is identical with Eq. (2.9) in Marchant & Smyth [105].

The full Lagrangian is obtained by integration over x. In dimensionless variables $(dx = L\,d\tilde{x})$ it gives

$$\mathscr{L} = E_0 \int_{-\infty}^{\infty} \left[\int_0^{1+\alpha\eta} \left[\tilde{\phi}_{\tilde{t}} + \frac{1}{2}\left(\alpha\tilde{\phi}_{\tilde{x}}^2 + \frac{\alpha}{\beta}\,\tilde{\phi}_{\tilde{y}}^2\right)\right] d\tilde{y} + \frac{1}{2}\alpha\eta^2\right] d\tilde{x}. \tag{8.68}$$

The factor in front of the integral, $E_0 = \rho ghaL = \rho gh^2 L\,\alpha$, has the dimension of energy.

Next, the signs ($\sim$) will be omitted, but we have to remember that we are working in scaled dimensionless variables in a fixed reference frame.

8.5.3 Energy in the fixed reference frame

Express the Lagrangian density by η and $f = \phi^{(0)}$. Now, up to first order in small parameters

$$\phi = f - \frac{1}{2}\beta y^2 f_{xx}, \quad \phi_t = f_t - \frac{1}{2}\beta y^2 f_{xxt}, \quad \phi_x = f_x - \frac{1}{2}\beta y^2 f_{xxx}, \quad \phi_y = -\beta y f_{xx}. \tag{8.69}$$

Then the expression under the integral in (8.67) becomes

$$[\,] = f_t - \frac{1}{2}\beta y^2 f_{xxt} + \frac{1}{2}\alpha f_x^2 + \frac{1}{2}\alpha\beta y^2\left(-f_x f_{xxx} + f_{xx}^2\right). \tag{8.70}$$

From properties of solutions at the limits $\left(-f_x f_{xxx} + f_{xx}^2\right) \Rightarrow 2f_{xx}^2$. Integration of (8.70) over y yields

$$\frac{\mathcal{L}}{\rho g h a} = \left(f_t + \frac{1}{2}\alpha f_x^2\right)(1 + \alpha\eta) - \frac{1}{2}\beta f_{xxt}\frac{1}{3}(1 + \alpha\eta)^3$$
$$+ \alpha\beta f_{xx}^2 \frac{1}{3}(1 + \alpha\eta)^3 + \frac{1}{2}\alpha\eta^2. \tag{8.71}$$

The dimensionless Hamiltonian density is $\left(f_t \frac{\partial \mathcal{L}}{\partial f_t} + f_{xxt}\frac{\partial \mathcal{L}}{\partial f_{xxt}} - \mathcal{L}\right)$

$$\frac{\mathcal{H}}{\rho g h^2 L} = -\alpha\left[\frac{1}{2}\alpha f_x^2(1 + \alpha\eta) + \alpha\beta f_{xx}^2 \frac{1}{3}(1 + \alpha\eta)^3 + \frac{1}{2}\alpha\eta^2\right]. \tag{8.72}$$

Again, we need to express the Hamiltonian by η and its derivatives, only. Inserting

$$f_x = \eta - \frac{1}{4}\alpha\eta^2 + \frac{1}{3}\beta\eta_{xx} \tag{8.73}$$

into (8.72) and leaving terms up to third order one obtains

$$\frac{\mathcal{H}}{\rho g h^2 L} = -\alpha\left[\alpha\eta^2 + \frac{1}{4}\alpha^2\eta^3 + \frac{1}{3}\alpha\beta(\eta_x^2 + \eta\eta_{xx})\right]. \tag{8.74}$$

The energy is

$$\frac{E}{\rho g h^2 L} = -\alpha\int_{-\infty}^{\infty}\left[\alpha\eta^2 + \frac{1}{4}\alpha^2\eta^3 + \frac{1}{3}\alpha\beta(\eta_x^2 + \eta\eta_{xx})\right]dx$$
$$= -\left[\alpha^2\int_{-\infty}^{\infty}\eta^2 dx + \frac{1}{4}\alpha^3\int_{-\infty}^{\infty}\eta^3 dx\right] \tag{8.75}$$

since the integral of the $\alpha\beta$ term vanishes. Here, in the same way as in calculations of energy directly from the definition (8.42), the energy is expressed by integrals of η^2 and η^3. The term proportional to $\alpha\eta$ is not present in (8.75), because it was dropped earlier [105].

8.5.4 Energy in a moving frame

Transforming into the moving frame one has

$$\bar{x} = x - t, \quad \bar{t} = \alpha t, \quad \partial_x = \partial_{\bar{x}}, \quad \partial_t = -\partial_{\bar{x}} + \alpha\partial_{\bar{t}}, \tag{8.76}$$

$$\phi = f - \frac{1}{2}\beta y^2 f_{\bar{x}\bar{x}}, \quad \phi_x = f_{\bar{x}} - \frac{1}{2}\beta y^2 f_{\bar{x}\bar{x}\bar{x}}, \quad \phi_y = -\beta y f_{\bar{x}\bar{x}}, \tag{8.77}$$

$$\phi_t = -f_{\bar{x}} + \frac{1}{2}\beta y^2 f_{\bar{x}\bar{x}\bar{x}} + \alpha(f_{\bar{t}} - \frac{1}{2}\beta y^2 f_{\bar{x}\bar{x}\bar{t}}). \tag{8.78}$$

Up to second order

$$\frac{1}{2}\left(\alpha\phi_x^2 + \frac{\alpha}{\beta}\phi_y^2\right) = \frac{1}{2}\left[\alpha f_{\bar{x}}^2 + \alpha\beta y^2(-f_{\bar{x}}f_{\bar{x}\bar{x}\bar{x}} + f_{\bar{x}\bar{x}}^2)\right] = \frac{1}{2}\alpha f_{\bar{x}}^2 + \alpha\beta y^2 f_{\bar{x}\bar{x}}^2.$$

(8.79)

Therefore the expression under the integral in (8.67) is

$$[\ \ ] = -f_{\bar{x}} + \frac{1}{2}\beta y^2 f_{\bar{x}\bar{x}\bar{x}} + \alpha(f_{\bar{t}} - \frac{1}{2}\beta y^2 f_{\bar{x}\bar{x}\bar{t}}) + \frac{1}{2}\alpha f_{\bar{x}}^2 + \alpha\beta y^2 f_{\bar{x}\bar{x}}^2. \qquad (8.80)$$

Integration yields

$$\frac{\mathcal{L}}{\rho g h a} = \left(-f_{\bar{x}} + \alpha f_{\bar{t}} + \frac{1}{2}\alpha f_{\bar{x}}^2\right)(1+\alpha\eta) \qquad (8.81)$$

$$+ \frac{1}{3}(1+\alpha\eta)^3\left(\frac{1}{2}\beta(f_{\bar{x}\bar{x}\bar{x}} - f_{\bar{x}\bar{x}\bar{t}}) + \alpha\beta f_{\bar{x}\bar{x}}^2\right) + \frac{1}{2}\alpha\eta^2.$$

Like in (8.72) above, the Hamiltonian density is

$$\frac{\mathcal{H}}{\rho g h^2 L} = -\alpha\left[\left(-f_{\bar{x}} + \frac{1}{2}\alpha f_{\bar{x}}^2\right)(1+\alpha\eta)\right. \qquad (8.82)$$

$$\left. + \frac{1}{3}(1+\alpha\eta)^3\left(\frac{1}{2}\beta f_{\bar{x}\bar{x}\bar{x}} + \alpha\beta f_{\bar{x}\bar{x}}^2\right) + \frac{1}{2}\alpha\eta^2\right].$$

Expressing $f_{\bar{x}}$ by (8.73) one obtains

$$\frac{\mathcal{H}}{\rho g h^2 L} = -\alpha\left[-\frac{1}{4}\alpha\eta^2 + \frac{1}{3}\beta\eta_{xx} - \frac{1}{2}\alpha^2\eta^3\right. \qquad (8.83)$$

$$\left. + \alpha\beta\left(-\frac{1}{4}\eta_x^2 - \frac{5}{12}\eta\eta_{xx}\right) - \frac{1}{18}\beta^2\eta_{xxxx}\right].$$

Finally the energy is given by

$$\frac{E}{\rho g h^2 L} = \alpha^2\frac{1}{4}\int_{-\infty}^{\infty}\eta^2 dx + \alpha^3\frac{1}{2}\int_{-\infty}^{\infty}\left(\eta^3 - \frac{1}{3}\frac{\beta}{\alpha}\eta_x^2\right)dx \qquad (8.84)$$

since integrals from terms with β, β^2 vanish at integration limits, and $-\frac{5}{12}\eta\eta_{xx} \Rightarrow \frac{5}{12}\eta_x^2$. The invariant term proportional to $\alpha\eta$ is not present in (8.84), because it was dropped in (8.67). If we include that term, the total energy is a linear combination of all three lowest invariants, $I^{(1)}, I^{(3)}, I^{(3)}$.

Comment   *An almost identical formula for the energy in a moving frame, for KdV expressed in dimensional variables (8.7), was obtained in [8]. That energy is expressed by all three lowest order invariants*

$$\mathcal{E} = -\frac{1}{2}c^2\int_{-\infty}^{\infty}\eta\,dx + \frac{1}{4}\frac{c^2}{h}\int_{-\infty}^{\infty}\eta^2\,dx + \frac{1}{2}\frac{c^2}{h^2}\int_{-\infty}^{\infty}\left(\eta^3 - \frac{h^3}{3}\eta_x^2\right)dx, \quad (8.85)$$
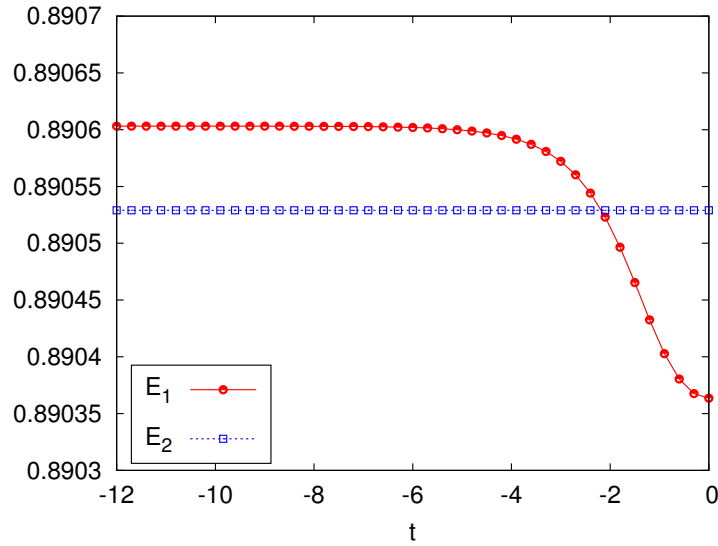
as well. Translation of (8.85) to nondimensional variables yields

$$\mathcal{E}_\varrho = \varrho g h^2 L \left(-\frac{1}{2}\alpha I^{(1)} + \frac{1}{4}\alpha^2 I^{(2)} + \frac{1}{2}\alpha^3 I^{(3)} \right).$$

8.5.5 How strongly is energy conservation violated?

The total energy in the fixed frame is given by equation (8.42). Taking into account its non-dimensional part we may write

$$E_1(t) = \frac{T + V}{\varrho g h^2 L} = \int_{-\infty}^{\infty} \left[\alpha\eta + (\alpha\eta)^2 + \frac{1}{4}(\alpha\eta)^3 \right] dx$$

$$= \alpha I^{(1)} + \alpha^2 I^{(2)} + \frac{1}{4}\int_{-\infty}^{\infty}(\alpha\eta)^3 dx. \tag{8.86}$$

Fig. 8.1. Precision of energy conservation for 3-soliton solution. Energies are plotted as open circles (E_1) and open squares (E_2) for 40 time instants. Reproduced with permission from [80]. Copyright (2015) by the American Physical Society

In order to see how much the changes of E_1 violate energy conservation we will compare it to the same formula but expressed by invariants

$$E_2(t) = \alpha I^{(1)} + \alpha^2 I^{(2)} + \frac{1}{4}\alpha^3 I^{(3)}. \tag{8.87}$$
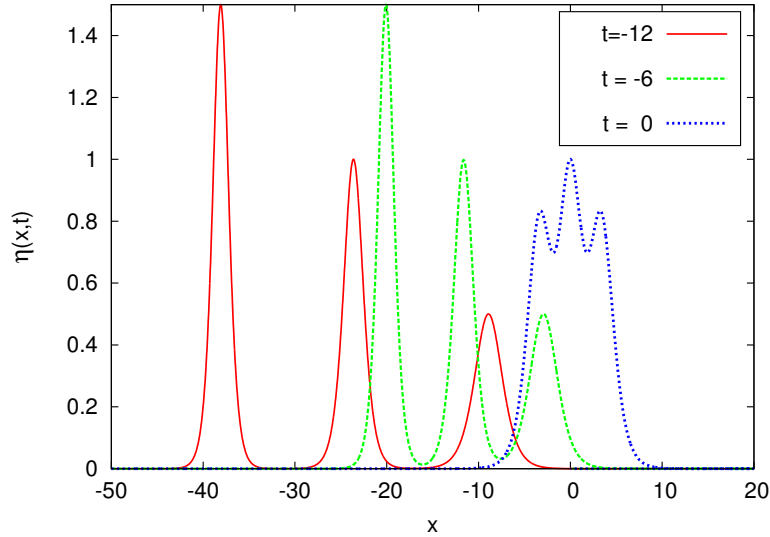
Fig. 8.2. Shape evolution of 3-soliton solution during collision. Reproduced with permission from [80]. Copyright (2015) by the American Physical Society

The time dependence of E_1 and E_2 is presented in figure 8.1 for a 3-soliton solution of KdV (8.1). Time evolution is calculated on the interval $t \in [-12, 0]$. The shape of the 3-soliton solution is presented only for three times $t = -12, -6, 0$ in order to show shapes changing during the collision.

For presentation, the example of the 3-soliton solution with amplitudes equals 1.5, 1 and 0.5 was chosen. In figure 8.2 the positions of solutions at given times were artificially shifted to set them closer to each other. The plots in figures 8.1 and 8.2 for $t > 0$ are symmetric to those which are shown in the figures.

For this example the relative discrepancy of the enregy E_1 from the constant value, is very small

$$\delta E = \frac{E_1(t = -12) - E_1(t = 0)}{E_1(t = -12)} \approx 0.000258. \tag{8.88}$$

However, the E_2 energy is conserved with the numerical precision of thirteen decimal digits in this example. In a similar example with a 2-soliton solution (with amplitudes 1 and 0.5) the relative error (8.88) was even smaller, with the value $\delta E \approx 0.00014$. This suggests that the degree of nonconservation of energy increases with n, where n is the number of solitons in the solution.

8.5.6 Conclusions for KdV equation

The main conclusions can be formulated as follows.

- The invariants of KdV in fixed and moving frames have the same form. (Of course when we have the same scaling factor for x and t in the transformation between frames).
- We confirmed some known facts. Firstly, that the usual form of the energy $H = T + V$ is not always expressed by invariants only. The reason lies in the fact, as pointed out by Luke in [103], that the Euler–Lagrange equations obtained from the Lagrangian $\mathscr{L} = T - V$ do not supply the right boundary conditions. Secondly, the variational approach based on Luke's Lagrangian density provides the correct Euler equations at the boundary and allows for a derivation of higher order KdV equations.
- In the frame moving with the velocity of sound all energy components are expressed by invariants. Energy is conserved.
- Numerical calculations confirm that invariants $I^{(1)}, I^{(2)}, I^{(3)}$ in the forms (8.12), (8.14), (8.17), (8.19) are exact constants of motion for two- and three-soliton solutions, both for fixed and moving coordinate systems. In all performed tests the invariants were exact up to fourteen digits in double precision calculations.
- For the extended KdV equation (4.27) we have only found one invariant of motion $I^{(1)}$ (8.27).
- The total energy in the fixed coordinate system as calculated in (8.42) is not exactly conserved but only altered during collisions, even then by minute quantities (an order of magnitude smaller than expected).

8.6 Extended KdV equation

In this section we calculate energy formula corresponding to a wave motion governed by second order equations in scaled variables, that is the equation (4.27) for the fixed coordinate system and the corresponding equation for a moving coordinate system. As previously we compare energies calculated from the definition with those Luke's Lagrangian.

8.6.1 Energy in a fixed frame calculated from definition

Now, instead of (8.1) we consider the extended KdV equation (KdV2), that is (4.27).

In section 8.3, the total energy of the wave governed by KdV equation, that is the equation (8.1) with terms only up to first order in small parameters was obtained in (8.42). In calculation according to equation (4.27) the potential energy is expressed by the same formula (8.35) as previously for KdV equation. In the expression for kinetic energy the velocity potential has to be expanded to second order in small parameters

$$\phi = f - \frac{1}{2}\beta y^2 f_{xx} + \frac{1}{24}\beta^2 y^4 f_{xxxx} \tag{8.89}$$

with derivatives

$$\begin{cases} \phi_x = f_x - \frac{1}{2}\beta y^2 f_{xxx} + \frac{1}{24}\beta^2 y^4 f_{xxxxx} \\[2mm] \phi_y = -\beta y f_{xx} + \frac{1}{6}\beta^2 y^3 f_{xxxx}. \end{cases} \tag{8.90}$$

Integrating over y and retaining terms up to fourth order yields

$$T = \frac{1}{2}\rho g h^2 L \int_{-\infty}^{+\infty} \alpha^2 \left[f_x^2 + \alpha \eta f_x^2 + \frac{1}{3}\beta \left(f_{xx}^2 - f_x f_{xxx} \right) + \alpha\beta(\eta f_{xx}^2 - \eta f_x f_{xxx}) \right.$$
$$\left. + \beta^2 \left(\frac{1}{20}f_{xxx}^2 - \frac{1}{15}f_{xx}f_{xxxx} + \frac{1}{60}f_x f_{xxxxx} \right) \right] dx. \tag{8.91}$$

Expression (8.91) limited to first line gives kinetic energy for KdV equation, compare (8.39).

Now, we use the expression for f_x (and its derivatives) up to second order, see, e.g., [105, equation (2.7)], [79, equation (17)]

$$f_x = \eta - \frac{1}{4}\alpha\eta^2 + \frac{1}{3}\beta\eta_{xx} + \frac{1}{8}\alpha^2\eta^3 + \alpha\beta \left(\frac{3}{16}\eta_x^2 + \frac{1}{2}\eta\eta_{xx} \right) + \frac{1}{10}\beta^2\eta_{xxxx}. \tag{8.92}$$

Insertion (8.92) and its derivatives into (8.91) gives

$$T = \frac{1}{2}\rho g h^2 L \int_{-\infty}^{+\infty} \alpha^2 \left[\eta^2 + \frac{1}{2}\alpha\eta^3 + \frac{1}{3}\beta \left(\eta_x^2 + \eta\eta_{xx} \right) \right.$$
$$- \frac{3}{16}\alpha^2\eta^4 + \alpha\beta \left(\frac{29}{24}\eta\eta_x^2 + \frac{3}{4}\eta^2\eta_{xx} \right) \tag{8.93}$$
$$\left. + \beta^2 \left(\frac{1}{20}\eta_{xx}^2 + \frac{7}{45}\eta_x\eta_{xxx} + \frac{19}{180}\eta\eta_{xxxx} \right) \right] dx.$$

From properties of solutions at $x \to \pm\infty$ terms with β and β^2 in square bracket vanish and the term with $\alpha\beta$ can be simplified. Finally one obtains

$$T = \frac{1}{2}\rho g h^2 L \int_{-\infty}^{+\infty} \alpha^2 \left[\eta^2 + \frac{1}{2}\alpha\eta^3 - \frac{3}{16}\alpha^2\eta^4 - \frac{7}{24}\alpha\beta\eta\eta_x^2 \right] dx. \tag{8.94}$$

Then total energy is the sum of (8.36) and (8.94)

$$E_{\text{tot}} = \rho g h^2 L \int_{-\infty}^{\infty} \left[\alpha\eta + (\alpha\eta)^2 + \frac{1}{4}(\alpha\eta)^3 - \frac{3}{32}(\alpha\eta)^4 - \frac{7}{48}\alpha^3\beta\eta\eta_x^2 \right] dx.$$

(8.95)

The first three terms are identical as in KdV energy formula (8.42), the last two terms are new for extended KdV equation (4.27).

8.6.2 Energy in a fixed frame calculated from Luke's Lagrangian

Calculate energy in the same way as in Section 8.5, but in one order higher. In scaled coordinates Lagrangian density is expressed by (8.67) (here we keep infinite constant term)

$$\mathcal{L} = \rho g h^2 L \left\{ \int_0^{1+\alpha\eta} \alpha \left[\phi_t + \frac{1}{2}\left(\alpha\phi_x^2 + \frac{\alpha}{\beta}\phi_y^2 \right) \right] dy + \frac{1}{2}(1+\alpha\eta)^2 \right\}.$$

(8.96)

From (8.89) we have

$$\phi_t = f_t - \frac{1}{2}\beta y^2 f_{xxt} + \frac{1}{24}\beta^2 y^4 f_{xxxxt}.$$

(8.97)

Inserting (8.97) and (8.90) into (8.96), integrating over y and retaining terms up to third order one obtains (constant term $\frac{1}{2}$ is dropped)

$$\begin{aligned}
\frac{\mathcal{L}}{\rho g h^2 L} = \alpha \Bigg\{ &(\eta + f_t) + \alpha\left(\frac{1}{2}\eta^2 + \eta f_t + \frac{1}{2}f_x^2 \right) - \frac{1}{2}\beta f_{xxt} \\
&+ \frac{1}{2}\alpha^2\eta f_x^2 + \alpha\beta\left(\frac{1}{6}f_{xx}^2 - \frac{1}{2}\eta f_{xxt} - \frac{1}{6}f_x f_{xxx} \right) + \frac{1}{120}\beta^2 f_{xxxxt} \\
&+ \frac{1}{2}\alpha^2\beta\left(\eta f_{xx}^2 - \eta^2 f_{xxt} - \eta f_x f_{xxx} \right) \\
&+ \alpha\beta^2\left(\frac{1}{40}f_{xxx}^2 - \frac{1}{30}f_{xx}f_{xxxx} + \frac{1}{24}\eta f_{xxxxt} + \frac{1}{120}f_x f_{xxxxx} \right) \\
&- \beta^3\frac{1}{5040}f_{xxxxxxt} \Bigg\}.
\end{aligned}$$

(8.98)

The the Hamiltonian density

$$\mathcal{H} = f_t\frac{\partial\mathcal{L}}{\partial f_t} + f_{xxt}\frac{\partial\mathcal{L}}{\partial f_{xxt}} + f_{(4x)t}\frac{\partial\mathcal{L}}{\partial f_{(4x)t}} + f_{(6x)t}\frac{\partial\mathcal{L}}{\partial f_{(6x)t}} - \mathcal{L}$$

is

$$\frac{\mathcal{H}}{\rho g h^2 L} = -\alpha\eta - \frac{1}{2}\alpha^2\left(\eta^2 + f_x^2\right) - \frac{1}{2}\alpha^3\eta f_x^2 + \alpha^2\beta\left(-\frac{1}{6}f_{xx}^2 + \frac{1}{6}f_x f_{xxx}\right)$$

$$+ \alpha^3\beta\left(-\frac{1}{2}\eta f_{xx}^2 + \frac{1}{2}\eta f_x f_{xxx}\right) \tag{8.99}$$

$$+ \alpha^2\beta^2\left(-\frac{1}{40}f_{xxx}^2 + \frac{1}{30}f_{xx}f_{xxxx} - \frac{1}{120}f_x f_{xxxxx}\right).$$

Now, we use f_x in the second order (8.92) and its derivatives. Insertion these expressions into (8.99) and retention terms up to third order yields

$$\frac{\mathcal{H}}{\rho g h^2 L} = -\alpha\eta - \alpha^2\eta^2 - \frac{1}{4}\alpha^3\eta^3 + \frac{3}{32}\alpha^4\eta^4 \tag{8.100}$$

$$+ \alpha^2\beta\left(-\frac{1}{6}\eta_x^2 - \frac{1}{6}\eta\eta_{xx}\right) + \alpha^3\beta\left(-\frac{29}{48}\eta\eta_x^2 - \frac{3}{8}\eta^2\eta_{xx}\right)$$

$$+ \alpha^2\beta^2\left(-\frac{1}{40}\eta_{xx}^2 - \frac{7}{90}\eta_x\eta_{xxx} - \frac{19}{360}\eta\eta_{xxxx}\right).$$

The energy is obtained by integration of (8.100) over x (using integration by parts and properties of η and its derivatives at $x \to \pm\infty$). Then terms with $\alpha\beta$ and $\alpha\beta^2$ vanish. The final result is

$$E = -\rho g h^2 L \int_{-\infty}^{+\infty}\left[\alpha\eta + (\alpha\eta)^2 + \frac{1}{4}(\alpha\eta)^3 - \frac{3}{32}(\alpha\eta)^4 - \frac{7}{48}\alpha^3\beta\eta\eta_x^2\right]dx, \tag{8.101}$$

the same as (8.95) but with the opposite sign.

8.6.3 Energy in a moving frame from definition

Let us follow arguments given by Ali and Kalisch [8, Sec. 3] and used already in Section 8.3. Working in a moving frame one has to replace ϕ_x by the horizontal velocity in a moving frame, that is, $\phi_x - \frac{1}{\alpha}$. Then in a frame moving with the sound velocity we have

$$\begin{cases} \phi_x = f_x - \frac{1}{2}\beta y^2 f_{xxx} + \frac{1}{24}\beta^2 y^4 f_{xxxxx} - \frac{1}{\alpha} \\ \\ \phi_y = -\beta y f_{xx} + \frac{1}{6}\beta^2 y^3 f_{xxxx}. \end{cases} \tag{8.102}$$

Then the expression under integral over y in (8.34) becomes (in the following terms up to fourth order are kept)

$$\left(\alpha^2\phi_x^2 + \frac{\alpha^2}{\beta}\phi_y^2\right) = 1 - 2\alpha f_x + \alpha^2 f_x^2 + y^2\alpha^2\beta f_{xx}^2 \tag{8.103}$$

$$+ y^2\alpha\beta f_{xxx} - y^2\alpha^2\beta f_x f_{xxx} - \frac{1}{12}y^4\alpha\beta^2 f_{xxxxx}$$

$$+ y^4\alpha^2\beta^2 \left(\frac{1}{4}f_{xxx}^2 - \frac{1}{3}f_{xx}f_{xxxx} + \frac{1}{12}f_x f_{xxxxx}\right).$$

After integration over y one obtains

$$T = \frac{1}{2}\rho g h^2 L \int_{-\infty}^{+\infty} \left[1 + \alpha\left(\eta - 2f_x\right) + \alpha^2\left(-2\eta f_x + f_x^2\right) + \frac{1}{3}\alpha\beta f_{xxx}\right.$$

$$+ \alpha^3\eta f_x^2 - \frac{1}{60}\alpha\beta^2 f_{xxxxx} + \alpha^2\beta\left(\frac{1}{3}f_{xx}^2 + \eta f_{xxx} - \frac{1}{3}f_x f_{xxx}\right)$$

$$+ \alpha^3\beta\left(\eta f_{xx}^2 + \eta^2 f_{xxx} - \eta f_x f_{xxx}\right) \tag{8.104}$$

$$+ \alpha^2\beta^2\left(\frac{1}{20}f_{xxx}^2 - \frac{1}{15}f_{xx}f_{xxxx} - \frac{1}{12}\eta f_{xxxxx} + \frac{1}{60}f_x f_{xxxxx}\right)\right] dx.$$

Then insertion f_x (8.92) and its derivatives yields

$$T = \frac{1}{2}\rho g h^2 L \int_{-\infty}^{+\infty} \left[-\alpha\eta - \frac{1}{2}\alpha^2\eta^2 - \frac{1}{3}\alpha\beta\eta_{xx} + \frac{3}{4}\alpha^3\eta^3 - \alpha^2\beta\left(\frac{5}{24}\eta_x^2 + \frac{1}{2}\eta\eta_{xx}\right)\right.$$

$$- \frac{19}{180}\alpha\beta^2\eta_{xxxx} - \frac{7}{16}\alpha^4\eta^4 + \alpha^3\beta\left(\frac{7}{12}\eta\eta_x^2 + \frac{3}{8}\eta^2\eta_{xx}\right) \tag{8.105}$$

$$+ \alpha^2\beta^2\left(\frac{11}{30}\eta_{xx}^2 + \frac{233}{360}\eta_x\eta_{xxx} + \frac{119}{360}\eta\eta_{xxxx}\right) + \frac{1}{36}\alpha\beta^3\eta_{xxxxxx}\right] dx,$$

where constant term is dropped. Using properties of solutions at $x \to \pm\infty$ this expression can be simplified to

$$T = \frac{1}{2}\rho g h^2 L \int_{-\infty}^{+\infty} \left[-\alpha\eta - \frac{1}{2}\alpha^2\eta^2 + \frac{3}{4}\alpha^3\eta^3 - \frac{7}{16}\alpha^4\eta^4\right. \tag{8.106}$$

$$\left. + \frac{7}{24}\alpha^2\beta\,\eta_x^2 + \frac{1}{12}\alpha^3\beta\,\eta\eta_x^2 + \frac{1}{20}\alpha^2\beta^2\eta_{xx}^2\right] dx.$$

Then total energy is

$$E_{\text{tot}} = \rho g h^2 L \int_{-\infty}^{+\infty} \left[\frac{1}{2}\alpha\eta + \frac{1}{4}\alpha^2\eta^2 + \frac{3}{8}\alpha^3\eta^3 - \frac{7}{32}\alpha^4\eta^4\right. \tag{8.107}$$

$$\left. + \frac{7}{48}\alpha^2\beta\,\eta_x^2 + \frac{1}{24}\alpha^3\beta\,\eta\eta_x^2 + \frac{1}{40}\alpha^2\beta^2\eta_{xx}^2\right] dx.$$

In special case $\alpha = \beta$ this formula simplifies to

$$E_{\text{tot}} = \rho g h^2 L \int_{-\infty}^{+\infty} \left[\frac{1}{2}\alpha\eta + \frac{1}{4}\alpha^2\eta^2 + \alpha^3\left(\frac{3}{8}\eta^3 + \frac{7}{48}\eta_x^2\right)\right. \tag{8.108}$$

$$\left. + \alpha^4\left(-\frac{7}{32}\eta^4 + \frac{1}{24}\eta\eta_x^2 + \frac{1}{40}\eta_{xx}^2\right)\right] dx.$$

8.6.4 Energy in a moving frame from Luke's Lagrangian

Follow considerations in Section 8.5, but with KdV2 equation (4.27). Transforming into the moving frame through (8.76) we have now

$$\phi \ = f - \frac{1}{2}\beta y^2 f_{\bar{x}\bar{x}} + \frac{1}{24}\beta^2 y^4 f_{\bar{x}\bar{x}\bar{x}\bar{x}}, \tag{8.109}$$

$$\phi_x = f_{\bar{x}} - \frac{1}{2}\beta y^2 f_{\bar{x}\bar{x}\bar{x}} + \frac{1}{24}\beta^2 y^4 f_{\bar{x}\bar{x}\bar{x}\bar{x}\bar{x}}, \tag{8.110}$$

$$\phi_y = -\beta y f_{\bar{x}\bar{x}} + \frac{1}{6}\beta^2 y^3 f_{\bar{x}\bar{x}\bar{x}\bar{x}}, \tag{8.111}$$

$$\phi_t = -f_{\bar{x}} + \frac{1}{2}\beta y^2 f_{\bar{x}\bar{x}\bar{x}} - \frac{1}{24}\beta^2 y^4 f_{\bar{x}\bar{x}\bar{x}\bar{x}\bar{x}} + \alpha(f_{\bar{t}} - \frac{1}{2}\beta y^2 f_{\bar{x}\bar{x}\bar{t}} + \frac{1}{24}\beta^2 y^4 f_{\bar{x}\bar{x}\bar{x}\bar{x}\bar{t}}). \tag{8.112}$$

Inserting (8.109)-(8.112) into (8.96) one obtains Lagrangian density in moving frame as (constant term $\frac{1}{2}$ is dropped as previously)

$$\frac{\mathcal{L}}{\rho g h^2 L} = \alpha(\eta - f_{\bar{x}}) + \alpha^2\left(\frac{1}{2}\eta^2 + f_{\bar{t}} - \eta f_{\bar{x}} + \frac{1}{2}f_{\bar{x}}^2\right)$$

$$+ \frac{1}{6}\alpha\beta f_{\bar{x}\bar{x}\bar{x}} + \alpha^3\left(\eta f_{\bar{t}} + \frac{1}{2}\eta f_{\bar{x}}^2\right) - \frac{1}{120}\alpha\beta^2 f_{\bar{x}\bar{x}\bar{x}\bar{x}\bar{x}}$$

$$+ \alpha^2\beta\left(\frac{1}{6}f_{\bar{x}\bar{x}}^2 - \frac{1}{6}f_{\bar{x}\bar{x}\bar{t}} + \frac{1}{2}\eta f_{\bar{x}\bar{x}\bar{x}} - \frac{1}{6}f_{\bar{x}}f_{\bar{x}\bar{x}\bar{x}}\right) \tag{8.113}$$

$$+ \alpha^3\beta\left(\frac{1}{2}\eta f_{\bar{x}\bar{x}}^2 - \frac{1}{2}\eta f_{\bar{x}\bar{x}\bar{t}} + \frac{1}{2}\eta^2 f_{\bar{x}\bar{x}\bar{x}} - \frac{1}{2}\eta f_{\bar{x}}f_{\bar{x}\bar{x}\bar{x}}\right)$$

$$+ \alpha^2\beta^2\left(\frac{1}{40}f_{\bar{x}\bar{x}\bar{x}}^2 - \frac{1}{30}f_{\bar{x}\bar{x}}f_{\bar{x}\bar{x}\bar{x}\bar{x}} + \frac{1}{120}f_{\bar{x}\bar{x}\bar{x}\bar{x}\bar{t}} - \frac{1}{24}\eta f_{\bar{x}\bar{x}\bar{x}\bar{x}\bar{x}} + \frac{1}{120}f_{\bar{x}}f_{\bar{x}\bar{x}\bar{x}\bar{x}\bar{x}}\right).$$

Then Hamiltonian density

$$\mathcal{H} = f_{\bar{t}}\frac{\partial\mathcal{L}}{\partial f_{\bar{t}}} + f_{\bar{x}\bar{x}\bar{t}}\frac{\partial\mathcal{L}}{\partial f_{\bar{x}\bar{x}\bar{t}}} + f_{\bar{x}\bar{x}\bar{x}\bar{x}\bar{t}}\frac{\partial\mathcal{L}}{\partial f_{\bar{x}\bar{x}\bar{x}\bar{x}\bar{t}}} - \mathcal{L} \tag{8.114}$$

after insertion of (8.113) into (8.114) yields

$$\frac{\mathcal{H}}{\rho g h^2 L} = \alpha\left(-\eta + f_{\bar{x}}\right) + \alpha^2\left(-\frac{1}{2}\eta^2 + \eta f_{\bar{x}} - \frac{1}{2}f_{\bar{x}}^2\right) - \frac{1}{6}\alpha\beta f_{\bar{x}\bar{x}\bar{x}} - \frac{1}{2}\alpha^3\eta f_{\bar{x}}^2$$

$$+ \frac{1}{120}\alpha\beta^2 f_{\bar{x}\bar{x}\bar{x}\bar{x}\bar{x}} + \alpha^2\beta\left(-\frac{1}{6}f_{\bar{x}\bar{x}}^2 - \frac{1}{2}\eta f_{\bar{x}\bar{x}\bar{x}} + \frac{1}{6}f_{\bar{x}}f_{\bar{x}\bar{x}\bar{x}}\right)$$

$$+ \alpha^3\beta\left(-\frac{1}{2}\eta f_{\bar{x}\bar{x}}^2 - \frac{1}{2}\eta^2 f_{\bar{x}\bar{x}\bar{x}} + \frac{1}{2}\eta f_{\bar{x}}f_{\bar{x}\bar{x}\bar{x}}\right) \tag{8.115}$$

$$+ \alpha^2\beta^2\left(-\frac{1}{40}f_{\bar{x}\bar{x}\bar{x}}^2 + \frac{1}{30}f_{\bar{x}\bar{x}}f_{\bar{x}\bar{x}\bar{x}\bar{x}} + \frac{1}{24}\eta f_{\bar{x}\bar{x}\bar{x}\bar{x}\bar{x}} - \frac{1}{120}f_{\bar{x}}f_{\bar{x}\bar{x}\bar{x}\bar{x}\bar{x}}\right).$$

In order to express (8.115) by η only we use $f_{\bar{x}}$ in the form (8.92) and its derivatives. It gives

$$\frac{\mathcal{H}}{\rho g h^2 L} = -\frac{1}{4}\alpha^2\eta^2 + \frac{1}{6}\alpha\beta\eta_{\bar{x}\bar{x}} - \frac{3}{8}\alpha^3\eta^3 + \alpha^2\beta\left(\frac{5}{48}\eta_x^2 + \frac{1}{4}\eta\eta_{xx}\right)$$

$$+ \frac{19}{360}\alpha\beta^2\eta_{\bar{x}\bar{x}\bar{x}\bar{x}} + \frac{7}{32}\alpha^4\eta^4 - \alpha^3\beta\left(\frac{7}{24}\eta\eta_{\bar{x}}^2 + \frac{3}{16}\eta^2\eta_{\bar{x}\bar{x}}\right) \quad (8.116)$$

$$- \alpha^2\beta^2\left(\frac{11}{60}\eta_{\bar{x}\bar{x}}^2 + \frac{233}{720}\eta_{\bar{x}}\eta_{\bar{x}\bar{x}\bar{x}} + \frac{119}{720}\eta\eta_{\bar{x}\bar{x}\bar{x}\bar{x}}\right) - \frac{1}{72}\alpha\beta^3\eta_{\bar{x}\bar{x}\bar{x}\bar{x}\bar{x}\bar{x}}.$$

Then energy is given by the integral

$$E = \varrho g h^2 L \int_{-\infty}^{+\infty} \left[-\frac{1}{4}\alpha^2\eta^2 + \frac{1}{6}\alpha\beta\eta_{\bar{x}\bar{x}} - \frac{3}{8}\alpha^3\eta^3 \right. \quad (8.117)$$

$$+ \alpha^2\beta\left(\frac{5}{48}\eta_x^2 + \frac{1}{4}\eta\eta_{xx}\right) + \frac{19}{360}\alpha\beta^2\eta_{\bar{x}\bar{x}\bar{x}\bar{x}} + \frac{7}{32}\alpha^4\eta^4$$

$$- \alpha^3\beta\left(\frac{7}{24}\eta\eta_{\bar{x}}^2 + \frac{3}{16}\eta^2\eta_{\bar{x}\bar{x}}\right) - \frac{1}{72}\alpha\beta^3\eta_{\bar{x}\bar{x}\bar{x}\bar{x}\bar{x}\bar{x}}$$

$$\left. - \alpha^2\beta^2\left(\frac{11}{60}\eta_{\bar{x}\bar{x}}^2 + \frac{233}{720}\eta_{\bar{x}}\eta_{\bar{x}\bar{x}\bar{x}} + \frac{119}{720}\eta\eta_{\bar{x}\bar{x}\bar{x}\bar{x}}\right)\right] dx.$$

From properties of solution integrals of terms with $\alpha\beta, \alpha\beta^2, \alpha\beta^3$ vanish and terms with $\alpha^2\beta, \alpha^3\beta, \alpha^2\beta^2$ can be simplified. Finally, energy is given by the follwing expression

$$E = \varrho g h^2 L \int_{-\infty}^{+\infty} \left[-\frac{1}{4}\alpha^2\eta^2 - \frac{3}{8}\alpha^3\eta^3 + \frac{7}{32}\alpha^4\eta^4 \right. \quad (8.118)$$

$$\left. - \frac{7}{48}\alpha^2\beta\eta_x^2 - \frac{1}{24}\alpha^3\beta\eta\eta_{\bar{x}}^2 - \frac{1}{40}\alpha^2\beta^2\eta_{\bar{x}\bar{x}}^2\right] dx.$$

In special case when $\beta = \alpha$ the result is

$$E = \varrho g h^2 L \int_{-\infty}^{+\infty} \left[-\frac{1}{4}\alpha^2\eta^2 - \alpha^3\left(\frac{3}{8}\eta^3 + \frac{7}{48}\eta_x^2\right)\right.$$

$$\left. + \alpha^4\left(\frac{7}{32}\eta^4 - \frac{1}{24}\eta\eta_{\bar{x}}^2 - \frac{1}{40}\eta_{\bar{x}\bar{x}}^2\right)\right] dx. \quad (8.119)$$

If the invariant term $I^{(1)} \equiv \int \alpha\eta\, dx$ is dropped in (8.95) or (8.101) then the energy calculated in the moving frame (8.118) have the same value but with oposite sign.

8.6.5 Numerical tests

Fixed frame

In order to check energy conservation for the extended KdV equation (4.27), we performed several numerical tests. First, let us discuss energy conservation in a fixed frame. We calculated time evolution governed by the equation (4.27) of waves which initial shape was given by 1-, 2- and 3-soliton solutions of the KdV (first order) equations. For presentation, the following initial conditions were chosen. The 3-soliton solution has amplitudes 1.5, 1 and 0.25, the 2-soliton solution has amplitudes 1 and 0.5, and the 1-soliton solution has the amplitude 1. The changes of energy presented in figures 8.4 and 8.5 are qualitatively the same also for different amplitudes. An example of such time evolution for the 3-soliton solution is presented in figure 8.3.
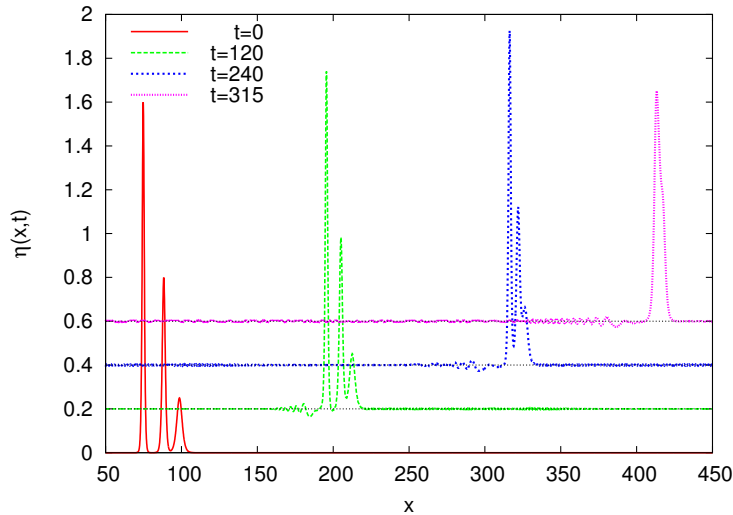
Fig. 8.3. Example of time evolution of 3-soliton solution. Reproduced with permission from [80]. Copyright (2015) by the American Physical Society

Time range in figure 8.3 contains the initial profile of 3-soliton solution with almost separated solitons at $t = 0$, intermediate shapes and almost ideal overlap of solitons at $t = 315$. In order to avoid overlaps of profiles and display details the subsequent shapes are shifted vertically with respect to the previous ones. Note behind the main wave additional slower waves which are generated by second order terms of the equation (4.27), that were already discussed in [79].
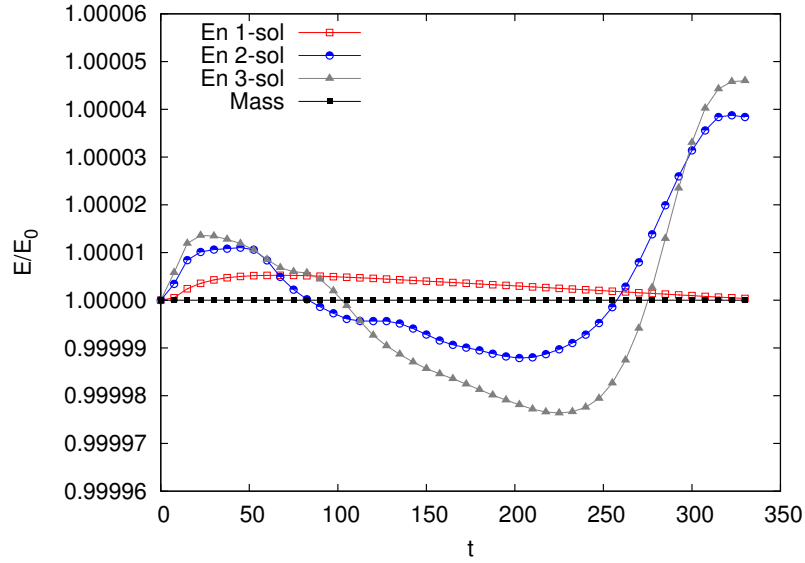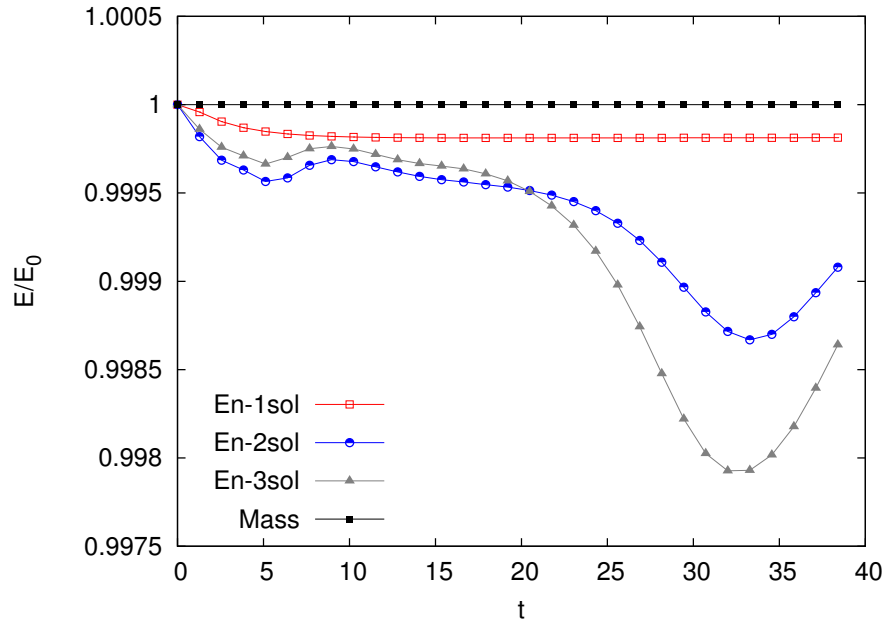
Fig. 8.4. Energy (non)conservation for the extended KdV equation in the fixed frame (4.27). Symbols represent values of the total energy given by formulas (8.95) or (8.101). Full square symbols represent the invariant $I^{(1)}$. Reproduced with permission from [80]. Copyright (2015) by the American Physical Society

We see that the total energy for waves which move according to the extended KdV equation is **not** conserved. Although energy variations are generally small (in time range considered they do not extend 0.001%, 0.004% and 0.005% for 1-, 2-, 3-soliton waves, respectively) they increase with more complicated waves. For additional check of numerics the invariant $I^{(1)} = \int_{-\infty}^{+\infty} \alpha \eta(x,t) dx$ for the eaquation (4.27) was plotted as Mass. In spite of approximate integration the value of $I^{(1)}$ was obtained constant up to 10 digits for all initial conditions.

Moving frame

Here we present variations of the energy calculated in a moving frame. The time evolution of the wave is given by the equation (4.27) transformed with (8.76), that is the equation

$$\eta_{\bar{t}} + \frac{3}{2}\eta\eta_{\bar{x}} + \frac{1}{6}\frac{\beta}{\alpha}\eta_{3\bar{x}} - \frac{3}{8}\alpha\,\eta^2\eta_{\bar{x}} + \beta\left(\frac{23}{24}\eta_{\bar{x}}\eta_{2\bar{x}} + \frac{5}{12}\eta\eta_{3\bar{x}}\right) + \frac{19}{360}\frac{\beta^2}{\alpha}\eta_{5\bar{x}} = 0.$$
$$(8.120)$$

Fig. 8.5. Energy (non)conservation for the extended KdV equation in the moving frame (8.120). Symbols represent values of the total energy given by the formula (8.107). Full square symbols represent the invariant $I^{(1)}$. Reproduced with permission from [80]. Copyright (2015) by the American Physical Society

The time range of the evolution was chosen for a convenient comparison with the numerical results obtained in the fixed reference frame, that is 2- and 3-soliton waves move from separate solitons to full overlap. The convention of symbols is the same as in figure 8.4, the energy is calculated according to the formula (8.107). In moving coordinate system energy variations are even greater than in the fixed reference frame because in the time considered it approaches values of 0.02%, 0.12% and 0.2% for 1-, 2- and 3-soliton waves, respectively. This increase of relative time variations of energy cannot be attributed only to two times smaller leading term ($\frac{1}{2}\alpha\eta$) in (8.107) with respect to (8.95). Again, despite of approximate integration, the value of $I^{(1)}$ was obtained constant up to 10 digits for all initial conditions.

8.6.6 Conclusions for KdV2 equation

We calculated energy of the fluid governed by the extended KdV equation (4.27) in two cases.

1. In the fixed frame (sections 8.6.1 and 8.6.2).
2. In the frame moving with the natural velocity $c = \sqrt{gh}$ (sections 8.6.3 and 8.6.4).

In both cases we calculated energy using two methods, from definition and from Luke's Lagrangian. Both methods give consistent results. For fixed frame energies (8.95) and (8.101) are the same. For moving frame the energy calculated from the definition contains one term more than energy calculated from Luke's Lagrangian, but this term ($\int \alpha \eta \, dx$) is the invariant $I^{(1)}$. When this term is dropped both energies in moving coordinate system (8.107) and (8.118) are the same and energies in both coordinate systems differ only by the sign.

The general conclusion concerning energy conservation for shallow water wave problem can be formulated as follows. Since there exists the Lagrangian of the system (Luke's Lagrangian), then exact solutions of Euler equations have to conserve energy. However, when approximate equations of different orders resulting from the exact Euler equations are considered, energy conservation is not a priori determined. **The KdV equation obtained in first order approximation has a miraculous property, an infinite number of invariants with energy among them. However, this astonishing property is lost in second order approximation to the Euler equations and energy in this order may be conserved only approximately.**

9

Adiabatic invariants for the extended KdV equation

It is common knowledge that KdV possesses an infinite number of invariants or conservation laws also known as integrals of motion [14, 36, 113, 122]. The two lowest KdV invariants are related to conservation of the fluid volume (mass) and its total momentum. The next one is related to energy conservation. Derivations of the first KdV invariants and their relations to volume momentum and energy conservation were presented in Chapter 8. The higher KdV invariants have no simple interpretation. KdV is, however, the result of an approximation of the set of the Euler equations within the perturbation approach, limited to the first order in expansion with respect to parameters assumed to be small. Several authors have extended KdV to the second order (KdV2), e.g., [24, 70, 82, 105, 108, 146]. In [78, 79] the authors have derived the KdV2 equation for an uneven bottom, that is KdV2B, introducing an additional small parameter related to bottom variation. However, this improved form is lacking in exactly conserved entities other than the ubiquitous mass law.

Many papers, e.g., [14,35,37–39,45,56,61–63,94,95,152] claim the existence of higher invariants and integrability of second order KdV type equations. In particular Benjamin and Olver [14] have discussed Hamiltonian structure, symmetries and conservation laws for water waves. A near-identity transformation (NIT), introduced by Kodama [94, 95] and then used by many authors, e.g., [35, 37–39, 45, 56, 61–63, 152], allows us to transform the second order KdV type equation to an asymptotically equivalent Hamiltonian form. The existence of the Hamiltonian form for the transformed equation supplies the full hierarchy of invariants, which appear to be adiabatic invariants for the original equation.

If there are no exact invariants in the system one looks for adiabatic (approximate) ones, as in [22]. Recently we developed a straightforward method to calculate adiabatic invariants, which allows us to find them directly from the original 'physical' equation (it also works for equations written in dimensional variables) [70]. Our method consists of the following: one proceeds with the KdV2 as with construction of KdV invariants and then uses the addition of KdV, multiplied by a small parameter, to cancel the nonintegrable terms. In [70] we focused on this direct method mentioning NIT-based derivation of adiabatic invariants rather briefly. In this chapter the NIT method is discussed more broadly with particular attention paid to energy conservation law.

In [132] it is shown that KdV2 for nonflat bottom [78, 79] admits no genuinely generalized symmetries, and thus is not symmetry-integrable.

9.1 Adiabatic invariants for KdV2 - direct method

We are interested in invariants of the extended KdV equation (4.27) called by us KdV2 (since it is obtained in second order perturbation approach), which is repeated below for reader's convenience

$$\eta_t + \eta_x + \frac{3}{2}\alpha\,\eta\eta_x + \frac{1}{6}\beta\,\eta_{3x} \tag{9.1}$$
$$- \frac{3}{8}\alpha^2\eta^2\eta_x + \alpha\beta\left(\frac{23}{24}\eta_x\eta_{2x} + \frac{5}{12}\eta\eta_{3x}\right) + \frac{19}{360}\beta^2\eta_{5x} = 0.$$

The equation was considered by several authors, see, e.g., [24, 70, 78–82, 105, 108].

In Section 8.2.2 we have recalled the fact that $I^{(1)} = \int_{-\infty}^{\infty} \eta\,dx$ is an invariant of equation (9.1) and represents the conservation of mass [80].

Below, we will be using the same notations as in Section 8.2.

9.1.1 Second invariant

The second invariant of KdV, $I^{(2)} = \int_{-\infty}^{\infty} \eta^2\,dx$ is **not** an invariant of KdV2, since, see [80, Sec. III B], upon multiplication of equation (9.1) by η one obtains

$$\frac{\partial}{\partial t}\left(\frac{1}{2}\eta^2\right) + \frac{\partial}{\partial x}\left[\frac{1}{2}\eta^2 + \frac{1}{2}\alpha\eta^3 + \frac{1}{6}\beta\left(-\frac{1}{2}\eta_x^2 + \eta\eta_{2x}\right) - \frac{3}{32}\alpha^2\eta^4 \tag{9.2}$$
$$+ \frac{19}{360}\beta^2\left(\frac{1}{2}\eta_{xx}^2 - \eta_x\eta_{3x} + \eta\eta_{4x}\right) + \frac{5}{12}\alpha\beta\,\eta^2\eta_{2x}\right] + \frac{1}{8}\alpha\beta\,\eta\eta_x\eta_{2x} = 0\,.$$

The last term in (9.2) can not be expressed as $\dfrac{\partial}{\partial x}X(\eta,\eta_x,\ldots)$. Therefore $\displaystyle\int_{-\infty}^{+\infty}\eta^2 dx$ is not a conserved quantity. There are no exact higher order invariants of (9.1), either.

It is possible, however, to find approximate invariants of (9.1), for which terms violating the invariance are of the third order in α,β. Our method allows us to find such approximate invariants with relatively low effort. It consists in forming an equation containing functions T and X through some manipulations with KdV2. Then some terms in X have nonintegrable form with respect to x similar to the last term in (9.2). We add some linear combination of type $(c_1\alpha+c_2\beta)\times KdV2(x,t)$ to that equation, drop the third order terms and require that nonintegrable terms cancel. (Equivalently, we add some linear combination of type $(c_1\alpha+c_2\beta)\times KdV(x,t)$ without dropping any term.) This action yields a new T' function and an approximate conservation law for $\int_{-\infty}^{\infty}T'dx$. Note that this procedure is analogous to that used in the construction of KdV invariants, described in detail in section 8.2.1. The term $KdV2(x,t)$ used above means the l.h.s. of the KdV2 equation (9.1).

The first approximate invariant can be obtained by adding to (9.2) equation (9.1) multiplied by $c_1\alpha\eta^2$, dropping third-order terms and choosing an appropriate value of c_1 in order to cancel the term $\dfrac{1}{8}\alpha\beta\,\eta\eta_x\eta_{2x}$. When this is done we are left with the expression

$$c_1\alpha\eta_t\eta^2 + c_1\alpha\eta^2\eta_x + c_1\frac{3}{2}\alpha^2\eta^3\eta_x + c_1\frac{1}{6}\alpha\beta\eta^2\eta_{3x}. \tag{9.3}$$

In integration over x of (9.3), the second and fourth terms are integrable with respect to x and then they can be included into the flux function X.

The last term in (9.3) can be transformed to $-\frac{1}{3}c_1\alpha\beta\eta\eta_x\eta_{2x}$. The condition for cancellation of this term with $\frac{1}{8}\alpha\beta\,\eta\eta_x\eta_{2x}$ gives $c_1=\dfrac{3}{8}$. Then the first term in (9.3) yields

$$c_1\alpha\eta_t\eta^2 = \frac{\partial}{\partial t}\left(\frac{1}{8}\alpha\eta^3\right) \tag{9.4}$$

and since the other terms are integrable we obtain an approximate invariant of KdV2 ($\frac{1}{2}$ is omitted)

$$I_{\mathrm{ad}}^{(2\alpha)} = \int_{-\infty}^{\infty}\left(\eta^2 + \frac{1}{4}\alpha\,\eta^3\right)dx \approx \mathrm{const.} \tag{9.5}$$

However, there is an alternative way to cancel the last term in (9.2) and obtain a second approximate invariant. This goal can be achieved by

adding to (9.2) equation (9.1) multiplied by $c_2\beta\eta_{2x}$, dropping again third-order terms and choosing an appropriate value of c_2 in order to cancel the term $\frac{1}{8}\alpha\beta\,\eta\eta_x\eta_{2x}$. Then new terms are

$$c_2\beta\eta_t\eta_{2x} + c_2\beta\eta_x\eta_{2x} + c_2\frac{3}{2}\alpha\beta\eta\eta_x\eta_{2x} + c_2\frac{1}{6}\beta^2\eta_{2x}\eta_{3x}. \tag{9.6}$$

In integration over x of (9.6), the second and fourth terms are integrable with respect to x and then they can be included into X. The condition for cancellation of nonintegrable terms

$$c_2\frac{3}{2}\alpha\beta\eta\eta_x\eta_{2x} + \frac{1}{8}\alpha\beta\,\eta\eta_x\eta_{2x} = 0$$

implies $c_2 = -\frac{1}{12}$.

Integration of the first term in (9.6) over x gives

$$\int_{-\infty}^{\infty} c_2\beta\eta_t\eta_{2x}dx = c_2\beta\left(\eta_t\eta_x|_{-\infty}^{\infty} - \int_{-\infty}^{\infty}\eta_{tx}\eta_x\right) = -c_2\beta\int_{-\infty}^{\infty}\frac{\partial}{\partial t}\left(\frac{1}{2}\eta_x^2\right). \tag{9.7}$$

Since terms with $\eta_x\eta_{2x}$ and $\eta_{2x}\eta_{3x}$ can be expressed as $\left(-\frac{1}{2}\eta_x^2\right)_x$ and $\left(-\frac{1}{2}\eta_{2x}^2\right)_x$, respectively, the final result is

$$\frac{\partial}{\partial t}\int_{-\infty}^{\infty}\frac{1}{2}\left(\eta^2 + \frac{1}{12}\beta\eta_x^2\right)dx + F(\eta,\eta_x,\eta_{2x})|_{-\infty}^{\infty} = O(\alpha^3), \tag{9.8}$$

where $F(\eta,\eta_x,\eta_{2x})$ comes from the flux term and vanishes due to properties of the solutions at $\pm\infty$. We assume that solutions at $\pm\infty$ vanish or are periodic.

Therefore we have an approximate (adiabatic) invariant of KdV2 (9.1) in the form

$$I_{ad}^{(2\beta)} = \int_{-\infty}^{\infty}\left(\eta^2 + \frac{1}{12}\beta\,\eta_x^2\right)dx \approx \text{const}. \tag{9.9}$$

The existence of two independent adiabatic invariants $I_{ad}^{(2\alpha)}$ and $I_{ad}^{(2\beta)}$ means also that

$$I_{ad}^{(2)} = \epsilon I_{ad}^{(2\alpha)} + (1-\epsilon)I_{ad}^{(2\beta)} = \int_{-\infty}^{\infty}\left(\eta^2 + \epsilon\frac{1}{12}\alpha\eta^3 + (1-\epsilon)\frac{1}{12}\beta\,\eta_x^2\right)dx \tag{9.10}$$

is an adiabatic invariant for any ϵ, that is, there exists one parameter family of adiabatic second invariant of KdV2.

9.1.2 Third invariant

In order to find the third invariant for KdV2 one can follow the procedure described in section 8.2.1, in equations (8.15)-(8.17), but with KdV2 equation. Let us take

$$3\eta^2 \times \mathrm{KDV2}(x,t) - \frac{2}{3}\frac{\beta}{\alpha}\eta_x \times \frac{\partial}{\partial x}\mathrm{KDV2}(x,t) = 0 \tag{9.11}$$

and consider a simpler case, when $\beta = \alpha$. The result is

$$\frac{\partial}{\partial t}\left(\eta^3 - \frac{1}{3}\eta_x^2\right) + \frac{\partial}{\partial x}\left(\eta^3 - \frac{1}{3}\eta_x^2 + \alpha\frac{9}{8}\eta^4 - \alpha^2\frac{9}{40}\eta^5\right) \tag{9.12}$$

$$+ \alpha\left(-\eta_x^3 - \eta\eta_x\eta_{2x} + \frac{1}{2}\eta^2\eta_{3x}\right) + \alpha^2\left(\frac{1}{2}\eta\eta_x^3 + \frac{25}{8}\eta^2\eta_x\eta_{2x} - \frac{23}{36}\eta_x\eta_{2x}^2\right.$$

$$\left. + \frac{5}{4}\eta^3\eta_{3x} - \frac{11}{12}\eta_x^2\eta_{3x} - \frac{5}{18}\eta\eta_x\eta_{4x} + \frac{19}{120}\eta^2\eta_{5x}\right).$$

In (9.12), we omitted terms which vanish under integration over x. All terms in the second and third rows of (9.12) are nonintegrable. However, taking an integral of the form $\int_{-\infty}^{\infty}...dx$ and integrating by parts they can be reduced to two types of nonintegrable terms. All terms in the bracket with α become proportional to $\eta\eta_x\eta_{2x}$. All terms in the bracket with α^2 reduce to $\eta\eta_x\eta_{2x}$ and $\eta_x\eta_{2x}^2$. Then using procedures described above for second adiabatic invariant, that is, by adding to (9.12) the KdV multiplied by proper factors one can cancel these nonintegrable terms. The added terms supply additional terms in the T function. As in the case of second invariant this action is not unique and there is some freedom in the form of final adiabatic invariant. One of admissibe forms is

$$I_{\mathrm{ad}}^{(3)} = \int_{-\infty}^{\infty}\left(\eta^3 - \frac{1}{3}\eta_x^2 - \alpha\eta^4 + \frac{7}{12}\alpha\,\eta\eta_x^2\right)dx. \tag{9.13}$$

Note that the first two terms in (9.13) are identical to the exact KdV invariant.

The presented method allows us to obtain higher order adiabatic invariants.

9.2 Near-identity transformation for KdV2 in fixed frame

All our considerations were performed in the fixed reference frame. They were motivated by two facts. First, as we have pointed out in [80, eq. (39)] even for KdV energy has **noninvariant form** (the same fact was shown, in dimension variables, in the paper of Ali and Kalisch [8]). Second, we aim to study invariants, and asymptotic invariants not only for KdV and KdV2 but also for

the KdV2 equation with uneven bottom, derived in [78, 79]. For this equation only the fixed reference frame makes sense.

Second order versions of KdV type equations are not unique since there exist transformations which transform the given equation into an equation of the same form but with some coefficients altered. These equations are asymptotically equivalent, that is, their solutions converge to the same form when small parameters tend to zero. Therefore such transformation, called *near-identity transformation* (NIT), is often used to convert higher order nonlinear differential equations to their asymptotically equivalent forms which can be integrable. Such NIT was first introduced by Kodama [94, 95] and then used and generalized by many authors, see, e.g., [37–39, 45, 54, 56, 63, 108]. Below we apply NIT in the form suitable for the KdV2 equation.

We employ the near-identity transformation in the form used by the authors of [37]

$$\eta = \eta' + \alpha a \eta'^2 + \beta b \eta'_{xx} + \cdots , \qquad (9.14)$$

where a, b are some constants. (Here, we choose $+$ sign. The inverse transformation, up to terms of second order, is $\eta' = \eta - \alpha a \eta^2 - \beta b \eta_{xx} + \cdots$).

NIT should preserve the form of the KdV2 (9.1), at most altering some coefficients. Then it is possible to choose coefficients a, b of NIT such that the transformed equation possesses a Hamiltonian (see the consequences in the subsection 9.2.2).

Insertion (9.14) into (9.1) yields (terms of order higher than the second in α, β are neglected)

$$\eta'_t + \eta'_x + \alpha \left[\left(\frac{3}{2} + 2a \right) \eta' \eta'_x + 2a \eta' \eta'_t \right] + \beta \left[\left(\frac{1}{6} + b \right) \eta'_{3x} + b \eta'_{xxt} \right] \qquad (9.15)$$

$$+ \alpha\beta \left\{ \left[\left(\frac{23}{24} + a + \frac{3}{2}b \right) \eta'_x \eta'_{2x} \right] + \left[\left(\frac{5}{12} + \frac{1}{3}a + \frac{3}{2}b \right) \eta' \eta'_{3x} \right] \right\}$$

$$+ \alpha^2 \left(-\frac{3}{8} + \frac{9}{2}a \right) \eta'^2 \eta'_x + \beta^2 \left[\left(\frac{19}{360} + \frac{1}{6}b \right) \eta'_{5x} \right] = 0.$$

Since terms with time derivatives (η'_t, η'_{xxt}) appear in first order with respect to small parameters we can replace them by appropriate expressions obtained from KdV2 (9.1) limited to first order, that is from KdV (3.29)

$$\eta'_t = -\eta'_x - \frac{3}{2}\alpha \eta' \eta'_x - \frac{1}{6}\beta \eta'_{3x} \qquad (9.16)$$

and

$$\eta'_{xxt} = \partial_{xx}\left(-\eta'_x - \frac{3}{2}\alpha\eta'\eta'_x - \frac{1}{6}\beta\eta'_{3x}\right) = -\eta'_{3x} - \frac{3}{2}\alpha(3\eta'_x\eta'_{2x} + \eta'\eta'_{3x}) - \frac{1}{6}\beta\eta'_{5x}.$$
(9.17)

Inserting (9.16) and (9.17) into (9.15) one obtains

$$\eta'_t + \eta'_x + \frac{3}{2}\alpha\eta'\eta'_x + \frac{1}{6}\beta\eta'_{3x} + \alpha^2\left(-\frac{3}{8} + \frac{3}{2}a\right)\eta'^2\eta'_x$$
(9.18)

$$+ \alpha\beta\left[\left(\frac{23}{24} + a - 3b\right)\eta'_x\eta'_{2x} + \frac{5}{12}\eta'\eta'_{3x}\right] + \frac{19}{360}\beta^2\eta'_{5x} = 0.$$

The equation (9.18) for η' has the same form as KdV2 (9.1) with only two coefficients altered. The coefficient in front of the term with $\alpha^2\eta^2\eta_x$ is changed from $-\frac{3}{8}$ to $-\frac{3}{8} + \frac{3}{2}a$ and the coefficient in front of the term with $\alpha\beta\eta_x\eta_{2x}$ is changed from $\frac{23}{24}$ to $\frac{23}{24} + a - 3b$.

9.2.1 NIT - second adiabatic invariant

For the NIT-transformed KdV2 equation (9.18) one can find the second invariant in the same way as previously, that is multiplying (9.18) by η' and requiring that the coefficient in front of the nonintegrable term vanishes. This gives

$$\int_{-\infty}^{\infty} \eta'\left[\frac{5}{12}\eta'\eta'_{3x} + \left(\frac{23}{24} + a - 3b\right)\eta'_x\eta'_{2x}\right] dx = 0.$$
(9.19)

Since

$$\int_{-\infty}^{\infty} \eta'^2\eta'_{3x} dx = -2\int_{-\infty}^{\infty} \eta'\eta'_x\eta'_{2x} dx$$
(9.20)

one obtains

$$\left(-2\frac{5}{12} + \frac{23}{24} + a - 3b\right)\int_{-\infty}^{\infty} \eta'\eta'_x\eta'_{xx} dx = 0 \quad\Longrightarrow\quad a - 3b + \frac{1}{8} = 0. \text{ (9.21)}$$

Then under the condition

$$a - 3b = -\frac{1}{8}$$
(9.22)

the integral $\int_{-\infty}^{\infty} \eta'^2 dx$ is the exact invariant of the equation (9.18).

Using inverse NIT

$$\eta' = \eta - \alpha a\eta^2 - \beta b\eta_{xx} + \cdots,$$
(9.23)

and neglecting higher order terms, one gets

$$\int_{-\infty}^{\infty} \eta'^2 dx \approx \int_{-\infty}^{\infty}\left[\eta^2 - 2\alpha a\eta^3 - 2\beta b\eta\eta_{xx}\right] = \int_{-\infty}^{\infty}\left[\eta^2 - 2\alpha a\eta^3 + 2\beta b\eta_x^2\right] dx,$$
(9.24)

where the last term was obtained through integration by parts. The r.h.s. of (9.24) is the most general form of the second adiabatic invariant of KdV2 under the condition (9.22), that is, one parameter family of adiabatic invariants

$$I_{\text{ad}}^{(2)} = \int_{-\infty}^{\infty} \left[\eta^2 - 2\alpha a \eta^3 + 2\beta b \eta_x^2 \right] dx \approx \text{const.} \tag{9.25}$$

In particular, with $a = 0$, $b = \frac{1}{24}$

$$I_{\text{ad}}^{(2)} = \int_{-\infty}^{\infty} \left(\eta^2 + \frac{1}{12} \beta \eta_x^2 \right) dx = I_{\text{ad}}^{(2\beta)} \tag{9.26}$$

and with $b = 0$, $a = -\frac{1}{8}$

$$I_{\text{ad}}^{(2)} = \int_{-\infty}^{\infty} \left(\eta^2 + \frac{1}{4} \alpha \eta^3 \right) dx = I_{\text{ad}}^{(2\alpha)}. \tag{9.27}$$

These adiabatic invariants are the same as those obtained in the direct way in (9.5) and (9.9).

The above formulas come from NIT (9.14) in which the sign $+$ was used. However, if in (9.14) the sign $-$ is chosen then the condition (9.22) is replaced by $a - 3b = \frac{1}{8}$. The signs of the inverse NIT become opposite and then the final forms of adiabatic invariants remain the same as in (9.25)-(9.27).

9.2.2 NIT - third adiabatic invariant

NIT-transformed KdV2 (9.18) describes waves in the fixed frame. In order to determine its Hamiltonian form let us convert (9.18) to a moving frame by transformation

$$\bar{x} = x - t, \quad \bar{t} = t, \quad \partial_x = \partial_{\bar{x}}, \quad \partial_t = -\partial_{\bar{x}} + \partial_{\bar{t}}. \tag{9.28}$$

Then (9.18) can be written in more general form as

$$\eta_{\bar{t}} + \alpha A \eta \eta_{\bar{x}} + \beta B \eta_{3\bar{x}} + \alpha^2 A_1 \eta^2 \eta_{\bar{x}} + \beta^2 B_1 \eta_{5\bar{x}} + \alpha\beta \left(G_1 \eta \eta_{3\bar{x}} + G_2 \eta_{\bar{x}} \eta_{2\bar{x}} \right) = 0, \tag{9.29}$$

where

$$A = \frac{3}{2}, \quad B = \frac{1}{6}, \quad A_1 = -\frac{3}{8} + \frac{3}{2}a, \quad B_1 = \frac{19}{360}, \quad G_1 = \frac{5}{12} \quad G_2 = \frac{23}{24} + a - 3b. \tag{9.30}$$

In the following we drop bars over t and x, remembering that now we work in the moving reference frame.

In particular, the parameters a, b of NIT can be chosen such that

$$G_2 = 2G_1. \tag{9.31}$$

In this case the Hamiltonian for the equation (9.29) exists. The condition (9.31) with (9.30) gives

$$\frac{23}{24} + a - 3b = 2\frac{5}{12} \qquad \Longrightarrow \qquad a - 3b = -\frac{1}{8}.$$

This is the same condition as (9.22). This condition supplies one parameter family of NIT, assuring Hamiltonian form of the NIT-transformed KdV2 (9.29) in the moving frame.

This Hamiltonian form is

$$\eta'_t = \frac{\partial}{\partial x}\left(\frac{\delta H}{\delta \eta'}\right), \tag{9.32}$$

where the Hamiltonian $H = \int_{-\infty}^{\infty} \mathcal{H}\, dx$ has density

$$\mathcal{H} = -\frac{1}{6}\alpha A\eta'^{3} + \frac{1}{2}\beta B\eta_x'^{2} - \frac{1}{12}\alpha^2 A_1\eta'^{4} - \frac{1}{2}\beta^2 B_1\eta_{xx}'^{2} + \frac{1}{2}\alpha\beta G_1\eta'\eta_x'^{2}. \tag{9.33}$$

Since $\mathcal{H} = \mathcal{H}(\eta', \eta'_x, \eta'_{xx})$, then the *functional derivative* in (9.32) is

$$\frac{\delta H}{\delta \eta'} = \frac{\partial \mathcal{H}}{\partial \eta'} - \frac{\partial}{\partial x}\frac{\partial \mathcal{H}}{\partial \eta'_x} + \frac{\partial^2}{\partial x^2}\frac{\partial \mathcal{H}}{\partial \eta'_{xx}} \tag{9.34}$$

$$= -\frac{1}{2}\alpha A\eta'^{2} - \beta B\eta'_{xx} - \frac{1}{3}\alpha^2 A_1\eta'^{3} - \alpha\beta G_1\left(\frac{1}{2}\eta_x'^{2} + \eta'\eta'_{xx}\right) - \beta^2 B_1\eta'_{4x}.$$

Insertion (9.34) into (9.32) yields

$$\eta'_t = -\alpha A\eta'\eta'_x - \beta B\eta'_{3x} - \alpha^2 A_1\eta'^{2}\eta'_x + \beta^2 B_1\eta'_{5x} - \alpha\beta G_1(2\eta'_x\eta'_{xx} + \eta'\eta'_{xxx}). \tag{9.35}$$

We see that the Hamiltonian form of KdV2 in the moving frame exists under the condition that the coefficient at the term $\eta'_x\eta'_{xx}$ is two times larger that the coefficient at the term $\eta'\eta'_{xxx}$. This is achieved by a proper choice of a, b parameters of NIT, which is the condition (9.22).

Now, the Hamiltonian is the exact constant of motion for the NIT-transformed equation (9.29) under the condition (9.22)

$$\int_{-\infty}^{\infty}\left[-\frac{1}{6}\alpha A\eta'^{3} + \frac{1}{2}\beta B\eta_x'^{2} - \frac{1}{12}\alpha^2 A_1\eta'^{4} \right. \tag{9.36}$$

$$\left. -\frac{1}{2}\beta^2 B_1\eta_{xx}'^{2} + \frac{1}{2}\alpha\beta G_1\eta'\eta_x'^{2}\right] dx = \text{const.}$$

In order to obtain the adiabatic invariant of the original equation (9.1) it is necessary to perform the inverse NIT, that is

$$\eta' = \eta - \alpha a \eta^2 - \beta b \eta_{xx} \tag{9.37}$$

and then to neglect in the Hamiltonian density all higher order terms. This yields

$$\mathcal{H} = -\frac{1}{6}\alpha A \eta^3 + \frac{1}{2}\beta B \eta_x^2 + \alpha^2 \left(\frac{1}{2}aA - \frac{1}{12}A_1\right)\eta^4 \tag{9.38}$$
$$+ \beta^2 \left(-\frac{1}{2}B_1\eta_{2x}^2 - bB\eta_x\eta_{3x}\right) + \alpha\beta \left[\left(\frac{1}{2}G_1 - 2aB\right)\eta\eta_x^2 + \frac{1}{2}bA\eta^2\eta_{2x}\right]$$

with the condition (9.22).

Now, we restore the original notation $A = \eta$ and numerical values of coefficients (9.30). Using relations which come from integration by parts

$$\int_{-\infty}^{\infty} \eta_x\eta_{3x}\, dx = -\int_{-\infty}^{\infty} \eta_{2x}^2\, dx, \quad \int_{-\infty}^{\infty} \eta^2\eta_{2x}\, dx = -2\int_{-\infty}^{\infty} \eta\eta_x^2\, dx$$

and changing irrelevant sign one obtains finally

$$I_{\mathrm{ad}}^{(3)} = \int_{-\infty}^{\infty} \left[\frac{1}{4}\alpha\eta^3 - \frac{1}{12}\beta\eta_x^2 - \alpha^2\left(\frac{1}{32} + \frac{5}{8}a\right)\eta^4 + \beta^2\left(\frac{19}{720} - \frac{1}{6}b\right)\eta_{2x}^2 \right.$$
$$\left. + \alpha\beta\left(\frac{1}{3}a + \frac{3}{2}b - \frac{5}{24}\right)\eta\eta_x^2\right]. \tag{9.39}$$

The result is one parameter family (9.22) of adiabatic invariants related to energy.

In a particular case, when in (9.22), we set $a = 0, \quad b = \frac{1}{24}$ and then

$$I_{\mathrm{ad}}^{(3)} = \int_{-\infty}^{\infty} \left[\frac{1}{4}\alpha\eta^3 - \frac{1}{12}\beta\eta_x^2 - \frac{1}{32}\alpha^2\eta^4 + \frac{7}{720}\beta^2\eta_{2x}^2 - \frac{7}{48}\alpha\beta\eta\eta_x^2\right] dx. \tag{9.40}$$

When in (9.22) we set $a = -\frac{1}{8}, \quad b = 0$, then we obtain

$$I_{\mathrm{ad}}^{(3)} = \int_{-\infty}^{\infty} \left[\frac{1}{4}\alpha\eta^3 - \frac{1}{12}\beta\eta_x^2 + \frac{3}{64}\alpha^2\eta^4 + \frac{19}{720}\beta^2\eta_{2x}^2 - \frac{1}{4}\alpha\beta\eta\eta_x^2\right] dx. \tag{9.41}$$

Another particular form of (9.39) can be received when one sets

$$\frac{19}{720} - \frac{1}{6}b = 0 \quad \Longrightarrow \quad b = \frac{19}{120}, \quad a = \frac{7}{20}.$$

Then, (9.39) reduces to

$$I_{\text{ad}}^{(3)} = \int_{-\infty}^{\infty} \left[\frac{1}{4}\alpha\eta^3 - \frac{1}{12}\beta\eta_x^2 - \frac{1}{4}\alpha^2\eta^4 + \frac{7}{240}\alpha\beta\eta\eta_x^2 \right] dx. \tag{9.42}$$

In a similar way one can set

$$\frac{1}{3}a + \frac{3}{2}b - \frac{5}{24} = 0 \quad \Longrightarrow \quad b = \frac{1}{10}, \quad a = \frac{7}{40}.$$

In this case the adiabatic invariant has the form

$$I_{\text{ad}}^{(3)} = \int_{-\infty}^{\infty} \left[\frac{1}{4}\alpha\eta^3 - \frac{1}{12}\beta\eta_x^2 - \frac{9}{64}\alpha^2\eta^4 + \frac{7}{720}\beta^2\eta_{2x}^2 \right] dx. \tag{9.43}$$

9.2.3 Momentum and energy for KdV2

Relations between invariants and conservation laws are not as simple as might be expected, even for KdV. In this subsection we present these relations for motion in a fixed reference frame. Expressions of energy for KdV and KdV2 in the moving frame can be found in [80, 81].

KdV case

The first KdV invariant, that is, $\int_{-\infty}^{\infty} \eta \, dx = $ const, represents volume (mass) conservation of the incompressible fluid.

When components of momentum are calculated as integrals over the fluid volume from momentum density the results are as follows

$$p_x = p_0 \int_{-\infty}^{\infty} \left[\eta + \frac{3}{4}\alpha\eta^2 \right] dx = p_0 \left[I_1 + \frac{3}{4}\alpha I_2 \right] \quad \text{and} \quad p_y = 0, \tag{9.44}$$

where p_0 is a constant in units of momentum. Since the vertical component of the momentum is zero and the horizontal component is expressed by the two lowest invariants we have the conservation of momentum law.

The total energy in the fixed frame is, see e.g. (8.43) (E_0 is a constant in energy units)

$$E_{\text{tot}} = E_0 \int_{-\infty}^{\infty} \left(\alpha\eta + (\alpha\eta)^2 + \frac{1}{4}(\alpha\eta)^3 \right) dx$$

$$= E_0 \left(\alpha I^{(1)} + \alpha^2 I^{(2)} + \frac{1}{4}\alpha^2 I^{(3)} + \frac{1}{12}\alpha^2\beta \int_{-\infty}^{\infty} \eta_x^2 \, dx \right).$$

This energy **has noninvariant form**. The last term in results in small deviations from energy conservation only when η_x changes in time in the soliton reference frame, which occurs only during soliton collisions.

KdV2 case

Volume conservation, that is, $I_1 = \int_{-\infty}^{\infty} \eta \, dx = \text{const}$, is fulfilled for KdV2, too.

   Calculation of momentum components within second order approximation of the Euler equations gives also a vanishing vertical component $p_y = 0$. For a horizontal component one gets

$$p_x = p_0 \int_{-\infty}^{\infty} \left(\eta + \frac{3}{4}\alpha\eta^2 - \frac{1}{8}\alpha^2\eta^3 - \frac{7}{48}\alpha\beta\eta_x^2 \right) dx \qquad (9.45)$$

$$= p_0 \left[I_1 + \frac{3}{4}\alpha \int_{-\infty}^{\infty} \left(\eta^2 - \frac{1}{6}\alpha\eta^3 - \frac{7}{36}\beta\eta_x^2 \right) dx \right].$$

The total momentum of the fluid is composed of two terms. The first is proportional to the volume. The second, an integral in the lower row of (9.45), contains the same functional terms η^2, η^3, η_x^2 as the expressions for the second adiabatic invariants (9.10) and (9.25) but with slightly different coefficients. Analogously to the KdV case (9.44) one can write

$$p_{x(\text{ad})} \approx p_0 \left[I_1 + \frac{3}{4}\alpha I_{\text{ad}}^{(2)} \right]. \qquad (9.46)$$

We will see in section 9.3 that $p_{x(\text{ad})}$, given by (9.46), has much smaller deviations from a constant value than p_x, given by (9.45).

   Energy $E_{\text{tot}} = T + V$ for the system governed by KdV2, see, e.g., [80, equation (91)], is as follows

$$E_{\text{tot}} = E_0 \int_{-\infty}^{\infty} \left(\alpha\eta + (\alpha\eta)^2 + \frac{1}{4}(\alpha\eta)^3 - \frac{3}{32}(\alpha\eta)^4 - \frac{7}{48}\alpha^3\beta\eta\eta_x^2 \right) dx. \quad (9.47)$$

This expression can be written as

$$E_{\text{tot}} = E_0 \left[\alpha I_1 + \alpha^2 \, I_{\text{ad}}^{2\beta} + \alpha^2 \int_{-\infty}^{\infty} \left(\frac{1}{4}\alpha\eta^3 - \frac{1}{12}\beta\eta_x^2 - \frac{3}{32}\alpha^2\eta^4 - \frac{7}{48}\alpha\beta\eta\eta_x^2 \right) dx \right]$$

$$\approx E_0 \, \alpha \left[I_1 + \alpha \left(I_{\text{ad}}^{2\beta} + \alpha I_{\text{ad}}^3 \right) \right], \qquad (9.48)$$

where $I_{\text{ad}}^{2\beta}$ is given by (9.9) and I_{ad}^3 was chosen in the form (9.42). Equation (9.48) shows that the energy of the system described by KdV2 in a fixed frame is approximately given by the sum of exact first invariant and combination of second and third adiabatic invariants. Since there is one parameter freedom in these adiabatic invariants other particular approximate formulas for the energy are admissible, as well. Because of the approximate character of adiabatic invariants the energy of the system is not a conserved quantity. When motion of several solitons is considered the largest changes in the energy occur when solitons change their shapes during collisions, see, e.g., [80, figure 4].
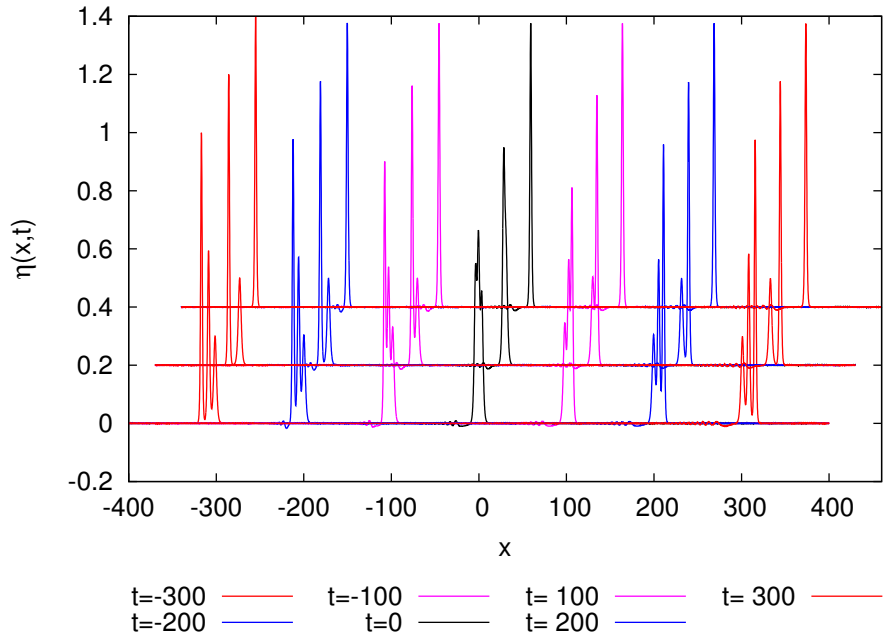
Fig. 9.1. Time evolution of initially 1-, 2- and 3-soliton KdV solution according to KdV2 (9.1). Reproduced with permission from [70]. Copyright (2017) by Elsevier

9.3 Numerical tests

One might wonder how good adiabatic invariants are. The calculations presented below give some insight.

First we calculated the time evolution, governed by equation (9.1), for three particular waves. The finite difference method (FDM) of Zabusky [149], generalized for precise calculation of higher derivatives [78, 79] was used. The finite element method (FEM) used for the same problems in [83] gives the same results for soliton's motion. As initial conditions 1-, 2- and 3-soliton solutions of KdV were taken. The amplitudes of the 3-soliton solution were chosen to be 1.0, 0.6 and 0.3, the amplitudes of the 2-soliton solution were chosen as 1.0 and 0.3 and the amplitude of this single soliton was chosen as 1.0. The motion of these waves according to (9.1) and their shapes at some instants are presented in figure 9.1. In order to avoid overlaps, vertical shifts by 0.2 and horizontal shifts by 30 were applied in the figure. In all calculations presented here the small parameters were both $\alpha = \beta = 0.1$.

The precision of numerical calculations of time evolution according to KdV2 can be verified by presentation of the exact invariant, that is volume conservation. Its numerical values displayed in figure 9.2 are constant up to 10 digits.
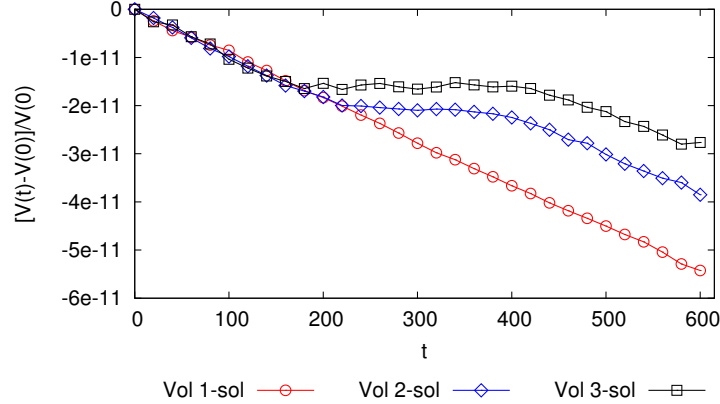
Fig. 9.2. Numerical precision of the volume conservation law for the three waves displayed in figure 9.1. Reproduced with permission from [70]. Copyright (2017) by Elsevier

9.3.1 Momentum (non)conservation and adiabatic invariant $I_{\mathrm{ad}}^{(2)}$

To study approximate invariants $I_{\mathrm{ad}}^{(2\beta)}$ and $I_{\mathrm{ad}}^{(2\alpha)}$ we write each of them as the sum of two terms

$$I_{\mathrm{ad}}^{(2\alpha)} = \int_{-\infty}^{\infty} \eta^2 \, dx + \int_{-\infty}^{\infty} \frac{1}{4} \alpha \, \eta^3 \, dx =: Ie(t) + Ia(t), \qquad (9.49)$$

$$I_{\mathrm{ad}}^{(2\beta)} = \int_{-\infty}^{\infty} \eta^2 \, dx + \int_{-\infty}^{\infty} \frac{1}{12} \beta \, \eta_x^2 \, dx =: Ie(t) + Ib(t). \qquad (9.50)$$

The first term in (9.49) and (9.50) is identical to the exact KdV invariant.

Values of adiabatic invariants $I_{\mathrm{ad}}^{(2\alpha)}$ (9.49) and $I_{\mathrm{ad}}^{(2\beta)}$ (9.50) calculated for the time evolution of waves displayed in figure 9.1 are presented in figure 9.3. In this scale both adiabatic invariants look perfectly constant. In order to see how good these invariants are we show how they change with respect to the initial values.

Figure 9.4 shows changes in the quantities Ie, Ia and Ib for all three 1-, 2-, and 3-soliton waves presented in figure 9.1. Displayed are the relative changes of
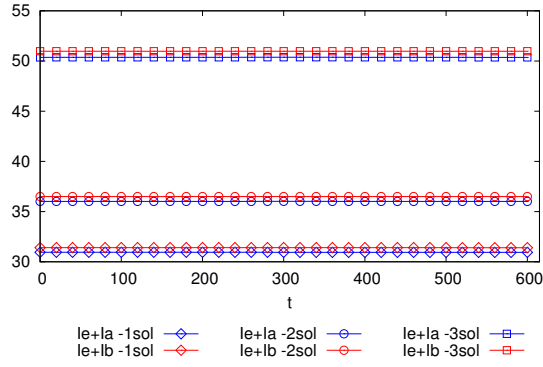
Fig. 9.3. Absolute values of the adiabatic invariants (9.49) and (9.50) for the time evolution shown in figure 9.1. Reproduced with permission from [70]. Copyright (2017) by Elsevier
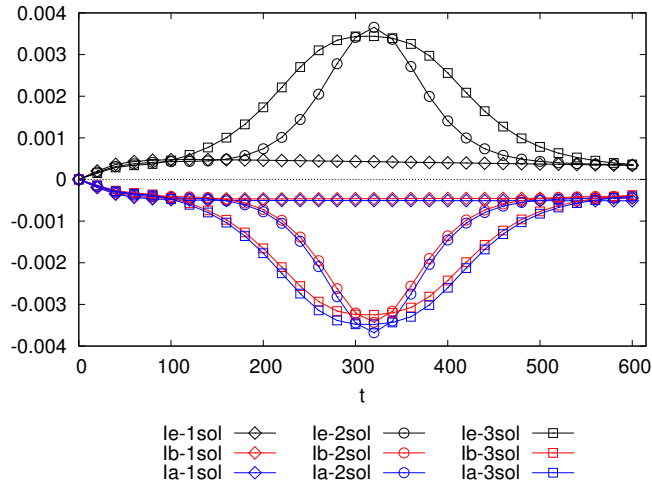
Fig. 9.4. Relative changes of Ia and Ib as a functions of time for the three waves presented in figure 9.1. Reproduced with permission from [70]. Copyright (2017) by Elsevier

$$Ie = \frac{Ie(t) - Ie(0)}{Ie(0) + Ia(0)}, \quad Ia = \frac{Ia(t) - Ia(0)}{Ie(0) + Ia(0)}, \quad Ib = \frac{Ib(t) - Ib(0)}{Ie(0) + Ia(0)}.$$

The figure shows that the corrections Ia, Ib to the KdV invariant Ie have very similar absolute values as Ie but opposite sign. Therefore one can expect that their sums with Ie should almost cancel ensuring that variations of approximate invariants $I_{\mathrm{ad}}^{(2\alpha)}$ and $I_{\mathrm{ad}}^{(2\beta)}$ will be very small.
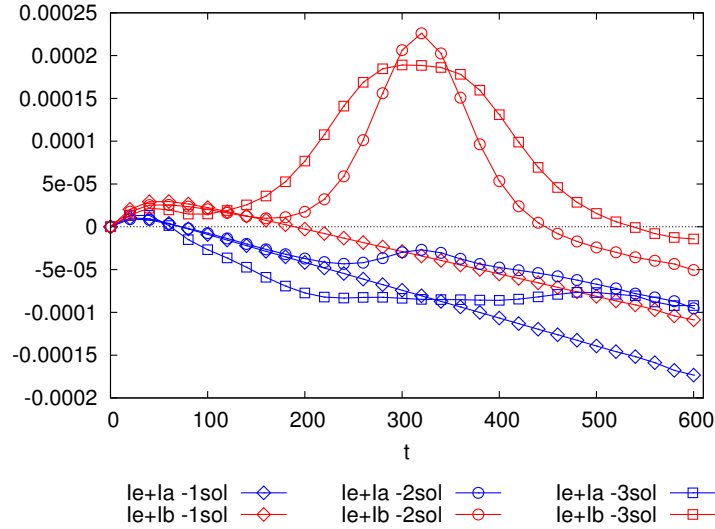
Fig. 9.5. Relative changes of the approximate invariants: $I_{\mathrm{ad}}^{(2\alpha)}$, denoted as $Ie +$ Ia and $I_{\mathrm{ad}}^{(2\beta)}$ denoted as $Ie + Ib$ for the three waves displayed in the figure 9.1. Reproduced with permission from [70]. Copyright (2017) by Elsevier

This expectation is confirmed by figure 9.5. For long term evolution, the relative changes of all approximate invariants are less than the order of 0.00025.

As we have already mentioned the fluid momentum is related to the adiabatic invariant $I_{\mathrm{ad}}^{(2)}$. Let us compare the momentum given by defintion (9.45) with its approximation expressed by adiabatic invariant (9.46). The former is presented in figure 9.6, top. In the latter, displayed in figure 9.6, bottom, for $I_{\mathrm{ad}}^{(2)}$ we used (9.10) with $\epsilon = \frac{1}{2}$. It is clear that the approximate momentum expressed by exact first invariant and adiabatic invariant $I_{\mathrm{ad}}^{(2)}$ sufers much smaller fluctuations than the exact momentum (9.45).

9.3.2 Energy (non)conservation and adiabatic invariant $I_{\mathrm{ad}}^{(3)}$

Relative changes of the energy, that is $(E(t) - E(0))/E(0)$ for time evolution of 1-, 2- and 3-soliton waves, presented in figure 9.1, are displayed in figure 9.7, top.

How good are adiabatic invariants $I_{\mathrm{ad}}^{(2)}$ and $I_{\mathrm{ad}}^{(3)}$? The energy (9.47) can be approximated by a linear combination of three terms (9.48), exact invariant I_1 and adiabatic invariants $I_{\mathrm{ad}}^{(2)}$ and $I_{\mathrm{ad}}^{(3)}$. Relative changes of that approximate
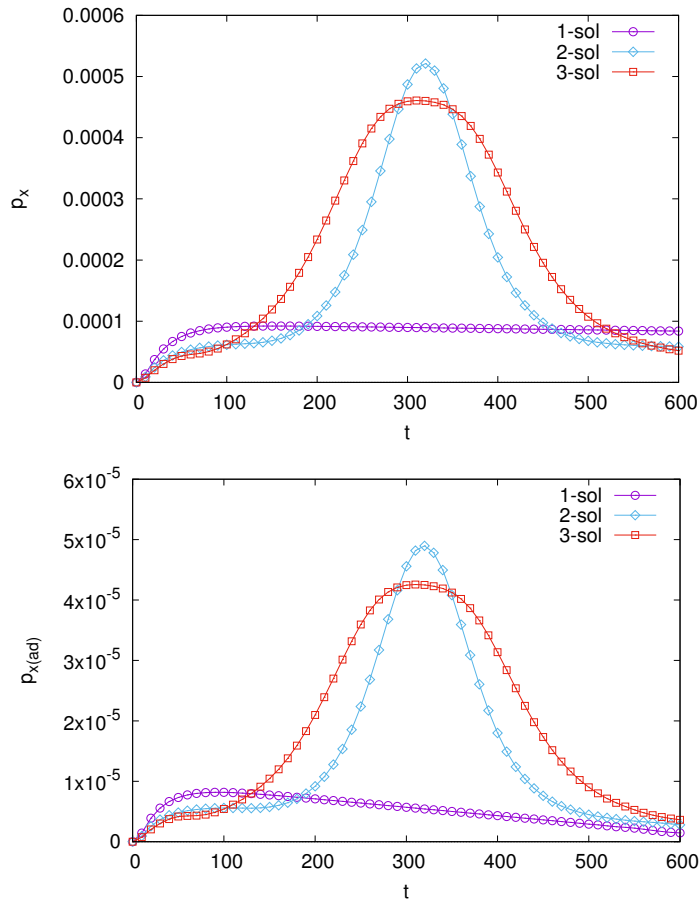
Fig. 9.6. Top: Relative changes of p_x (9.45) as a function of time for the three waves presented in figure 9.1. Bottom: The same for $p_{x(\text{ad})}$ (9.46).

energy (9.48) are displayed in figure 9.7, bottom. Comparing top and bottom parts of the figure 9.7, we see, that, as in the case of momentum, the approximate energy expressed by adiabatic invariants is closer to constant value than the exact one.

Apart from volume conservation, which holds almost to numerical precision (see figure 9.2), the adiabatic invariants presented in figures 9.5 and 9.6, and the energy shown in figure 9.7 for longer times slowly decrease with time. In our opinion the reason lies in the fact that initial conditions, taken as 1-, 2-, 3-soliton solutions of the KdV equation, **are not exact** solutions of the KdV2 equation. The known 1-soliton analytic solution of KdV2 equa-
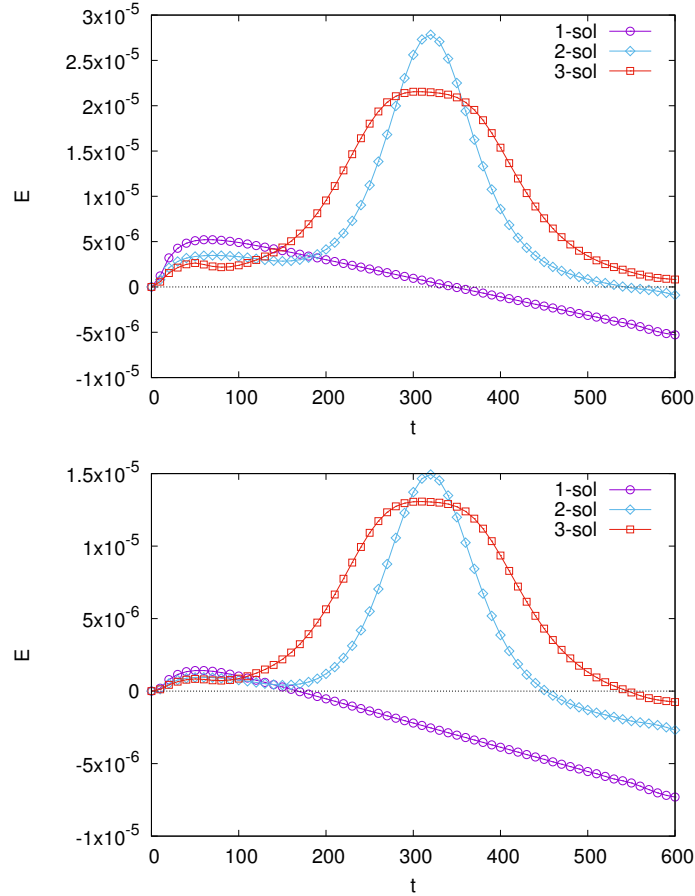
Fig. 9.7. Top: Relative changes of energy (9.47) as a function of time for the three waves presented in figure 9.1. Reproduced with permission from [82]. Copyright (2017) by Elsevier. Bottom: The same for energy approximated by adiabatic invariants (9.48).

tion found in [79] preserves exactly its shape and then possesses the infinite number of invariants. The same is true for recently found [70] exact analytic periodic solutions of KdV2. However, we do not expect the existence of exact n-soliton solutions for KdV2 since it does not belong to a hierarchy of integrable equations. On the other hand the 2- or 3-soliton solutions of an integrable equation like those obtained through NIT are likewise not exact solutions of (9.1) and the deviations from exactness will cause dissipation.

9.4 Summary and conclusions

In this chapter adiabatic invariants of KdV2 are described in detail. A method of direct calculation of adiabatic invariants for KdV2, developed in [82], is presented. This method can be applied directly to equations written in the fixed reference frame and with different small parameters of similar order, for instance $\alpha \neq \beta$. The method does not require a transformation to a particular moving frame, nor a near-identity transformation and therefore calculations of second invariant are simpler. It can be applied also to higher order invariants.

The NIT-based method, developed in section 9.2, seems to be more suitable for the adiabatic invariant related to energy since it gives the most general form of this invariant directly.

Numerical tests have proved that adiabatic invariants related to momentum and energy have indeed almost constant values. The largest deviations from these nearly constant values appear during soliton collisions.

Since the KdV2 equation has nonintegrable form, momentum and energy are not exact constants (see, e.g., figure 9.6 and figure 9.7).

There is, however, an intriguing kind of paradox with KdV2 invariants. On the one hand, exact invariants related to momentum and energy do **not exist**, only adiabatic ones are found. On the other hand, despite the non-integrability of KdV2, there exist exact analytic solutions of KdV2. The form of the single soliton solution of KdV2 was found in [79, Sect. IV]. Recently, in [70, 129, 130], we found several kinds of analytic periodic solutions of KdV2 known as *cnoidal waves*. These KdV2 solutions have the same form as corresponding KdV solutions, but with different coefficients. Both of these solutions preserve their shapes during motion, so for such initial conditions the infinite number of invariants like those given by (8.25) exists. When initial conditions have the form different from analytic solutions only adiabatic invariants are left.

Numerical simulations for KdV2B equation - Finite Difference Method

10.1 FDM algorithm

Let us briefly describe the scheme of our FDM code. This is a Zabusky-Kruskal type of algorithm [150] extended for second order terms and terms introduced by the non-flat bottom and modified in order to compute space derivatives of $\eta(x, t)$ with high accuracy.

We calculate time evolution of waves assuming periodic boundary conditions. This assumption is natural for periodic solutions (cnoidal waves). For soliton solutions, these conditions require a wide space interval, such that values of $\eta(x, t)$ at both ends of this interval are very close to zero.

Denote by

$$\eta_i^j = \eta(x_i, t_j), \qquad (i = 0, 1, 2, \ldots, N), \tag{10.1}$$

the value of the solution of (4.31) in the grid point $x_i = i\,dx$ at time instant $t_j = j\,dt$. Discrete values of space derivatives of the wave profile are consequently denoted by

$$\eta_x(x_i, t_j) = (\eta_x)_i^j, \quad \eta_{2x}(x_i, t_j) = (\eta_{2x})_i^j, \quad \ldots \quad \eta_{5x}(x_i, t_j) = (\eta_{5x})_i^j. \tag{10.2}$$

Similarly the values of the bottom function and its derivatives in the mesh points are denoted by

$$h_i, \quad (h_x)_i, \quad (h_{2x})_i, \quad (h_{3x})_i. \tag{10.3}$$

With such notations the N-dimensional vector of the wave profile at time t_{j+1} is given by so-called *leap-frog*

$$\eta_i^{j+1} = \eta_i^{j-1} + 2dt \left((\eta_x)_i^{j-1} + \frac{3}{2}\alpha\, \eta_i^{j-1}\, (\eta_x)_i^{j-1} + \frac{1}{6}\beta\, (\eta_{3x})_i^{j-1} \right) \qquad (10.4)$$

$$+ 2dt \left[-\frac{3}{8}\alpha^2\, (\eta_i^{j-1})^2\, (\eta_x)_i^{j-1} + \frac{19}{360}\beta^2\, (\eta_{5x})_i^{j-1} \right.$$

$$\left. +\alpha\beta \left(\frac{23}{25}\, (\eta_x)_i^{j-1}\, (\eta_{2x})_i^{j-1} + \frac{5}{12}\, \eta_i^{j-1}\, (\eta_{3x})_i^{j-1} \right) \right]$$

$$+ 2dt\, \beta\delta \left[-\frac{\left(h_i\, (\eta_x)_i^{j-1} + (h_x)_i \eta_i^{j-1} \right)}{2\beta} \right.$$

$$-\frac{1}{4} \left(h_i\, (\eta_{3x})_i^{j-1} + (h_x)_i\, (\eta_{2x})_i^{j-1} \right)$$

$$\left. +\frac{1}{4} \left((h_{2x})_i (\eta_x)_i^{j-1} + (h_{3x})_i \eta_i^{j-1} \right) \right].$$

For a given instant of time, high-order space derivatives η_{nx} are calculated sequentially from the profile η using nine-point central difference formula.

This scheme can be used to calculate time evolution according to KdV equation (3.29), KdV2 equation (4.27) and KdV2B equation (4.31). For the first one, it is enough to keep only terms in the first line in (10.4). For the second case, one has to keep terms in the first three lines of (10.4). Time evolution of a wave moving over an uneven bottom is obtained from the full equation (10.4).

10.2 Numerical simulations, short evolution times

In this section, some examples of numerical calculations of time evolution according to the second order equation (4.31) are presented and discussed. All calculations are done in non-dimensional variables (4.1). The initial condition was always taken in the form of the exact KdV soliton (the solution of first order KdV equation (3.29)). Calculations were performed on the interval $x \in [0, X]$ with periodic boundary conditions. The space step in the grid was chosen to be $\Delta x = 0.05$ and the time step $\Delta t = (\Delta x)^3/4$, like in [150]. In all simulations, the volume of the fluid was conserved up to 10-11 digits.

First, we calculated the time evolution of the exact KdV soliton according to second order equation (4.27). When $\alpha = \beta = 0.1$ the soliton moves almost unchanged for a long time. That behavior persists even for larger values of small parameters ($\alpha = \beta = 0.15$) though distortions of the tails of the soliton, tiny in the previous case, become a little bigger.

In the case $\alpha > \beta$ one obtains that nonlinear terms prevail and the initial soliton quickly evolves into the two-soliton solution. In the opposite case $\alpha < \beta$ dispersive terms predominate, and one observes decreasing amplitude of the wave, increasing width, distortion of the shape and creation of the wave trains at the tails. All these effects are known from the analysis of the pure KdV equation (3.29). Up to reasonable values of small parameters, $\alpha, \beta \lessapprox 0.15$, the same behavior is preserved for solutions to the second order equation (4.27).

Below several early results obtained in [78] for the time evolution of solutions to the second order equation with bottom topography included (4.31) are presented.
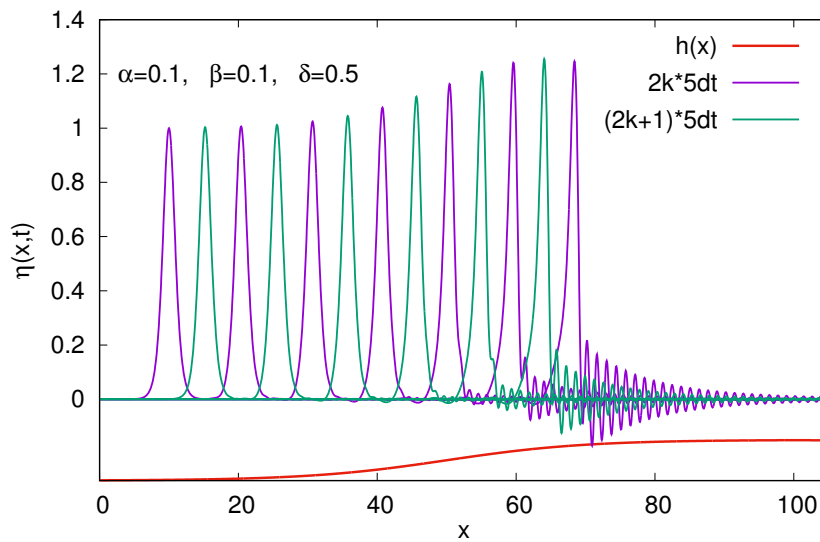
Fig. 10.1. Time evolution of the KdV soliton according to the equation (4.31) for decreasing water depth.

The simulations show the influence of $h(x)$-dependent terms. For the beginning let us present the case of smooth decreasing (or increasing) of the water depth. The cases are shown in figures 10.1 and 10.2, respectively. The non-dimensional $h(x)$ function was chosen in the form $h(x) = \pm\frac{1}{2}(\tanh(0.05(x-50))+1)$. In both cases the calculations were performed on the interval $x \in [0, 200]$ with $N = 4000$ grid points, where the bottom function for the subinterval $x \in [100, 200]$ was symmetric to that in the subinterval $x \in [0, 100]$. Such setting assured almost exact smoothness of the function $h(x)$ and its derivatives. The cases shown in figures 10.1 and 10.2 model incoming and outgoing sea-shore waves.
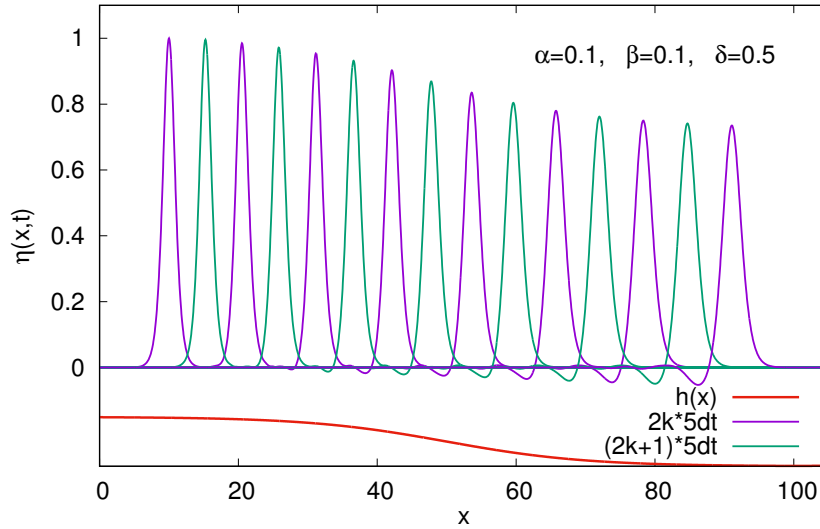
Fig. 10.2. Time evolution of the KdV soliton for $\alpha = \beta = 0.1$ $\delta = 0.5$ for increasing water depth.

In the figures 10.1-10.7 the bottom function is drawn with the thick red line (not in scale). Medium thick blue lines represent the wave shapes at $t = 0, 10, 20, \ldots$ and the green ones at $t = 5, 15, 25, \ldots$. In figure 10.1 we see a growth of the wave amplitude, forward scattering and formation of the shock wave when the soliton approaches the shallow region. In figure 10.2 the wave slows down and decreases its amplitude when the water depth increases. At the same time, a backward scattered wave appears.

Figures 10.3 and 10.4 show the soliton motion for the bottom containing a well and a hump. In both cases $\alpha = \beta = 0.1$ and $\delta = 0.5$. The bottom function was chosen as a sum of two Gaussians centered at $x = 15$ and $x = 25$ with widths $\sigma = 2$. Calculations were performed on the interval $X \in [0:50]$ with $N = 1000$ grid points and periodic boundary conditions. In order to show details of the evolution thin yellow lines are plotted for $t \in [5, 35]$ with the step $\Delta t = 1$. In both cases, we see decreasing/increasing amplitudes of the wave passing over the well/hump, respectively. However, when the wave comes back to the flat part of the bottom, it almost comes back to its original shape.

The shape of the soliton evolving with respect to the equation (4.31) is resistant to bottom variations extended on long distances. The case presented
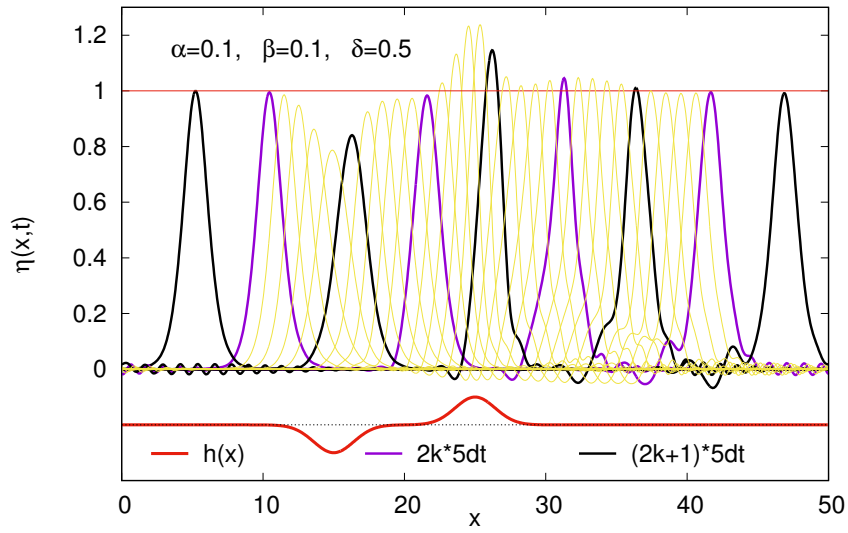
Fig. 10.3. Time evolution of the KdV soliton according to KdV2B for the Gaussian well followed by the symmetric hump.
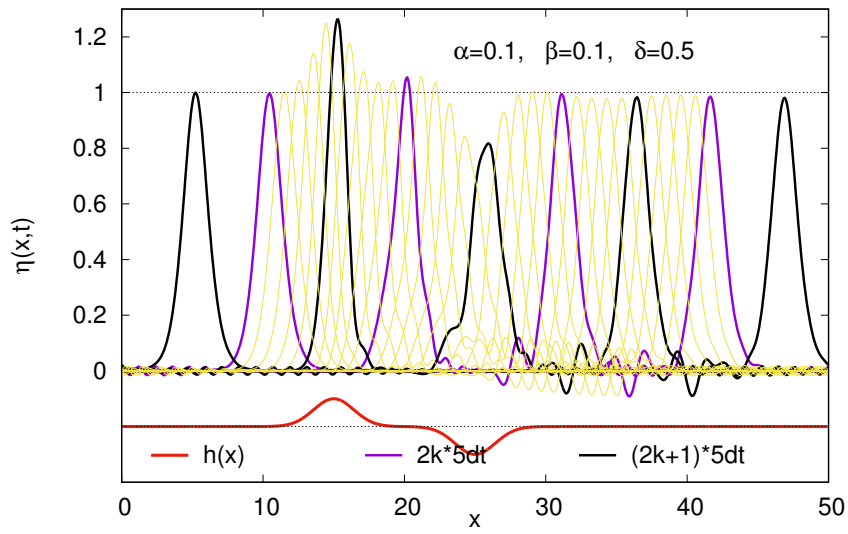
Fig. 10.4. Time evolution of the KdV soliton according to KdV2B for the Gaussian hump followed by the symmetric well.
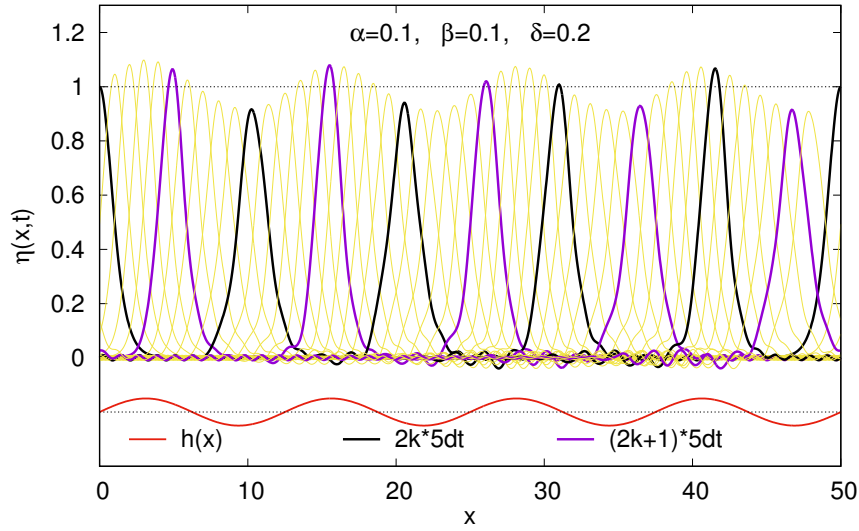
Fig. 10.5. Motion of the soliton according to the equation (4.31) for periodically varying bottom.

in figure 10.5 shows the time evolution of the KdV soliton when the bottom function is the sinus function with the period $2\pi/12.5$ and the amplitude $0.2\,H$. The soliton wave moves with its shape almost unchanged modifying its amplitude, width, and speed. This behavior maintains for larger values of δ, only the distortions of tails become larger.

The numerical simulations presented above exhibit the fact that KdV soliton persist its form even for substantial changes of the bottom.

10.3 Further numerical studies

In the previous section, we reported the earliest examples of numerical calculations for the time evolution of a KdV soliton according to the KdV2B equation (4.31) performed in [78]. However, the examples for a non-flat bottom were limited to short time evolution. In this section, we present results obtained for much longer times of evolution in [79]. Several cases of a long term evolution of wave motion according to the KdV2B equation, obtained with FDM algorithm (10.4) have been already shown in previous chapters (see figures 6.16, 7.7, 8.3, 9.1).
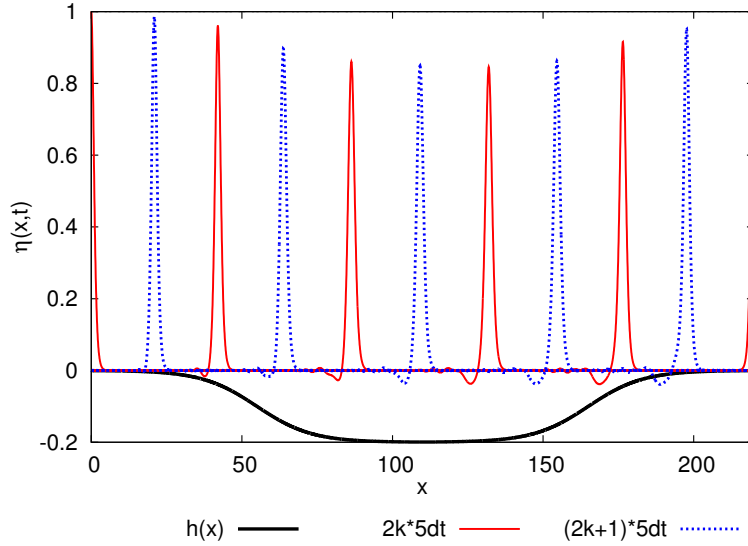
Fig. 10.6. Time evolution of the initial KdV soliton according to Eq. (4.31) for bottom shape function $h_-(x)$ and $\alpha = \beta = 0.1$, $\delta = 0.2$. See detailed explanations in the text. Reproduced with permission from [79]. Copyright (2014) by the American Physical Society

10.3.1 Initial condition in the form of KdV soliton

All the calculations presented below are performed in non-dimensional variables (4.1). In all examples presented in this subsection we assume the initial wave as the exact single KdV soliton $\eta(x,t) = \text{sech}\left[\frac{\sqrt{3}}{2}\left(x - x_0 - t(1 + \frac{\alpha}{2})\right)\right]^2$ at $x_0 = 0$, $t = 0$ (in non-dimensional variables we took the amplitude of the soliton to be 1). Calculations were performed on the interval $x \in [0, D]$ with the periodic boundary conditions of N grid points. The space grid points were separated by $\Delta x = 0.05$. The time step Δt was chosen as in [150], i.e., $\Delta t = (\Delta x)^3/4$. The calculations shown in this section used grids with $N = 4400$ and $N = 13200$, implying $D = 220$ and $D = 660$. For the soliton motion covering the interval $x \in [0, D]$ the number of time steps reaches $2 \cdot 10^7$. In all cases, the algorithm secures the volume (mass) conservation (8.12) up to 8-10 decimal digits. The initial position of the soliton is $x_0 = 0$ in all cases.

We begin calculations with the bottom function defined as $h_\pm(x) = \pm\frac{1}{2}[\tanh(0.055(x - 55)) + 1]$ for $x \leq 110$ and its symmetric reflection with respect to $x = 110$ for $x > 110$. figure 10.6 presents snapshots of the time evo-

lution of the initial wave, according to Eq. (4.31), over the bottom, defined by $h_-(x)$ function. The red (solid) curves show the profiles of the wave at time instants $t_i = 0, 10, 20, 30, 40\,dt$, where $dt = 4$, whereas the blue (dotted) ones correspond to times $t_i = 5, 15, 25, 35\,dt$. The same color and line scheme is used in the next figures. One observes a decrease in the amplitude of the wave when the depth of water increases and the inverse behavior when the bottom slants up. The small backscattered tail increases slowly with time.

In figure 10.7 the same sequence of snapshots for the soliton motion is presented for the bottom function $h_+(x)$. Here one observes at first an increase then a decrease in the amplitude of the main wave. In the case when the main part of the wave approaches a shallower region a forward scattering occurs and creates waves of much smaller amplitude outrunning the main one.

A closer inspection of the results presented above brings to light apparent relations between the bottom changes and amplitude and velocity of the main wave. When the pure KdV equation is considered (corresponding to a limitation of Eq. (4.31) to first order and flat bottom) the amplitude of the soliton and its velocity is greater when the water depth is smaller. Therefore, from this point of view, one expects a slower soliton motion when it enters a
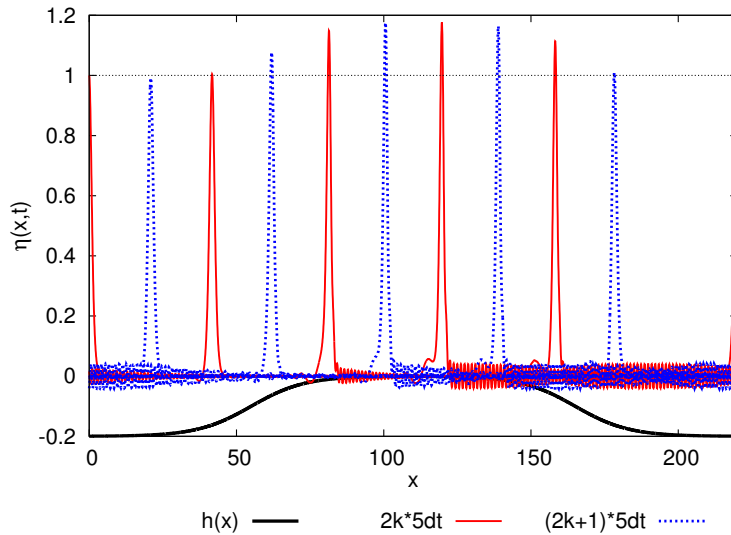
Fig. 10.7. The same as in figure 10.6 but for the bottom shape function $h_+(x)$. Reproduced with permission from [79]. Copyright (2014) by the American Physical Society
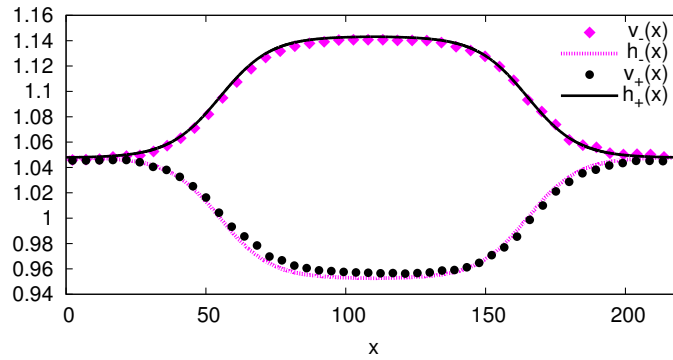
Fig. 10.8. Anticorrelations between the soliton's velocity and the water depth. Dots indicate the average velocities of the tops of solitons for given positions, lines with the same color the shape of the bottom function. Reproduced with permission from [79]. Copyright (2014) by the American Physical Society

deeper basin and a faster motion when it moves towards a shallowing. On the other hand, inspection of solutions to the KdV-type equation obtained in [59], (see, e.g., figures 3 and 4), which is second order in the small parameter for slow bottom changes, shows qualitatively that when the depth decreases, the amplitude of the solitary wave increases with simultaneous decrease of its wavelength and velocity. (The small parameter used in [59, 126] is different from ours, as it measures the ratio of the bottom variation to a wavelength.) A decrease of the velocity with simultaneous increase of the amplitude (and a creation of slower secondary waves) is obtained for the solitary wave entering a shallower region in [140, see, figure1], as well.

The distances between the peaks shown in figures 10.6 and 10.7 indicate that the main waves in figure 10.6 cover, in the same time periods, larger distances over a deeper water than the waves in figure 10.7 traveling over shallower water. The corresponding sequence of decrease/increase and increase/decrease of the wave's amplitude is apparently visible in figure 10.6 and figure 10.7, respectively.

Can we get more details on these velocities from our numerical data? Having recorded the profiles of solitons $\eta(x, t_k)$ in smaller time steps than those presented in figures 10.6-10.7, we made an effort to estimate the average values of the velocities for a given time step. Define

$$v(x, t_i) = \frac{X(t_i) - X(t_{i-1})}{t_i - t_{i-1}}, \qquad (10.5)$$
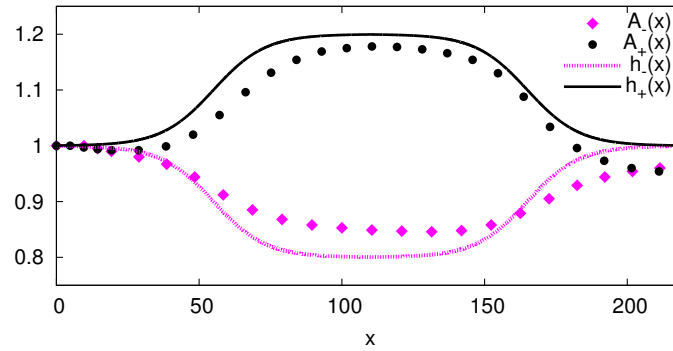
Fig. 10.9. Correlations between the soliton's amplitude and the water depth. Case $\alpha = \beta = 0.1$, $\delta = 0.2$. Dots indicate amplitudes of solitons for given positions, lines with the same color the shape of the bottom function. Reproduced with permission from [79]. Copyright (2014) by the American Physical Society

where $X(t_i)$ is the position of the top of the wave. Because this position, due to the finite space grid, is read off by interpolation, the values of $X(t_i)$ have precision limited to 4-5 digits. This is enough, however, to observe an almost perfect anticorrelation of these velocities with the depth. Contrary to "obvious" conclusions from KdV reasoning, figure 10.8 shows that when the water depth increases, the average velocity of the top of the wave likewise increases and vice versa. From plots of the bottom functions $h(x)$, appropriately scaled and vertically shifted, one sees that this correlation is almost linear. Concerning numerical values, note that the velocity of the KdV soliton is $v_{KdV} = 1 + \frac{\alpha}{2} = 1.05$. Similar, however less linear, correlations occur between the water depth and the soliton's' amplitude. It is presented in figure 10.9.

The forwardly scattered waves seen in figure 10.7 suggest that something interesting can occur at later stages of the wave motion. However, in order to eliminate the influence of "neighbor cell effects" arising from the periodic boundary conditions, we decided to check this with an interval three times longer, $x \in [0 : 660]$ in which the bottom varies only in the first part of that interval. Several snapshots of the wave motion in that setting are shown in figure 10.3.1. In this case, the calculated data are plotted at time steps of $2k\,dt$ and $(2k + 1)\,dt$, $k = 0, 1, \ldots, 7$, where $dt = 8$. Comparing waves at time instants $t = 15\,dt$, $20\,dt$, $25\,dt, \ldots$ (where the parts of the waves are still far from the boundary) one sees a sequential formation of the forward wave train in the form of a wave packet. This wave packet comes from the main
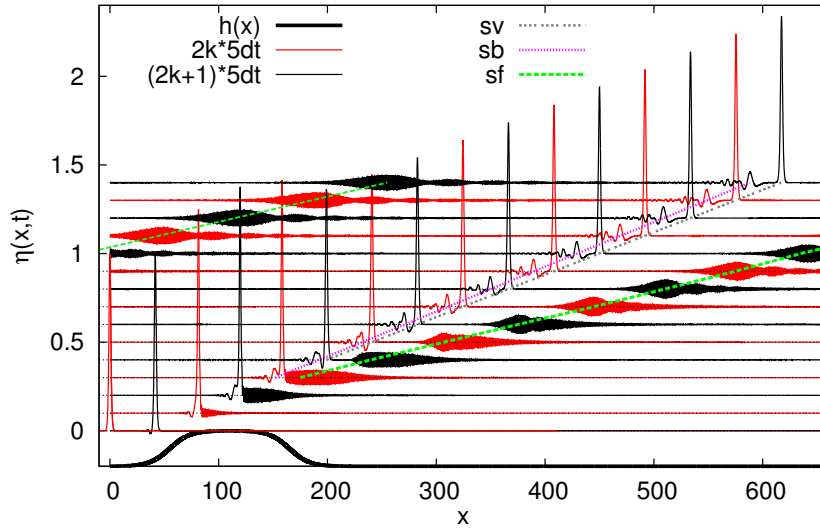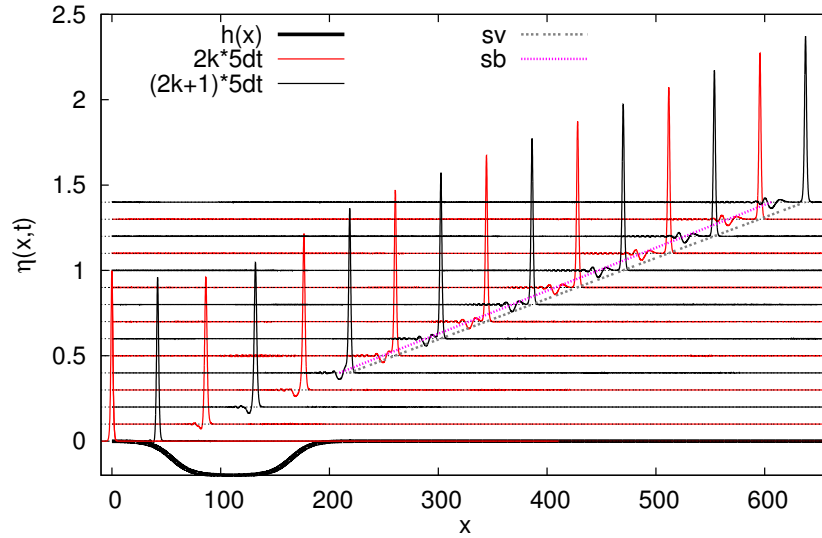
Fig. 10.10. Distortions of solitary wave due to the motion over an extended obstacle for $\alpha = \beta = 0.1$, $\delta = 0.2$. See details in the text. Reproduced with permission from [79]. Copyright (2014) by the American Physical Society

part (a solitary wave) and moves faster than the main wave. Then this wave packet divides at later stages of the motion. The thick green line (sf) going through the positions of the top of the envelope of this wave packet indicates the constant velocity of that part of the wave. Two other thick lines, grey (sv) and magenta (sb), join the positions of the main soliton and the smaller one, scattered backward, respectively. All three lines show the constant (but different) velocities of these objects when the wave has already passed the obstacle and moves over a flat bottom.

Figure 10.11 shows the longtime evolution of the initial soliton above an extended well of the same shape and amplitude as the obstacle in the previous case. Here only one backward scattered wave is seen. Its velocity, indicated by the thick magenta line (sb), is only a little smaller than the velocity of the main part of the wave.

Does the main part of the wave preserve the shape of the KdV soliton when it is moving over the flat bottom region after passing the interval of the varying bottom? In order to answer this question, we compared the shapes of the main part of the wave at temporal points $t = 440, 520, 600$ with the shape of KdV soliton.

Fig. 10.11. Distortions of a solitary wave due to motion over an extended well. Case $\alpha = \beta = 0.1$, $\delta = 0.2$. Reproduced with permission from [79]. Copyright (2014) by the American Physical Society

In figure 10.12 the shapes of the main part of the waves after a long period of evolution, shown in figures 10.3.1 and 10.11, are compared with the shape of the KdV soliton. The comparison was made as follows. For each time instant t_i, we selected an interval $x \in [x_{top}(t) - 5, x_{top}(t) + 5]$, where $x_{top}(t)$ was the position of the top of that wave. Then we fitted the formula $f(x,t) = a \operatorname{sech}[b(x - ct)]^2$ to values of $\eta(x,t)$ recorded in grid points as solutions of Eq. (4.31). The symbols in figure 10.12 represent numerical solutions to (4.31), whereas the green lines (sol) represent the fitted KdV solitons. It is remarkable that, for the given case, it is the same soliton for all time instants when the wave has already passed the obstacle or a well. In the case when the obstacle forms a bump, figure 10.3.1, the fitted parameters are $a = 0.9367$, $b = 0.8073$, $c = 1.0467$. In the case of a well, figure 10.11, the corresponding set is $a = 0.9707$, $b = 0.8206$, $c = 1.0488$. This means that after formation of smaller waves scattered forward and/or backward during interaction with a bottom obstacle the main part preserves the shape of a KdV soliton, although with slightly smaller amplitude, width and velocity.
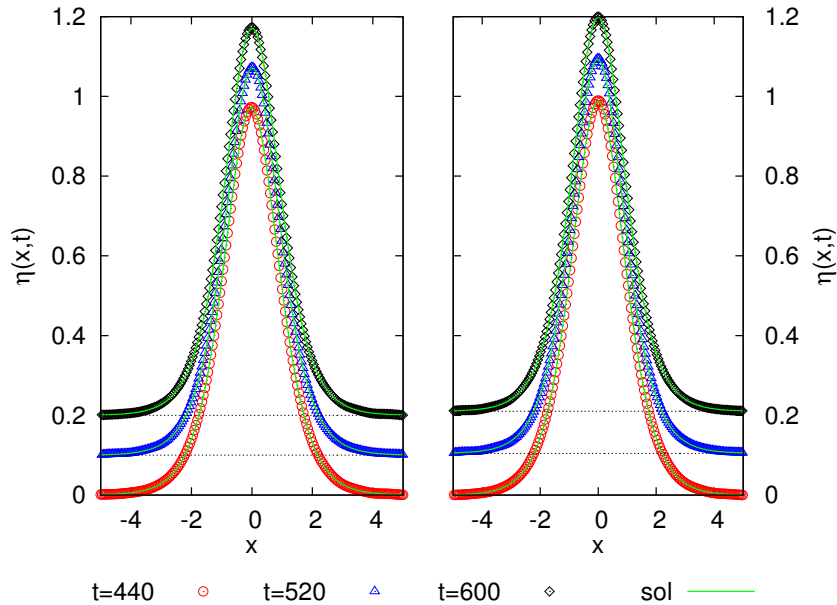
Fig. 10.12. Comparison of shapes of the main part of the waves at $t = 440, 520, 600$ from figure 10.3.1 (left) and figure 10.11 (right) with the shape of the KdV soliton (sol) after shifts to the same position. Reproduced with permission from [79]. Copyright (2014) by the American Physical Society

10.3.2 Initial condition in the form of KdV2 soliton

In this subsection we present some examples of the time evolution of the wave which at $t = 0$ is given by (5.2), with coefficients A, B, v fulfilling (5.31)-(5.32), i.e., it is the exact solution of the second order KdV-type equation for a flat bottom (4.27). In figure 10.13 three cases of solitons, corresponding to three different sets of (α, β) and moving according to the second order equation (4.27) are displayed. In all cases, the soliton's velocity is the same, given by (5.32), which is different from the KdV case, where the velocity depends on α. It is clear from the figure 10.13 that the numerical solution preserves its shape and amplitude for all cases in agreement with the analytic solution.

In figures 10.14 and 10.15 we show time evolution of the initial soliton (5.2) according to the equation (4.31) which contains terms from an uneven bottom. In order to compare these cases with the evolution of initial KdV soliton, all parameters of the calculations are the same as those related to results shown in figures 10.3.1 and 10.11.
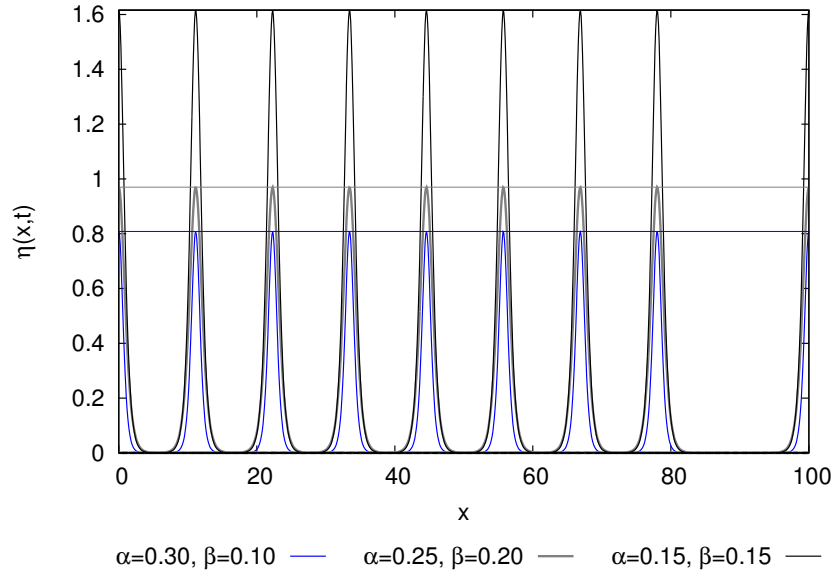
Fig. 10.13. Time evolution of the exact solitons $\eta(x,t) = A\,\mathrm{Sech}^2\,(B(x - vt))$, according to the KdV2 equation (4.27) obtained in numerical simulations for three different sets of parameters α and β. Reproduced with permission from [79]. Copyright (2014) by the American Physical Society

In general, the time evolution of initial KdV2 soliton is qualitatively very similar to the evolution of KdV soliton. In particular, as seen in figures 10.11 and 10.15, time evolution is roughly the same when soliton encounters firstly deepening and next shallowing of the bottom. There are, however, some differences. First of all the initial velocities of the solitons are slightly different. For exact KdV soliton it is $v_{\mathrm{KdV}} = 1 + \frac{\alpha}{2} = 1.05$ for $\alpha = 0.1$. The velocity of KdV2 soliton (5.32) is $v_{\mathrm{KdV2}} \approx 1.11455$.

In cases displayed in figures 10.3.1 and 10.14, when soliton enters firstly shallowing and then deepening, the wave packet created in front of the KdV2 soliton is broader than that in the case of KdV soliton. It moves faster and its fragmentation, in later stages of the evolution, is more pronounced.

In conclusion, we stress that numerical simulations according to the KdV2 equation containing terms originating from a varying bottom (4.31) revealed quantitative results concerning the velocity and amplitude of the solitary wave. The initial soliton almost preserves its parameters (shape, amplitude) during the motion over bottom topography being resistant to distortions.
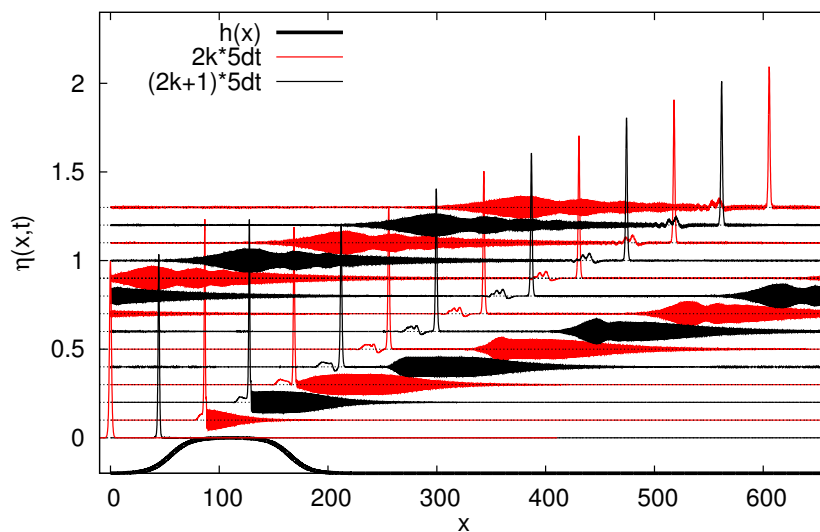
Fig. 10.14. The same as in figure 10.3.1 but for initial condition given by the exact KdV2 soliton. Reproduced with permission from [79]. Copyright (2014) by the American Physical Society
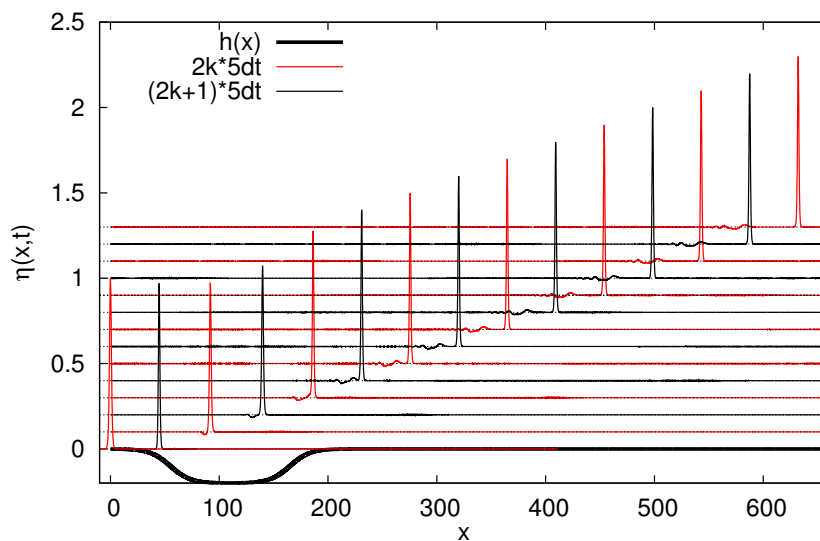
Fig. 10.15. The same as in figure 10.11 but for initial condition given by the exact KdV2 soliton. Reproduced with permission from [79]. Copyright (2014) by the American Physical Society

11

Numerical simulations: Petrov-Galerkin and Finite Element Method

Results of numerical simulations presented in all previous chapters have been obtained with the finite difference method (FDM for short) discussed in Chapter 10.

It was demonstrated in [32] that finite element method (FEM) describes properly the dynamics of the KdV equation in standard, mathematical form (3.33), which is the equation in a moving frame of reference resulting from a particular scaling of x and t variables (3.32). In [84] we extended this version of FEM for the second order equations, that is, KdV2 (4.27) and KdV2B (4.31). In [83] we generalized the method to include a white stochastic noise which can simulate the random influence of such factors like air pressure fluctuations and/or wind gusts. Next, we compared the results obtained in this numerical scheme with some of the results obtained earlier using the finite difference method in [78] and [79].

11.1 Numerical method

The emergence of soliton solutions to the KdV equation was observed in numerics fifty years ago [150]. Several numerical methods used for solving the KdV equation are discussed in [138]. Among them is the finite difference explicit method [150], the finite difference implicit method [49] and several versions of the pseudospectral method, as in [47]. It is also worth mentioning papers using the FEM and Galerkin methods [17, 26, 31]. Most numerical applications use periodic boundary conditions, but there also exist calculations that apply Dirichlet boundary conditions on a finite interval [133, 147, 148].

Below we describe the construction of a method which will be applicable not only for the numerical simulation of the evolution of nonlinear waves governed by equations (4.27) or (4.31) but also for their stochastic versions. Such stochastic equations are studied in the next section. Since stochastic noise is irregular, solutions are not necessarily smooth, neither in time nor in space. A finite element method (FEM) seems to be suitable for such a case.

11.1.1 Time discretization

In [83], we have adapted the Crank–Nicholson scheme for time evolution, beginning with the KdV equation (3.29) in a fixed coordinate system. Note that $\eta\eta_x = \frac{1}{2}(\eta^2)_x$. Denote also $v = \eta_x$ and $w = v_x$. Let us choose time step τ. Then the KdV equation (3.29) in the Crank–Nicholson scheme can be written as a set of coupled first order differential equations

$$\eta^{n+1} - \eta^n + \tau\left(\frac{\partial}{\partial x}\eta^{n+\frac{1}{2}} + \frac{3\alpha}{4}\frac{\partial}{\partial x}(\eta^{n+\frac{1}{2}})^2 + \frac{\beta}{6}w^{n+\frac{1}{2}}\right) = 0, \qquad (11.1)$$

$$\frac{\partial}{\partial x}\eta^{n+\frac{1}{2}} = v^{n+\frac{1}{2}},$$

$$\frac{\partial}{\partial x}v^{n+\frac{1}{2}} = w^{n+\frac{1}{2}},$$

where

$$\eta^{n+\frac{1}{2}} = \tfrac{1}{2}\left(\eta^{n+1} + \eta^n\right),$$
$$v^{n+\frac{1}{2}} = \tfrac{1}{2}\left(v^{n+1} + v^n\right), \qquad (11.2)$$
$$w^{n+\frac{1}{2}} = \tfrac{1}{2}\left(w^{n+1} + w^n\right).$$

For second order equations (4.27) or (4.31) we need to introduce two new auxiliary variables, $p = w_x$ and $q = p_x$. Note that $\eta^2\eta_x = \frac{1}{3}(\eta^3)_x$, $\eta_x\eta_{2x} = \frac{1}{2}(\eta_x^2)_x = \frac{1}{2}(v^2)_x$. Moreover, $\eta_{5x} = q = p_x$ and

$$\frac{23}{24}\eta_x\eta_{2x} + \frac{5}{12}\eta\eta_{3x} = \frac{13}{48}(v^2)_x + \frac{5}{12}(\eta w)_x.$$

This setting allows us to write the Crank–Nicholson scheme for (4.27) as the following set of first order equations

$$\eta^{n+1} - \eta^n + \tau \frac{\partial}{\partial x}\left[\eta^{n+\frac{1}{2}} + \frac{3\alpha}{4}\left(\eta^{n+\frac{1}{2}}\right)^2 + \frac{\beta}{6}w^{n+\frac{1}{2}} - \frac{1}{8}\alpha^2\left(\eta^{n+\frac{1}{2}}\right)^3 \right. \quad (11.3)$$

$$\left. + \alpha\beta\left(\frac{13}{48}\left(v^{n+\frac{1}{2}}\right)^2 + \frac{5}{12}\left(\eta^{n+\frac{1}{2}}w^{n+\frac{1}{2}}\right)\right) + \frac{19}{360}\beta^2\left(q^{n+\frac{1}{2}}\right)\right] = 0,$$

$$\frac{\partial}{\partial x}\eta^{n+\frac{1}{2}} - v^{n+\frac{1}{2}} = 0,$$

$$\frac{\partial}{\partial x}v^{n+\frac{1}{2}} - w^{n+\frac{1}{2}} = 0,$$

$$\frac{\partial}{\partial x}w^{n+\frac{1}{2}} - p^{n+\frac{1}{2}} = 0,$$

$$\frac{\partial}{\partial x}p^{n+\frac{1}{2}} - q^{n+\frac{1}{2}} = 0,$$

where

$$p^{n+\frac{1}{2}} = \tfrac{1}{2}\left(p^{n+1} + p^n\right),$$
$$q^{n+\frac{1}{2}} = \tfrac{1}{2}\left(q^{n+1} + q^n\right). \qquad (11.4)$$

For the second order KdV type equation with an uneven bottom (4.31) the first equation in the set (11.3) has to be supplemented by terms originating from bottom variations, yielding

$$\eta^{n+1} - \eta^n + \tau \frac{\partial}{\partial x}\left[\eta^{n+\frac{1}{2}} + \frac{3\alpha}{4}\left(\eta^{n+\frac{1}{2}}\right)^2 + \frac{\beta}{6}w^{n+\frac{1}{2}} - \frac{1}{8}\alpha^2\left(\eta^{n+\frac{1}{2}}\right)^3 \right. \quad (11.5)$$

$$+ \alpha\beta\left(\frac{13}{48}\left(v^{n+\frac{1}{2}}\right)^2 + \frac{5}{12}\left(\eta^{n+\frac{1}{2}}w^{n+\frac{1}{2}}\right)\right) + \frac{19}{360}\beta^2\left(q^{n+\frac{1}{2}}\right)$$

$$\left. \frac{1}{4}\beta\delta\left(-\frac{2}{\beta}\left(h^{n+\frac{1}{2}}\eta^{n+\frac{1}{2}}\right) + \eta^{n+\frac{1}{2}}g^{n+\frac{1}{2}} + h^{n+\frac{1}{2}}w^{n+\frac{1}{2}}\right)\right] = 0,$$

where $g = h_{xx}$.

Below we focus on the second order equations (4.27) and (11.3), pointing out contributions from bottom variation later.

11.1.2 Space discretization

Following the arguments given by Debussche and Printems [32] we apply the Petrov-Galerkin discretization and finite element method. We use piecewise linear shape functions and piecewise constant test functions. We consider wave motion on the interval $x \in [0, L]$ with periodic boundary conditions. Given $N \in \mathbb{N}$, then we use a mesh M_ν of points $x_j = j\nu$, $j = 0, 1, \ldots, N$, where $\nu = L/N$. Let V_ν^1 be a space of piecewise linear functions $\varphi_j(x)$, such that $\varphi_j(0) = \varphi_j(L)$, defined as

$$\varphi_j(x) = \begin{cases} \frac{1}{\nu}(x - x_{j-1}) & \text{if} \quad x \in [x_{j-1}, x_j] \\ \frac{1}{\nu}(x_{j+1} - x) & \text{if} \quad x \in [x_j, x_{j+1}] \\ 0 & \text{otherwise.} \end{cases} \tag{11.6}$$

As test functions we have chosen the space of piecewise constant functions $\psi_j(x) \in V_\nu^0$, where

$$\psi_j(x) = \begin{cases} 1 & \text{if} \quad x \in [x_j, x_{j+1}) \\ 0 & \text{otherwise.} \end{cases} \tag{11.7}$$

An approximate solution and its derivatives may be written as an expansion in the basis (11.6)

$$\begin{aligned} \eta_\nu^n(x) &= \sum_{j=1}^N a_j^n \, \varphi_j(x), \\ v_\nu^n(x) &= \sum_{j=1}^N b_j^n \, \varphi_j(x), \\ w_\nu^n(x) &= \sum_{j=1}^N c_j^n \, \varphi_j(x), \\ p_\nu^n(x) &= \sum_{j=1}^N d_j^n \, \varphi_j(x), \\ q_\nu^n(x) &= \sum_{j=1}^N e_j^n \, \varphi_j(x), \end{aligned} \tag{11.8}$$

where $a_j^n, b_j^n, c_j^n, d_j^n, e_j^n$ are expansion coefficients. Therefore, in a weak formulation we can write (11.1) as

$$\left(\eta_\nu^{n+1} - \eta_\nu^n, \psi_i\right) + \tau \left\{ \left(\partial_x \eta_\nu^{n+\frac{1}{2}}, \psi_i\right) + \frac{3\alpha}{4} \left(\partial_x \left(\eta_\nu^{n+\frac{1}{2}}\right)^2, \psi_i\right) \right. \tag{11.9}$$

$$+ \frac{\beta}{6} \left(\partial_x w_\nu^{n+\frac{1}{2}}, \psi_i\right) - \frac{1}{8}\alpha^2 \left(\partial_x \left(\eta_\nu^{n+\frac{1}{2}}\right)^3, \psi_i\right)$$

$$+ \alpha\beta \left[\frac{13}{48} \left(\partial_x \left(v_\nu^{n+\frac{1}{2}}\right)^2, \psi_i\right) + \frac{5}{12} \left(\partial_x \left(\eta_\nu^{n+\frac{1}{2}} w_\nu^{n+\frac{1}{2}}\right), \psi_i\right) \right]$$

$$\left. + \frac{19}{360}\beta^2 \left(\partial_x \left(q_\nu^{n+\frac{1}{2}}\right), \psi_i\right) \right\} = 0,$$

$$\left(\partial_x \eta_\nu^{n+\frac{1}{2}}, \psi_i\right) - \left(v_\nu^{n+\frac{1}{2}}, \psi_i\right) = 0,$$

$$\left(\partial_x v_\nu^{n+\frac{1}{2}}, \psi_i\right) - \left(w_\nu^{n+\frac{1}{2}}, \psi_i\right) = 0,$$

$$\left(\partial_x w_\nu^{n+\frac{1}{2}}, \psi_i\right) - \left(p_\nu^{n+\frac{1}{2}}, \psi_i\right) = 0,$$

$$\left(\partial_x p_\nu^{n+\frac{1}{2}}, \psi_i\right) - \left(q_\nu^{n+\frac{1}{2}}, \psi_i\right) = 0,$$

for any $i = 1, \ldots, N$, where for abbreviation ∂_x is used for $\frac{\partial}{\partial x}$. In (11.9) and below scalar products are defined by appropriate integrals

$$(f, g) = \int_0^L f(x)g(x)dx.$$

In the case of equation (4.31), the first equation of the set (11.9) has to be supplemented inside the bracket { } by the terms

$$+\frac{1}{4}\beta\delta\left(\partial_x\left[-\frac{2}{\beta}\left(h^{n+\frac{1}{2}}\eta_\nu^{n+\frac{1}{2}}\right)\right.\right. \tag{11.10}$$
$$\left.\left.+\eta_\nu^{n+\frac{1}{2}}g^{n+\frac{1}{2}} + h^{n+\frac{1}{2}}w_\nu^{n+\frac{1}{2}}\right], \psi_i\right).$$

Insertion of (11.8) into (11.9) yields a system of coupled linear equations for coefficients $a_j^n, b_j^n, c_j^n, d_j^n, e_j^n$. The solution to this system supplies an approximate solution to (4.27) given in the mesh points x_j.

KdV equation

In order to demonstrate the construction of the matrices involved we limit at this point our considerations to the first order equation (3.29). It means that we drop temporarily in (11.9) terms of second order, that is, the terms with $\alpha^2, \alpha\beta, \beta^2$. Equations with p and q do not apply because η_{4x} and η_{5x} do not appear in (3.29). This leads to equations

$$\sum_{j=1}^N (a_j^{n+1} - a_j^n)(\varphi_j, \psi_i) + \tau\frac{1}{2}\sum_{j=1}^N (b_j^{n+1} + b_j^n)(\varphi_j, \psi_i) \tag{11.11}$$

$$+\tau\alpha\frac{3}{16}\sum_{j=1}^N\sum_{k=1}^N (a_j^{n+1} + a_j^n)(a_k^{n+1} + a_k^n)(\varphi_j'\varphi_k + \varphi_j\varphi_k', \psi_i)$$

$$+\tau\beta\frac{1}{12}\sum_{j=1}^N (c_j^{n+1} + c_j^n)(\varphi_j, \psi_i) = 0,$$

$$\sum_{j=1}^N \left[(a_j^{n+1} + a_j^n)(\varphi_j', \psi_i) - (b_j^{n+1} + b_j^n)(\varphi_j, \psi_i)\right] = 0,$$

$$\sum_{j=1}^N \left[(b_j^{n+1} + b_j^n)(\varphi_j', \psi_i) - (c_j^{n+1} + c_j^n)(\varphi_j, \psi_i)\right] = 0.$$

Define

$$C_{ij}^{(1)} = (\varphi_j, \psi_i), \qquad\qquad C_{ij}^{(2)} = (\varphi_j', \psi_i),$$
$$C_{ijk}^{(3)} = (\varphi_j'\varphi_k + \varphi_j\varphi_k', \psi_i), \tag{11.12}$$

where $\varphi_j' = \frac{d\varphi}{dx}(x_j)$. Simple integration shows that

$$C_{ij}^{(1)} = \begin{cases} \frac{1}{2}\nu & \text{if} \quad i = j \quad \text{or} \quad i = j - 1 \\ 0 & \text{otherwise,} \end{cases} \tag{11.13}$$

$$C_{ij}^{(2)} = \begin{cases} -1 & \text{if} \quad i = j \\ 1 & \text{if} \quad i = j - 1 \\ 0 & \text{otherwise.} \end{cases} \tag{11.14}$$

Similarly one obtains

$$C_{ijk}^{(3)} = C_{ij}^{(2)} \delta_{jk}. \tag{11.15}$$

The property (11.15) reduces the double sum in the term with $\tau\alpha\frac{3}{16}$ to the single one of the square of $(a_j^{n+1} + a_j^n)$. Insertion of (11.13)–(11.15) into (11.11) gives

$$\sum_{j=1}^{N} \left[(a_j^{n+1} - a_j^n)C_{ij}^{(1)} + \tau\left(\frac{1}{2}(b_j^{n+1} + b_j^n)C_{ij}^{(1)} \right. \right. \tag{11.16}$$

$$\left. \left. + \alpha\frac{3}{16}(a_j^{n+1} + a_j^n)^2 C_{ij}^{(2)} + \beta\frac{1}{12}(c_j^{n+1} + c_j^n)C_{ij}^{(2)} \right) \right] = 0,$$

$$\sum_{j=1}^{N} \left[(a_j^{n+1} + a_j^n)C_{ij}^{(2)} - (b_j^{n+1} + b_j^n)C_{ij}^{(1)} \right] = 0,$$

$$\sum_{j=1}^{N} \left[(b_j^{n+1} + b_j^n)C_{ij}^{(2)} - (c_j^{n+1} + c_j^n)C_{ij}^{(1)} \right] = 0.$$

Define the $3N$-dimensional vector of expansion coefficients

$$X^n = \begin{pmatrix} A^n \\ B^n \\ C^n \end{pmatrix}, \tag{11.17}$$

where

$$A^n = \begin{pmatrix} a_1^n \\ a_2^n \\ \vdots \\ a_N^n \end{pmatrix}, \quad B^n = \begin{pmatrix} b_1^n \\ b_2^n \\ \vdots \\ b_N^n \end{pmatrix}, \quad C^n = \begin{pmatrix} c_1^n \\ c_2^n \\ \vdots \\ c_N^n \end{pmatrix}. \tag{11.18}$$

In (11.16), $A^{n+1}, B^{n+1}, C^{n+1}$ represent the unknown coefficients and A^n, B^n, C^n the known ones. Note that the system (11.16) is nonlinear. The single nonlinear term is quadratic in unknown coefficients. For the second order equations (4.27) and (4.31) there are more nonlinear terms.

In an abbreviated form the set (11.16) can be written as

$$F_i(X^{n+1}, X^n) = 0, \quad i = 1, 2, \ldots, 3N. \tag{11.19}$$

Since this equation is nonlinear we can use the Newton method for each time step. That is, we find X^{n+1} by iterating the equation

$$(X^{n+1})_{m+1} = (X^{n+1})_m + J^{-1}(X^{n+1})_m = 0, \tag{11.20}$$

where J^{-1} is the inverse of the Jacobian of $F(X^{n+1}, X^n)$ (11.19). Choosing $(X^{n+1})_0 = X^n$ we obtain the approximate solution to (11.19), $(X^{n+1})_m$ in $m = 3 - 5$ iterations with very good precision. The Jacobian itself is a particular $(3N \times 3N)$ sparse matrix with the following block structure

$$J = \begin{pmatrix} (A_a) & (A_b) & (A_c) \\ (C2) & -(C1) & (0) \\ (0) & (C2) & -(C1) \end{pmatrix}, \tag{11.21}$$

where each block $(\cdot)$ is a two-diagonal sparse $(N \times N)$ matrix. The matrix A_a is given by

$$A_a = \begin{pmatrix} a_1^1 & 0 & 0 & \cdots & 0 & a_{N-1}^1 & a_N^1 \\ a_1^2 & a_2^2 & 0 & \cdots & 0 & 0 & a_N^2 \\ 0 & a_2^3 & a_3^3 & 0 & \cdots & 0 & 0 \\ \vdots & \vdots & \vdots & \ddots & \vdots & \vdots & \vdots \\ 0 & 0 & \cdots & a_{N-4}^{N-3} & a_{N-3}^{N-3} & 0 & 0 \\ 0 & 0 & \cdots & 0 & a_{N-3}^{n-2} & a_{N-2}^{N-2} & 0 \\ a_1^N & 0 & \cdots & 0 & 0 & a_N^{N-1} & a_N^n \end{pmatrix}. \tag{11.22}$$

In (11.22) the nonzero elements of A_a are given by

$$a_j^i = \frac{\partial F_i}{\partial a_j^{n+1}}, \tag{11.23}$$

where F is given by (11.19). The elements in the upper right and lower left corners result from periodic boundary conditions. Matrices A_b and A_c have the same structure as A_a, with only elements a_j^i having to be replaced by $b_j^i = \frac{\partial F_i}{\partial b_j^{n+1}}$ and $c_j^i = \frac{\partial F_i}{\partial c_j^{n+1}}$, respectively.

Matrices $C1$ and $C2$ are constant. They are defined as

$$Ck = \begin{pmatrix} C_{11}^{(k)} & 0 & \cdots & C_{11}^{(k)} & C_{1N}^{(k)} \\ C_{21}^{(k)} & C_{22}^{(k)} & \cdots & 0 & C_{2N}^{(k)} \\ \vdots & \vdots & \ddots & \vdots & \vdots \\ 0 & 0 & \cdots & C_{N-1N-1}^{(k)} & 0 \\ C_{N1}^{(k)} & 0 & \cdots & C_{N-1N}^{(k)} & C_{NN}^{(k)} \end{pmatrix}, \tag{11.24}$$

where $k = 1, 2$.

Extended KdV equation (KdV2)

For the second order equation (4.27) there are more nonlinear terms. These are terms with α^2 and $\alpha\beta$. According to the Petrov–Galerkin scheme we get for the term with α^2

$$\partial_x \left(\eta^{n+\frac{1}{2}} \right)^3 = \frac{1}{8} \left(\partial_x \sum_{j=1}^{N} \left(a_j^{n+1} + a_j^n \right) \varphi_j \right)^3 \tag{11.25}$$

$$= \frac{1}{8} \partial_x \sum_{j=1}^{N} \sum_{k=1}^{N} \sum_{l=1}^{N} [a_j^{n+1} + a_j^n][a_k^{n+1} + a_k^n][a_l^{n+1} + a_l^n]\varphi_j\varphi_k\varphi_l$$

$$= \frac{1}{8} \sum_{j=1}^{N} \sum_{k=1}^{N} \sum_{l=1}^{N} [a_j^{n+1} + a_j^n][a_k^{n+1} + a_k^n][a_l^{n+1} + a_l^n]$$

$$\times \left(\varphi_j'\varphi_k\varphi_l + \varphi_j\varphi_k'\varphi_l + \varphi_j\varphi_k\varphi_l' \right).$$

Denote
$$C_{ijkl}^{(4)} = \left(\left[\varphi_j'\varphi_k\varphi_l + \varphi_j\varphi_k'\varphi_l + \varphi_j\varphi_k\varphi_l' \right], \psi_i \right). \tag{11.26}$$

Similarly as for $C_{ijk}^{(3)}$ in (11.15) the following property holds

$$C_{ijkl}^{(4)} = C_{ij}^{(2)} \, \delta_{jk} \, \delta_{kl}. \tag{11.27}$$

In a similar way, for terms with $\alpha\beta$ we obtain

$$\partial_x \left(v^{n+\frac{1}{2}} \right)^2 = \frac{1}{4} \partial_x \left(\sum_{j=1}^{N} \left(b_j^{n+1} + b_j^n \right) \varphi_j \sum_{k=1}^{N} \left(b_k^{n+1} + b_k^n \right) \varphi_k \right)$$

$$= \frac{1}{4} \sum_{j=1}^{N} \sum_{k=1}^{N} [b_j^{n+1} + a_j^n][b_k^{n+1} + b_k^n] \left(\varphi_j'\varphi_k + \varphi_j\varphi_k' \right)$$

and

$$\partial_x \left(\eta^{n+\frac{1}{2}} w^{n+\frac{1}{2}} \right) = \frac{1}{4} \partial_x \left(\sum_{j=1}^{N} \left(a_j^{n+1} + a_j^n \right) \varphi_j \sum_{k=1}^{N} \left(a_k^{n+1} + a_k^n \right) \varphi_k \right)$$

$$= \frac{1}{4} \sum_{j=1}^{N} \sum_{k=1}^{N} [a_j^{n+1} + a_j^n][b_k^{n+1} + b_k^n] \left(\varphi_j'\varphi_k + \varphi_j\varphi_k' \right).$$

The scalar products appearing in the terms proportional to α^2 and $\alpha\beta$ are already defined: $\left(\left(\varphi_j'\varphi_k + \varphi_j\varphi_k' \right), \psi_i \right) = C_{ijk}^{(3)}$.

Due to properties (11.27) and (11.15) triple and double sums reduce to single ones. With these settings the second order KdV equation (11.9) gives the following system of equations

$$\sum_{j=1}^{N}\left\{(a_j^{n+1}-a_j^n)C_{ij}^{(1)}+\tau\left[\frac{1}{2}(b_j^{n+1}+b_j^n)C_{ij}^{(1)}\right.\right. \tag{11.28}$$

$$+\left(\alpha\frac{3}{16}(a_j^{n+1}+a_j^n)^2+\beta\frac{1}{12}(c_j^{n+1}+c_j^n)\right.$$

$$-\alpha^2\frac{1}{64}(a_j^{n+1}+a_j^n)^3+\alpha\beta\frac{13}{192}(b_j^{n+1}+b_j^n)^2$$

$$\left.\left.\left.+\alpha\beta\frac{5}{96}(a_j^{n+1}+a_j^n)(c_j^{n+1}+c_j^n)\ +\beta^2\frac{19}{720}(e_j^{n+1}+e_j^n)\right)C_{ij}^{(2)}\right]\right\}=0,$$

$$\sum_{j=1}^{N}\left[(a_j^{n+1}+a_j^n)C_{ij}^{(2)}-(b_j^{n+1}+b_j^n)C_{ij}^{(1)}\right]=0,$$

$$\sum_{j=1}^{N}\left[(b_j^{n+1}+b_j^n)C_{ij}^{(2)}-(c_j^{n+1}+c_j^n)C_{ij}^{(1)}\right]=0,$$

$$\sum_{j=1}^{N}\left[(c_j^{n+1}+c_j^n)C_{ij}^{(2)}-(d_j^{n+1}+d_j^n)C_{ij}^{(1)}\right]=0,$$

$$\sum_{j=1}^{N}\left[(b_j^{n+1}+b_j^n)C_{ij}^{(2)}-(e_j^{n+1}+e_j^n)C_{ij}^{(1)}\right]=0,$$

where $i=1,2,\ldots,N$.

In this case the vector of expansion coefficients X^n is $5N$-dimensional

$$X^n=\begin{pmatrix}A^n\\B^n\\C^n\\D^n\\E^n\end{pmatrix}, \tag{11.29}$$

where A^n, B^n and C^n are already defined in (11.18) and

$$D^n=\begin{pmatrix}d_1^n\\d_2^n\\\vdots\\d_N^n\end{pmatrix},\ E^n=\begin{pmatrix}e_1^n\\e_2^n\\\vdots\\e_N^n\end{pmatrix}. \tag{11.30}$$

The Jacobian becomes now $(5N\times 5N)$ dimensional. Its structure, however, is similar to (11.21), that is

$$J = \begin{pmatrix} (A_a) & (A_b) & (A_c) & (0) & (A_e) \\ (C2) & -(C1) & (0) & (0) & (0) \\ (0) & (C2) & -(C1) & (0) & (0) \\ (0) & (0) & (C2) & -(C1) & (0) \\ (0) & (0) & (0) & (C2) & -(C1) \end{pmatrix}, \qquad (11.31)$$

where the matrices $(A_a), (A_b), (A_c)$ are defined as previously and $(A_e)_{ij} = \frac{\partial F_i}{\partial e_j^{n+1}}$. Now F_i represents the set (11.28) which contains four nonlinear terms.

KdV2B equation

For the extended KdV with non-flat bottom we have to include into (11.28) three additional terms contained in the last line of formula (4.31). Expanding the bottom function $h(x)$ and its second derivative $h_{2x}(x)$ in the basis $\{\varphi_j(x)\}$

$$h(x) = \sum_{j=1}^{N} H_j^0 \varphi_j(x), \quad h_{2x}(x) = \sum_{j=1}^{N} H_j^2 \varphi_j(x) \qquad (11.32)$$

we can write the terms mentioned above in the following form

$$\partial_x \left(h \eta^{n+\frac{1}{2}} \right) = \frac{1}{2} \sum_{j=1}^{N} \sum_{k=1}^{N} H_j^0 \left(a_k^{n+1} + a_k^n \right) \left(\varphi_j' \varphi_k + \varphi_j \varphi_k' \right), \quad (11.33)$$

$$\partial_x \left(h_{2x} \eta^{n+\frac{1}{2}} \right) = \frac{1}{2} \sum_{j=1}^{N} \sum_{k=1}^{N} H_j^2 \left(a_k^{n+1} + a_k^n \right) \left(\varphi_j' \varphi_k + \varphi_j \varphi_k' \right), \quad (11.34)$$

$$\partial_x \left(h \eta_{2x}^{n+\frac{1}{2}} \right) = \frac{1}{2} \sum_{j=1}^{N} \sum_{k=1}^{N} H_j^0 \left(c_k^{n+1} + c_k^n \right) \left(\varphi_j' \varphi_k + \varphi_j \varphi_k' \right). \quad (11.35)$$

Since
$$\left(\left(\varphi_j' \varphi_k + \varphi_j \varphi_k' \right), \psi_i \right) = C^{(3)}(i, j, k) = C^{(2)}(i, j) \, \delta_{jk},$$

terms proportional to $\beta\delta$ can be reduced to single sums like those proportional to $\alpha^2, \alpha\beta$ and β^2 discussed in previous subsections. Finally, taking the bottom terms into account, one obtains (4.31) as a system of coupled nonlinear equations $(i = 1, 2, \ldots, N)$

$$\sum_{j=1}^{N}\left\{(a_j^{n+1}-a_j^n)C_{ij}^{(1)}+\tau\left[\frac{1}{2}(b_j^{n+1}+b_j^n)C_{ij}^{(1)}+\left(\alpha\frac{3}{16}(a_j^{n+1}+a_j^n)^2\right.\right.\right. \quad (11.36)$$

$$+\beta\frac{1}{12}(c_j^{n+1}+c_j^n)-\alpha^2\frac{1}{64}(a_j^{n+1}+a_j^n)^3+\beta^2\frac{19}{720}(e_j^{n+1}+e_j^n)$$

$$+\alpha\beta\left(\frac{13}{192}(b_j^{n+1}+b_j^n)^2+\frac{5}{96}(a_j^{n+1}+a_j^n)(c_j^{n+1}+c_j^n)\right)$$

$$\left.\left.\left.-\frac{1}{4}\delta H_j^0(a_k^{n+1}+a_k^n)+\frac{1}{8}\beta\delta H_j^2(a_k^{n+1}+a_k^n)-\frac{1}{8}\beta\delta H_j^0(c_j^{n+1}+c_j^n)\right)C_{ij}^{(2)}\right]\right\}=0,$$

$$\sum_{j=1}^{N}\left[(a_j^{n+1}+a_j^n)C_{ij}^{(2)}-(b_j^{n+1}+b_j^n)C_{ij}^{(1)}\right]=0,$$

$$\sum_{j=1}^{N}\left[(b_j^{n+1}+b_j^n)C_{ij}^{(2)}-(c_j^{n+1}+c_j^n)C_{ij}^{(1)}\right]=0,$$

$$\sum_{j=1}^{N}\left[(c_j^{n+1}+c_j^n)C_{ij}^{(2)}-(d_j^{n+1}+d_j^n)C_{ij}^{(1)}\right]=0,$$

$$\sum_{j=1}^{N}\left[(b_j^{n+1}+b_j^n)C_{ij}^{(2)}-(e_j^{n+1}+e_j^n)C_{ij}^{(1)}\right]=0.$$

In this case the sizes and structures of the vector X^n and all matrices remain the same as in (11.29)-(11.31). However the matrix elements of matrices A_a and A_c are now different from those in the subsection 11.1.2, due to new terms in (11.36) related to the bottom function.

11.2 Simulations

It was demonstrated in [32] that the method described in the previous section works reasonably well for the KdV equation (3.33). We aimed to apply the finite element method in order to numerically solve the second order equations with a flat bottom (4.27) and with an uneven bottom (4.31). There exist two kinds of solutions to KdV equations: soliton (in general, multi-soliton) solutions and periodic solutions called cnoidal waves, see, e.g., [33, 144]. In subsections 11.2.1 and 11.2.2 we present some examples of numerical simulations for soliton solutions, whereas in the subsection 11.2.3 we give some examples for cnoidal solutions.
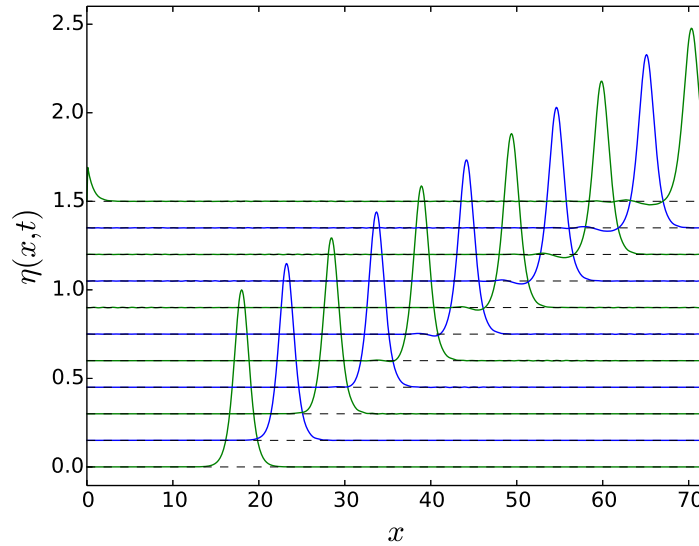
Fig. 11.1. Time evolution of the initial KdV soliton according to the KdV2 equation (4.27). Profiles are obtained by numerical solution of the set of equations (11.28). Dashed lines represent the undisturbed fluid surface.

11.2.1 KdV2 equation

In figure 11.1 we present several steps of the time evolution of the soliton wave (at $t = 0$ it is the KdV soliton) according the the extended KdV equation (4.27) and numerical scheme (11.28) on the interval $x \in [0, L]$ with $L = 72$. The mesh size is $N = 720$, with a time step $\tau = \nu^2$, $\nu = L/N$, and parameters $\alpha = \beta = 0.1$. Plotted are the calculated profiles of the wave $\eta(x, t_k)$ where $t_k = 5 \cdot k$, $k = 0, 1, ..., 10$. In order to avoid overlaps of profiles at different time instants, each subsequent profile is shifted up by 0.15 with respect to the previous one. This convention is used in figures 11.2 and 11.3, as well. Here and in the next figures, the dashed lines represent the undisturbed fluid surface. As the initial condition we chose the standard KdV soliton centered at $x_0 = 18$. That is, in the applied units,

$$\eta(x, t = 0) = A \operatorname{sech}^2 \left[\frac{\sqrt{3}}{2}(x - x_0) \right].$$

Note, that in simulations presented below the amplitude of the soliton is chosen to be equal 1. In figures 11.2-11.4 we use the same initial conditions.

The soliton motion shown in figure 11.1 is in agreement with the numerical results obtained with the finite difference method in [78,79]. With parameters,

$\alpha = \beta = 0.1$ the resulting distortion of the KdV soliton due to second order terms in (4.27), (11.28) is in the form of a small amplitude wavetrain created behind the main wave.

11.2.2 KdV2B equation
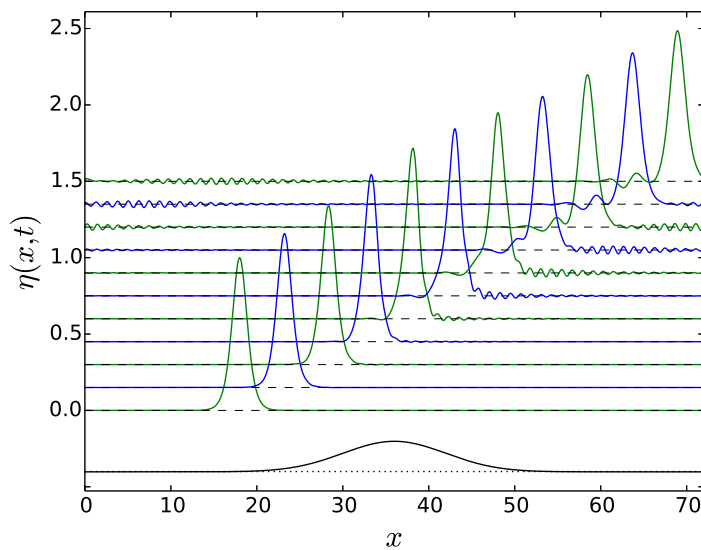
Fig. 11.2. Time evolution of the initial KdV soliton governed by the KdV2B equation (4.31) when the bottom has one hump. Here and in the following figures the dotted line shows the position of (the) undisturbed bottom.

We may question whether the FEM numerical approach to the extended KdV (11.36) is precise enough to reveal the details of soliton distortion caused by a varying bottom. The examples plotted in figures 11.2-11.4 show that it is indeed the case. In all the presented calculations the amplitude of the bottom variations is $\delta = 0.2$. The bottom profile is plotted as a black line below zero on a different scale than the wave profile.

In figure 11.2 the motion of the KdV soliton over a wide bottom hump of Gaussian shape is presented. Here, the bottom function is

$$h(x) = \exp\left[-\left(\frac{x-36}{7}\right)^2\right].$$

In the scaled variables the undisturbed surface of the water (dashed lines) is at $y = 0$. The soliton profiles shown in figure 11.2 are almost the same as the

profiles obtained with the finite differences method (FDM) used in [78, 79]. There are small differences due to a smaller precision of our FEM calculations. The FEM allows for the use of larger time steps then FDM. However, in the FEM the computing time grows fast with the increase in the number N of the mesh, since calculation of the inverse of the Jacobian ($5N \times 5N$) matrices becomes time-consuming.
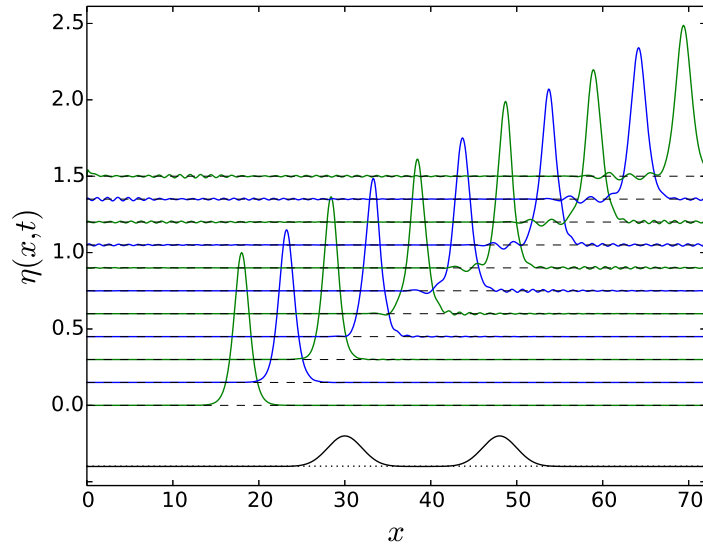
Fig. 11.3. Time evolution of the initial KdV soliton governed by the KdV2B equation (4.31) when the bottom has two narrow humps.

Figure 11.3 displays the motion of the KdV soliton above a double humped Gaussian shaped bottom defined by

$$h(x) = \exp\left[-\left(\frac{x-30}{6\sqrt{2}}\right)^2\right] + \exp\left[-\left(\frac{x-48}{6\sqrt{2}}\right)^2\right].$$

Here both Gaussians are rather narrow, and therefore deviations of the wave shape from the ideal soliton are smaller than those in figure 11.2.

In figure 11.4 we see the influence of a bottom well with horizontal size extending the soliton's wavelength. The bottom function is chosen as

$$h(x) = 1 - \frac{1}{2}[\tanh(x-28) + \tanh(44-x)].$$

Figure 11.4 shows that during the motion above smooth obstacles two effects appear. First, some additional 'waves' of small amplitude, but moving faster
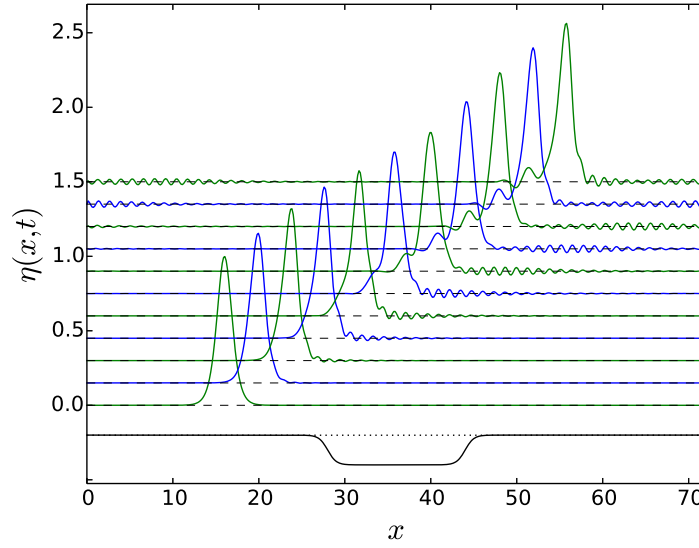
Fig. 11.4. Time evolution of the initial KdV soliton governed by the KdV2B equation (4.31) when the bottom has a well.

than the main solitary wave appear. Second, a wave of smaller amplitude and smaller velocity appears behind the main wave. Both these properties were observed and described in detail in previous chapters.

11.2.3 Motion of cnoidal waves

The cnoidal solutions to KdV equation are expressed by the Jacobi elliptic cn^2 function. The explicit formula for cnoidal solutions is, see, e.g., [33]

$$\eta(x,t) = \eta_2 + H\mathrm{cn}^2\left(\frac{x-ct}{\Delta}\bigg| m\right), \qquad (11.37)$$

where

$$\eta_2 = \frac{H}{m}\left(1 - m - \frac{E(m)}{K(m)}\right), \quad \Delta = h\sqrt{\frac{4mh}{3H}}, \qquad (11.38)$$

and

$$c = \sqrt{gh}\left[1 + \frac{H}{mh}\left(1 - \frac{m}{2} - \frac{3E(m)}{2K(m)}\right)\right]. \qquad (11.39)$$

The solution (11.37)-(11.39) is written in dimensional quantities, where H is the wave height, h is mean water depth, g is the gravitational acceleration and m is an elliptic parameter. $K(m)$ and $E(m)$ are complete elliptic integrals of

the first kind and the second kind, respectively. The value of $m \in [0, 1]$ governs the shape of the wave.

For $m \to 0$ the cnoidal solution converges to the cosine function. For $m \to 1$ the cnoidal wave exhibits peaked crests and flat troughs, such that for $m = 1$ the distance between crests increases to infinity and the cnoidal wave converges to a soliton solution.

For (4.31) and (4.27) we have to express the formulas (11.37)-(11.39) in dimensionless variables.
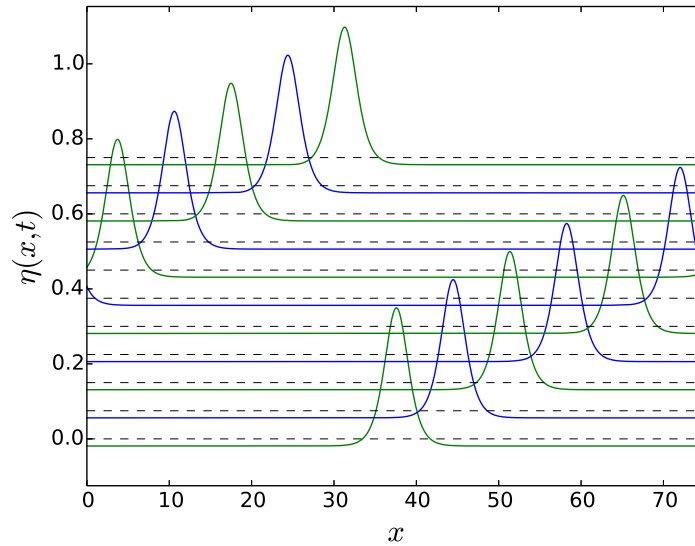
Fig. 11.5. Time evolution of the initial KdV cnoidal wave governed by the KdV2 equation (4.27) and numerical scheme (11.28).

Figure 11.5 shows the time evolution of the cnoidal wave according to the KdV2 equation (4.27), that is, the second order KdV equation with the flat bottom. The parameters of the simulation are: $\alpha = \beta = 0.14$, $m = 1 - 10^{-16}$. With this value of m the wavelength of the cnoidal wave is equal to $d \approx 75.1552$ in dimensionless units, and calculations were performed on the interval of that length, $x \in [0, 75.1552]$ with a periodic boundary condition. The mesh size was taken as $N = 752$. The initial position of the wave peak was chosen at the center of chosen interval, that is $x_0 = 37.5776$. The explicit form of the initial condition in this case was $\eta(x, t = 0) = -0.0189862 + 0.368486 \, \mathrm{cn}^2 \left(\frac{x - x_0}{1.90221} \big| m \right)$. Profiles of the wave are plotted at time instants
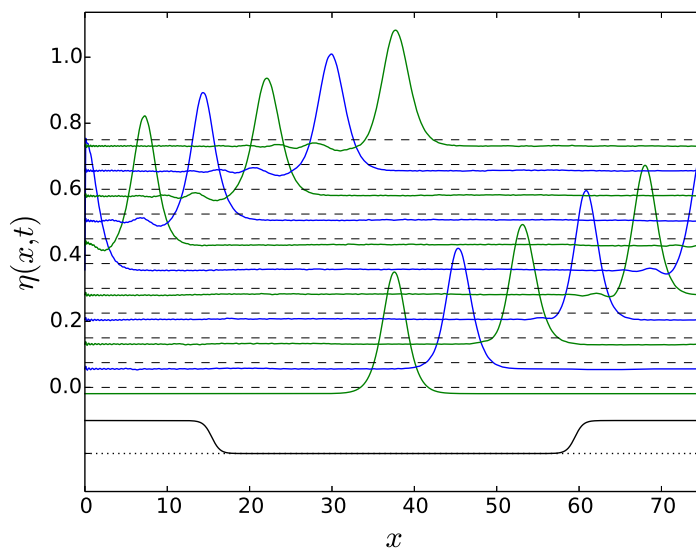
Fig. 11.6. Time evolution of the initial KdV cnoidal wave governed by the KdV2B equation (4.31).

$t_k = 10 \cdot k$, where $k = 0, 1, ..., 8$. Since the amplitudes of cnoidal waves are smaller than 1, the vertical shift for the sequential profiles in figures 11.5-11.7 is chosen to be 0.075.

In figure 11.6 we display the motion of the cnoidal wave over the bottom which is flat in the center of the interval but with an extended hump at the borders. In this simulation the value of parameters α, β, m and x interval are the same as in the figure 11.5. In this case the bottom is flat in the center of the x-interval and raises towards its borders according to the function $h(x) = 1 + \frac{1}{2}[\tanh(2(x - 15) - \frac{1}{2}) - \tanh(2(x - 60) - \frac{1}{2})]$. Therefore, the evolution was calculated according to equation (4.31) and numerical scheme (11.36). Profiles of the wave are plotted at time instants $t_k = 10 \cdot k$, where $k = 0, 1, ..., 8$. Figure 11.6 shows that during the wave motion over the obstacle a kind of slower wave with smaller amplitude is created following the main peak.

In figure 11.7 we present the initially cnoidal wave moving over an extended, almost flat hump centered at the border of the x-interval. In this simulation $m = 1 - 10^{-8}$. The intial condition is given by $\eta(x, t = 0) = 0.0359497 + 0.368486 \, \mathrm{cn}^2(\frac{x - x_0}{1.90221}|m)$ with $x_0 = 20.1571$. Because m is smaller than in the previous cases, the wavelength d of the cnoidal wave is also smaller, $d \approx 40.3241$. Calculations were made on the interval $x \in [0, 2d]$ with $N = 807$.
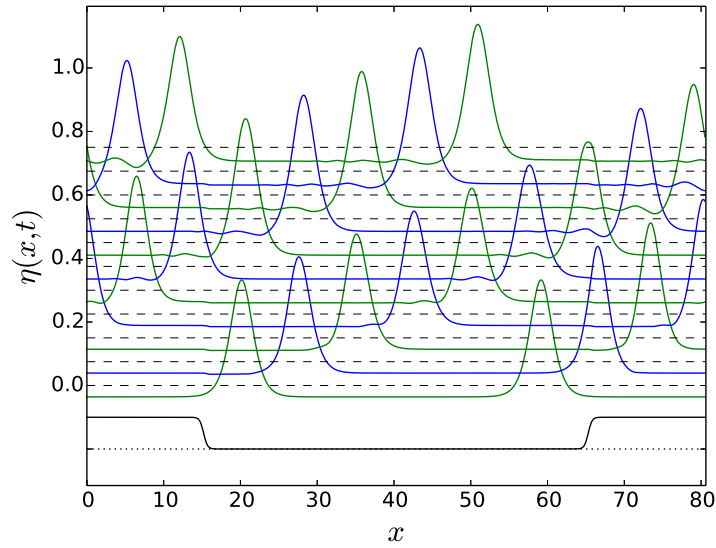
Fig. 11.7. Time evolution of the initial KdV cnoidal wave governed by the extended KdV equation (4.31). The bottom function is here $h(x) = 1 + \frac{1}{2}[\tanh(2(x - 15) - \frac{1}{2}) - \tanh(2(x - 65) - \frac{1}{2})]$.

Profiles of the wave are plotted at time instants $t_k = 10 \cdot k$, where $k = 0, 1, ..., 8$. Figure 11.7 shows qualitatively similar features to those in figure 11.6.
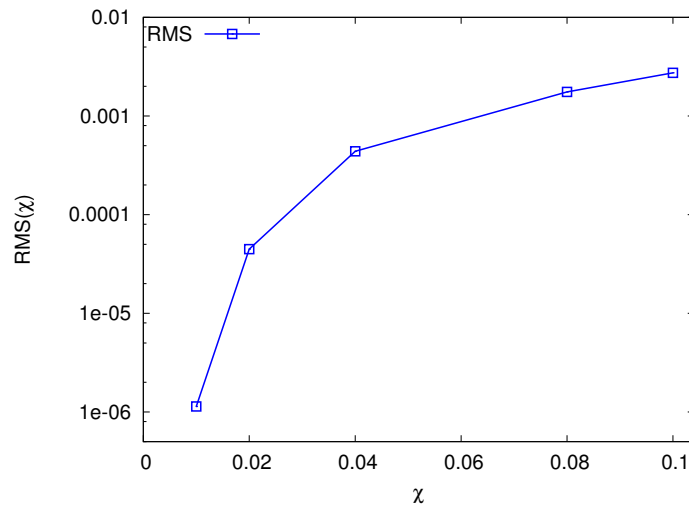
Fig. 11.8. Precision of numerical calculations for KdV equation in the fixed frame as a function of mesh size.

11.2.4 Precision of numerical calculations

The KdV equation (3.29) or (3.33) is unique since it possesses an infinite number of invariants, see, e.g., [36, 113]. As we have already written, the lowest invariant, $I_1 = \int_{-\infty}^{+\infty} \eta \, dx$, represents the conservation law for the mass (volume) of the liquid. The second, $I_2 = \int_{-\infty}^{+\infty} \eta^2 \, dx$, is related to momentum conservation, and the third, $I_3 = \int_{-\infty}^{+\infty} (\eta^3 - \frac{1}{3}\eta_x^2) \, dx$, is related to energy conservation. However, as pointed by [4, 8, 80] and in Chapters 8-9 of this book, the relations between I_2 and momentum and I_3 and energy are more complex.

Approximate conservation of these invariants often serves as a test of the precision of numerical simulations. However, this is not the case for the second order KdV type equations (4.31) and (4.27). It was noted in [80] that I_1 is an invariant of equations (4.31) and (4.27) but I_2 and I_3 are not invariants. Therefore, only I_1 can be used as a test for the precision of numerical calculations of waves moving according to the second order extended KdV equations. In all the presented calculations the precision of the numerical values of I_1 was consistently high (the values $\frac{I_1(t) - I_1(0)}{I_1(0)} \le 10^{-6}$).

Wave motion according to KdV and extended (second order) KdV equations is usually calculated in the reference frame moving with the natural velocity $c = 1$ in scaled dimensionless variables (in original variables $c = \sqrt{gh}$). The KdV and extended KdV equations for a moving reference frame are obtained by the transformation $\hat{x} = (x - t), \quad \hat{t} = t$ which removes the term η_x from the equation (4.27). Then the soliton velocity in the fixed frame is proportional to $1 + \frac{\alpha}{2}$ whereas in the moving frame it is proportional to $\frac{\alpha}{2}$. Therefore, for the value of $\alpha = 0.1$ the distance covered by a soliton in the moving frame is $\frac{\alpha}{2}/(1 + \frac{\alpha}{2}) = \frac{1}{21}$ times shorter than the distance covered in the fixed frame for the same duration. Then, with the same number of the mesh points N the mesh size ν can be more than 20 times smaller assuring a much higher precision of calculation in the moving frame at the same operational cost. For instance [32] obtained a good precision for motion of KdV soliton with the FEM method using $N = 200$, $\nu = 0.01$ and time step $\tau = \nu$ on the interval $x \in [0, 2]$.

Precision of FEM method in the fixed frame can be tested by calculation of a root mean square (RMS) of deviations of wave profile obtained numerically from those obtained from the analytic solution. Denote by $\eta_i^{anal}(t)$ and $\eta_i^{num}(t)$ the values of the solutions at given mesh point i an time instant t, analytic and numerical, respectively. Then the RMS is expressed as

$$\text{RMS}(\nu, t) = \left(\frac{1}{N} \sum_{i=1}^{N} (\eta_i^{anal}(t) - \eta_i^{num}(t))^2 \right)^{1/2}. \qquad (11.40)$$

We checked our implementation of the FEM on the interval $x \in [0, 20]$ using several different sizes ν of the mesh and several time values. Figure 11.8 displays the RMS (11.40) values for $t = 10$. It shows that deviations from the analytic solution decrease substantially with decreasing ν. Small ν assures a very high precision in numerical simulations, however, at the expense of large computation time. Other tests (not shown here) in which ν was fixed and RMS was calculated as a function of time showed that for $\tau = \nu^2$ RMS increases with time linerly and very slowly.

When the bottom is not flat simulations *have to be done in the fixed reference frame*. For our purposes, we needed to choose the x intervals of the order of 70 or 80. Even for $\nu = 0.1$ the size of Jacobian matrices (11.31) reaches (4000×4000) and its inversion is time consuming. In a compromise between numerical precision and reasonable computing times, we made our simulations with $\nu = 0.1$. This choice resulted in about one week of computing time for a single run on the cluster. Despite of the insufficient precision the results presented in figures 1-7 reproduce details of evolution known from our previous studies, obtained with the finite difference method. These details, resulting from second order terms in extended KdV (4.27), are seen in figure 11.1 as a wavetrain of small amplitude created behind the main one (compare with figure 2 in [79]). A similar wavetrain behind the main one was observed in numerical simulations by [108], see e.g., figure 2 therein. For waves moving with the presence of bottom obstacle these secondary waves behind the main one are amplified by interaction with the bottom and new faster secondary waves appear (see, e.g., figures 2-4). We already observed these effects, see figures 6 and 7 in [79].

Conclusions

The main conclusions of this chapter can be summarized as follows.

- A weak formulation of the finite element method (FEM) for extended KdV equation (4.27) can be effectively used for numerical calculations of the time evolution of both soliton and cnoidal waves when calculations are done in a moving frame.
- Since numerical calculations for equation (4.31) have to be performed in a fixed frame, the presented FEM method is not as effective as the FDM

method used by us and our co-workers in previous papers because the computer time necessary for obtaining sufficiently high precision becomes impractical. On the other hand, the presented results (though not as precise as FDM ones) exhibit all secondary structures generated by higher order terms of the equations.

11.3 Stochastic KdV type equations

In this section we report on numerical solutions to stochastic versions of second order KdV type equations (4.27) and (4.31) obtained in [83]. In a first step let us recall the finite element method (FEM) used by Debussche and Printems in [32]. Their method was good enough for the the stochastic Korteweg-de Vries equation of the form [32, equation 1.2]

$$u_t + u\,u_x + \epsilon\,u_{xxx} = \gamma\,\dot{\xi}. \tag{11.41}$$

In Eq. (11.41) the noise term $\xi(x,t)$ is a Gaussian process with correlations

$$\mathbb{E}\,\dot{\xi}(x,t)\,\dot{\xi}(y,s) = c(x-y)\,\delta(t-s) \tag{11.42}$$

and γ is the amplitude of the noise. Equation (11.41) with r.h.s. equal zero is the Korteweg-de Vries equation written in a moving reference system with coordinates scaled in a particular way. This form was convenient for the authors in order to apply the finite element method (FEM) in their numerical simulation.

In the case of periodic boundary conditions, the noise term ξ has to be introduced differently. Since the Brownian motions are nowhere differentiable, we have to introduce the mathematical form of (11.41).

The Itô form of (11.41) can be written as follows

$$du + \left(u\frac{\partial u}{\partial x} + \epsilon\frac{\partial^3 u}{\partial x^3}\right)dt = \gamma\,\Phi\,dW. \tag{11.43}$$

In (11.43), W is a Wiener process on $L^2(0,T)$, $T < \infty$, of the form

$$W(t,x) = \sum_{i=0}^{\infty} \beta_i(t)\,e_i(x), \tag{11.44}$$

where $\{e_i\}_{i\in\mathbb{N}}$ is an orthonormal basis of $L^2(0,T)$ and $\{\beta_i\}_{i\in\mathbb{N}}$ is a sequence of independent real valued Brownian motions. In (11.43), Φ is an appropriate linear map from $L^2(0,T)$ to $L^2(0,T)$. For more details, see [32].

11.3.1 Numerical approach

Our aim was to extend the approach used in [32] in order to solve numerically stochastic version of the KdV2B equation (4.31)

$$\eta_t + \eta_x + \alpha \frac{3}{2}\eta\eta_x + \beta \frac{1}{6}\eta_{3x} \tag{11.45}$$

$$- \frac{3}{8}\alpha^2\eta^2\eta_x + \alpha\beta\left(\frac{23}{24}\eta_x\eta_{2x} + \frac{5}{12}\eta\eta_{3x}\right) + \frac{19}{360}\beta^2\eta_{5x}$$

$$+ \beta\delta\left(-\frac{1}{2\beta}(h\eta)_x + \frac{1}{4}(h_{2x}\eta)_x - \frac{1}{4}(h\eta_{2x})_x\right) = \gamma\dot{\xi}.$$

Note that this equation, in contrast to KdV equation, has to be solved in the fixed coordinate system because transformation to a moving frame would make the bottom function time dependent.

Setting $\delta = 0$ in (11.45) one obtains second order stochastic KdV type equation (that is the equation for the flat bottom)

$$\eta_t + \eta_x + \alpha \frac{3}{2}\eta\eta_x + \beta \frac{1}{6}\eta_{3x} - \frac{3}{8}\alpha^2\eta^2\eta_x \tag{11.46}$$

$$+ \alpha\beta\left(\frac{23}{24}\eta_x\eta_{2x} + \frac{5}{12}\eta\eta_{3x}\right) + \frac{19}{360}\beta^2\eta_{5x} = \gamma\dot{\xi}.$$

which can be solved within the same algorithm.

The details of numerical scheme for solution of equations (4.27), (4.31) were described in section 11.1 (see, also [83]). Therefore in this section we only briefly summarize that description emphasizing the stochastic part. We focus on (11.45) because in our scheme (11.46) is the particular case of (11.45) when $\delta = 0$.

We adopt the same, as in section 11.1, Crank-Nicholson scheme for time evolution using the time step τ. Introducing the following variables

$$v = \eta_x, \quad w = v_x, \quad p = w_x, \quad q = p_x, \quad g = h_{xx} \tag{11.47}$$

we can write fifth order differential equation (11.45) as the coupled set of first order differential equations

$$\eta^{n+1} - \eta^n - \Phi\left(W^{n+1} - W^n\right) + \tau\frac{\partial}{\partial x}\left[\eta^{n+\frac{1}{2}} + \frac{3\alpha}{4}\left(\eta^{n+\frac{1}{2}}\right)^2 + \frac{\beta}{6}w^{n+\frac{1}{2}}\right. \quad (11.48)$$

$$-\frac{1}{8}\alpha^2\left(\eta^{n+\frac{1}{2}}\right)^3 + \alpha\beta\left(\frac{13}{48}\left(v^{n+\frac{1}{2}}\right)^2 + \frac{5}{12}\left(\eta^{n+\frac{1}{2}}w^{n+\frac{1}{2}}\right)\right) + \frac{19}{360}\beta^2\left(q^{n+\frac{1}{2}}\right)$$

$$\left. +\frac{1}{4}\beta\delta\left(-\frac{2}{\beta}\left(h^{n+\frac{1}{2}}\eta^{n+\frac{1}{2}}\right) + \eta^{n+\frac{1}{2}}g^{n+\frac{1}{2}} + h^{n+\frac{1}{2}}w^{n+\frac{1}{2}}\right)\right] = 0,$$

$$\frac{\partial}{\partial x}\eta^{n+\frac{1}{2}} - v^{n+\frac{1}{2}} = 0,$$

$$\frac{\partial}{\partial x}v^{n+\frac{1}{2}} - w^{n+\frac{1}{2}} = 0,$$

$$\frac{\partial}{\partial x}w^{n+\frac{1}{2}} - p^{n+\frac{1}{2}} = 0,$$

$$\frac{\partial}{\partial x}p^{n+\frac{1}{2}} - q^{n+\frac{1}{2}} = 0,$$

where

$$
\begin{aligned}
\eta^{n+\frac{1}{2}} &= \tfrac{1}{2}\left(\eta^{n+1} + \eta^n\right), & v^{n+\frac{1}{2}} &= \tfrac{1}{2}\left(v^{n+1} + v^n\right), \\
w^{n+\frac{1}{2}} &= \tfrac{1}{2}\left(w^{n+1} + w^n\right), & p^{n+\frac{1}{2}} &= \tfrac{1}{2}\left(p^{n+1} + p^n\right), \\
q^{n+\frac{1}{2}} &= \tfrac{1}{2}\left(q^{n+1} + q^n\right), & h^{n+\frac{1}{2}} &= \tfrac{1}{2}\left(h^{n+1} + h^n\right), \\
g^{n+\frac{1}{2}} &= \tfrac{1}{2}\left(g^{n+1} + g^n\right).
\end{aligned}
\quad (11.49)
$$

In (11.48), $\eta^n = \eta(x, n\tau)$, $\eta^{n+1} = \eta(x, (n+1)\tau)$ and so on.

Finite element method

Since solutions to the stochastic equation are not expected to be smooth, we follow the arguments given in [32] and apply Petrov-Galerkin space discretization and the finite element method like in Section 11.1. We use the same piecewise linear shape function and piecewise constant test functions with the same definition of the mesh. So the shape functions $\varphi_j(x)$ and the test functions $\psi_j(x)$ are define by (11.6) and (11.7), respectively.

Approximate solution and its derivatives may be expanded in the basis (11.6) according to (11.50)

$$
\begin{aligned}
\eta_\nu^n(x) &= \sum_{j=1}^N a_j^n\,\varphi_j(x), & v_\nu^n(x) &= \sum_{j=1}^N b_j^n\,\varphi_j(x), \\
w_\nu^n(x) &= \sum_{j=1}^N c_j^n\,\varphi_j(x), & p_\nu^n(x) &= \sum_{j=1}^N d_j^n\,\varphi_j(x), \\
q_\nu^n(x) &= \sum_{j=1}^N e_j^n\,\varphi_j(x). & &
\end{aligned}
\quad (11.50)
$$

Therefore in a weak formulation we can write (11.48) as

$$
\left(\eta_\nu^{n+1} - \eta_\nu^n, \psi_i\right) - \left(\Phi\left(W_\nu^{n+1} - W_\nu^n\right), \psi_i\right) \tag{11.51}
$$
$$
+\tau\left\{\left(\partial_x\eta_\nu^{n+\frac{1}{2}}, \psi_i\right) + \frac{3\alpha}{4}\left(\partial_x\left(\eta_\nu^{n+\frac{1}{2}}\right)^2, \psi_i\right) + \frac{\beta}{6}\left(\partial_x w_\nu^{n+\frac{1}{2}}, \psi_i\right)\right.
$$
$$
-\frac{1}{8}\alpha^2\left(\partial_x\left(\eta_\nu^{n+\frac{1}{2}}\right)^3, \psi_i\right) + \frac{19}{360}\beta^2\left(\partial_x\left(q_\nu^{n+\frac{1}{2}}\right), \psi_i\right)
$$
$$
+\alpha\beta\left[\frac{13}{48}\left(\partial_x\left(v_\nu^{n+\frac{1}{2}}\right)^2, \psi_i\right) + \frac{5}{12}\left(\partial_x\left(\eta_\nu^{n+\frac{1}{2}} w_\nu^{n+\frac{1}{2}}\right), \psi_i\right)\right]
$$
$$
\left.+\frac{1}{4}\beta\delta\left(\partial_x\left[-\frac{2}{\beta}\left(h^{n+\frac{1}{2}}\eta_\nu^{n+\frac{1}{2}}\right) +\eta_\nu^{n+\frac{1}{2}}g^{n+\frac{1}{2}} + h^{n+\frac{1}{2}}w_\nu^{n+\frac{1}{2}}\right], \psi_i\right)\right\} = 0,
$$
$$
\left(\partial_x\eta_\nu^{n+\frac{1}{2}}, \psi_i\right) - \left(v_\nu^{n+\frac{1}{2}}, \psi_i\right) = 0,
$$
$$
\left(\partial_x v_\nu^{n+\frac{1}{2}}, \psi_i\right) - \left(w_\nu^{n+\frac{1}{2}}, \psi_i\right) = 0,
$$
$$
\left(\partial_x w_\nu^{n+\frac{1}{2}}, \psi_i\right) - \left(p_\nu^{n+\frac{1}{2}}, \psi_i\right) = 0,
$$
$$
\left(\partial_x p_\nu^{n+\frac{1}{2}}, \psi_i\right) - \left(q_\nu^{n+\frac{1}{2}}, \psi_i\right) = 0,
$$

for any $i = 1, \ldots, N$, where abbreviation ∂_x is used for $\frac{\partial}{\partial x}$. Here and in the following,

$$
(f, g) = \int_0^L f(x)g(x)dx
$$

denotes the scalar product of functions.

In order to obtain a noise in space, at each time step n and each node j a random number $\kappa_{j,n}^{\nu,\tau}$ is computed according to a normal law and such that it forms a sequence of independent random variables. Then we can set

$$
\Phi\left(W_\nu^{n+1} - W_\nu^n\right) = \sqrt{\tau}\sum_{j=1}^N \frac{1}{||\phi_j||_{L^2(0,T)}}\kappa_{j,n}^{\nu,\tau}\phi_j = \sqrt{\tau}\,N_\phi\sum_{j=1}^N \kappa_{j,n}^{\nu,\tau}\phi_j, \tag{11.52}
$$

where notation $N_\phi = \dfrac{1}{||\phi_j||_{L^2(0,T)}}$ was introduced for abbreviation.

Insertion (11.8) and (11.52) into (11.51) yields a system of coupled linear equations for coefficients $a_j^n, b_j^n, c_j^n, d_j^n, e_j^n$. Solution of this system supplies an approximate solution of (4.27) given in the mesh points x_j.

$$\text{Denote} \quad \begin{cases} C_{ij}^{(1)} = (\varphi_j, \psi_i), \\[2mm] C_{ij}^{(2)} = (\varphi_j', \psi_i), \\[2mm] C_{ijk}^{(3)} = (\varphi_j'\varphi_k + \varphi_j\varphi_k', \psi_i), \\[2mm] C_{ijkl}^{(4)} = \left(\left[\varphi_j'\varphi_k\varphi_l + \varphi_j\varphi_k'\varphi_l + \varphi_j\varphi_k\varphi_l' \right], \psi_i \right), \end{cases} \tag{11.53}$$

where $\varphi_j' = \frac{d\varphi}{dx}(x_j)$. Simple integration shows that

$$C_{ij}^{(1)} = \begin{cases} \frac{1}{2}\nu & \text{if} \quad i = j \quad \text{or} \quad i = j - 1 \\[2mm] 0 & \text{otherwise}, \end{cases} \tag{11.54}$$

$$C_{ij}^{(2)} = \begin{cases} -1 & \text{if} \quad i = j \\[2mm] 1 & \text{if} \quad i = j - 1 \\[2mm] 0 & \text{otherwise}. \end{cases} \tag{11.55}$$

A little more complicated calculation yields

$$C_{ijk}^{(3)} = C_{ij}^{(2)}\,\delta_{jk} \quad \text{and} \quad C_{ijkl}^{(4)} = C_{ij}^2\,\delta_{jk}\,\delta_{kl}. \tag{11.56}$$

Properties (11.56) allow reducing double and triple sums arising in nonlinear terms in (11.51) to single ones.

The final system of nonlinear equations for coefficients $a_j^{n+1}, b_j^{n+1}, c_j^{n+1}$, d_j^{n+1}, e_j^{n+1} of expansion of the solution in the basis $\{\phi_i\}$ has the form (for details of derivation, see [83])

$$\sum_{j=1}^{N} \left\{ \left(a_j^{n+1} - a_j^n + \sqrt{\tau} \, N_\phi \kappa_{j,n}^{\nu,\tau} \right) C_{ij}^{(1)} + \tau \left[\frac{1}{2} (b_j^{n+1} + b_j^n) C_{ij}^{(1)} \right. \right. \qquad (11.57)$$

$$+ \left(\alpha \frac{3}{16} (a_j^{n+1} + a_j^n)^2 + \beta \frac{1}{12} (c_j^{n+1} + c_j^n) - \alpha^2 \frac{1}{64} (a_j^{n+1} + a_j^n)^3 \right.$$

$$+ \alpha\beta \left[\frac{13}{192} (b_j^{n+1} + b_j^n)^2 + \frac{5}{96} (a_j^{n+1} + a_j^n)(c_j^{n+1} + c_j^n) \right]$$

$$\left. \left. \left. + \beta^2 \frac{19}{720} (e_j^{n+1} + e_j^n) \right) C_{ij}^{(2)} \right] \right\} = 0,$$

$$\sum_{j=1}^{N} \left[(a_j^{n+1} + a_j^n) C_{ij}^{(2)} - (b_j^{n+1} + b_j^n) C_{ij}^{(1)} \right] = 0,$$

$$\sum_{j=1}^{N} \left[(b_j^{n+1} + b_j^n) C_{ij}^{(2)} - (c_j^{n+1} + c_j^n) C_{ij}^{(1)} \right] = 0,$$

$$\sum_{j=1}^{N} \left[(c_j^{n+1} + c_j^n) C_{ij}^{(2)} - (d_j^{n+1} + d_j^n) C_{ij}^{(1)} \right] = 0,$$

$$\sum_{j=1}^{N} \left[(b_j^{n+1} + b_j^n) C_{ij}^{(2)} - (e_j^{n+1} + e_j^n) C_{ij}^{(1)} \right] = 0,$$

where $i = 1, 2, \ldots, N$.

Define $5N$-dimensional vector of expansion coefficients (11.50)

$$X^n = \begin{pmatrix} A^n \\ B^n \\ C^n \\ D^n \\ E^n \end{pmatrix}, \qquad (11.58)$$

where

$$A^n = \begin{pmatrix} a_1^n \\ a_2^n \\ \vdots \\ a_N^n \end{pmatrix}, \quad B^n = \begin{pmatrix} b_1^n \\ b_2^n \\ \vdots \\ b_N^n \end{pmatrix}, \quad C^n = \begin{pmatrix} c_1^n \\ c_2^n \\ \vdots \\ c_N^n \end{pmatrix},$$

$$D^n = \begin{pmatrix} d_1^n \\ d_2^n \\ \vdots \\ d_N^n \end{pmatrix}, \quad \text{and} \quad E^n = \begin{pmatrix} e_1^n \\ e_2^n \\ \vdots \\ e_N^n \end{pmatrix}.$$

In (11.57), $A^{n+1}, B^{n+1}, C^{n+1}, D^{n+1}, E^{n+1}$ represent the unknown coefficients whereas A^n, B^n, C^n, D^n, E^n the known ones. Note that the system (11.57) is a nonlinear one.

In an abbreviated form the set (11.57) can be written as

$$F_i(X^{n+1}, X^n) = 0, \quad i = 1, 2, \ldots, 5N. \tag{11.59}$$

Since this equation is nonlinear we can use Newton method at each time step. That is, we find X^{n+1} by iterating the equation

$$(X^{n+1})_{m+1} = (X^{n+1})_m + J^{-1}(X^{n+1})_m = 0, \tag{11.60}$$

where J^{-1} is the inverse of the Jacobian of the $F(X^{n+1}, X^n)$ (11.59). Choosing $(X^{n+1})_0 = X^n$ we usually obtain the approximate solution to (11.59), $(X^{n+1})_m$ in $m = 3 - 5$ iterations with very good precision. The Jacobian itself is a particular sparse matrix $(5N \times 5N)$ with the following block structure

$$J = \begin{pmatrix} (A_a) & (A_b) & (A_c) & (0) & (A_e) \\ (C2) & -(C1) & (0) & (0) & (0) \\ (0) & (C2) & -(C1) & (0) & (0) \\ (0) & (0) & (C2) & -(C1) & (0) \\ (0) & (0) & (0) & (C2) & -(C1) \end{pmatrix}, \tag{11.61}$$

where each block $(\cdot)$ is a two-diagonal sparse $(N \times N)$ matrix. The matrix A_a is given by

$$A_a = \begin{pmatrix} a_1^1 & 0 & 0 & \cdots & 0 & a_{N-1}^1 & a_N^1 \\ a_1^2 & a_2^2 & 0 & \cdots & 0 & 0 & a_N^2 \\ 0 & a_2^3 & a_3^3 & 0 & \cdots & 0 & 0 \\ \vdots & \vdots & \vdots & \ddots & \vdots & \vdots & \vdots \\ 0 & 0 & \cdots & a_{N-4}^{N-3} & a_{N-3}^{N-3} & 0 & 0 \\ 0 & 0 & \cdots & 0 & a_{N-3}^{n-2} & a_{N-2}^{N-2} & 0 \\ a_1^N & 0 & \cdots & 0 & 0 & a_N^{N-1} & a_N^n \end{pmatrix}. \tag{11.62}$$

In (11.62) the nonzero elements of (A_a) are given by

$$a_j^i = \frac{\partial F_i}{\partial a_j^{n+1}}, \tag{11.63}$$

where F_i, $i = 1, \ldots, N$ is given by the first equation of the set (11.57). Elements in the upper right and lower left corners come from periodic boundary conditions. Matrices $(A_b), (A_c), (A_e)$ have the same structure as (A_a), only elements a_j^i have to be replaced, respectively, by

$$b_j^i = \frac{\partial F_i}{\partial b_j^{n+1}}, \quad c_j^i = \frac{\partial F_i}{\partial c_j^{n+1}} \quad \text{and} \quad e_j^i = \frac{\partial F_i}{\partial e_j^{n+1}}.$$

Matrix (A_d) vanishes since there is no fourth order derivative in the extended KdV equation and d^n does not appear in F.

Matrices $C1$ and $C2$ are constant. They are defined as $Ck, \;\; k = 1, 2$

$$Ck = \begin{pmatrix} C_{11}^{(k)} & 0 & \cdots & C_{11}^{(k)} & C_{1N}^{(k)} \\ C_{21}^{(k)} & C_{22}^{(k)} & \cdots & 0 & C_{2N}^{(k)} \\ \vdots & \vdots & \ddots & \vdots & \vdots \\ 0 & 0 & \cdots & C_{N-1N-1}^{(k)} & 0 \\ C_{N1}^{(k)} & 0 & \cdots & C_{N-1N}^{(k)} & C_{NN}^{(k)} \end{pmatrix}, \tag{11.64}$$

where $C_{ij}^{(k)}$ are defined in (11.54) and (11.55).

11.3.2 Results of simulations

In this section, some examples of numerical calculations of soliton waves with stochastic forces are presented. Simulations were performed by solving the set of equations (11.57) step by step. The main aim was to compare time evolution of waves described by second order KdV-type equation with the bottom dependent term with stochastic forces to those obtained without these forces (obtained in [83] and presented in the previous section). In order to do this several cases of time evolution are presented in the following convention. For each particular case of the bottom function $h(x)$ a sequence of three figures is presented in which the amplitude of the stochastic force is 0, 0.001 and 0.002, respectively. In this way, the influence of an increasing stochastic term on the wave evolution is exhibited. In all presented cases $\delta = 0.2$, that is, the amplitude of the bottom variation is 20% of the average water depth. In order to avoid overlaps of the wave profiles at different time instants, the consecutive profiles are shifted vertically by 0.15.

Soliton waves

In figures 11.9-11.10 we compare time evolution of the wave (initialy a KdV soliton) when the bottom function represents a wide Gaussian hump,

$$h_1(x) = \exp\left(-\frac{(x - 40)^2}{72}\right).$$
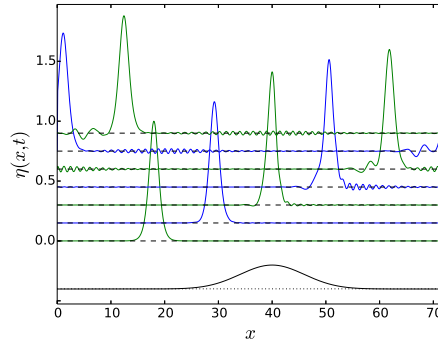
Fig. 11.9. Time evolution of the initial KdV soliton governed by the extended KdV equation (4.31) obtained with FEM method, by numerical solution of the set of equations (11.57) with $\gamma = 0$. Dashed lines represent the undisturbed fluid surface.
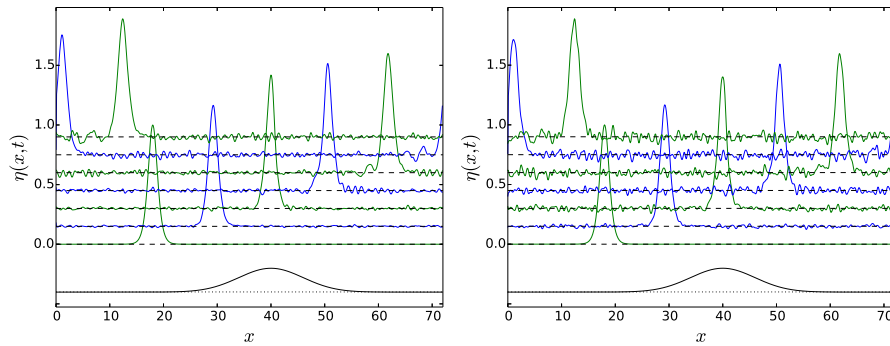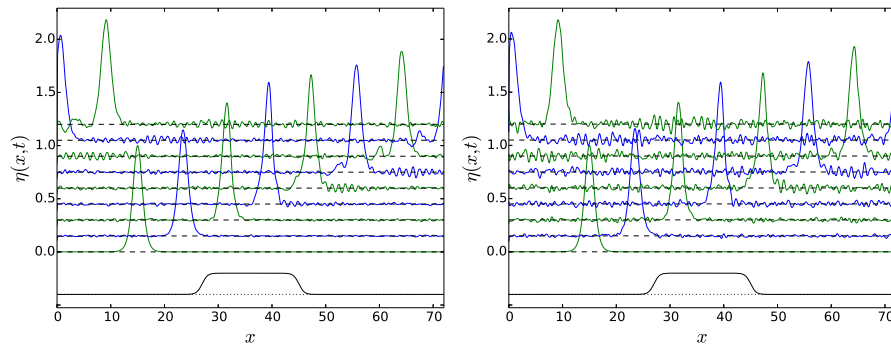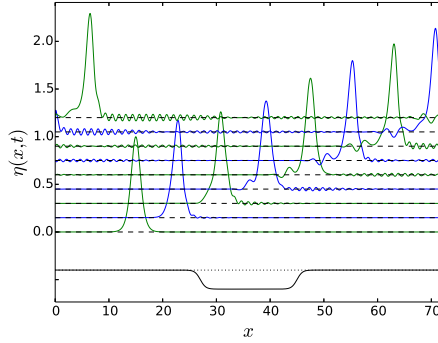

Fig. 11.10. The same as in figure 11.9 but with a moderate amplitude of stochastic force, $\gamma = 0.001$ (left) and with a larger one $\gamma = 0.002$ (right).

In figures 11.11-11.12 we compare time evolution of the wave (initialy a KdV soliton) when the bottom function represents a double Gaussian hump,

$$h_2(x) = \left[\exp\left(-\frac{(x-30)^2}{4} \right) + \exp\left(-\frac{(x-48)^2}{4} \right) \right].$$

In figures 11.13-11.14 we compare time evolution of the initial KdV soliton when the bottom function represents an extended hump,

$$h_3(x) = \left(\frac{\tanh(x-27) - \tanh(x-45)}{2} \right).$$

In figures 11.15-11.16 time evolution of the initial KdV soliton is compared for different amplitude of the stochastic term when the bottom function represents a valley, $h_4(x) = -h_3(x)$.
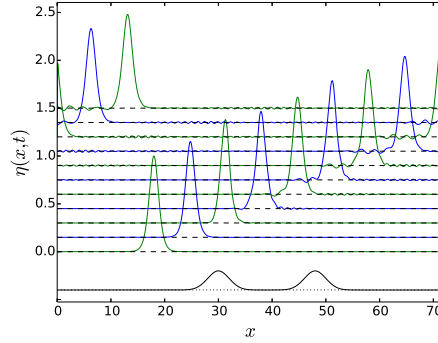
Fig. 11.11. The same as in figure 11.9 but for a double Gaussian hump bottom function.
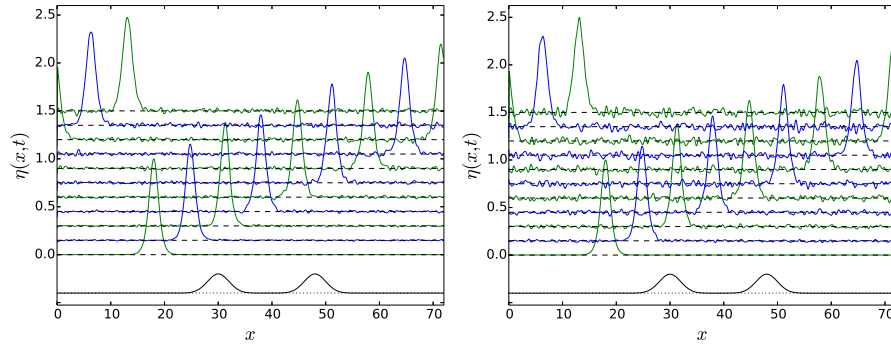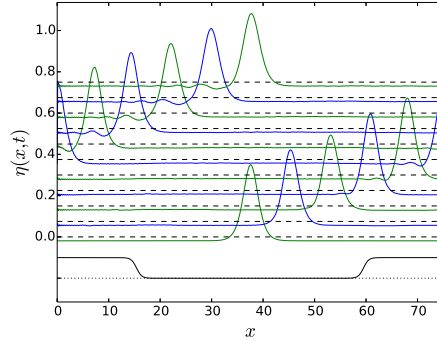

Fig. 11.12. The same as in figure 11.11 but with a moderate amplitude of stochastic force, $\gamma = 0.001$ (left) and with a larger one $\gamma = 0.002$ (right).

In all the examples presented, with different shapes of bottom functions, one observes the same general trend. When the amplitude of the stochastic force is relatively small ($\gamma = 0.001$), some small structures originated from second order terms in the evolution equation (4.31) can be still visible. Simultaneously, the main soliton wave is disturbed only a little by the stochastic term.

When the amplitude of the stochastic force increases, through $\gamma = 0.0015$ which case is not shown here, to $\gamma = 0.002$, the structures from second order terms begin to be more and more obscured by the noise and are not visible at $\gamma = 0.002$. The main wave, however, appears to be strongly resistant to the noise and preserves its soliton character.
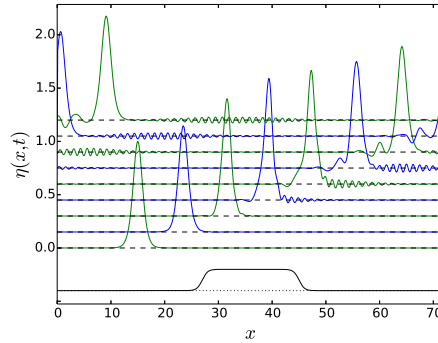
Fig. 11.13. The same as in figure 11.9 but for the bottom function in the form of an extended hump.

Fig. 11.14. The same as in figure 11.13 but with a moderate amplitude of stochastic force, $\gamma = 0.001$ (left) and with a larger one $\gamma = 0.002$ (right).

This character is preserved also for times much longer than in presented examples. To see that we needed, however, to adapt our different code, based on the finite difference method, to the stochastic case. That code proved to be very efficient in numerical calculations presented in [78–80]. The reasons why the finite difference method is more effective than finite element method presented here are explained in detail in the next section.

Cnoidal waves

In figures 11.17-11.18 we present examples of time evolution of cnoidal wave with $m = 1 - 10^{-16}$ (the same as this shown in figure 11.6) for stochastic noise with the strength $\gamma = 0, 0.001$ and 0.0015.

Fig. 11.15. The same as in figure 11.9 but for the bottom function in the form of an extended valley.
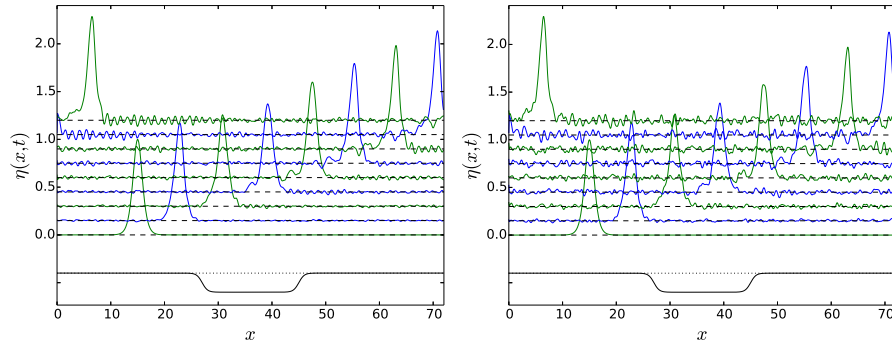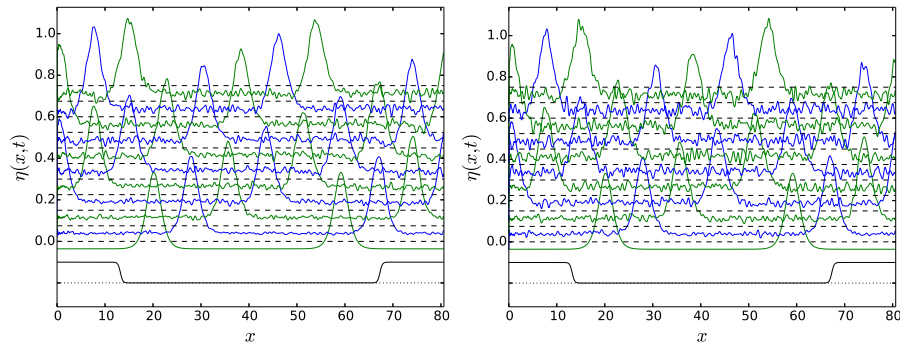

Fig. 11.16. The same as in figure 11.15 but with a moderate amplitude of stochastic force, $\gamma = 0.001$ (left) and with a larger one $\gamma = 0.002$ (right)

In figures 11.19-11.20 we display time evolution of the wave, initialy cnoidal solution of KdV equation with $m = 1 - 10^{-8}$ for $\gamma = 0, 0.001$ and 0.0015. In this case the bottom function is $h(x) = 1 + \frac{1}{2}[-\tanh(2(x-15)-\frac{1}{2})+\tanh(2(x-65)-\frac{1}{2})]$ and the wavelength of the cnoidal wave is $d \approx 40.324$, the same as in figure 11.7.

11.3.3 Conclusions

The main conclusions obtained from our numerical simulations of the time evolution of KdV-type waves with respect to second order equations with bottom terms are the following.

- Both solitary and cnoidal solutions of KdV equations are extremely robust structures for many possible distortions. In [78–80] we showed the resis-

Fig. 11.17. Time evolution, according to eq. (4.31), of the cnoidal wave for the bottom function in the form of an extended valley. The x interval is equal to the wavelength of the cnoidal wave with $m=1\text{-}10^{-16}$.
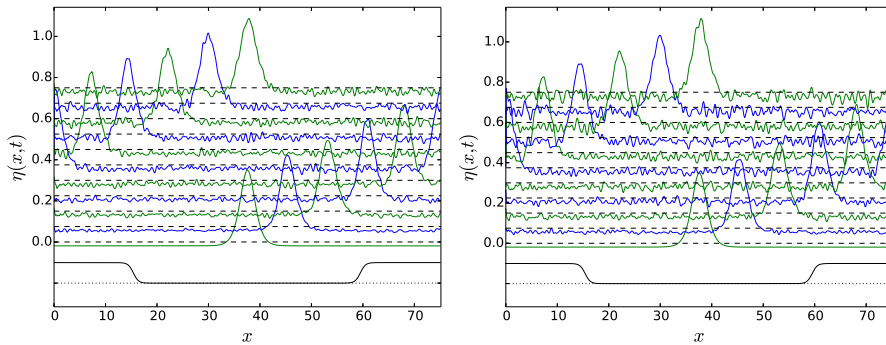
Fig. 11.18. The same as in figure 11.17 but with a moderate amplitude of stochastic force, $\gamma = 0.001$ (left) and with a larger one $\gamma = 0.0015$ (right).

tance of these waves to second order terms in extended KdV equation, including terms from an uneven bottom.

- In this chapter, we showed that inclusion of a stochastic force into second order KdV-type equation does not disturb much the shape of the main wave even for a large amplitude of the noise, although the noise can completely obscure the secondary wave structures. It seems, however, that the main wave is the most robust for solitary waves (which is a limiting case of cnoidal waves when m tends to 1). That robustness with respect to stochastic noise diminishes when parameter m decreases below 1.

- Finite element method, though sufficient for numerical study of stochastic KdV equation in [32] is not so well suited for the higher order KdV type
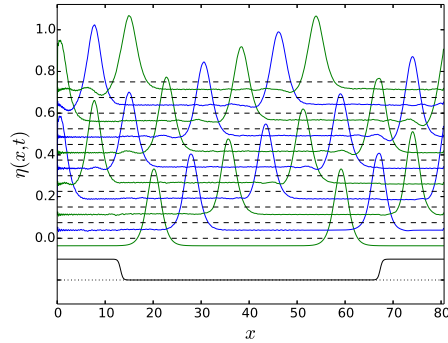
Fig. 11.19. Time evolution, according to eq. (4.31), of the cnoidal wave for the bottom function in the form of a wide hump. The x interval is equal to the double wavelength of the cnoidal wave with m=1-10^{-8}.

Fig. 11.20. The same as in figure 11.19 but with a moderate amplitude of stochastic force, $\gamma = 0.001$ (left) and with a larger one $\gamma = 0.0015$ (right).

equation, and particularly less satisfactory when the bottom is not flat. For the KdV equation considered in a moving frame (11.41) the wave motion is slow and vital time evolution can be calculated using not very long space and time intervals. This property allowed the authors of [32] to use relatively low number $N = 200$ of the mesh size to obtain relevant results. Consequently, since KdV is a third order differential equation, the size of the Jacobian matrix used in the numerical scheme, $(3N \times 3N)$ is still low and allows for fast calculations. The KdV2 equation (4.27), which is a differential equation of fifth order, can be studied both in a moving reference frame and in a fixed frame. In the first case the size of the Jacobian increases to $(5N \times 5N)$ and when N is of the same order the

results can still be obtained in reasonable computing time. The KdV2B equation which takes into account bottom variation (4.31), however, has to be solved in the fixed frame. Then, since waves move much faster, in order to obtain a good description of the wave evolution, substantially longer space intervals have to be used. For a resolution of fine structures of the wave relatively dense mesh has to be applied so N is usually an order of magnitude larger than in the case of moving reference frame. Then computer time for inversion of the Jacobian becomes very large, and detail calculations are not practical. In these cases, the finite difference method used in [78, 79], adapted for the stochastic equation, proves to be more efficient.

References

1. Ablowitz, A.: *Nonlinear dispersive waves. Asymptotic Analysis and solitons*, Cambridge University Press, Cambridge, 2001
2. Ablowitz, A. and Clarkson, A.: *Solitons, Nonlinear Evolution Equations and Inverse Scattering.*, London Mathematical Society Lecture Note Series, **149**, Cambridge University Press, Cambridge, 1991
3. Ablowitz, A., Prinari, B. and Trubatch, A.D.: *Discrete and Continuous Nonlinear Schrdinger Systems.*, London Mathematical Society Lecture Note Series, **302**, (2003)
4. Ablowitz, M. and Segur, H.: *On the evolution of packets of water waves* Journal of Fluid Mechanics, **92**, (4), 691-715, (1979)
5. Ablowitz, M. and Segur, H.: *Solitons and the Inverse Scattering Transform* SIAM, Philadelphia, PA, 1981
6. Abraham-Shrauner, B.: *Exact Solutions of Nonlinear Differential Equations*, Discr. Cont. Dyn. Syst. S, **11** (4), 577, (2018)
7. Abraham-Shrauner, B.: *Analytic Solutions of Nonlinear Differential Equations by the Power Index Method*, Symmetry, **10**, 76, (2018)
8. Ali, A. and Kalisch, H.: *On the formulation of mass, momentum and energy conservation in the KdV equation*, Acta Applicandae Mathematicae, **133**, 113-133, (2014)
9. Banach, S.: *Mechanika*, Instytut Matematyczny Polskiej Akademi Nauk, Warszawa-Lwów-Wilno, (1938)
10. Belashov, V.Y. and Vladimirov, S.V.: *Solitary Waves in Dispersive Complex Media*, Springer Series in Solid-State Sciences, **149**, 2005
11. Benilov, E.S. and Howlin, C.P.: *Evolution of Packets of Surface Gravity Waves over Strong Smooth Topography*, Studies Appl. Math. **116**, 289, (2006)
12. Benjmin, T.B.: *The stability of solitary waves*, Proc. R. Soc. London A, **32**, 153, (1972)

13. Benjamin, T.B., Bona J.L. and Mahony, J.J.: *Model equations for long waves in nonlinear dispersive media*, Phil. Trans. Roy. Soc. London, Series A, **272**, 47-78, (1972)

14. Benjamin, T.B. and Olver, P.J.: *Hamiltonian structure, symmetries and conservation laws for water waves*, J. Fluid Mech., **125**, 137-185, (1982)

15. Bernard K. Ee, Grimshaw, R. H. J., Zhang, D. H., Chow, K. W.: *Steady transcritical flow over a hole: Parametric map of solutions of the forced Korteweg-de Vries equation*, Physics of Fluids, **22**, 056602, (2010)

16. Bona, J.L., Pritchard W.G. and Scott L.R.: *An evaluation of a model equation for water waves*, Phil. Trans. Roy. Soc. London, Series A, **302** 457-510, (1981)

17. Bona, J.L., Chen, H., Karakashian, O. and Xing, Y.: *Conservative, discontinuous-Galerkin methods for the generalized Korteweg-de Vries equation*, Mathematics of Computation **82** (283) 14011432, (2013)

18. Bottman, N., Deconinck, B.: *KdV cnoidal waves are spectrally stable*, AIMS, **25** (4), 1163 - 1180, (2009)

19. de Bouard, A. and Debussche, A.: *On the stochastic Korteweg-de Vries equation.*, Journal of Functional Analysis, **154** (1), 215-251, (1998)

20. Boussinesq, J. V. : *Théorie générale des mouvements qui sont propagés dans un canal rectangulaire horizontal.*, Comptes Rendus de l'Académie des Sciences, **73**, 256-260, (1871)

21. Brauer, K.: *The Korteweg-de Vries Equation: History, exact Solutions, and graphical Representation*, University of Osnabrück, (2000)
https://www.researchgate.net/publication/2806104_The_Korteweg-de_Vries_Equation_History_exact_Solutions_and_graphical_Representation

22. Bullough, R.K., Fordy, A.P. and Manakov, S.V.: *Adiabatic invariants theory of near-integrable systems with damping*, Phys. Lett. A, **91**, 98-100, (1982)

23. Burde, G.I.: *Solitary wave solutions of the higher-order KdV models for bidirectional water waves*, Commun. Nonlinear Sci. Numer. Simulat. **16**, 1314, (2011)

24. Burde, G.I. and Sergyeyev, A.: *Ordering of two small parameters in the shallow water wave problem*, J. Phys. A: Math. Theor. **46**, 075501, (2013)

25. Byatt-Smith, J.G.B.: *On the change of amplitude of interacting solitary waves*, J. Fluid Mech. **182**, 485, (1987)

26. Canivar, A., Sari, M. and Dag, I.: *A Taylor-Galerkin finite element method for the KdV equation*, Physica B **405** 3376-3383, (2010)

27. Chow, K.W.: *A second-order solution for the solitary wave in a rotational flow*, Physics of Fluids **1** (7), 1235, (1989)

28. Cooper, F., Lucheroni, C., Shepard, H., Sodano, P.: *Variational Method for Studying Solitons in the Korteweg-DeVries Equation*, Physics Letters A **173**, 33-36, (1993)

29. Courant, R. and Hilbert, D.: *Methods of mathematical physics*, Interscience publishers Inc., New York, 1953

30. Craik, A.D.D.: *The Origins of Water Wave Theory*, Annual Review of Fluid Mechanics **37**, 23-42, (2004)

31. Cui, Y. and Ma, D.: *Numerical method satisfying the first two conservation laws for the Korteweg-de Vries equation*, Journal of Computational Physics **227** (1), 376399, (2007)

32. Debussche, A. and Printems, I.: *Numerical simulation of the stochastic Kortewegde Vries equation*, Physica D **134**, 200-226, (1999)

33. Dingemans, M.: *Water wave propagation over uneven bottoms*, World Scientific, Singapore, 1997

34. Djordjević, V.D. and Redekopp, L.G.: *On the development of packets of surface gravity waves moving over an uneven bottom*, J. Appl. Math. and Phys. (ZAMP) **29**, 950-962, (1978)

35. Dodd, R. and Fordy, A.P.: *On the integrability of a system of coupled KdV equations*, Phys. Lett. A **89**, 168-170, (1982)

36. Drazin, P.G. and Johnson, R.S.: *Solitons: An introduction*, Cambridge University Press, Cambridge, 1989

37. Dullin, H.R., Gottwald, G.A. and Holm, D.D.: *An integrable shallow water equation with linear and nonlinear dispersion*, Phys. Rev. Lett. **87** (19), 194501, (2001)

38. Dullin, H.R., Gottwald, G.A. and Holm, D.D.: *Camassa-Holm, Korteweg-de Vries-5 and other asymptotically equivalent equations for shallow water waves*, Fluid Dyn. Res. **33**, 7395, (2003)

39. Dullin, H.R., Gottwald, G.A. and Holm, D.D.: *On asymptotically equivalent shallow water equations*, Physica D **190**, 1-14, (2004)

40. Eckhaus, W. and van Harten, A.: *The Inverse scattering method and the theory of solitons. An introduction*, North-Holland Mathematics studies, Utrecht, 1981

41. El, G.A., Grimshaw, R.H.J. and Smyth, N.F.: *Unsteady undular bores in fully nonlinear shallow-water theory*, Physics of Fluids, **18**, 027104, (2006)

42. Farin, G.: *Curves and Surfaces for Computer Aided Geometric Design - A Practical Guide, 4th Edition*, Academic Press, 1997

43. Fenton, J.D.: *A high-order cnoidal wave theory*, *J. Fluid Mech.*, **94** (1), 129 (1979)

44. Fenton, J.D.: *Nonlinear wave theories*, in: Ocean Engineering Science, The Sea, Vol. 9, Eds. B. Le Méhauté, D.M Hanes, Wiley Interscience, New York, 1990

45. Fokas, A.S. and Liu, Q.M.: *Asymptotic Integrability of Water Waves*, Phys. Rev. Lett., **77**, 2347, (1996)

46. Fordy, A. P.: *A Historical Introduction to Solitons and Bäcklund Transformations*, Aspects of Mathematics, **E 23**, 7-28, (1994)

47. Fornberg, B. and Whitham, G. B.: *A numerical and theoretical study of certain nonlinear wave phenomena*, Phil. Trans. Royal Soc. Lond. A **289** (1361), 373404, (1978)

48. Gardner, C.S., Greene, J.M., Kruskal, M.D. and Miura, R.M.: *Method for Solving the Korteweg-deVries Equation.*, Physical Review Letters, **19**, 1095, (1967)

49. Goda, K.: *On instability of some finite difference schemes for the Korteweg de Vries equation*, Journal of the Physical Society of Japan **39**, 229236, (1975)

50. Green, A.E. and Naghdi, P.M.: *A derivation of equations for wave propagation in water of variable depth*, Journal of Fluid Mechanics, **78**, 237-246, (1976)

51. Grilli, S.T., Subramanya, R., Svendsen, I.A. and Veeramony, J.: *Shoaling of solitary waves on plane beaches*, Journal of Waterway Port Coastal and Ocean Engineering, **120**, 609-628, (1994)

52. Grilli, S. T., Svendsen, I.A. and Subramanya, R.: *Breaking Criterion and Characteristics for Solitary Waves on Slopes*, Journal of Waterway Port Coastal and Ocean Engineering, **123**, 102-112, (1997)

53. Grimshaw, R.: *The solitary wave in water of variable depth*, J. Fluid Mech. **42**, 639-656, (1970)

54. Grimshaw, R.: Internal solitary waves (2001). Presented at the international conference PROGRESS IN NONLINEAR SCIENCE, held in Nizhni Novogrod, July 2001. Dedicated to the 100-th Anniversary of Alexander A. Andronov

55. Grimshaw, R. H. J., Chan, K. H., Chow, K. W.: *Transcritical flow of a stratified fluid: The forced extended Korteweg-de Vries model*, Physics of Fluids, **14**, 755, (2002)

56. Grimshaw, R., Pelinovsky, E. and Talipova, T.: *Modelling internal solitary saves in the coastal ocean*, Surv. Geophys., **28**, 273298, (2007)

57. Grimshaw, R., Pelinovsky, E. and Talipova, T.: *Fission of a weakly nonlinear interfacial solitary wave at a step*, Geophys. Astrophys. Fluid Dynam. **102**, 179-194, (2008)

58. Grimshaw, R.H.J. and Smyth, N. F: *Resonant flow of a stratified fluid over topography.*, Journal of Fluid Mechanics, **169**, 429-464, (1986)

59. van Greoesen, E. and Pudjaprasetya, S. R.: *Uni-directional waves over slowly varying bottom. Part I: Derivation of a KdV-type of equation* , Wave Motion **18**, 345, (1993)

60. Hereman, W.: *Shallow Water Waves and Solitary Waves* in *Encyclopedia of Complexity and Applied System Science* ed. Robert A. Meyers, Entry 480, pp. 8112-8125 Springer Verlag, Heidelberg, 2009. http://arxiv.org/abs/1308.5383

61. He, Y.: *New exact solutions for a higher order wave equation of KdV type using multiple G'/G-expansion methods*, Advances in Mathematical Physics, 148132, (2014)

62. He, Y., Zhao, Y.M. and Long, Y.: *New exact solutions for a higher-order wave equation of KdV type using extended f-expansion method*, Mathematical Problems in Engineering, 128970, (2013)

63. Hiraoka, Y. and Kodama, Y.: *Normal form and solitons*, Lect. Notes Phys. **767**, 175214, (2009)

64. Hirota, R.: *Exact solution of the Korteweg-de Vries equation for multiple collisions of solitons*, Phys. Rev. Lett. **27**, 1192, (1972)

65. Hirota, R.: *The Bäcklund and inverse scatering transform of the KdV equation with nonuniformities*, J. Phys. Soc. Jpn. **46** 1681-1682, (1979)

66. Hirota, R.: *The Direct Method in Soliton Theory*, Cambridge Tracts in Mathematics, **155**, (2004)

67. Infeld, E., Rowlands, G.and Hen, M.: *Three-dimensional stability of Korteveg de Vries waves and soliton*, Acta Phys. Pol. A **54**, 623, (1978)

68. Infeld, E. and Rowlands, G.: *Three-dimensional stability of Korteveg de Vries waves and solitons, II*, Acta Phys. Pol. A **56**, 329-332, (1979)

69. Infeld, E.: *Three-dimensional stability of Korteweg de Vries waves and solitons. III. Lagrangian methods, KdV with positive dispersion*, Acta Phys. Pol. A **60**, 623-643, (1981)

70. Infeld, E., Karczewska, A., Rowlands, G. and Rozmej, P.: *Exact cnoidal solutions of the extended KdV equation*, Acta Phys. Pol. A, **133**, 1191-1199, (2018). DOI: 10.12693/APhysPolA.133.1191

71. Infeld, E. and Rowlands, G.: *Stability of nonlinear ion sound waves and solitons in plasma*, Proc. R. Soc. Lond. A **366**, 537, (1979)

72. Infeld, E. and Rowlands, G.: *Nonlinear Waves, Solitons and Chaos*, Cambridge University Press, 1990

73. Infeld, E., Rowlands, G. and Senatorski, A.: *Instabilities and oscillations in one and two dimensional Kadomtsev-Petviashvili waves and solitons*, Proc. Roy. Soc. London A, **455**, 4363-4381, (1999)

74. ul-Islam, S., Haq, S. and Ali, A.: *A meshfree method for the numerical solution RLW equation*, J. Comp. Appl. Math. **223** 997-1012 (2009)

75. Jeffrey, A.: *Role of the Korteweg-de Vries Equation in Plasma Physics*, Quarterly Journal of the Royal Astronomical Society, **14**, 183, (1973)

76. Kadomtsev, B.B. and Petviashvili, V.I.: *On the stability of solitary waves in weakly dispersive media*, Dokl. Akad. Nauk SSSR **192**, 753, (1970) [Sov. Phys. Dokl. **15**, 539, (1970)]

77. Kamchatnov, A. M., Kuo, Y.-H., Lin, T.-C., Horng, T.-L., Gou, S.-C., Clift, R., El, G. A. and Grimshaw, R. H. J.: *Undular bore theory for the Gardner equation*, Physical Review E, **86**, 036605, (2012)

78. Karczewska, A., Rozmej, P. and Rutkowski, L.: *A new nonlinear equation in the shallow water wave problem*, Physica Scripta, **89**, 054026, (2014). DOI: 10.1088/0031-8949/89/5/054026

79. Karczewska, A., Rozmej, P. and Infeld, E.: *Shallow water soliton dynamics beyond KdV*, Physical Review E, **90**, 012907, (2014). DOI: 10.1103/PhysRevE.90.012907

80. Karczewska, A., Rozmej, P. and Infeld, E.: *Energy invariant for shallow-water waves and the Korteweg-de Vries equation: Doubts about the invari-*

ance of energy, Physical Review E, **92**, 053202 (2015). DOI: 10.1103/Phys-RevE.92.053202

81. Karczewska, A., Rozmej, P. and Rutkowski, Ł.: *Problems with energy of waves described by Kortewg-de Vries equation*, Annales UMCS Sectio AAA Physica **70**, 41-54, (2015)

82. Karczewska, A., Rozmej, P., Infeld, E. and Rowlands, G.: *Adiabatic invariants of the extended KdV equation*, Phys. Lett. A, **381**, 270-275, (2017). DOI: 10.1016/j.physleta.2016.11.035

83. Karczewska, A., Rozmej, P., Szczeciński, M. and Boguniewicz, B.: *A finite element method for extended KdV equations*, Int. J. Appl. Math. Comput. Sci. **26**, (3), 555-567, (2016). DOI: 10.1515/amcs-2016-0039

84. Karczewska, A., Szczeciński, M., Rozmej, P. and Boguniewicz, B.: *Finite element method for stochastic extended KdV equations*, Comput. Meth. Phys. Tech. **22**, (1), 19-29, (2016). DOI: 10.12921/cmst.2016.22.01.002

85. Karczewska, A. and Szczeciński, M.: *Existence of mild solution to stochastic extended Korteweg-de Vries equation*, submitted.

86. Karczewska, A. and Szczeciński, M.: *Stochastic hybrid Korteweg-de Vries-Burgers equations*, submitted.

87. Kenig, C.E, Ponce, G. and Vega, L.: *Well-posedness of the initial value problem for the Korteweg-de Vries equation*, J. Amer. Math. Soc. **4**, 323-347, (1991)

88. Kichenassamy, S. and Olver, P.: *Existence and nonexistence of solitary wave solutions to higher-order model evolution equations*, SIAM J. Math. Anal. **23**, 1141, (1992)

89. Kim, J.W., Bai, K.J., Ertekin, R.C. and Webster, W.C.: *A derivation of the Green-Naghdi equations for irrotational flows*, Journal of Engineering Mathematics, **40**, (1), 17-42, (2001)

90. Khare, A. and Saxena, A.: *Linear superposition for a class of nonlinear equations*, Phys. Lett. A **377**, 2761-2765, (2013)

91. Khare, A. and Saxena, A.: *Superposition of elliptic functions as solutions for a large number of nonlinear equations*, J. Math. Phys. **55**, 032701, (2014)

92. Khare, A. and Saxena, A.: *Periodic and hyperbolic soliton solutions of a number of nonlocal nonlinear equations*, J. Math. Phys. **56**, 032104, (2015)

93. Khusnutdinova, K.R., Stepanyants, Y. and Tranter, M.: *Soliton solutions to the fifth-order Korteweg - de Vries equation and their applications to surface and internal water waves*, Phys. of Fluids, **30**, 022104, (2018)

94. Kodama, Y.: *On integrable systems with higher order corrections*, Phys. Lett. A, **107**, 245-249, (1985)

95. Kodama, Y.: *Normal forms for weakly dispersive wave equations*, Phys. Lett. A, **112**, 193-196, (1985)

96. Korteweg, D.J. and de Vries, H: *On the change of form of long waves advancing in a rectangular canal, and on a new type of long stationary waves.*, Philosophical Magazine, **39**, 422-443, (1895)

97. Kurkina, O.E., Kurkin, A.A., Soomere, T., Pelinovsky, E.N. and Rouvinskaya, E.A.: *Higher-order (2+4) Korteweg-de Vries-like equation for interfacial waves in a symmetric three-layer fluid*, Physics of Fluids, **23**, (2011)

98. Lax, P.D.: *Integrals of nonlinear equations of evolution and solitary waves.*, Communications on Pure and Applied Mathematics, **21** (5), 467-490, (1968)

99. Landau, L.D. and Lifschitz, E.M.: *Fluid mechanics*, sec. ed., Pergamon Press, 1987

100. Leitner, M. and Mikikits-Leitner, A.: *Nonlinear differential identities for cnoidal waves*, Math. Nachr., **287**, 2040-2056, (2014)

101. Linares, F. and Ponce, G.: *Introduction to Nonlinear Dispersive Equations*, Universitext, Springer, 2009

102. Longuet-Higgins, M.S. and Fenton, J.D.: *On the mass, momentum, energy and circulation of a solitary wave. II*, Proc. R. Soc. London A **340**, 471, (1974)

103. Luke, J.C.: *A variational principle for a fluid with a free surface*, Journal of Fluid Mechanics, **27**, part 2, 395-397, (1967)

104. Maimistov, A.I.: *Solitons in nonlinear optics*, Quantum Electronics, **40**, No 9, 756, (2010)

105. Marchant, T.R. and Smyth, N.F.: *The extended Korteweg-de Vries equation and the resonant flow of a fluid over topography*, Journal of Fluid Mechanics, **221**, 263-288, (1990)

106. Marchant, T.R.: *Coupled Korteweg-de Vries equations describing, to high-order, resonant flow of a fluid over topography*, Physics of Fluids, **11**, (1999)

107. Marchant, T.R.: *High-Order Interaction of Solitary Waves on Shallow Water*, Studies in Applied Mathematics, **109** (1), (2002)

108. Marchant, T.R. and Smyth, N.F.: *Soliton interaction for the extended Korteweg-de Vries equation*, IMA J. Appl. Math. **56**, 157-176, (1996)

109. Marchant, T.R.: *Asymptotic solitons for a higher-order modified Korteveg-de Vries Equations*, Phys. Rev. E **66**, 046623, (2002)

110. Le Méhauté, B., Divoky, D. and Lin, A.: *Shallow Water Waves: A Comparison of Theories and Experiments*, Coastal Engineering, (1968)

111. Mei, C.C. and Le Méhauté, B.: *Note on the equations of long waves over an uneven bottom*, J. Geophys. Res. **71**, 393-400, (1966)

112. Miura, R.M.: *Korteweg-de Vries equation and generalizations. I A remarkable explicit nonlinear transformation*, Journal of Mathematical Physics, **9**, 1202-1204, (1968)

113. Miura, R.M., Gardner, C.S. and Kruskal, M.D.: *Korteweg-de Vries equation and generalizations. II Existence of conservation laws and constants of motion*, Journal of Mathematical Physics, **9**, 1204-1209, (1968)

114. MULTIWAVE PROJECT @ 2012 University College Dublin, http://www.ercmultiwave.eu

115. Nadiga, B.T., Margolin, L.G. and Smolarkiewicz, P.K.,: *Different approximations of shallow fluid flow over an obstacle*, Physics of Fluids, **8**, 2066, (1996)

116. Nakoulima, O., Zahibo, N., Pelinovsky, E., Talipova, T. and Kurkin, A.: *Solitary wave dynamics in shallow water over periodic topography*, Chaos **15**, 037107, (2005)

117. Newell, A.C.: *Solitons in Mathematics and Physics*, Society for Industrial and Applied Mathematics, Philadelphia, PA, 1985

118. Niu, X. and Yu, X.: *Analytical Solution of Long Wave Propagation over a Submerged Hump*, Coastal Engineering **58**, 143, (2011); Liu H-W. and Xie, J-J.: *Discussion of "Analytic solution of long wave propagation over a submerged hump" by Niu and Yu (2011)*, **58**, 948, (2011)

119. Oh, T.: *Periodic stochastic Korteweg-de Vries equation with additive space-time white noise*, Analysis & PDE **2**, 281-304 (2009)

120. Oh, T.: *Invariance of the White Noise for KdV*, Commun. Math. Phys. **292**, 217236, (2009)

121. Olver, P.J. and Sattinger, D.H. (Eds.): *Solitons in Physics, Mathematics, and Nonlinear Optics*, Springer, New York, 1990

122. Olver, P.J.: *Applications of Lie groups to differential equations*, Springer, New York, 1993

123. Osborne, A.: *Nonlinear Ocean Waves and the Inverse Scattering Transform*, Elsevier, Amsterdam, 2010

124. Pelinovsky, E., Choi, B.H, Talipova, T., Woo, S.B. and Kim D.C.: *Solitary wave transformation on the underwater step: Asymptotic theory and numerical experiments*, Applied Mathematics and Computation, **217**, 1704-1718, (2010)

125. Peregrine, D.H.: *Long Waves on Beach*, Journal of Fluid Mechanics, **27**, 815-827, (1967)

126. Pudjaprasetya, S.R. and van Greoesen, E.: *Uni-directional Waves over slowly varying bottom. Part II: Quasi-static approximation of distorting wave*, Wave Motion **23**, 23, (1996)

127. Remoissenet, M.: *Waves Called Solitons*, Springer-Verlag, Berlin Heidelberg, 1994

128. Rowlands, G., Rozmej, P., Infeld, E. and Karczewska, A.: *Single soliton solution to the extended KdV equation over uneven depth*, Eur. Phys. J. E, **40**, 100, (2017). DOI: 10.1140/epje/i2017-11591-7

129. Rozmej, P., Karczewska, A. and Infeld, E.: *Superposition solutions to the extended KdV equation for water surface waves*, Nonlinear Dynamics **91**, 1085-1093, (2018). DOI: 10.1007/s11071-017-3931-1

130. Rozmej, P. and Karczewska, A.: *New Exact Superposition Solutions to KdV2 Equation*, Advances in Mathematical Physics. **2018**, Article ID 5095482, 1-9, (2018). DOI: 10.1155/2018/5095482

131. Russel, J.S.: *Report on Waves*, Murray, London, 311-390, (1844)

132. Sergyeyev, A. and Vitolo, R.: *Symmetries and conservation laws for the Karczewska-Rozmej-Rutkowski-Infeld equation*, Nonl. Anal.: Real World Appl. **32**, 1-9, (2016)

133. Skogstad, J. and Kalisch, H.: *A boundary value problem for the KdV equation: comparison of finite difference and Chebyshev methods*, Mathematics and Computers in Simulation **80** (1), 151163, (2009)

134. Smyth, N. F.: *Modulation theory solution for resonant flow over topography*, Proceedings of the Royal Society A, **409**, 79-97, (1987)

135. Stokes, G.G.: *On the theory of oscillatory waves*, Camb. Trans. **8**, 441-473 (1847). (*Papers* **1**, 197-229)

136. Strutt, J.W. (Lord Rayleigh): *On waves*, Philosophical Magazine, **5**, 257-279, (1876)

137. Taniuti, T. and Wei, CC.: *Reductive perturbation method in nonlinear wave propagation*, *J. Phys. Soc. Jpn.*, **24**, 941-847, (1968)

138. Taha, T.R. and Ablowitz, M.J.: *Analytical and numerical aspects of certain nonlinear evolution equations III. Numerical, the Korteweg de Vries equation*, Journal of Computational Physics **55** (2), 231253, (1984)

139. Tzirtzilakis, E., Marinakis, V., Apokis, C. and Bountis, T.: *Soliton-like solutions of higher order wave equations of the Korteweg-de Vries type*, Journal of Mathematical Physics, **43**, (2002)

140. Viotti, C., Dutykh, D. and Dias, F.: *The Conformal-mapping Method for Surface Gravity Waves in the Presence of Variable Bathymetry and Mean Current*, Procedia IUTAM **11**, 110, (2014)

141. Villegas J.G., Castano J.B., Duarte J.V. and Fierro E.Y.: *Wavelet-Petrov-Galerkin method for the numerical solution of the KdV equation*, Appl. Math. Sci. **6**, 3411-3423, (2012)

142. Vvedensky, D.: *Partial Differential equations with Mathematica*, Addison-Wesley, 1993

143. Wazwaz, A.M.: *A fifth-order Korteweg-de Vries equation for shallow water wth surface tension: multiple soliton solutions*, Acta Phys. Pol. A, **130** (3) 679, (2016)

144. Whitham, G.B.: *Linear and Nonlinear Waves*, John Wiley & Sons Inc., 1974

145. Xiaofeng, L., Ricketts, D.S. and Donhee, H.: *Solitons in Electrical Networks*, Yearbook of Science and Technology, 2008

146. Yang, J.: *Dynamics of embedded solitons in the extended Korteweg-de Vries equations*, Studies in Applied Mathematics 106, 337365, (2001)

147. Yi, N., Huang, Y. and Liu, H.: *A direct discontinous Galerkin method for the generalized Korteweg-de Vries equation: energy conservation and boundary effect*, Journal of Computational Physics, **242**, 351-366, (2013)

148. Yuan, J.-M., Shen, J. and Wu, J.: *A dual-Petrov-Galerkin method for the Kawahara-type equations*, Journal of Scientific Computing, **34**, 48-63, (2008)

149. Zabusky, N. J.: *Solitons and Bound States of the Time-Independent Schrdinger Equation*, Physical Review, **168**, 124-128, (1968)

150. Zabusky, N. J. and Kruskal, M. D.: *Interaction of "Solitons" in a Collisionless Plasma and the Recurrence of Initial States.*, Physical Review Letters, **15**, 240-243, (1965)

151. Zhao, M., Teng, B. and Cheng, L.: *A new form of generalized Boussinesq equations for varying water depth*, Ocean Engineering, **31** (16), 2047-2072, (2004)

152. Zhao, Y.M.: *New exact solutions for a higher-order wave equation of KdV type using the multiple simplest equation method.* Journal of Applied Mathematics, **2014**, 848069 (2014)

153. Q. Zou, Q. and Su, CH-H.: *Overtaking collision between two solitary waves*, Phys. Fluids **29**, 2113, (1986)

Index